3D Crop Modelling

Jillian Watt

Remote Sensing Unit
Department of Geography
University College London

Thesis Submitted for the Fulfilment
of a Masters of Philosophy

Crop models have become increasingly useful tools for understanding and implementing sustainable agricultural techniques and as a way of accurately predicting crop yields for economists and policy decision makers.

Using remotely sensed imagery can significantly reduce the effort required to obtain the inputs for crop models and can provide regular sets of observations throughout a growing season. Empirical models can be used to extract information regarding the crop from remotely sensed images but have well-documented limitations. Coupling a crop model with a radiative transfer model allows comparison between modelled and actual reflectance, across a range of potential crop model states. The potential difference observed can then allow for recalibration of the crop model. This technique enables the crop model to be updated throughout crop development and growth, increasing its accuracy at predicting the development of the crop. As the structure of the crop changes significantly during growth and development, affecting the remote sensing signal, a 3D structural model which can represent this change is required.

This thesis presents work developing and re-parameterising an existing 3D crop model to make it more generic, as well as coupling it with a radiative transfer model. The crop model being re-parameterised is ADEL-wheat. Extensive field work spanning two growing seasons has been carried out to measure the phenological and structural differences that occurred during the growth and development of different genotypes of winter wheat. These observed differences, particularly in phenology, have been implemented within the model, and then used to test the impact on the remote sensing signal. The work shows that structural differences between genotypes tend to have a greater impact on the resulting modelled signal than phenological variation. The combined structural and radiative transfer modelling approach is shown to be very flexible and can be used to improve/augment existing crop modelling approaches.

Contents

List of Figures

List of Tables

Chapter 1

Introduction

Crop models at their simplest predict yield and at their most complex simulate the processes involved in crop growth and development. Recent advances within this area of research have led to the coupling of more complex crop models with, both optical and microwave remote sensing data. This chapter aims to justify this area of research and put it in context of the wider scientific field.

Wheat (Triticum spp) was one of the first crops easily cultivated on a large scale yielding a harvest which provided long term storage of food. The combination of these attributes made it a key factor enabling the emergence of city-based societies at the start of civilisation. It is now cultivated worldwide and in 2007 world production of wheat was 607 million tons, making it the third most produced cereal after maize (784 million tons) and rice (651 million tons) (Faostat 2007). Globally wheat has been the leading source of vegetable protein in human food, having a higher protein content than the other major cereals; maize and rice. In terms of total production tonnages used for food, it has been second to rice as the main human food crop and ahead of maize. Wheat grain is a staple food used to make flour, noodles, pasta, breakfast cereals and couscous and is used for fermentation to make beer and other alcoholic beverages as well as bio fuel. It is therefore an important crop socially and economically and a worthy focus of this thesis (Sources 2013).

It is important to acknowledge that agriculture produces a variety of food and fuel, both of which are vital for humans and the local, regional and global economies. Scientific evidence suggests that the global climate is changing (Watson *et al.* 1996, Watson *et al.* 1998, Parry *et al.* 2001, Van Vuren *et al.* 2011). Global agriculture must confront this change and in addition provide for the predicted increased population (Bank 1994). Recently due to severe drought and rampaging wildfires, Russia dropped its grain crop forecast for 2010, sending wheat prices to a two year high (Welle 2011).This highlights the impact wheat yield can have on the global economy and the importance of being able to forecast yields accurately to maintain food security. Crop models play an important part in this challenge providing accurate and timely predictions of food security and related issues with food pricing (Parry *et al.* 1999).

Globally, agriculture contributes to climate change through the consumption of energy and the release of soil carbon as well as affecting the carbon and water cycles (Desjardins *et al.* 2007). It has a crucial influence on runoff, albedo, evapotranspiration and ultimately atmospheric composition and global climate energy exchanges between its surface and the atmosphere (Foley

et al. 2005). Crop models can increase the understanding of these complex relationships. This is important as agriculture affects, but is also vulnerable to, climate change. Predicted increased temperatures are suggested to eventually reduce yields and encourage weed and pest proliferation. Predicted changes in precipitation patterns are forecast to increase the likelihood of short-run crop failures and long run production declines. The overall impact of climate change on agriculture is thus expected to be negative. Crop models enable a greater understanding of these complex relationships which are important within the climate change and agricultural sectors but also due to the knock on affect such changes can have on global food security as already mentioned (Nelson *et al.* 2009).

Locally, the conversion and maintenance of natural land to agricultural land affects the local environment contributing significantly to water, air and soil pollution and adversely affects the local biodiversity of flora and fauna (FAO 2002). In order to minimise the environmental impacts, crop models can be used to help inform optimal agricultural management strategies. This allows high quality and quantity yield to be produced with minimal inputs (Launey *et al.* 2009).

Within research crop models can reduce the need for resource intensive glasshouse and field trials by, within reason, enabling model simulation runs to take their place. Examples of such research include; competition within crop canopies (Lawless *et al.* 2005), spread of foliar disease (Zhang *et al.* 2007) and pest damage (Pinnschmidt *et al.* 1995). By constructing a model of a system such as a growing plant or crop canopy, knowledge gaps are identified which enables research to progress more efficiently. Within education (Graves *et al.* 2002) they have also been shown to be a useful visual and practical aid.

Crop models therefore have a variety of applications within important areas not limited to agricultural research but also within economics, food security and climate change and conservation. This variety of use has produced a range of crop models which can be categorised into empirical and mechanistic. The main difference between these types of model are that mechanistic models describe the system it is simulating based on knowledge of the processes that are taking place, whereas an empirical model describes the system based directly on observation. It is important to note that all models are empirical at some level. The main issue of empirical models are that at the forecast level they cannot be extrapolated easily and are limited in use to conditions similar to those in which they were generated. Mechanistic models however do not have this limitation and can be extrapolated outside the boundaries from which they were generated (Chanter 1981).

There are also different types of mechanistic models, some which describe the canopy as a vertical layers of homogeneous vegetation and others that model the structure of the plants within the canopy (some of which are empirical). Detailed description and examples of such models are given in the next chapter (Chapter 2).

All crop models, mechanistic or empirical, require data which can be collected using field measurements or the trawling through of data files in the case of regional yield estimates. This thesis concentrates on the use of an alternative method of data collection, remote sensing, which is considered far more efficient (Pinter *et al.* 2003) than in-field measurements. The temporal and spatial frequency of remotely sensed data is high enough to enable data to be collected throughout the growing season of a crop and the problems which arise with cloud cover being overcome by using microwave data (Vescovi and Gomarasca 1998).

Remotely sensed data has been used within precision farming to create yield maps (Sehgal *et al.* 2005). These maps enable within season anomaly to be detected and resolved directly reducing input requirement and cost to the farmer and environment. The use of remote sensing is also used to predict yield at regional scales (DiBella *et al.* 2005), where remote sensing data is used as inputs into models which aid in policy making, such as CAP, food security and food pricing, and with real time estimates enable prior warning of low crop yield.

Extracting the relevant information from the remotely sensed data has in the past required empirical models. Empirical models, as mentioned, are limited in that they are applicable only under the conditions in which the data was collected (Lewis 2007). With the prediction of environmental change such models may therefore fall short of predicting anything meaningful. In response there has been a move to combining more mechanistic crop models with canopy reflectance models. Mechanistic models incorporate the current understanding of the processes involved within the system being modelled. This enables a greater understanding of the system and in forward mode ‘better’ prediction of its state. Canopy reflectance models predict the reflectance from a canopy. Coupling a crop model with a canopy reflectance model allows comparison between modelled and actual reflectance, across a range of potential crop model states (Moulin *et al.* 1998, Rickman and Klepper 1991) and enables the crop model to be updated throughout crop development and growth, increasing its accuracy at predicting the development of the crop (Lewis 2007).

There has been published research on this and the next chapter gives more detail on this work. In such cases, where the crop model has been mechanistic, the crop is modelled as vertical layers of homogeneous vegetation. The structure of the plants within the canopy is not included and the canopy is considered homogeneous. The remote sensing signal is sensitive to structural variation within the canopy and so crop models that simulate the structure of the crop are considered in this thesis to be more useful crop models. Functional-Structural crop models are the 'new' crop model, which model the structure of the plant as it grows using biological rules. ADEL-Maize (Fournier and Andrieu 1998) is one example of such a model. This model has been adapted to model wheat; ADEL-Wheat, and is used as the basis of this thesis (a description of which is given in Chapter 2). ADEL-Wheat is however classified as a structural model rather than a Functional-Structural model. It models the architecture of the wheat canopy but relies more on empirical rather than mechanistic relationships to describe the growth and development of the wheat. The coupling of a truly Functional-Structural model with a canopy reflectance model would require heavy parameterisation and computation time. Instead the approach here is to concentrate on the main influence on the reflectance from the canopy, the structure, and use sound semi-empirical relationships to 'grow' the wheat, which require less parameters. Currently ADEL-wheat is parameterised using data collected from only one genotype of winter wheat. To increase the applicability of the model, the parameterisation needs to be checked that it is appropriate for many genotypes of winter wheat, especially if it is to be used at the regional scale.

One aim of this work is to build a useful database of information on wheat growth and development. It is to hold information on many genotypes over one experimental period and information for two genotypes over two growing seasons. The database is to include phenological and architectural data which can help feed into continuing research with wheat growth and development. Apart from actual quantitative data on 10 genotypes over one growing season and 2 over two growing seasons, it also gives feedback on the drawbacks and advantages of certain measurement techniques which should aid in future experimental research. This database has already proven useful to other applications of crop research and has contributed to two published papers (Dornbusch *et al.* 2011, Dornbusch *et al.* 2010) and no other published work can be found that details such an extensive database of information from the same growing season on winter wheat genotypes.

The crop model that this thesis is focused on is ADEL-wheat which is considered to be a dynamic 3D model of winter wheat and as mentioned simulates explicitly the structure of the crop at the

plant level. There is no published work available on the coupling of a radiative transfer model with a 3D dynamic crop model in relation to wheat.This thesis aims to investigate the idea of this combination of models and illustrate its potential use within remote sensing studies to understand more about the how the structure of the canopy affects the radiometric signal.

Chapter 2 gives a review of the crop models currently developed as well as an overview of the methods used to couple such models with canopy reflectance models, making full use of remotely sensed data. A description of ADEL-wheat is given within this chapter and an overview of the suggested changes to be made within this thesis, highlighted. The Methodology chapter describes the methods used to collect the data required for the updating of ADEL-wheat over the two growing seasons that data was collected. The updating of ADEL-wheat has been split into two chapters, the first covering aspects of the model that simulate phenological properties of wheat and the second that simulate architectural properties of the wheat. Chapter 5 covers the models that describe the final organ dimensions, leaf appearance and tillering, and chapter 6 covers the models which describe 3D and 2D leaf shape. Suggested changes to the ADEL-wheat model are implemented into the model. Using radiometric data and canopy cover data collected during one experiment, these model outputs are compared with collected measurements and discussed. The final chapter concludes the findings within the thesis and gives an overview of future work to improve the modelling process further.

Chapter 2

Review

This chapter follows on from the introduction which justified the use of crop models and the coupling with remote sensing for efficient data collection, to give a review of existing crop models and how these models can utilise remote sensing data to improve their predictions. A review of the methods used to couple the models with remote sensing sensing data is given and the future of this area of agricultural research discussed.

A crop model is a mathematical representation of a canopy. Since such models may be constructed for a variety of purposes they may differ substantially in complexity, focus and scope. This has led to a range of models simulating particular crops or particular aspects of the processes involved in plant growth and development to be created. The simplest type of models are empirical in which no knowledge of underlying processes are involved. At the other end is purely mechanistic modelling which incorporate knowledge of the processes acting within the system and intermediate between these two are semi-empirical models. Mechanistic models have the advantage over empirical models that due to the process involved in the system being described they are more general and can aid in the increased understanding of the system, however they require more parameters and computationally are more expensive than empirical models.

Crop models may also be subdivided in terms of the basic units modelled. The most simple, model the canopy as a homogeneous medium with state variables representing spatial averages of interest such as biomass or LAI (Leaf Area Index) which is the one-sided leaf area per unit ground area. In recent times, advances in computing power have made possible the modelling of the canopy as a population of individually modelled plants, which in turn may be modelled as an ensemble of individual organs. In theory modelling at the organ/plant level should be more accurate and satisfying since many important processes such as assimilation occur at the level of the individual organ/plant, however such models tend to require heavy parameterisation and thus present their own particular problems.

The area of crop modelling covers numerous plants and trees of interest, from flowers (Fisher and Lieth 2000) to mainstream financial crops, maize (Jones 1985, Fournier and Andrieu 1999) and rice (Jame and Cutforth 1996, Pinnschmidt *et al.* 1995). Models also exist which concentrate on genetics of the plant growth and development and also root structure and development (Wang *et al.* 2004). Since the focus of this project is on winter wheat and remote sensing applications only a subset of the above models that have relevance to both (one or the other) of these areas is reviewed here.

2.1 Empirical Model and Semi-Empirical Models

The simplest crop-growth models are statistical relationships, or mathematical functions, such as polynomials, exponential functions, and sigmoidal curves representing the state of the canopy as a function of time (Marcelis *et al.* 1998). Where regression techniques are used to fit a model to observed data, the resulting model can be referred to as 'statistical'. Statistical models require extensive data collection, preferably throughout the growing season of the crop of interest and over many years. Regression or statistical models although useful are inherently limited in their application to the conditions and genotype from which the data was collected in order to create the models. However the predictive value of such descriptive models can be high, because they implicitly take into account all unknown affects as well (Marcelis *et al.* 1998). In summary empirical models are made up of statistical relationships usually between a variable of interest such as LAI or biomass and time. They have little heuristic value but can produce good predictions, especially when the environmental conditions for which the models are applied are within the range of variation upon which the model is parameterised. When empirical models are used outside such a range they may fail or may require substantial re-calibration. Their use is now reduced, although empirical elements in models are still common in many mechanistic models.

In order to increase the generality of these models and their ability to be applied in different locations they must encompass more knowledge of the processes involved. These models are known as semi-empirical models and an example of which is a dynamic empirical model. This is driven by temperature instead of time and is based on the observation that growth rate is constant within a limited range of temperature (Fournier *et al.* 2000). Equation 2.1 is a dynamic model expressing growth, if y is biomass, as a differential equation. The actual behaviour of the system is obtained through integration of the model.

$$dy/dt = f(x) \tag{2.1}$$

where
y = variable of system such as biomass
t = time variable
f = some function of y, t and other parameters

x= the system under examination, i.e a vector containing parameters describing the state of the canopy at time t.

Additional variables can also be included into the model to increase its generality, such as the model created by Waggoner (1984) which predicts wheat yield as a function of meteorological variables, such as temperature, precipitation and number of days warmer than $32\,^{\circ}\mathrm{C}$. Inclusion of these extra variables within the model aid in increasing its applicability as it can be more easily re-calibrated to areas other than those where the data was collected to create the model, however data is still required to be collected from the new sites in order to re-calibrate the model.

This top down approach has been adopted by Sinclair (1986), Muchow *et al.* (1990) and Hammer and Muchow (1991) to develop models of soybean, maize and sorghum growth respectively. It has also been used by Jensen (1968) and Stewart *et al.* (1977) to calculate decrease in yield in respect of water stress.

The advantages of such an approach is that it is often simple and quick and is most useful when a prediction of yield is required (Robertson and Foong 1977, Mall *et al.* 2004) or if an interpolation between various measured points i.e for analysing inter annual variability of regional production (Goetz *et al.* 2000). As mentioned in Chapter 1, regional estimates or prediction of crop yield is critical for many applications such as decision support systems, food security warning systems, food trading policy and carbon cycle research (Tao *et al.* 2005). Predicting yield is not the only application of empirical models, others include simulating the response of crop yield to fertiliser application (Reid 202) and simulating structure or development (Andrieu and Sinoquet 1993, Sinoquet *et al.* 1998).

Semi-empirical models aim to introduce some level of generality that purely empirical models lack by incorporating some understanding of the processes involved in the modelled system. In order to estimate growth (biomass accumulation) in any condition it is thought necessary that the model takes into account the process of energy absorption, conversion and allocation to dry mass. The Production Efficiency Model (PEM) (Monteith 1977) is an earlier example of a modular empirical model, than the Waggoner (1984) model. It has the option of re-calibration to new sites using data from remote sensing, which means that extensive field measurements are not needed.

The PEM was created after the observation by (Monteith 1977) that throughout a wide range of crops and environmental conditions, the ratio of absorbed light to carbon assimilation over the growing season is relatively constant. As carbon assimilation is related to biomass accumulation, crop growth can thereby be estimated from the amount of absorbed light. Using a satellite derived faction of absorbed photosynthetically available radiation as an input within the model. The model incorporates knowledge of the system by calculating dry matter production according to the amount of light received which is weighted according to the efficiency of radiation interception, photosynthesis and assimilation. This model can then be integrated during the growing season to give final biomass which is related to yield (Moulin *et al.* 1998). There are different versions of the PEM model (CASA, GLO-PEM, TURC, C-Fix, MOD17 and BEAMS for review of all models see McCallum *et al.* (2009)), sometimes referred to as diagnostic models, all developed to monitor primary production by taking advantage of available satellite data. It is important to note that the modern PEMs should not be confused with early experimental models based solely on correlation relationships between spectral vegetation indices and crop yield (Goetz *et al.* 2000). These models are now generally global and depend heavily on spatial and temporal resolution. They typically consider GPP and NPP (net primary productivity) separately and contain terms to describe plant respiration. Typically the PEMS require inputs of meteorological data such as radiation and temperature and the satellite-derived fraction of absorbed photosynthetically available radiation (FAPAR). In general all PEMs employ a similar basic methodology to calculated NPP involving two steps. The first calculates GPP (equation:2.2) and the second subtracts autotrophic respiration (equation:2.3). Variation among the different methods generally appears in the determination of LUE the use of scalars and autotrophic respiration. Time steps range from daily to yearly and spatial resolution from 1 km to 1°.

$$GPP = PAR * FAPAR * LUE * Scalars \tag{2.2}$$

$$NPP = GPP - Ra \tag{2.3}$$

GPP Gross Primary Productivity ($gCm^{-2}yr^{-1}$)
PAR Photosynthetically Active Radiation (MJm^{2})
FAPAR Fraction of Absorbed PAR (dimensionless percentage)
LUE Light Use Efficiency ($gCMJ^{-1}$)

Scalars Temperature (VPD) Vapour Pressure Deficit, etc (0-1)
NPP Net Primary Production (gCm^2)
Ra Autotrophic respiration (gCm^2)

The modular structure of the PEM has enabled it to be adapted by other researchers, in particular by Prince (1991) who included different 'stress' factors which enable the departure from maximum efficiency caused by physiological responses to limiting environmental conditions. Additional improvements have included making the light use efficiency a function of temperature, water and nutrient stress and by combining the model with satellite data (Carnegie-Ames-Stanford-Approach(CASA))(Potter *et al.* 1993, Field *et al.* 1995). The PEM is widely used to estimate terrestrial ecosystem net primary production (NPP), global carbon cycle, (Potter *et al.* 1993, Field *et al.* 1995, Lobell *et al.* 1982-1998) and crop production at regional scale (Lobell *et al.* 2003, Bastiaanssen and Ali 2003, Samarasinghe 2003) utilising satellite data.

The models mentioned so far are concerned with crop growth and have been applied within the agricultural industry to predict yield and within research to aid in the understanding of global carbon cycles, however their applicability within research at the level of crop science is limited as no real understanding of the biophysical processes are included and the models are essentially box models, whereby varying amounts of input are put into the model and an output generated without gaining much knowledge and understanding of the systems involved.

2.1.1 Crop Development and Structure

Crop Development

Empirical plant developmental models simulate the progress of phenological stages with time. They predict harvest date and date of important phenological stages important for agricultural management strategies, where certain inputs are required at different stages of plant development. Within this review they are considered as an important component within crop simulation models rather than as a stand alone model due to their reduced application within research and yield

prediction.

Crop Structure

Empirical models of crop structure require data on the plant's geometric features. The architecture of a plant plays a fundamental role in the acquisition and allocation of resources, tolerance to damage and competition (Bloomenthal 1985). Such models which incorporate the structure and geometry are useful tools for plant scientists and teachers in biology, agronomy, ecology, pest management (Hanan *et al.* 2003, Room and Prusinkiewicz 1996, Prusinkiewicz 1998, Godin and Sinoquet 2005) and remote sensing.

In order to discuss such models it is important to firstly understand the methods used to obtain 3D information and also the methods used to analyse the data and create the models.

There are two main ways of collecting 3D data, contact and non-contact. Contact methods capture individual data points whereas non-contact use an alternative approach using point-cloud measurements. In their simplest form, contact methods involve using a compass and ruler or articulated arms where rotation angles are recorded (Lang 1973) or a pocometer which consists of a tape measure to measure the distance and two protractors to measure the zenith and azimuth angle (Takenaka *et al.* 1998). More popular contact measures include FASTRAK magnetic 3D digitiser (Polhemus Colchester VT USA). This uses a magnetic signal receiver and pointer and enables the user to record the 3D spatial coordinates of the pointer within a hemisphere of 3m diameter from the receiver. Individual plants are digitally reconstructed by recording a series of point co-ordinates and the relevant connectivity between the points. Disadvantages are that due to it creating a magnetic field, it can be used outside but in a greenhouse the frames can disturb measurements. The error in measuring spatial coordinates with the Fastrak-polhemus apparatus was reported to be within 1mm in the laboratory (Moulia and Sinoquet 1993) and about 1cm in the field (Thanisawanyangkura *et al.* 1997) for medium-size leaves.

The sonic digitiser GTCO Freepoint 3D consists of a hand-held probe with 2 or more sonic emitters and a triangular detector array with 3 microphones. It is necessary to calibrate for difference in temperature and humidity in the air and is more adapted for greenhouse experiments since they are sensitive to wind.

A large advantage of contact points is that the points can be annotated but the disadvantage is that it disturbs the structure of which analysis and data recording is being made.

Volumetric intersection is where the 3D scene is reconstructed by capturing the silhouette of an object against a monochrome background, which is disregarded during analysis by chroma-keying. This has been used by De Viser *et al.* (2003) with chrysanthemum plants. This requires the plant to be turned on a table and a silhouette created at different angles of view. Problems occur if there is too much occlusion and if the stems are too thin. The movement of the plant increases error, however reverse intersection (an alternative approach) can reduce such errors. Once the 3D scene is obtained, points can be taken from the image. Stereo Vision is an alternative method which uses two camera's set at a fixed distance from a scene from which 3D position on the real word can be computed. It has been used by Ivanov *et al.* (1995), where a canopy of maize plants was reconstructed. This method has been associated with high errors, new software has led to less manual input. Structured light, another alternative, but which is not suitable for complex planes, uses spacial light which is projected on the object and from transformation of the grid depth estimated. These methods require the plants to be removed from the field or for the clearance of neighbouring plants within the field.

Recently laser profile scanners, such as the Polhemus FastSCAN have meant that 3D plant data can be captured holistically and without contact with the canopy. The data acquired from the laser surface scanners is in unordered point cloud form, with points collected only on the surface of the object under study. A magnetic field is generated by which the position of the wand is determined at any time. Pressing the trigger causes a scan line of red laser light to be emitted. When the scan line is swept over the object, intersections of the laser line with the surface of the object (the profiles) are captured by video cameras mounted at an angle to the laser line generator on the wand and processed into data points by joining sweeps. It is a non contact method and therefore has an advantage over contact devices which encounter measurement error if the object is displaced during measurement and leads to smaller data sets than non-contact methods since every single data point needs to be selected by the operator. A disadvantage is that since a green surface will absorb light of any colour but green and laser light is relatively pure in colour not enough of a red laser beam may be reflected from the object and received by the scanner camera's to calculate positions of data points. Options include changing the laser to green rather than red, which is expensive or using fine chalk and water sprayed over the plant and left to dry. The affect this chalk may have on the plant's further growth and development has not be investigated.

Recently image based, automated, non-invasive, and non-destructive high-throughput plant phenotyping platforms have started to be used to collect this data (Paproki *et al.* 2012). These platforms acquire and record large amounts of raw data which can be processed in two ways; 2D image processing and 3D mesh processing algorithms, see Paproki *et al.* (2012) for an introduction into a novel mesh processing based technique for 3D plant analysis.

Various methods are also used to process such data to obtain mathematical descriptions required by growth models (Sinoquet and Bonhomme 1992, Drouet and Pages 2003, Evers *et al.* 2005, Dornbusch *et al.* 2007, Dauzat *et al.* 2008, Zheng *et al.* 2008). The two main methods of analysing this extensive field data in order to simulate crop structure are; reconstruction and curve fitting.

- Reconstruction can be thought of as the simplest empirical crop structure model. Such an approach requires large amount of data in order to represent features of a single plant and cannot be manipulated to simulate other species or used for predictive purposes (Prusinkiewicz 1998).
- Curve fitting uses statistical methods to obtain a best fit model to measurements taken in the field. Stochastic and deterministic models can be created (Prusinkiewicz 1998).

These structural representations lead to models which are static. However a series of such models throughout the development of the plant can give a dynamic ‘picture’ of structural development throughout a growing season. This method is resource intensive, however it does enable actual plants rather than a stochastic instance generated from a model to be used in simulations.

This feature is important with regard to light interception because the actual distribution of foliage in space may be quite different from that described by theoretical models whereby the distribution of leaves is based on simple rules of phyllotaxy. Such models have been used by Andrieu and Sinoquet (1993) to derive gap fractions by image analysis and also by Sinoquet *et al.* (1998) to compute attributes of light interception. Limitations of such models are that although very effective when light is assumed to be in one direction, in conditions of diffuse light the models are unable to simulate the system as well, which is a problem if used to derive canopy reflectance data .

Empirical models of crop structure and development, although limited, have been of use to crop research scientists and in particular to those that wish to understand more about light attenuation within the canopy and also reflectance patterns for remote sensing studies.

Beyond the instantaneous description of canopy structure, dynamic structural models have also been proposed. They enable the structure to grow using a minimum set of rules or empirical relationships between various structural properties which aim to reproduce observed plant forms at different stages of growth. Examples of the relationships the models take advantage of are those between leaf length and leaf width, leaf length and relative leaf insertion height (Espana *et al.* 1999). As an alternative to these empirical relations a set of rules can instead be given and used to 'grow' the plant structure for which L-systems have been utilised. A description of L-systems is given towards the end of this review, however for a detailed review see (Prusinkiewicz 1998) and references within.

In summary, the predictive value of empirical models can be high, because they implicitly take into account all unknown affects (Marcelis *et al.* 1998). They also have a short computing time and usually contain few state variables and relatively easy to estimate model parameters (Moulin *et al.* 1998). However, empirical models require data to be collected at several intervals and preferably during a number of growing seasons in order to be created. Not only is this process resource extensive, but the resulting model is applicable only for the conditions under which the data was collected, which makes them inherently limited due to their lack of generality and being difficult to scale and inability to be extrapolated. Poluektov and Topaj (2001) commented that 'Any attempt to extend the scope of an empirical model beyond the events or conditions for which it was developed and tested is not simulation but speculation. Therefore the empirical approach cannot be used with confidence as a method of scientific speculation'. However, the semi-empirical approach has been found to be extremely useful and accurate and so have their uses, however within scientific research limited understanding can be gained from such models.

2.2 Mechanistic Models

Mechanistic models overcome the main drawbacks of empirical models, as they simulate the processes governing canopy growth and development with an understanding of underlying physical,

physiological and biochemical processes. The description of all of these processes and especially their integration within a model at the same level of accuracy, is an extremely difficult problem with some phenomena, particularly of the biological nature, not having yet been studied in sufficient detail to enable such a level of integration to occur. Instead a mechanistic model which, for example, aims to predict yield will be mechanistic only down to organ level processes, such as photosynthesis, where the model will become empirical. Empirical relationships are also used where knowledge gaps may be present (Dourado-Neto *et al.* 1998). For these reasons as well as the requirement of the developers to be skilled specialists in various branches of science, the development of mechanistic models is regarded to be difficult and is why there is still no complex agroecosystem model that is truly mechanistic (Poluektov and Topaj 2001).

2.2.1 Non-Architectural Models

Mechanistic crop models are generally driven by photosynthesis. The rate of photosynthesis depends on the amount of light intercepted and the efficiency of this light to be absorbed and converted to photosynthate. Leaf area is therefore an important consideration as it directly affects the amount of light absorbed and as such photosynthesis and growth. The proportion of photosynthate distributed to certain organs such a leaves, stems, roots and grain is dependent on phenological stage. Therefore prediction of phenological stage is also of importance. Progression of phenological stage of winter wheat is dependent on vernalisation, temperature and photoperiod, which also therefore have to be considered within the model. Potential growth is predicted usually over a time step of one day with limiting factors, such as temperature, nitrogen and water availability etc causing the expected response within the processes of crop growth.

Model Structure

In general mechanistic crop models have two components in which the important processes, mentioned, are described. These are plant and soil. Both of these components have further sub modules each of which deal with specific mechanisms. The sub modules of the plant module consider phenology (developmental stages), organ growth, and yield formation and the sub modules of the soil component consider root growth, water balance, nitrogen balance and soil transfers.

Most mechanistic crop models require the same inputs which include genetic information about the cultivar reaction to certain conditions. Management such as sowing depth and density and environmental factors such as temperature and solar radiation. The outputs are usually yield quality and quantity. The output is the quantification of above ground biomass usually in terms of quality and quantity of yield. There are various mechanistic crop models that simulate winter wheat growth, such as AFRCWheat (Weir *et al.* 1984, Porter 1993), CERES-Wheat (Ritchie and Otter 1984), SIRIUS (Jamieson *et al.* 1998b), SUCROS (Spitters *et al.* 1989) and STICS (Brisson *et al.* 2003a). They have each been built for specific purposes and therefore differ in their calculation of various plant growth and development processes, however the structure of these models is similar to the one described (Brisson *et al.* 2003b).

SIRIUS which is the simplest of AFRCWHEAT, CERES-wheat and SUCROS calculates grain yield and quality and nitrogen leaching and water and nitrogen uptake and assumes the canopy is a single entity, producing biomass as a product of light and RUE (radiation use efficiency). No calculation of yield components is included. By dealing with leaf layers it avoids the need to consider tillers and reduces the parameters required for calibration. Biomass accumulation is calculated from intercepted PAR (photosynthetic active radiation) and grain growth from simple partitioning rules. LAI is developed from a simple thermal time sub model. STICS was primarily designed to investigate agronomic and environmental impacts such as leaching at regional scale and is similar to SIRIUS in that it does not separate simulated ground biomass into organs and biomass accumulation is a product of intercepted light and RUE. SUCROS (Simple and Universal Crop growth Simulator) simulates growth (rate of dry matter accumulation) based on CO_2 assimilation (photosynthesis) of the canopy which is a function of incoming radiation and light. The rate of dry matter accumulation is a function of irradiation, temperature, crop characteristics and water supply. After subtraction of maintenance respiration, growth of leaf stem, root and storage organs are simulated. Biomass partitioning depends on crop development stage, which is computed as a function of temperature only. Different crops can be simulated by altering specific input parameters. Influence on respiration can also be included by alerting environmental conditions such as temperature.

CERES-wheat and AFRCWHEAT consider the separation of biomass accumulation into separate organs within the canopy. They both simulate the process of crop growth and development by including the timing of phenological events during the life cycle of the crop and development of canopy and the interception of PAR and its use to fix carbon which is then converted to dry

matter. They both include an algorithm to reduce potential production via strategies of water and nitrogen (effects of other nutrients such as potassium and phosphorus and effects of weeds and pests are not considered although can be 'added' to the model). Both models assume a linear relationship between rate of crop development and temperature. AFRCWHEAT includes the partitioning of photosynthesis, growth of leaf and stems, senescence biomass accumulation and root system dynamics and uses temperature to regulate growth. This model has been used to investigate effects of climate change at national scale and uses GIS technology. CERES-wheat has been applied at regional scale to estimate yield and forecasting and analysis of policy questions related to crop production and resource conservation and at the farm level for decision making and for multi year analysis for risk assessment. Its primary purpose was to predict alternative management strategies and tactics that affect yield at intermediate steps. It does this by simulation crop yield and focus on 3 import stages of growth, duration, rate and extent and the stress influence on such process(in terms of water and Nitrogen). These are beyond its initial goal which was to predict leaf number and sizes and quantify genetic and climate interactions.

Harnos and Kovacs (1999) compared CERES-Wheat, AFRCWHEAT2, CROPSIM and SUCROS2 in order to select an appropriate model for climate change studies and found that although CERES-Wheat and AFRCWHEAT2 fitted the best with the historical data, used within the study, that all models showed different sensitivity to environmental parameters, creating different simulated yields for the climate scenarios. From these results no decision was made on the most applicable model for this purpose and instead the inaccuracies associated with using these models, for such an application, were instead just highlighted. More worryingly when Jamieson *et al.* (1998a) compared CERES-wheat, AFRCWHEAT2 and SIRIUS using observed UK grain yields from well managed agricultural experiments, none of the models were found to accurately predict yield and substantial disagreement was found between the models' predictions of both yield and yield loss due to water limitation. This disagreement between the models predictions was concluded to highlight the differences in the underlying hypothesis in the models. These comparisons highlight the fact that some models simulate different aspects of plant growth and development to differing degrees of accuracy and that the models although mechanistic should be used out of their 'experimental scope' with caution. In this study the ADEL-wheat model is used with the main aim to parameterise the model structure for predicting the EO signal, rather than predicting yield directly, and so these weaknesses common with such models are not so important in the first instance. However, the improvement of the response of crop-growth models to environmental drivers is clearly an active area of research.

In general the models mentioned are constructed using mechanistic models at the level of organ growth, however as discussed when first introducing mechanistic models, empirical relationships are used, to describe certain relationships. For example the PAR extinction canopy coefficient in AFRCWHEAT2 is set as 0.44 and in CERES to be 0.85. This coefficient affects the rate of dry matter accumulation and as such the allocation of daily assimilates to leaves. The use of inaccurate coefficients within a relation affecting canopy development such as this, may possibly, lead to errors on the estimation of biomass production (Porter 1993).

It has been suggested that main parameters driving crop growth could be replaced or updated by estimations derived from remote sensing within the growing season (Moulin *et al.* 1998). The methods and models used for this coupling is discussed in section 2.3.

A recent advance in mechanistic crop models is to consider the architecture of the canopy resulting in architectural which consider crop growth using empirical and mechanistic models. Such models are refereed to as Functional-Structural models.

2.2.2 Functional-Structural Models (Architectural models)

FSPM are particularly suited to analyse problems in which spatial structure of the system is an essential factor contributing to the explanation of the behaviour of the system of the study. Examples include intra-specific and interspecifc competition phenomena, analyses of mechanisms of physiological response to environmental signal that affect allocation of carbon and nitrogen in the plant and exploration of alternative manipulation plant architecture on production of fruits or flowers. Functional-Structural models simulate a canopy as a selection of individual plants rather than a homogeneous canopy in which horizontal heterogeneity and plant to plant variability is neglected. Important considerations within FSPM, are the development and geometry of organs, carbon production and assimilation at the scale of the organs. The micro-climate and development of organs can be considered new modules added to a non-architectural model. The addition of a micro-climate model enables the micro-climate of developing organs to be simulated. This is important as light quantity at certain organs affects carbon availability and photosynthesis and therefore growth.

ADEL-maize (Fournier and Andrieu 1998) is one relevant example of a Functional-Structural

models which take into account the micro-climate of the organs. Other examples do exist such as LIGNUM (Perttunen *et al.* 1998, Perttunen *et al.* 1996), Cotons (Jallas *et al.* 2000) which was derived from Gossyn (McKinion *et al.* 1989, Watkins *et al.* 1998), AMAPHydro (de Reffye *et al.* 1988), GRoGra (Kurth *et al.* 1994), ADEL-Wheat (Fournier *et al.* 2003) and ADEL-maize (Fournier and Andrieu 1998)).

FSPM usually use L-systems to represent plant structure, a brief description is given below however for a more detailed description see (Prusinkiewicz 1998).

L-systems

L-systems are a language which use a collection of symbols which when set into a sequence are referred to as a string. There are two main parts to an L-system, the axiom and the set of production rules. The axiom is the starting point on which the production rules are applied. When production rules are applied more strings are produced, the rules can then be applied to these new strings.

The advantage of using L-systems to simulate plant development is that they provide a modular approach to the modelling problem which enables plants and canopies to be described as a collection of modules and the connections between these modules to be described (topology). Each module, in the case of winter wheat, can be considered to be a phytomer, which consists of a lamina (leaf and sheath), internode and apical bud, where at each successive step (growth) a new module is formed.

L-systems can be open or closed. Closed L-systems consider the structure and its development as always being the same over sequential steps, however in open L-systems the development of the structure between successive steps can be made dependent on external forces acting on each module or the plant as a whole. The initial plant module is referred to as the axiom. At each step production rules are applied, initially to the axiom, giving rise to a new structure, to which the production rules are then applied and this is repeated as necessary.

In closed L-systems production rules contain an, only when, statement, so that for instance in the case above, the bud may produce a new module only when three modules are already present. In

reality this relates to tiller production, which in winter wheat generally occurs after three leaves or more have been produced on the main stem. The geometric parameters such as length and width or diameter of organs and branching angles are also subject to the production rules, all of which result in a realistic 3D structural representation of a crop. Probabilities can also be given to each production rule, for example the death of a tiller may only occur 90% of the instances it is applied. This gives rise to non-identical plants and allows for statistically observed differences in the growth and development to be incorporated in the simulated canopy.

Simple development models belong to the simplest L-systems, known as context free. This is where a production rule can be applied to a module irrespective of its adjacent modules. In more complex models, context sensitive L-systems are used, in which the applicability or outcome of a production rule depends not only on the module being replaced, but also on its neighbours and the external environment (Prusinkiewicz 1998). This is a key feature of L-systems for functional-structural crop models which enables the simulation of information between plant modules (endogenic) and also between plant modules and their micro-climate, such as light intensity or water availability.

Mechanistic models of crop growth and development are superior to empirical models in that they are more general, more applicable, and have the ability to increase the understanding and knowledge of the canopy system. The downfall is that they require more parameters which increases computation time dramatically compared to that of empirical models. Non-architectural models have however shown poor predictability in comparison studies. The new Structural-Functional models are the improved mechanistic crop models, and are consequently a more powerful tool. They enable light attenuation to be simulated throughout the crop, an important resource to the plant which directly affects photosynthesis, as well as competition and spread of foliar diseases. Comparison or validation of architectural models has not been as wide spread as non-architectural crop models however the combination with remote sensing data has found them to be a valuable resource.

2.3 Crop Models and the Role of Remote Sensing

Remote sensing enables such extensive spatial and temporal data to be collected with minimal to no field work. Techniques to estimate vegetation characteristics from reflective optical measurements have either been based on the empirical-statistical approach that relates surface measurements of canopy variables to single spectral reflectances or vegetation indices (VI), or on the inversion of a physically based canopy reflectance (CR) model (Houborg *et al.* 2009). A description of both vegetation indices and CR models is given below highlighting their advantages and disadvantages.

Vegetation Indices

Vegetation indices are empirical models used within agriculture to extract biophysical properties such as LAI (leaf area index, the ratio of green leaf area per area of ground) and biomass from remotely sensed images (from optical sensors) which in turn can be related to yield. The indices are based on the observation that red light is strongly absorbed by photosynthetic pigments (e.g. chlorophyll) found within living plants, while near-infrared light either passes through or is reflected. As such, on a satellite image, areas covered with green vegetation will be very bright in the near-infrared, due to higher reflectance and very dark in the red part of the spectrum due to higher absorption. Vegetation indices use a ratio of the reflected NIR and reflected RED wavebands in various ways to obtain a value which is representative to the amount of vegetation present. The most popular index is the NDVI (eqn:2.4), normalized difference vegetation index, which calculates the difference in reflectance divided by the sum of the reflectance in both wavebands. The value of NDVI can range from -1 to 1. A surface with a low contrast between the NIR and R channels will have an NDVI value closer to 0, while surfaces of high contrast, particularly green vegetetation, will have NDVI values much closer to 1.

$$NDVI = \rho(NIR) - \rho(RED)/(\rho(NIR) + \rho(RED)) \tag{2.4}$$

where:
ρ(NIR) = Reflectance in the Near Infra Red
ρ(RED) = Reflectance in the Red reflected
In order to relate NDVI to parameters of interest, such as LAI, an empirical model can be cre-

ated by comparing actual measurements of LAI and observed measurements of NDVI from one or more sites over a number of growing seasons. By analysing the relationship found between NDVI and the parameter of interest a simple empirical model can be created. This method is suggested to be a useful, cheap and real-time method for crop monitoring. (A similar method is carried out to obtain the relationship of back scatter to parameters of interest). In summary the potential of VIs for the determination of crop parameters have been demonstrated in numerous studies (Broge and Leblanc 2001, Colombo *et al.* 2003, Gitelson *et al.* 2005, Tucker 1979)and the simplicity and computational efficiency of the approach makes it highly desirable for large-scale remote sensing applications. However, a fundamental problem with the VI approach for estimating biophysical variables is its lack of generality. Since canopy reflectance depends on a complex interaction of several internal and external factors (Baret and Guyot 1991) that may vary significantly in time and space and from one crop type to another, no universal relationship between a single canopy variable and a spectral signature can be expected to exist. Consequently, spectral reflectance relationships will be site, time and crop specific, making the use of a single relationship for an entire region unfeasible (Baret and Guyot 1991, Colombo *et al.* 2003).

Physically Based Models

Physically-based models have proven to be a promising alternative as they describe the transfer and interaction of radiation inside the canopy based on physical laws and thus provide an explicit connection between the biophysical variables and the canopy reflectance (Houborg *et al.* 2009). Coupling these physical models of canopy reflectance with crop models allows the crop model to inform the canopy model which can be used to obtain parameters of interest from remote sensing data. The two main methods of coupling the models are described below which are: (see review by (Moulin *et al.* 1998) for more detail)

- Inversion of canopy reflectance model to estimate canopy variables of interest, which are then forced or used to recalibrate parameters of the crop model using optimisation techniques.
- Coupling of the crop model and canopy reflectance model, enabling the whole process from canopy functioning to radiometric data to be simulated. The parameters of the cou-

pled models are re-calibrated to find the best agreement between observed and simulated remote sensed data. (Prévot *et al.* 2003).

The first method can simply involve using the estimated model parameter inverted from satellite images directly within the model, removing the need for the state variable to be modelled altogether or if it is still calculated within the model to update it. The main drawback of such an approach is that data (if used to run the model) is required at the same time step of the model, which is usually daily. Problems arise due to cloud cover and low temporal frequency of satellite images which reduces the sampling frequency of this required data. Interpolation of the state variable over time can be used to overcome this problem, which was a technique used by Delecolle and Guerif (1988) who used high spatial resolution satellite data over a wheat field to improve predictions of ARCWHEAT to predict a yield estimation with a reduced mean error (Moulin *et al.* 1998).

In such cases where the variable is calculated by the model, and the data from satellite images is used to update the model, optimisation techniques are used to obtain the most appropriate value of the parameter by comparing actual and modelled values. Instead of altering the actual state variable, the model can alternatively be re-initialised, whereby the initial conditions of the model are altered to enable the observed and modelled state of the crop to match (Maas 1988, Maas 1991).

The second method, the assimilation strategy, combines a crop model and a model of canopy reflectance which using inversion strategies enables the direct use of radiometric information to re-parameterise the crop model. Advantages of this method are that the predictions are continuous and not reliable on discontinuous data from remote sensing and that it permits a better integration of both spectral and radar domains which is of great interest when the cloud cover limits the number of optical images (Prévot *et al.* 2003).

There are many different types of radiative transfer or canopy reflectance models which can be categorised into turbid medium, geometric-pptical, radiosity and ray tracing models, of which further description is to be given. These models work in different ways but share the same aim to predict reflectance for a given canopy type. They use data regarding the canopy as estimated from the crop model to predict the reflectance from the canopy. Inversion of these models must however be carried out if information about the canopy is to be extracted from remote sensing

images to be used within the crop models.

The method of inversion used depends on the complexity of the model to be inverted. Very simple problems can use analytical methods but cannot be used for non-linear model inversion. Maximum-likelihood and least-square methods can be used for more complex models with larger parameter sets, however they are computationally expensive (Jacquemoud *et al.* 2000, Jacquemoud *et al.* 1995). The most widely used inversion methods for the problem of highly complex models are LUT (Look Up Tables) (Combal 2002, Knyazikhin *et al.* 1998a, Knyazikhin *et al.* 1998b, Weiss *et al.* 200) and ANN (Artificial Neural Networks)(Bacour *et al.* 2006, Fang and Liang 2005)

LUT inversion requires a canopy model and canopy reflectance model to be run for various scenarios of canopy development and structural and radiometric properties, spanning the possible range of parameter space it is thought likely will be experienced in practice. The outputs of these forward model runs are stored in a table, indexed by the various driving parameter values. Inversion is then simply a process of finding the parameter set in the table which minimises the difference between observed and the LUT-modelled reflectance values. This enables a matching process to be carried out when remote sensing data is acquired. This method assumes that the behaviour of the canopy surface reflectance as observed from satellite images is unique to a specific canopy structure.

ANN are software tools that mimic the way the way in which information is processed in the brain through a network of interconnected neurons (Rumulhart *et al.* 1986) they work by learning relationships between a set of input variables and output variables, the most commonly used in Remote Sensing being the MLP, the multilayer perceptron. Baret and Buis (2008) review and compare approaches for inverting CR models to estimate biophysical properties including, iterative numerical optimisation, LUT and ANN. They concluded that ANNs are computational fast, can incorporate a priori knowledge of canopy and environmental variables and that they can be tuned to estimate one or more canopy biophysical variables of interest.

Look up table and neural network approaches both require a training database consisting of canopy reflectance spectra together with the corresponding biophysical variables, and their performances rely on the training database and the training process itself. Ideally, these approaches should be learnt on experimental data which is not readily available for most places on the globe.

The advantages of LUTs however are that the forward and inversion process is separated and as such the inversion is quite rapid and also that as developments and improvements are made to the underlying CR model the LUT table can be recomputed and updated accordingly. Overall the choice of inversion is largely dependent on type of canopy reflectance model used.

The iterative optimisation approach facilitates a direct retrieval of biophysical parameters from observed reflectance without the prior use of calibration or training data of any kind. However, this method suffers from its expensive computational requirement (Jacquemoud *et al.* 2000) making the retrieval of biophysical variables unfeasible for large geographic areas. A limitation shared by all of the physically based models is the ill-posed nature of model inversion (Atzberger 2004, Combal 2002); the fact that different combinations of canopy parameters may correspond to almost identical spectra. This makes the choice of the initial parameter values important, and some regularisation of the inverse problem may be required implying the use of a priori knowledge or information on the spatial or temporal variability of key canopy parameters to constrain the inversion process (Atzberger 2004, Combal 2002) The crop-specific sensitivity of spectral reflectance relationships to canopy geometry (e.g. leaf angle distribution and clumping) and leaf properties (e.g. dry matter and mesophyll structure) and the site-specific sensitivity to atmospheric and background influences must be properly accounted for in order to apply spectral reflectance relationships for the mapping of LAI and Cab (leaf chlorophyll a and b content)

An important aspect of having an explicity defined 3D description of plant architecture within a canopy is that it can be used to reduce effectively the parameter space in the inversion algorithm. In effect by using a 3D representation of a particular plant or set of plants) we are defining constraints on inversion, further, if the 3D model is dynamic in a way that can be related to the time interval between sets of remote-sensing observations, then time development can be used as a further constraint (Lewis 2007).

Although the computational cost is higher than using simpler analytical models, the advantages are that structural influences can be explicitly investigated and that the derivation of models is no longer reliant on making assumptions purely for mathematical convenience.

Both FSPM and empirical structural plant models provide realistic images of structural representation for part vegetation canopies. These can be used effectively to restrict biophysical parameter spaces to feasible ranges of conditions and inherent dependencies between canopy

structural variables. They also have the great potential for integrating optical and microwave remote sensing data as they can provide a common structure basis for modelling both regions of e, spectrum.

2.3.1 Canopy Reflectance Models

Danson *et al.* (2003) summarised that canopy reflectance models are a key tool in investigating the factors that control vegetation canopy reflectance due to their ability to simulate a wide range of canopy structures, leaf optical properties and measurement conditions. A variety of canopy reflectance models exist all of which attempt to describe the scattering and absorption mechanisms in vegetation canopies using the radiative transfer theory and differ mainly in the way that the canopy structure is described (Espana *et al.* 1999). As Baret and Buis (2008) state 'a compromise should be found between the realism of the description of the canopy structure, and its complexity'. This is due to the observations that a more realistic description of canopy architecture requires a greater number of input variables and will be computationally more demanding yet will not necessarily improve the performance of the model.

Turbid Medium Model

Turbid medium canopy reflectance models assume the canopy to be a layer or layers of homogenised scattering medium, each consisting of randomly oriented and scattering leaves. They simulate the reflectance from the canopy by considering the law of conservation of energy between each layer and using data that can be acquired using crop models. In the case of horizontally heterogeneous or discontinuous canopies such as row of crops, or chards with isolated tree crowns, the turbid medium analogy is not considered applicable because foliage enclosures are not finite (Kimes and Kirchner 1982, Kimes 1968). The SAIL model (Verhoef 1984) is based on the turbid medium concept, where the vegetation canopy is considered as a homogeneous layer characterised by leaf area index, leaf angle distribution, soil reflectance, diffuse skylight and illumination and viewing angle. In an extended version by Andrieu *et al.* (1997) the specular reflectance and transmittance of the leaves was included.

SIRASCA (Sinoquet *et al.* 1990) is another turbid medium model which aims to compute light partitioning in mixed canopies. It is assumed to provide accurate estimates of light interception and has been validated on a large range of canopies and also against other models (Sinoquet *et al.* 2000). This model computes light interception in multispecies canopies from its LAI and mean leaf inclination angle. SIRASCA was set within a paper by Barillot *et al.* (2011) to gradually account for vertical heterogeneity of the foliage i.e canopy described as one, two or ten horizontal layes of leaves. The conclusion of the study being that the turbid medium analogy could infact be successfully used in a wide range of canopies. However, a more detailed description of the canopy is required for mixtures exhibiting vertical stratification and inter or intra species foliage overlapping and therefore architectural models remain a relevant tool for studying light partitioning in inter cropping systems that exhibit strong vertical heterogeneity.

Geometrical Models

These models describe the vegetation canopy as a collection of geometrical objects for which the surface properties are known. Scattering within the objects is calculated using beers law or some other model of attenuation. These models take into account shadowing within the canopy. Their application is most frequent within the modelling of trees (Li and Strahler 1985) and no work could be found in relation to modelling winter wheat canopies.

Hybrid Models

These are semi-empirical models that combine the benefits of geometrical models, which include their inherent ability to describe the discrete nature of discontinuous canopy with a Radiative Transfer approach to the scattering within the objects.

Radiosity Models

The radiosity approach takes into account detailed canopy structure, but divides the canopy into small elementary plane surfaces or ‘patches’ each with an associated emissivity and reflectiv-

ity. The idea is that each patch exchanges radiation with all others. This approach enables the shadowing of leaves to be taken into account and also the amount of radiation received that has come from other leaves. This method is computationally fast although a downside is that is assumes lambertian surfaces. Specular surfaces have however been included in this type of model but result in high computation (Rushmeier and Torrence 1990). DIANA (Goel *et al.* 1991) is a radiosity based model which has been shown to demonstrate good accordance of analytical CR models in the case of a random canopy.

Ray Tracing

Ray tracing models are developed from computer graphics techniques and are based on the concept of tracing photon paths through a scene, defined by a detailed 3D description of canopy architecture, either from source to observer (forward ray tracing) or from the observer to source (reverse ray tracing). The radiometric properties of the objects in the scene determine whether the photons are absorbed or scattered at each intersection, The total scene scattering is determined by summing many such photon paths, usually via Monte Carlo sampling. Disney *et al.* (2000) review the various options for MC ray tracing in canopy applications. These models also use detailed architecture of the canopy structure and calculate the intersections of rays fired into the 3D scene. The objects within the scene determine whether the photons are absorbed or scattered at each intersection. This method can use realistic images or static empirical models of the canopy. Large computational times are associated with this model especially when diffuse scattering is simulated (Govaerts *et al.* 1996).

SAIL (Verhoef 1984, Verhoef 1985) is the most widely used turbid medium model and has been combined with non mechanistic crop models (and PROSPECT) to increase the accuracy of the model by using remote sensing data. Barnes *et al.* (2001) combined AFRCWheat and SAIL and found that only by updating the model later on in development with the use of remote sensing data that LAI prediction was improved. This is not of great value for farmers as at this late stage in development no methods exist to aid in increasing the yield if it predicted to be reduced. However, it can help to produce a more accurate yield map which is of use in precision farming.

Combination of crop models with both microwave and optical canopy models has also been carried using the STICS crop models, and the CLOUD and SAIL reflectance models (Prévot

et al. 2003). It was concluded that the introduction of optical data lead to a clear improvement in the prediction of LAI and above ground biomass but that the inclusion of RADAR data had little impact on the improvement of prediction. However it was concluded that this may have been because of the high quality and quantity of optical data available and as such suggested that the inclusion of both data sets is possible and that when cloud cover does not permit optical data collection, then inclusion of RADAR is of interest.

Overall the inclusion of remote sensing data with crop models has been shown to improve the accuracy of predictions, if only the yield. These examples given however use non-architectural models and turbid medium canopy reflectance models. The combination of architectural models and ray tracing canopy reflectance models does, although maybe computationally more extensive, seem the way forward.

2.4 Discussion and Future Progression

As illustrated, there are a vast array of crop models available including a significant number specific to winter wheat, many of which consider the canopy to be one or more homogeneous layers of vegetation. In the case of intensive farming, this situation is not rare, due to the high inputs used during the growing season. However as mentioned in chapter 1, the environmental and financial impact of such farming practises is considerable and that in the future more sustainable practises should instead be considered. If this is indeed the future of farming as suggested, then models that can cope with heterogeneity are required. Structural-functional models are as such, incredibly important. As a consequence of considering the 3D structure of the crop, plants competition, foliar disease and many other important factors within crop science can also be investigated, simulated and predicted requiring less resource expensive field trials.

One main consequence of incorporating structural development using biological rules into a crop model is the ability to couple the model with remote sensing data using Ray Tracing canopy reflectance models. This is a powerful model that uses less approximations in the calculation of the canopy reflectance compared to other methods mentioned due to the structure of the canopy being described explicitly.

The coupling of a structural-functional model and ray tracing canopy reflectance models in both the optical and microwave is an important and powerful tool within agriculture and especially within the UK. It enables crops growth and development to be simulated throughout the growing season with regular updates from both optical and microwave data regardless of the weather conditions.

ADEL-wheat, a functional-structural model of wheat and DRAT a ray tracing canopy reflectance model and PROSPECT a leaf reflectance model are combined, within this PhD, to create a powerful and useful tool for the prediction of canopy characteristics. The models combined have been introduced and an overview of the alternatives given. It is thought however that these models, and their combination not only give a greater understanding of the system but also a more accurate prediction of the state of the crop throughout development. A description of each model is given in the following chapter 3

The phenology chapter looks at the trend in final organ length over phytomer rank for various genotypes of winter wheat and for two genotypes over two environmental conditions. This is a purely empirical relationship implemented within ADEL wheat. The final number of leaves on all stems is investigated over the different genotypes. Investigation into any linkages between the pattern over different organ types. It is also discussed in this chapter the idea of modelling tillers are delayed main stems, which enables tillers to be included within the model with a simple parameter describing the delay in phytomer number. In addition, leaf appearance rate is compared between genotypes and also to confirm the idea of tillers being delayed main stems.

The Architecture chapter looks at 3D leaf shape, which is the midrib curvature and phyllotaxy of two different genotypes and 2D leaf shape for various genotypes and ranks of leaves. Observations are implemented into the ADEL model and it is parameterised according to two genotypes and compared against radiometric observations.

Chapter 3

ADEL

3.1 Overview of ADEL-wheat

In the previous chapter emphasis is placed on the advantages of Functional-Structural models compared to non-architectural models. Discussion is also given on canopy reflectance models, favouring Ray Tracing models for this highly complex system. Within this chapter the crop model ADEL-wheat is described.

ADEL-wheat is a 3D dynamic model of the above ground growth and development of wheat, from emergence to heading, based on thermal time steps. It was produced as part of an ESA (European Space Agency)(Fournier *et al.* 2000) funded project. It was during this project that it was adapted from ADEL-maize (Fournier and Andrieu 1998) for the primary purpose of being of use within remote sensing studies. The underlying rationale of the project was based on answering the question 'if exploitation of remote sensing data can be made more robust by using physically-based models for the reflection and scattering of radiation from vegetation and soil', it was also to investigate whether such 'models enable a link to be built between radiation measurements and quantitative estimates of vegetation and soil characteristics' (Fournier *et al.* 2000).

The model can be considered as two L-system models (plante.lsys and field.lsys), the first defines the growth and development of wheat and the second the plant's structural arrangement in a virtual field which is necessary for radiometric simulations. These L-systems use three parameter files, the first of which documents physiological characteristics (physio.h) such as final organ length, the second contains information on geometrical features (geom.h) of the plants an example being the midrib curvature of leaves and the third is dedicated to the arrangement of plants in the field (field.h) which includes the number of rows to be simulated (see Figure 3.1)

There are three steps within the model. The first converts the temperature data into a useful format to be used within the second step. At this second step the plant organs are generated and aged accordingly (see figure3.2 for the rules used within this step) and the final third step is when the geometry of the organs is calculated and the turtle instructions generated. It is at this point that plants are organised into bounding boxes for efficient ray tracing. Turtle instructions work slightly differently from Cartesian geometry (x,y) in that they are vector-based, so relative to direction and distance from its current position. The use of this turtle is common within L-system modelling (Prusinkiewicz 1990). The field.lsys is the second L-system within the model.

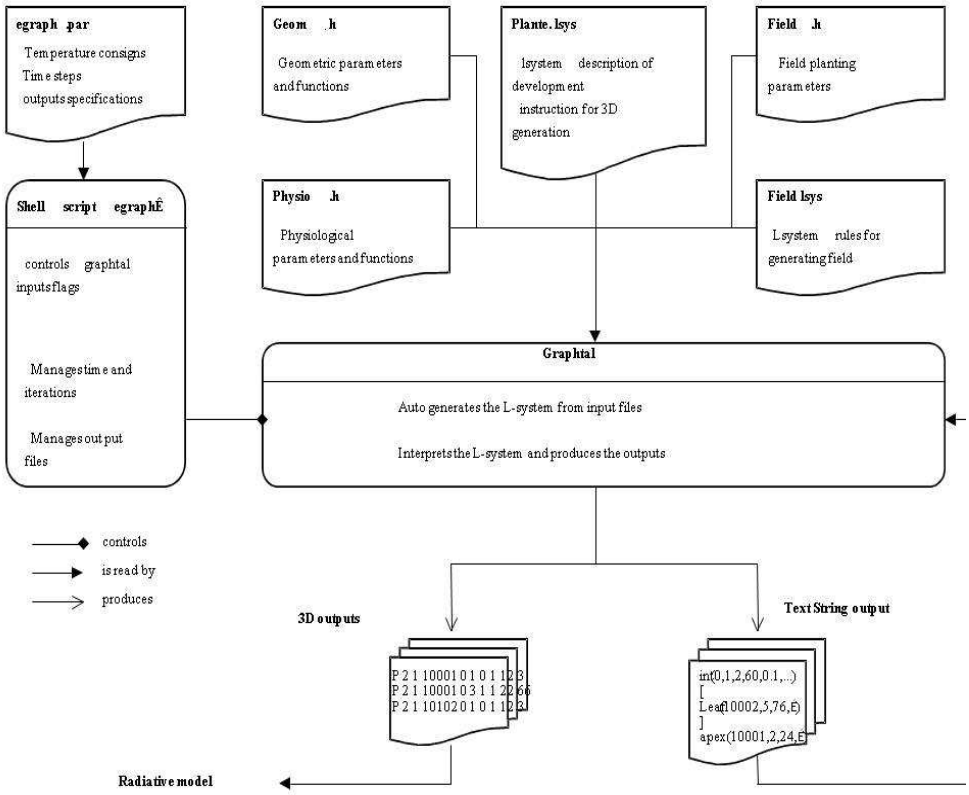

(a)

Figure 3.1: Structure of ADEL-wheat model. Boxes are for executable, single sheet for input files and multiple sheets for output files. Reproduced from (Fournier et al. *2000) pg 92.*

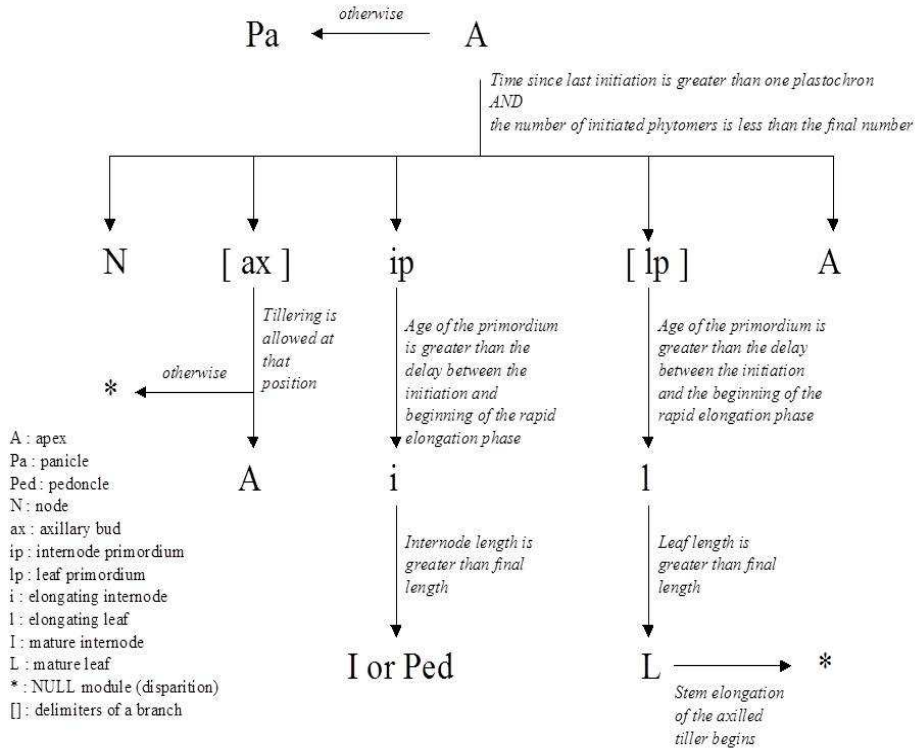

(a)

Figure 3.2: Flow diagram showing the qualitative transformations of the modules and the conditions for these transformations to apply. Reproduced from (Fournier et al. *2000) page 94.*

This places the cloned plants in the virtual field, the size and dimensions of which are determined within the setup.dat file. A file containing turtle directions are constructed at each time step. The thermal interval between each time step and the number of time steps can also be altered within the shell script.

There are two outputs of the L-systems, one is a text file containing a string of modules describing physiological parameters only and the other are files detailing the output from the geometrical calculations and the turtle instructions for generating a 3D representation of the modelled crop.

Below is an example of a string describing a fully grown lamina. The string within the brackets detail the plant no (1), axis rank (0, main stem), organ identification number (1) and phytomer rank (2). This is followed by physiological parameters which are needed to describe the lamina. These include information on the final length (8.4322), associated sheath length (3.43) and maximum width (0.3051). The following three values are associated with the age of the lamina and the rest geometry parameters (which include the insertion angle (70.0805), pcass (1, purely ascending), parabola top angle (10.2162), ellipse top angle (-20), angular curvature of ellipse (60), minimal length for a blade polygon to be represented (0.2), azimuth (-33) and basal inclination (0):

L(1, 0, 1, 2, 8.4322, 3.43, 0.3051, 0.1121, 266.3132, 46.5632, 70.0805, 1, 10.2162, -20, 60, 0.2, -33, 0)

The ‘L’ in the string above defines the organ the parameters are defining, so in this example a lamina which has a ligule (so fully grown). Within Figure 3.2 there is a list of the other organs which are also described in this format.

Once this information is read within graphtal, another file is created. Below is a sample of what such a file looks like. This is also describing a fully grown lamina:

p 2 100003003002 9 3 -3.3566 -0.3761 10.9398 -4.1163 -0.2423 10.7592 -3.2575 -0.6579 7.2705
p 2 100003003002 9 3 -3.2575 -0.6579 7.2705 -2.6863 -0.7585

....additional information in the same format ended with..
p 2 100003003002 10 3 -5.9827 1.7122 21.5975 -5.8966 1.6970 21.618 -6.0294 1.9246 22.1479
.... continued to describe the rest of the plant

Here the plant number is given (p 2) followed by a twelve digit number (100003003002) which includes plant number, axis, rank and organ type. The next two numbers (9 3 or 10 3 in the last line) identify which part of, in this case, the lamina the string is describing. The two numbers, 9 and 3 highlight that the data on that line describes the main part of the lamina and the numbers 10 and 3 that the data on that line is describing the tip of the lamina. The data on each line after these codes are co-ordinates from which the turtle can construct the leaf. The leaf is made up of numerous triangles.

The files within the model that are discussed within this thesis are; setup.dat, density.par, physio.h and geom.h files. A description of each file is given below:

setup.dat

The setup.dat allows some model parameters to be easily altered according to user preference. These include plant and axis density, inter row spacing, number of real plants (set as 9 plants which are then cloned and randomly chosen to represent the canopy), field size, thermal interval (thermal time step at each model run), number of simulations, germination period (thermal time delay until germination). It also allows radiometric parameters to be altered such as the number of rays per pixel and number of rows to view and image dimensions in pixels.

density.par

The density.par file lists the model parameters which describe the progression of final organ length per rank for all organs modelled, stem angle, final number of leaves, the form factor which is associated with leaf shape and discussed more in section 6.1.7, the delay in terms of phytomer rank of tillers (discussed in section 5.2.4), the leaf and internode extension rate and the phyllochron.

Inclusion of coordination of plant growth and development

The initiation and extension of successive organ in grasses is highly coordinated and this coordination is taken advantage of within the model (Fournier *et al.* 2003). The assumptions included within the model regarding kinetics of organ extension are that once the collar on lamina rank n appears, extension of sheath rank n ceases and linear extension of internode rank n starts as well as extension of lamina rank n+2. Another important feature is that the duration of extension of leaves and internodes remains constant between phytomer rank, the rate of extension is assumed proportional to the final organ length which further reduces parameters. It is well recognised that the rate of these processes is dependent on temperature, and thus why thermal time is used as the variable to express the kinetics of development and extension ADEL (Fournier *et al.* 2000).

Thermal time

Thermal time often has a considerable advantage over the use of normal calendar time, particularly in analysing field data where the temperature varies from season to season or from one planting to another. Thermal time is simply a summation of the cumulative differences between daily mean temperature and a specified base temperature and has units of degree days ($^{\circ}\mathrm{Cd}$). The thermal time within ADEL-wheat takes into account the non linear dependence of the rate of processes with temperature, so that a linear dependence is assumed at temperatures below 17.5 $^{\circ}\mathrm{C}$ and a greater dependence above such temperatures. The thermal time concept is commonly used to assess crop development rate as impacted by temperature (Gordon and Bootsma 1993, Shaykewich 1995, Saiyed *et al.* 2009) and as mentioned is considered more accurate than using the calendar-day method for estimating crop phenology (Bauer *et al.* 1984, Russelle *et al.* 1984, Slafer and Savin 1991). There are different thermal time models and Mkhabela *et al.* (2012) has compared five different thermal time models for modelling spring wheat phenological development on the Canadian Prairies.

Organ dimension, another important factor within ADEL-wheat, is assumed to be similar over all axes for each organ; sheath, internode, lamina length and lamina width. A developmental shift, that refers to the delay in development of the additional axes in relation to the main stem is the only additional parameter required to model the final organ lengths over all axes.

2D leaf shape is assumed to be the same for all leaves regardless of rank or axis and the ADEL model assumes the Prévot model to be the most suitable The 3D leaf shape is simulated using either a combination of a parabolic and ellipse model or purely parabolic. Differences are assumed for lower ranks of leaves, which are simulated with a bias towards a combination of parabolic

and ellipse. Higher leaves are assumed to be more parabolic in shape with less need for the additional ellipse model for the tip of the leaf. The phyllotaxy is assumed to not be regular with leaf position and instead the leaves are categorised into base (8 ranks below panicle), middle and upper (last three leaves). Each category of leaf, regardless of axis is allocated a probability of producing an opposite phyllotaxy pattern and a probability distribution function for azimuth angle. The overall differences between the group are that the leaves are shown to be less and less spread from the base to the top of the plant.

3.2 Overview of *librat* MCRT model

Lewis (2011) is a monte carlo ray tracing simulation library. MCRT is a method of estimating canopy radiative transfer. It uses stochastic sampling of the possible photon ray trajectories from the source to the sensor, so in this case the canopy to the field sensor. It moderates the photon attenuation at each ray interaction according to specified material reflectance and transmittance properties which are stored within the ADEL-wheat model and can be adapted/updated easily if field measurements are available. It has been tested and validated against EO measurements and other models and used for a wide range of EO applications (Disney *et al.* 2006, Disney *et al.* 2011, Hancock *et al.* 2012). The object files are used from the ADEL-wheat model as the input in this model with the output being files which contain information on the sunlit and shaded reflectance and transmittance of the leaves and the reflectance of the stem and soil. An additional file is used to describe the sun angle at the time of the observed measurements.

Chapter 4

Methodology

Two field experiments were carried out at the INRA campus of Thiverval-Grignon, France (48 ° 51' North 1 ° 58' East) during the years 2003-2004 and 2004-2005. Different varieties of winter wheat were sown on silty loam soil (Typic Eutrochrept, Soil Survey Stafff, 1996, Silt70%, Clay 23%, Sand 7%) and their development monitored. Different experimental setups were used to address the key aims of the thesis during these two experiments. Additional data from a previous experiment, also carried out at INRA campus of Thiverval-Grignon but not carried out by myself is also referred to in section5.2.4 of Chapter 5. This experiment is referenced within this thesis as Experiment 99, due to it being carried out in 1999.

This chapter gives a description of the data collection methods used during these three field experiments. General descriptions of the measurements made to acquire specific data are given in the relevant chapters that follow, but this chapter can be referred back to if more specific details of methods used to acquire measurements are required.

4.0.1 Selection of median plants

In all experiments, we were interested in obtaining an estimation of the dimensions of a median plant, and not in characterising a mean plant, representative of the whole variability within the field. We therefore always calculated the median of data (and not mean), and used sampling procedures that almost always included a selection of the plants to be measured. For selecting median plants, we measured two simple criteria on the entire sample and eliminated the extremes. One criterion was related to plant development (the number of visible leaves and length of the last visible leaf), and the other to organ dimension (the length of the most recent ligulated lamina). In experiment 1 and 2, for the non destructively measured plants, we also performed a post-selection of plants, by eliminating the few ones that did not produce the median number of phytomers on their main stem. More detailed description is given per experiment below

4.1 Experiment 1

4.1.1 Aims

- Parameterisation of leaf senescence
- Parameterisation of profiles of final organ dimensions against phytomer rank
- Development and parameterisation of a 2D model for leaf shape
- Characterisation of the plants' 3D-geometry including parameterisation for the 3D form of the leaf midrib.
- Comparison of parameterisation of the different genotypes in order to

  Verify that the same model is appropriate for all genotypes

  Evaluation of ADEL-wheat (developed from a single experiment in 1999) against these independent datasets. Analysis of the models' parameters across several genotypes to explore interdependence.
- To validate ADEL-wheat and the reflectance model against radiometric measurements at the canopy scale.

Parameterisation of leaf appearance and the profile of final organ dimensions was planned to be carried using both destructive and non destructive measurements, however time limitations meant that senescence was not parameterised within the scope of this thesis even though the data was available. Scans of a range of lamina over various ranks are collected and used to investigate a 2D model for leaf shape. Digitising of the leaf architecture is carried out within this experiment to investigate the plants 3D geometry including the 3D form of the leaf midrib and tiller and main stem angles. Limited radiometry measurements are collected to aid in the validation of the output of the ADEL-wheat combined within the reflectance model against observed radiometric measurements at the canopy scale. Thermal time, necessary to compare observed and modelled data is calculated from data collected within this experiment using a combination of temperature as measured in the canopy using the thermocouples and from the meteorological station.

4.1.2 Method

Ten different genotypes of winter wheat were sown in September 2003 using a precision sowing technique, which aims to have precise, even spacing between individual seeds in the row. The genotypes sown were Soisson, Isengrain, Caphorn, Arminda, Apache, Recital, Florence-Aurore, Recital, Thesee and Oratario. (A schematic diagram of a generalised wheat plant is given in Figure 4.1.) These were chosen due to being the more popular genotypes used within European farming. They were sown at high density 250 pl/m^2 (250 plants per square meter). Each genotype was sown in its own plot which consisted of eight rows. Between each plot a gap of 30cm was left bare to allow access to the plots (as illustrated in Figure 4.2). The plants were grown under non-limiting conditions of water and nutrients and were kept free of disease and weeds by appropriate fungicide and herbicide applications. Soil and canopy temperature were monitored directly by thermocouples and in addition meteorological data (air temperature at 2 meters, global radiation) were registered by a Stevenson screen located no more than 500 meters from the experimental field.

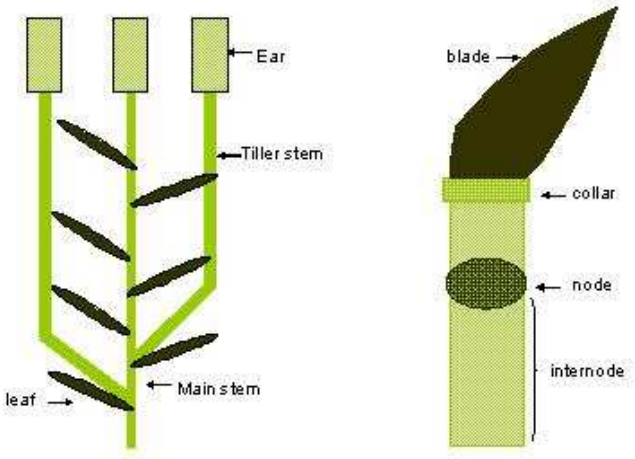

Figure 4.1: Diagrams of a wheat plant. To the left shows the whole plant, including tillers, lamina, ear (head). To the right a section of the plant is shown including the internode, node, collar and blade (lamina).

Selection of Median Plants

Median plants were used within the experiments described within this chapter. The idea of selecting median plants was to attempt to exclude variation within genotypes.

In experiment 1, all plants measured, except those of the first destructive sampling, were selected in the field at Haun Stage 5 (January). For the selection, we first randomly sampled 30 plants per genotype and calculated the value of the two criteria for the first and last quartile of the sample. These values were then used to select and tag plants in the field. For genotypes Soisson and Isengrain, 20 plants were measured non destructively weekly, from Haun stage 6 to flowering and then destructively sampled. Main stem was measured on the whole sample, whereas tillers were measured on half of the sample. The same procedure occurred for other genotypes, but with 13 plants measured instead of 20, and with a bi-weekly frequency. For Soisson and Isengrain, 4 destructive sampling sessions occurred. The first one occurred at Haun stage 2, where 50 (non selected) plants were measured. Other destructive sampling occurred monthly from February to May, where all axis of 20 plants per genotypes were measured. For other genotypes, 10 to 15 plants were measured at the first destructive sampling date, and 13 plants were destructively sampled in February and March.

Tagging

Sixty median plants of each cultivar were identified and tagged on the third row in from the gap between each plot. It was expected that the first 2 rows from the path would be affected by the edge effect, the 3rd row was chosen as it was not possible to reach further into the canopy without damaging the plants. The minimum distance between the tagged plants per row was set at 10cm. This was to reduce the risk of damaging other plants to be measured during sampling.
The plants were tagged using a small piece of wire coated with white plastic that was manipulated to produce a loop with a long straight end. The loop was placed over the plant and the straight edge used to secure the tag into the ground, as shown in Figure 4.3. A main stem leaf of each tagged plant was marked so that when the plants were subsequently sampled, the rank of the main stem blades would be easy to identify. This tagging process continued throughout the growing season. When the last tagged leaf started to senesce the highest ranking liguled leaf that was

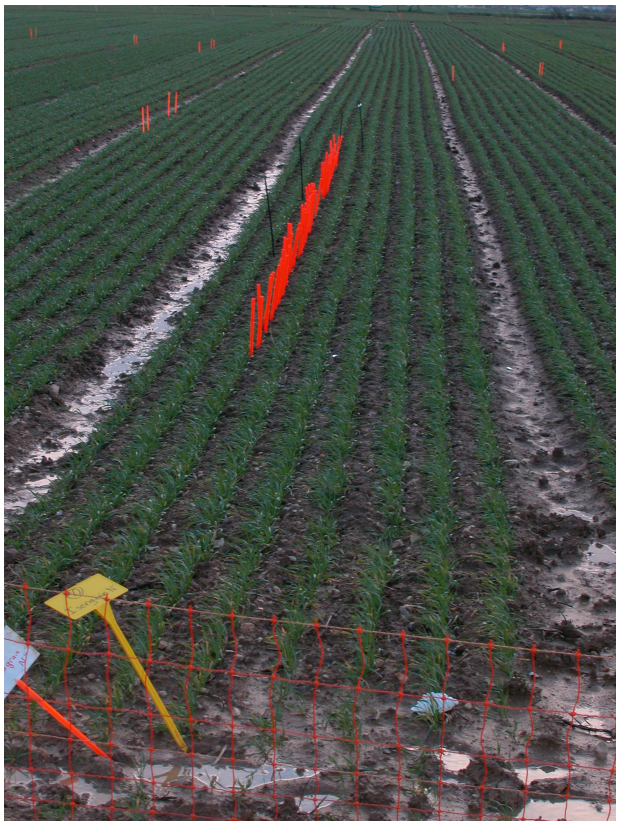

Figure 4.2: View of a plot containing one genotype of winter wheat. Selected median plants are tagged and marked with an orange picket

present on all tagged plants for each genotype would then be marked. On the initial tagging date the leaf to be marked was placed through the white tag so that is rested on top of it. It was then marked with a small black dot or some correction fluid as shown in Figure 4.3. Tillers of some of the tagged plants were similarly marked although with different coloured tags. Different colour wire loops were placed over the tillers to represent the different rank of each tiller. A blade per tiller was also marked with its phytomer rank using a black marker pen.

The sixty plants initially tagged can be thought of as three sets of twenty. For plants of genotypes Soisson and Isengrain ten of each of these sets of twenty plants had their tillers tagged whereas for the other genotypes only five per twenty were fully tagged. It was due to time restrictions and weather conditions that not all plants were re-tagged. It was found that ten plants were taking too long and not all data would be collected on all genotypes, this number was halved, allowing a sufficient collection of repeated data per genotype and could be collected within the time available. In order to make the tagged plants easier to locate a fluorescent orange plastic picket was secured into the ground near the plant. It was ensured that these markers were located far enough away in order to minimise the shading the plant and disturbance of the soil around it. Figure 4.4 shows the field, once all plants had been tagged, where each orange marker represents

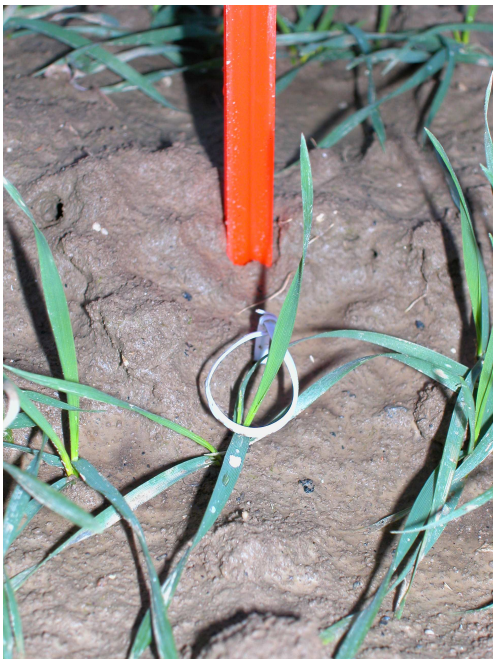

Figure 4.3: Photograph of a young wheat plant that has been identified as a median plant. A white tag has been placed over the plant. A white mark is also placed on one leaf and the rank of this leaf will have been recorded.

one median plant per genotype. The frequency and type of sampling strategy applied to the sixty

Figure 4.4: An image of the experimental field (experiment 1). Orange pickets are placed next to each selected median plants within the experimental field. These are the plants that are measured throughout development within this growing season.

plants varied and specific details of the methodology used, are given in subsequent chapters. Figure 4.5, gives an overview of how the tagged plants were sampled during the growing season.

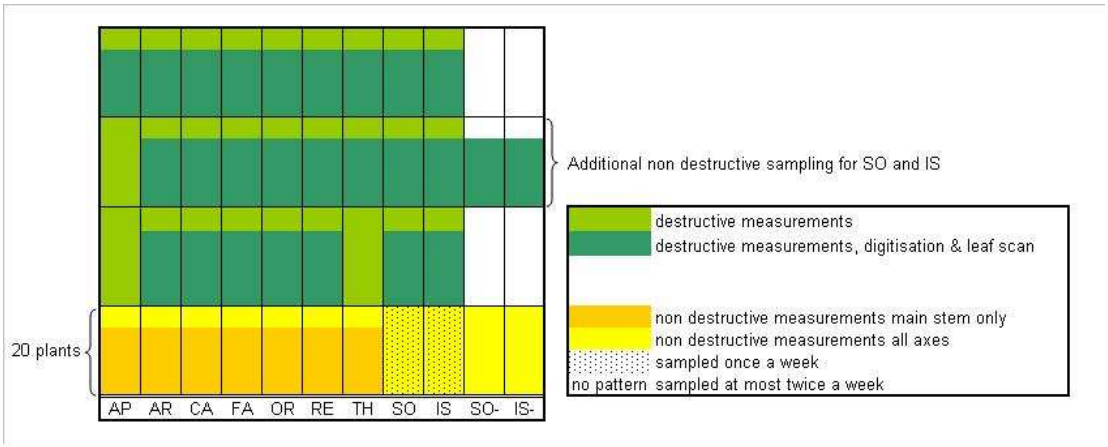

Figure 4.5: Schematic plan of experimental field for Experiment 1 showing the number of plants per genotype that are measured during experiment 1. Detail is given to how these measurements are taken (non-destructive sampling or destructive sampling)(AP=Apache, AR=Arminda, CA=Ca Horn, FA=Florence-Aurore, OR=Oratario, RE=Recital, TH=Thesee, SO=Soisson, IS=Isengrain, SO-=Soisson (no nitrogen), IS-=Isengrain(no nitrogen))

4.1.3 Measurements

Non-Destructive

Non-destructive measurements were performed weekly on genotypes, Soisson and Isengrain, and fortnightly on the remaining genotypes. At each measurement date the number of visible leaves, number of liguled leaves, the length of the last visible leaf and the length, width and percentage senescence of liguled leaves was recorded.

Destructive

Destructive sampling was carried out 3-4 times during the growing season, coinciding with digitisation and leaf 2D shape measurements (described below). In addition to the measurements made during non-destructive sampling the length of the sheaths and internodes were also recorded. The length of the sheath being the distance from the collar of one phytomer to that of the preceding one and the length of an internode being the distance between the middle of the node of one phytomer to the middle of the preceding node. These measurements are illustrated in figure 4.7.

Digitisation

Digitising was carried out in the field using a digitiser and Polhemus software, (Adam 1999). Figure 4.6 shows digitising in progress within the experimental plot. Points were recorded up the main stem with the position of liguled leaves recorded with their rank. Where internodes had started to elongate the location of the node was also recorded. Points were also taken along each non senescing lamina of the main stem, with points recorded at the base of the lamina (collar) and then at 1-2cm intervals along the leaf until the tip. The architecture of the tillers and angle from the main stem was measured for plants of genotype Soisson and Isengrain again only non senescing lamina were measured. Figure 4.7 is a schematic illustration of where measurements were made on the plant.

Figure 4.6: Jillian Watt(on floor) and Jonathon Hillier(sitting on chair), digitising some young winter wheat plants

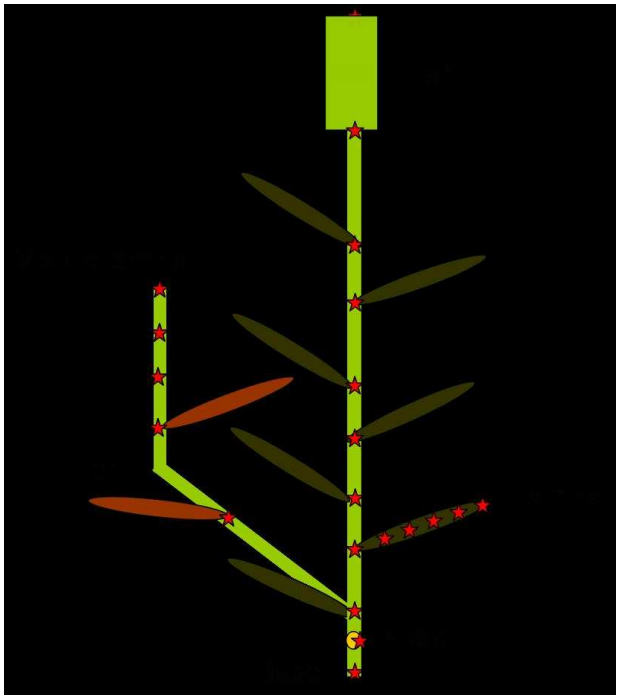

Figure 4.7: Schematic representation of where digitisation measurements were made on the wheat plants

Table 6.3 documents the number of plants measured per genotype and if the tillers were measured or not. On the last sampling date, the plants of some genotypes were removed from the field and digitised within the laboratory, this was due to the wind moving the plants whilst measurements were being taken. The data collected on tiller angle cannot therefore be used for analysis of tiller angle.

	SO	***IS***	***AR***	***CA***	***FA***	***OR***	***RE***
Date 1	**20**	**20**	**15**	**13**	**8**	**13**	**13**
Date 2	**19**	**20**	**12**	**13**	**13**	**13**	**13**
Date 3	**15**	**16**	**8**	**6**	**13**	**13**	**12**
Date 4	**14**	**16**					

Table 4.1: Summary of the number of plants per sampling date per genotype digitised. Digitising on the main stem and tillers was carried out on Soisson (SO) and Isengrain (IS) plants and for the other genotypes, the main stem only.

Leaf Scan

Lamina were removed from plants that had been destructively sampled. Non damaged lamina or those that had minimal senescence were then placed on a A4 piece of paper with the base of the lamina located at the top of the page and the tip at the bottom making sure the lamina ran as vertical as possible, as shown is Figure 4.8, (this is a requirement of the software used to analyse lamina shape). They were scanned using a flatbed scanner and the gimp software (GNU 2002) used within the subsequent analysis. Gimp is a software developed at INRA-grignon (Dornbusch and Andrieu 2009). Main stem and tiller leaves were scanned from genotypes Soisson and Isengrain whereas only main stem leaves were scanned from other genotypes. At each sampling date, the number of leaves scanned per relative phytomer rank and genotype differed, due to the quality of the lamina. At least ten lamina per phytomer rank per genotype were, however attempted to be scanned.

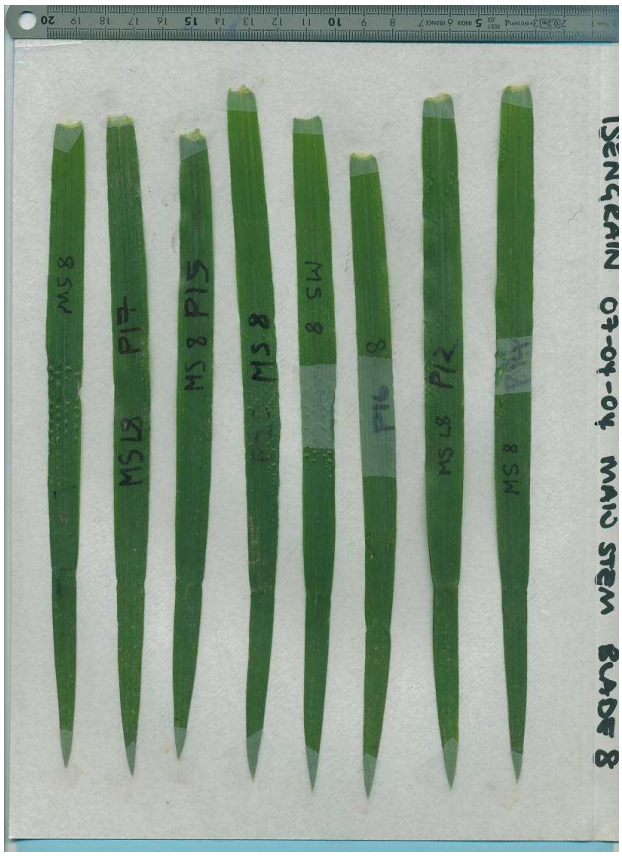

Figure 4.8: Illustration of how lamina were layed out to be scanned

Radiometry

Radiometric measurements were made over the canopies of genotypes Soisson and Isengrain at several dates during the growing season using an ASD FieldSpec PRO(ASD Inc., Boulder, CO., USA). The Analytical Spectral Devices (ASD) is a backpack mounted instrument which allows with some ease collection of high resolution solar reflectance, radiance and irradiance measurements with a 350-2500 nm spectral range and a field of view of three degrees. As it is backpack mounted one person wore the instrument and took measurements at shoulder height (approx 150 m) whilst the other held the white reference panel which was used after every three measurements. Ten horizontal hand held canopy cover photographs were taken on the same day or the day after radiometric measurements of each canopy. They were taken at random locations within each plot during cloudy or overcast parts of the day to avoid shadowing. It was also ensured that they were taken parallel to the rows with two inter rows present. The radiometric data collected was limited due to resource constraints. The second experiment however was designed to overcome the limited radiometric data collected within the first experiment.

4.2 Experiment 2

4.2.1 Aims

- To construct a comparable data set to Experiment 1 to test for year-to-year variation in parameterisation.
- To validate ADEL wheat and the reflectance model against radiometric measurements at the canopy scale (repeated as limited radiometric data was obtained during Experiment 1).

The final organ measurements collected throughout this experiment are used to construct a comparable data set with experiment 1. This enables year-to-year variation within genotypes when considering parameterisation of final organ length and the proposed tiller delay parameters used within the ADEL model. Specifically within this experiment, the additional data on presence and absence of tillers is used to develop and improve parameterisation on tiller presence and

abortion over thermal time. Radiometric measurements using the GER1500 and also from the Skye sensors is used in the validation of the output from the combination of ADEL-wheat and the reflectance model against observed oradiometric measurements at the canopy scale. Canopy cover photographs, leaf moisture content (dry weight), leaf reflectance and chlorophyll data are collected to aid in understanding any discrepancies found between observed and modelled radiometric measurements. The non-destructive and destructive measurements are also of use for this purpose as the age of the plant at the time radiometric measurements were obtained can be estimated.

4.2.2 Method

Two winter wheat varieties, Soisson and Caphorn were sown in October 2004 using agronomic sowing techniques at density 250 pl/m^2. The plots were 30 m by 30 m instead of long rectangular plots as used in Experiment 1. Nitrogen, herbicides and fungicides were added when necessary so growth and development were not inhibited. Irrigation was not required as the experiment was only due to continue to mid-May.

The genotype Soisson was chosen to be measured as a substantial amount of data has been collected on the growth and development of this variety over the last few years. Caphorn was chosen due to the difference in its structure compared to genotype Soisson. It is erectophile, whereas Soisson is more plagiophile in structure.

Due to available resources a maximum six week sampling period was available for the measurements to be recorded in Experiment 2. As such, the time of year in which rapid growth occurs was chosen to be the most optimal period in the growing season to obtain measurements. This rapid period can be described as begining at the onset of internode elongation on the main stem and finishing at the appearance of the flag leaf ligule on all axes was chosen as the. In addition to this sampling period, crop development was measured from January up until the beginning of this six week sampling date by Alain Fortineau, a Senior Technician at INRA Grignon, which helped to identify the start of this sampling period and also enabled certain early plant phenology data to be obtained.

Median Plant Selection

In Experiment 2, 30 randomly chosen plants per genotype were measured non-destructively from Haun stage 5 to flag leaf appearance. Dimensions of final organ lengths associated with the main stem were measured on all plants through out the period, whereas the dimensions of final organ lengths associated with the tillers were measured on all plants until the start of stem elongation and on the 15 plants whose criteria was in the inter-quartile interval of the sample afterwards. For each genotypes, 10 of these plants were destructively measured one week before the end of the period, and 15 were destructively measured at the end of the period. For Soisson, two additional destructive sampling occurred, without selection, at Haun stage 2 (30 plants) and Haun stage 5 (10 plants). For Caphorn one additional destructive sampling occurred at Haun Stage 2 (30 plants).

Tagging

Plants to be measured per genotype were chosen using a different sampling strategy than the one used in Experiment 1 which meant that no criterion was set for the chosen plants prior to tagging. Instead thirty plants on the same row for each genotype were tagged on the third row in from one set of tractor marks left from sowing. The third row in from this gap was, as in Experiment 1, used so that the plants measured were not affected by the edge effect. The plants chosen, per genotype, were approximately 30 cm apart and were tagged using a white tag and orange marker as in Experiment 1. Correction fluid or black marker pens were not used to mark the leaves as this was found, in Experiment 1, to cause localised senescence of the leaves. Instead different colour wire was twisted loosely around certain ranks of leaves per axis during the plants development in order that phytomer rank and axis rank were able to be identified at each subsequent sampling date. During subsequent weekly sampling of these plants, by Alain Fortineau, fifteen plants that did not display abnormal development such as, behind or ahead in development were identified as the median plants.

4.2.3 Measurements

Non-destructive

Weekly non-destructive measurements were made on all 30 plants from January 2004, with measurements made on the identified median plants up until the start of the six week sampling period. During this period of sampling all thirty plants were measured at each sampling date, however, on the 15 chosen median plants, measurements were made on all axes whereas on the remaining 15 plants, measurements were made on the main stem only. The measurements taken included those recorded using non-destructive sampling during Experiment 1, which were; the number of visible leaves, number of liguled leaves, the length of the last visible leaf and the length, width and percentage senescence of liguled leaves. In addition and where possible, the absence and presence of tillers was also noted on all thirty tagged plants.

Destructive

At the beginning of Experiment 2, plants were tagged in a different location from those on which non-destructive sampling was to occur. However, due to time constraints in the months before the sampling period, some of these plants were not re-tagged and as such, the rank of the leaves were unknown during the six week sampling period. In addition, in previous experiments within the same area of the field, variations of nitrogen had been applied and had altered the growth and development of the plants within this experiment rendering them unsuitable. Destructive measurements were to be made on these additionally tagged plants, however for the reasons mentioned this was not possible. Instead, fifteen non tagged plants were used at the beginning of the six week sampling period, per genotype, and at the end, the 30 plants that had been non-destructively sampled were sampled destructively. The same measurements were made using non-destructive sampling but, as in experiment 1, also included the length of the sheaths and internodes.

Leaf scan

Leaf scans were made on lamina from the main stem and tillers when destructive sampling took place using the same methodology as Experiment 1.

Digitisation

Digitisation of both genotypes was intended to occur at the beginning of the six week sampling period and at the end, however due to weather conditions only one set of data was obtained for genotype Soisson (two were obtained for genotype Caphorn). The plants that were due to be digitised were the additionally tagged plants, however for the reason mentioned they could not be used. Instead representative plants were chosen away from these affected sites and non tagged plants digitised from the top of the plant down. This enabled each lamina to be digitised and its rank recorded as flag leaf, flag leaf -1 and so on. Tillers were also digitised, however the rank could not be identified with a high degree of accuracy and so instead identified as 'non main stem'.

Radiometry

Canopy cover measurements were made weekly before and during the six week sampling period, see Figure4.9 for an example. At each sampling date ten hand held horizontal photographs of each canopy were taken, each at the same location, which was marked by a numbered orange picket. During the six week sampling period canopy cover measurements were attempted to be made the same day as radiometry measurements or if not possible the day before or after.

Radiometry measurements, using a GER1500 with a viewing angle of 8 degrees, were taken as often as possible during the set six week sampling period with weather conditions dictating the sampling frequency. The GER 1500 (Geophysical and Environmental Research Corporation) is a single-beam field spectroradiometer measuring over the visible to near infrared wavelength range. Radiometry measurements were taken on fully overcast or clear sunny days of which there were six during the sampling period. On these six dates, however both measurements over

both canopies was not always possible and as such each canopy was sampled on four dates only. Radiometric measurements were taken at nadir angle of both canopies and a bare patch of soil each hour, throughout the day sampling occurred. If the weather deteriorated during the day measurements were only taken during one half of the day.

Additional radiometric measurements were taken of the canopy once the heads of the wheat had fully appeared. The sampling involved removing the heads of each plant and the flag leaf within a 2 m squared area and measuring the reflectance before and after the removal at one hour intervals during the day. A 2 m area was used as this was just bigger than the sampled area from the radiometer.

A 2 channel Skye sensor (channel 1: 600-750 nm and channel 2: 700-850 nm) was located using a tripod approximately 2 m above the ground, over the canopy of genotype Soisson in February 2005 and left to monitor the crop signal during development, it was removed in March 2005 and placed over the Caphorn canopy for two weeks before being returned to the Soisson canopy in April. In April 2005 an additional 2 channel Skye sensor was located over the Caphorn canopy and left until two weeks after the end of the six week sampling period. Both sensors were removed from the field in June 2005. Instaneous weather conditions were not measured as sensors were operating throughout the growing season.

Leaf Reflectance was measured at the end of the six week sampling period (by Dr.P. Bowyer and Dr. P. Lewis). An ASD leaf clip device connected to an ASD was used to measure leaf reflectance in the laboratory. Representative plants within a 1 m transect (along one row) were taken from each plot and the leaves from the stems removed. Each leaf was labelled as leaf 1 through to leaf n from the first leaf at the top of the plant, through to the last leaf at the bottom of

(a)

Figure 4.9: An example of a canopy cover photograph. This photo was taken in January over a canopy of Caphorn plants

the plant. Due to the size of the port on the ASD contact probe, leaves (of same rank and species) were taped together to provide an area large enough to fill the sample port. Leaf reflectance and transmittance measurements were then made at the base, middle, and top of the leaf sample, by placing the leaf sample between the probe and the panel background. The procedure was repeated for both the abaxial and adaxial surfaces.For each leaf sample (position on stem, and section of leaf (top, middle, base)) up to 3 leaves were sampled for each leaf position. Given the heating of the leaves by the probe, together with the size of sample required to fill the sample port, it was not viable to make replicate measurements on the same leaf sample.

Dry weights of the leaves were measured by taking a sample of plants from a transect of 1m on one row from the field plots. Estimations of the density were made by counting the number of plants within 1 m. The leaves of 20-50 of these plants were removed and grouped per layer. Each layer corresponded to the distance from the top of the canopy. Leaves were scanned into the computer by group and subsequently analysed to calculate the 'sample surface'. Their fresh weight was also measured before being placed in an oven for 48 hours. Once fully dried, their dry weight was measured. This was carried out twice for both genotypes. The chlorophyll concentration of a selection of these leaves was also measured using a chlorophyll meter (spad meter). Three measurements along the leaf (as carried out for the leaf reflectance measurements) were made. This was repeated on 15^{th} April, 28^{th} April and the 12^{th} May.

Chapter 5

Phenology

Crop models are built for specific purposes and their structure and focus adopted accordingly. This has led to a range of models simulating particular crops or particular aspects of the processes involved in plant growth and development to be created. Plant architecture is generally described within crop models using descriptive models. This is due to the regulatory mechanisms that lead to the observed patterns of final organ length not being fully understood. The descriptive models used rely on identification and formalisation of patterns found in the architectural traits of organs according to their age and position within the plant. Identifying these patterns as stable relationships of organ dimension with position that are constant over a range of environments has been the method used to build and parameterise architectural models. This chapter details work carried out to help validate or propose alternative models of organ dimension with position. Comparison of data collected over various genotypes and also between experiment 1 and 2 allows the opportunity to identify how constant these relationships are. The overall aim being to create a generic dynamic architectural winter wheat model with minimal parameterisation. There are many architectural models, currently developed and being applied for a range of purposes, however the furthering of this area of research within the remote sensing area leads to the need for more generic models and particularly those requiring less parameter inputs.

This chapter is focused on the phenology of wheat, which can be considered as the pattern of organ development. It is split into two main parts, the first which concentrates on the pattern of final organ length and the second the pattern of tiller development.

5.1 Final Organ Length

In most architectural models, the pattern of final organ length is simulated using phytomer rank. In ADEL-wheat the relative phytomer number (RPN) is used to model observed patterns over all axes. The relative phytomer number is the decimal number of phytomers, characteristic for the delay in development of each tiller (relative to the main stem) added to the actual phytomer rank. This works where the pattern in final organ length is similar on all axes. For example if Tiller two has a delay shift value of 2.7, this would mean phytomer 3 on tiller two would have a RPN value of 5.7. The dimension of this phytomer would then have properties similar to an imaginary phytomer 5.7 on the main stem (Jochem 2006). Exceptions however have been highlighted, such as with lamina width. For lamina width the normalised relative phytomer rank (nrpn) can instead

be used due to a difference in lamina width over the lower phytomers of the tillers and main stem. The normalised relative phytomer number is the relative phytomer number normalised to the number of leaves on the main stem axis.

In general for all organ types, there is a pattern of final length with phytomer rank over different densities (with the same species) and also between different crop types.

Lamina length has been shown to increase in length over phytomer rank until around the penultimate phytomer after which a decrease in length is expected. This pattern has been reported for rice (Jaffuel and Dauzat 2005), maize (Fournier and Andrieu 1999) and spring (Jochem 2006) and winter wheat (Fournier *et al.* 2003), but with the decrease in lamina length occurring at differing phytomer ranks which for rice is dependent on the final number of phytomers.

It has been observed for final internode length that only the last 4-5 internodes (Fournier *et al.* 2000) extend significantly (over 1-2 cm) with the last extending internodes increasing at a different increment between phytomer rank compared to the initial extending internodes. This difference in rate of increase was only noticed between the final internode and peduncle by (Fournier *et al.* 2003) but Evers *et al.* (2005) found in spring wheat that this change in rate occurred over the last two phytomer ranks. In Maize a linear increase of internode length is observed for the first five internodes that elongate but is followed by a moderate decrease with rank for higher internodes and that maximum length was dependent on genotypes (Fournier and Andrieu 1998).

Not as much work has been carried out on sheath length. For winter wheat it has been observed that sheath length remains similar up until around RPN (relative phytomer number) 5 after which it increases linearly until the final rank (Fournier *et al.* 2003). Evers *et al.* (2005) found that for spring wheat the pattern over phytomer rank could be better described by a logistic sigmoid curve, where the relationship between phytomer rank and sheath length is an initial slow increase followed by a rapid increase then over the final phytomers an increase occurs again at a reduced rate. For Maize the pattern follows a regular increase in final length of successive sheaths for the first six or seven leaves, followed by a moderate decrease for higher leaves (Fournier and Andrieu 1998, Robertson 1994, Grant and Hesketh 1992).

The pattern of maximum final blade width has not been found to yield a single association with phytomer rank in spring or winter wheat (Hotsonyame and Hunt 1997, Evers *et al.* 2005). It has

however been found to be well correlated with sheath length when using a linear function. This relation is used to model final maximum blade width and results in a sigmoid curve that describes maximum blade width as a function of phytomer rank because sheath length was modelled as a logistic function of phytomer rank. A sigmoid shape has also been shown by Pararajasingham and Hunt (1995), who observed a similar pattern for main stems of several spring and winter wheat cultivars grown at different photoperiods. However, some showed a decrease in maximum final blade width over the top three or four phytomers and others a linear function. This variability in blade width has also observed by Hotsonyame and Hunt (1997) and reinforces the idea of Fournier *et al.* (2005) and Evers *et al.* (2005) that maximum blade width of Graminae cannot be modelled solely as a function of RPN (relative phytomer number) as it varies depending on photoperiod, light intensity (Bos *et al.* 2000), plant density and nitrogen level. Patterns of maximum blade width of rice was however found over phytomer rank by Tivet *et al.* (2001), where it is observed to gradually increase over phytomer rank and then achieve a plateau for the last four to five leaves.

Parameterisation of final organ length and leaf width as a function of phytomer rank has been established for the winter wheat genotype, Soisson (Fournier *et al.* 2005). This work is based on empirical observation of organ dimensions with relative phytomer rank (and normalised relative phytomer rank). Here, the aim is to evaluate the parameterisation given and attempt to generalise it to a range of genotypes. We also aim to ascertain whether the relationships are robust for all genotypes and if fewer parameters can be used whilst maintaining the most optimal models.

5.1.1 Materials and Method

Experiments

Wheat vegetative development was measured at the level of individual phytomer in 3 field experiments during 3 growing seasons all within the INRA-INAPG Research Unit Environnement et Grandes Cultures of Thiverval-Grignon, near Paris ($48°51$'N,$1°58$' E). Plants were grown on a deep loamy soil under non-limiting conditions of water (irrigation) and nutrients (two nitrogen applications were applied). They were kept free of disease and weeds by appropriate fungicide and herbicide applications. Stem growth regulator was applied in experiments 1 and 2, but not in

the alternative experiment carried out in 1999. After plant emergence, we verified that the actual density conformed to the nominal density. In 1999 Soisson was grown at two densities (250 and 70 pl/m^2). In experiment 1, a panel of ten varieties, including Soisson, were grown at standard density (250 pl/m^2). In experiment 2, two cultivars selected from the panel for their contrast in architecture, Soisson and Caphorn, were grown at standard density (250 pl/m^2). The experiment in 1999 was not detailed within the methodology chapter In this experiment the plants were sown on the 15th October 1998 in a 10m x 60m plot (30m for each density), organised in 5 band of 9 rows, separated by a 0.3 m interval. Within a band, inter-row distance was 0.175m, whereas inter-plant interval was adjusted according to nominal density. In experiment 1, plants were sown on the 16th October 2003, in a 100m x 100m plot, organised in 50 bands with similar characteristics as those of experiment 1. In experiment 2, the wheat was sown on the 26th October 2004 in a 30m x 30m homogeneous plot (without bands), with an inter-row distance of 0.14 m.

Measurements

Data collected methods can be found in the Methodology Chapter. Data came from either destructive (experiment 1), or a mix of destructive and non-destructive samples (experiment 1 and 2). Destructive measurements allow for measuring all phytomer dimensions (internode, lamina and sheaths) and the plant developmental stage. As leaves continuously senesce and disappear measurements on successive phytomers are performed during the season on different plants. Non-destructive measurements allow for measuring data on the same individual plant throughout the season, but only lamina dimension and developmental stage could be measured precisely in the field. By destructively sampling these individuals at the end of the growing season, the dimensions of all internodes could be determined, but only the dimensions of sheath for some phytomer ranks. In experiment 1 and 2, these measurements were completed by a few additional destructive measurements earlier in the season.

The following dimensions are recorded: lamina length (from collar to tip), lamina width at the widest part of the lamina, sheath length (from the middle of the node to the collar) and internode length (distance between the middle of two successive nodes). Plant developmental stage was characterised by a slightly modified version of the decimal Haun Stage (Haun 1973). Here, Haun stage is calculated by adding the rank of the last visible leaf plus the fraction of the lamina of that leaf that is visible. This requires measuring, a posteriori, the mature lamina length, but avoided

overlapping between Haun-Stages. For non-destructively followed plants, mature lamina length was known for each individuals, and was used to compute Haun stage. For destructively sampled plants, we used the median value of mature lamina length instead. For all non-destructively measured plants, and for half of the destructively measured plants in Experiment 2, leaf and axis were tagged to allow a non ambiguous numbering of phytomer and axes. This was achieved by placing, early in the season, a non-intrusive loop of wire placed over the main stem and using ink mark. The tags were updated regularly throughout the season. For non-tagged plants, phytomer position and axis number were guessed with the help of tagged plant. This led to un-ambiguous numbering, except for the last measurements, where an uncertainty of 1 rank is plausible.

In experiments 99 and 1, air and soil temperature were continuously measured in the field by thermocouples. Thermal time (base 0) was calculated using the temperature of the soil as long as the apex was in the soil (before stem elongation), and air temperature afterwards. In experiment 2, thermal time was calculated from air temperature registered by a Stevenson screen, which was positioned within 500 m of the experimental plots.

Data Collection

In all experiments, we were interested in obtaining an estimation of the dimensions of a ‘median plant’, and not in characterising a ‘mean plant’, representative of the whole variability within the field. We therefore always calculated the median of data (and not mean), and used sampling procedures that almost always included a selection of the plants to be measured. For selecting median plants, we measured two simple criteria on the entire sample and eliminated the extremes. One criterion was related to plant development (the number of visible leaves and length of the last visible leaf), and the other to organ dimension (the length of the most recent ligulated lamina). In experiment 2 and 3, for the non destructively measured plants, we also performed a post-selection of plants, by eliminating the few ones that did not produce the median number of phytomers on their main stem.

In an experiment carried out in 1999, 60 (normal density) or 30 (for the low density) randomly chosen plants were destructively sampled every $20°$Cd, from Haun Stage 2.8 to flowering. Out

of these, ten (at the beginning of the experiment) to five (at the end of the experiment) median plants were selected and measured. Half of the sample was eliminated using the developmental criteria, and then the dimension criteria were used.

In experiment 1, all plants measured, except those of the first destructive sampling, were selected in the field at Haun Stage 5 (January). For the selection, we first randomly sampled 30 plants per genotype and calculated the value of the two criteria for the first and last quartile of the sample. These values were then used to select and tag plants in the field. For genotypes Soisson and Isengrain, 20 plants were measured non destructively weekly, from Haun stage 6 to flowering and then destructively sampled. Main stem was measured on the whole sample, whereas tillers were measured on half of the sample. The same procedure occurred for other genotypes, but with 13 plants measured instead of 20, and with a bi-weekly frequency. For Soisson and Isengrain, 4 destructive sampling sessions occurred. The first one occurred at Haun stage 2, where 50 (non selected) plants were measured. Other destructive sampling occurred monthly from February to May, where all axes of 20 plants per genotypes were measured. For other genotypes, 10 to 15 plants were measured at the first destructive sampling date, and 13 plants were destructively sampled in February and March.

In Experiment 2, 30 randomly chosen plants per genotype were measured non-destructively from Haun stage 5 to flag leaf appearance. Dimensions of final organ lengths associated with the main stem were measured on all plants through out the period, whereas the dimensions of final organ lengths associated with the tillers were measured on all plants until the start of stem elongation and on the 15 plants whose criteria was in the inter-quartile interval of the sample afterwards. For each genotypes, 10 of these plants were destructively measured one week before the end of the period, and 15 were destructively measured at the end of the period. For Soisson, two additional destructive sampling occurred, without selection, at Haun stage 2 (30 plants) and Haun stage 5 (10 plants). For Caphorn one additional destructive sampling occurred at Haun Stage 2 (30 plants).

5.1.2 Data Analysis

Processing of the data involved excluding any non-destructive measurements taken during the growing season from an axis that did not produce the median final number of leaves. For destructive sampling this was not possible as the final number of leaves was not known, except when destructively sampled data was collected on plants when all leaves were present. Visual analysis per organ type over rank was also made, any obvious outlying data was checked for data entry or rank allocation mistakes and rectified appropriately.

The first part of the analysis is a visual check that the profiles of organ length over phytomer rank between axes can be accounted for by the parameterisation incorporated in ADEL-wheat (Fournier and Bruno 2002). This involves (i) simply overlaying the data collected on all axes and visually checking that it superimposes when taking into account a 'shift' parameter which is a time offset and (ii) qualitatively checking whether the parameterisation can be fitted to the change in organ size as a function of phytomer number. From this qualitative phase, it is concluded that the concept of a shift can be kept (and in-depth evaluated), but that in most cases, a more general parameterisation of the change of organ size with RPN (relative phytomer number), including additional parameters, must be proposed compared to that currently applied within the ADEL-wheat model. An analysis of LAR (Lamina Appearance Rate) over all ranks of all axes for a range of genotypes is discussed in the next chapter to further investigate and prove the idea that tillers can be regarded as delayed main stems.

The second part of the analysis involves fitting consistent models profiling organ size for all genotypes and years. The fitting of suggested models for each organ type is carried out using the gnls function (Pinheiro and Bates 2004) in the free statistical package R (R Development Core Team 2005), which performs numerical non-linear regression using a modified Newton-Raphson method. Consistent models of organ type are suggested and fitted to the data collected on the various genotypes during the three experiments.

Choice of Models

Figure 5.1 illustrates the model per organ type, with the data collected from experiment two on genotype Soisson (SO04). All final organ lengths are shown using the relative phytomer number

except lamina width where the normalised relative phytomer number is instead used. It can be observed that the pattern of final sheath and internode length over phytomer rank is the same on all axes. For final lamina length and final maximum lamina width the pattern of final length and width differs between the main stem and tillers over the lower to mid phytomers but is shown to be similar over the mid to higher phytomers. It is also observed that the pattern of final organ length or width is the same over all phytomer ranks between the tillers. These patterns are the same for all genotypes measured during the three experiments and suggest that parameterisation of final organ change can be fitted as a function of relative phytomer number. By displaying the data over RPN, it can be easily observed that the idea of a shift can be kept albeit slightly modified for lamina width and length models.

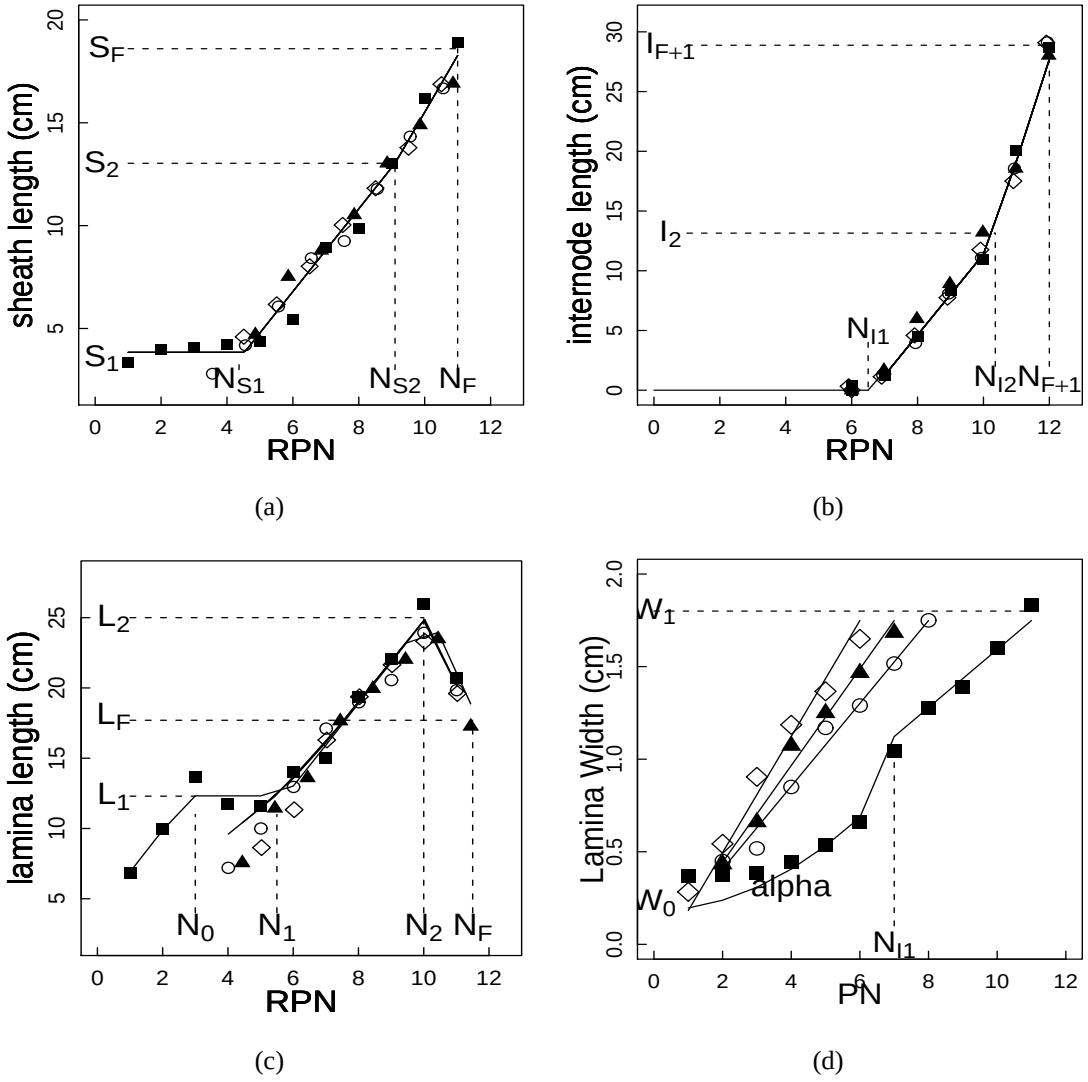

Figure 5.1: Final organ lengths per axis per relative phytomer number ,except lamina width, which is per normalised relative phytomer rank collected. The data shown was collected on genotype Soisson (SO04). The model for each organ type is shown by a solid line, the parameters of each model are also shown. Observed data of the main stem is represented by black squares, tiller one, clear circles, tiller two, triangles and tiller three by diamonds.

Sheath length

The pattern is described using a 'broken line' model, consisting of a plateau and two phases of linear variation with leaf rank as shown in Figure 1a. Sheath length of phytomer n of the main stem, S (n, 0) is modelled as:

$$S(n,0) = \begin{pmatrix} S_1 & \text{for } n \leq N_{S1} \\ S_1 + inc_{S1}(n - N_{S1}) & \text{for } N_{S1} < n \leq N_{S2} \\ S_2 + inc_{S2}(n - N_{S2}) & \text{for } N_{S2} < n \leq N_F(i) \end{pmatrix} \quad (5.1)$$

with

$$inc_{S1} = \frac{S_2 - S_1}{N_{S2} - N_{S1}}$$

$$inc_{S2} = \frac{S_F - S_2}{N_F(i) - N_{S2}}$$

For tillers, i, the same model applies, but using the relative phytomer rank, n+ sh(i). The relative phytomer rank is used thus

$$S(n,i) = S(n + sh(i), 0) \quad \text{i = 1,2,3}$$

The parameters of the model are:
S_1, length of sheath at rank N_{S1}
S_2, length of sheath at rank N_{S2}
S_F, length of final sheath
N_{S1}, rank at end of plateau
N_{S2}, rank at end of first increment phase and beginning of second
N_F(i), (i = 0-3) number of phytomers on axis i, where i=0 is the main stem
sh(i), (i = 1-3) phytomer shift between the main stem and tiller i

In the case of genotype Soisson at low density in experiment 1, two successive slopes for the increment of length were not observed; this can be seen as a special case of the model, where $inc_{S1} = inc_{S2}$; practically, this was dealt with by fitting a simplified model with only one phase of linear increment.

Internode length

The pattern of internode length as a function of phytomer rank, including the length of the peduncle, is shown in Figure 5.1. The internodes of the lower phytomers on the main stem do not extend and the internodes of the higher phytomers are found to extend in two linear stages.

$$I(n,0) = \begin{pmatrix} 0 & \text{for n} \leq N_{I1} \\ inc_{I1}(n - N_{I1}) & \text{for } N_{I1} < n \leq N_{I2} \\ I_2 + inc_{I2}(n - N_{I2}) & \text{for } N_{I2} < n \leq N_{F+1}(i) \end{pmatrix} \quad (5.2)$$

with constraints analogous to those for sheaths

For tillers, i, the same model applies, but using the relative phytomer rank, n+ sh(i). The relative phytomer rank is used thus

$$I(n,i) = I(n + sh(i), 0) \quad \text{i = 1,2,3}$$

:

$$inc_{I1} = \frac{I_2}{N_{I2} - N_{I1}}$$

$$inc_{I2} = \frac{I_{F+1} - I_2}{N_{F+1}(i) - N_{I2}}$$

The model's parameters are:
I_2, internode length at rank N_{I2}
I_{F+1}, length of the peduncle
N_{I1}, the rank at which internodes start to elongate
N_{I2}, rank at end of first increment phase and beginning of second
$N_{F+1(i)}$, (i = 0-3) final phytomer number per axis, where i=0 is the main stem
sh(i), (i = 1-3) phytomer shift between the main stem and tiller i

Lamina Length

The pattern of lamina length over phytomer rank was observed to be the same on all axes over the top phytomers only. Over the lower phytomers the pattern, although the same between tillers, differs from that observed on the main stem.

An increase in lamina length over the top five or six phytomers is observed to be of a similar rate on all axes. Over the lower phytomers on tillers a slower increase in length is observed compared to that over the higher phytomers. On the main stem an increase over the initial phytomers is followed by a plateau in length which lasts over a few phytomers (as shown in Figure 1c). A different model is thus proposed for the lower phytomers of the main stem and tillers.

A model consisting of two connecting straight lines is applied to the data over the top phytomers where the pattern is thought to be similar for all axes. This data is then used to calculate an intercept of this model with the data from below the set cut off rank (above which the pattern is similar). A separate model is then applied to the main stem which includes an increase in lamina over the initial phytomers, followed by a plateau. Where increments in lamina length before and after the plateau can be sufficiently estimated (more than one data point) both are found to be approximately 3 cm per phytomer and as such the increment in the model is assumed to be the same. Although this assumption presents a small error in estimated lamina length over the initial two phytomers it does enable a simpler model to be created. For tillers, three different models were considered. One which modelled the different linear increase over the initial phytomers and calculated the phytomer rank at which the upper phytomer model converged. An alternative option, models the initial increase in lamina length but assumes the the point of convergence of the model over higher ranks, is the same rank at the end of the plateau noticed on the main stem and also assumes that the initial lamina length is the same as that observed on the main stem thus removing the need for additional parameters. The third model, which is the one chosen as the most appropriate simply applies the linear model observed on the main stem before and after the plateau. The simple linear model was shown to fit well and reduced the complexity of the model and parameters required. The fit being found to be similar to that of the two linear model but slightly less that the two linear model requiring extra parameters. Due to the requirement of keeping parameters to a minimum it is suggested that the linear model is the most appropriate and that again the error over the smaller leaves is assumed to be acceptable.

The suggested models of lamina length of phytomer n of the main stem, L(n,0) is modelled as:

$$L(n,0) = \begin{pmatrix} L_0 + inc_{L1}(n-1) & \text{for } 1 < n \leq N_{L0} \\ L_1 & \text{for } N_{L0} < n \leq N_{L1} \\ L_1 + inc_{L1}(n - N_{L1}) & \text{for } N_{L1} < n \leq N_{L2} \\ L_2 + inc_{L2}(n - N_{L2}) & \text{for } N_{L2} < n \leq N_F(i) \end{pmatrix} \tag{5.3}$$

whereas for tillers there is no plateau,

$$L(n,t) = \begin{pmatrix} L_0 + inc_{L1}(n-1) & \text{for } 1 < n \leq N_{L2} \\ L_2 + inc_{L2}(n - N_{L2}) & \text{for } N_{L2} < n \leq N_F(i) \end{pmatrix} \tag{5.4}$$

For tillers, i, the same model applies, but using the relative phytomer rank, n+ sh(i). The relative phytomer rank is used thus

$$L(n,i) = L(n + sh(i), 0) \quad \text{i = 1,2,3}$$

Where:

$$inc_{L1} = \frac{L_2 - L_c}{N_{L2} - N_c}$$

$$inc_{L2} = \frac{L_F - L_2}{N_{F(i)} - N_{L2}}$$

The model parameters are:
L_0, lamina length at rank calculated as inc_{L1} *(N_{L0}-1)-L_1
L_1, lamina length at plateau (N_{L1})
L_2, maximum lamina length
L_F ,lamina length at N_F
N_{L0},rank at which plateau starts
N_{L1},rank at which plateau ends
N_{L2},rank at which lamina length is greatest
$N_{F(i)}$, (i = 0-3) final phytomer number per axis, where i=0 is the main stem
sh(i), (i = 1-3) phytomer shift between the main stem and tiller i

Lamina width

The pattern of lamina width as a function of phytomer rank is shown in Figure 5.1. It can be observed that the lamina width for all final and initial leaves is similar regardless of axis rank. The linear property of lamina width with rank is not observed on the lower phytomer of the main stem where instead a curvilinear relationship is present. The normalised phytomer rank was considered an option for modelling the lamina on the tillers and the upper lamina on the main stem. However the simpler model as shown, which has fewer parameters was decided upon. This model assumes the lamina width of rank one is the same for all axes and the final lamina of all axes is the same. It applies a linear model in between. For the lower phytomers of the main stem and curvilinear parameter is required and to distinguish between the lower and upper phytomer of the main stem the NI1 is used as the cut off point between the two models. No shift parameters are required, just the final number of assumed lamina on each axis.

Equation 5.5 is the proposed model for leaves of phytomers on the main stem and equation 5.6 for the tillers.

$$W(n,0)\begin{pmatrix} W_0 + a(n-1)^2 & \text{for } n < N_{I1} \\ W_0 + inc_w(n-1) & \text{for } N_{I1} < n \leq NF_i \end{pmatrix} \tag{5.5}$$

$$W(n,i) = \begin{pmatrix} W_i + inc_w(n-1) & \text{for } 1 < n \leq NF_i \end{pmatrix} \tag{5.6}$$

where

$$inc_w = \frac{W_1 - W_0}{NF_i - 1} \tag{5.7}$$

Where
i is tiller rank 1-3
n is the phytomer rank
W_0 is the lamina width for the rank 1 lamina
W_1 is the lamina width at NF_i (where i is 0 to 3)

$N_{F(i)}$ is the total phytomer number on axis i (0 for main stem)
N_{I1} is the rank of the first internode that extends as defined within the internode model
a is curved model parameter

5.2 Results

5.2.1 Model Fitting

Phytomer Number per Axis

Each final organ length model requires the final number of leaves per axis. The median final number of leaves produced was used. The median final number of leaves on the main stem was between 10 and 12 depending on genotype and year of experiment (see Table 5.1).

Genotype	Main stem		T1		T2		T3	
	Med	Mean $\pm$ sd	Med	Mean $\pm$ sd	Med	Mean $\pm$ sd	Med	Mean $\pm$ sd
S099	11		8		7		7	
S099low	12		9		8		8	
SO05	12	11.8 ± 0.4	9	8.7 ± 0.6	8	7.9 ± 0.4	7	7.0 ± 0.5
CA05	12	11.8 ± 0.4	9	8.7 ± 0.5	8	8.2 ± 0.4	7	6.8 ± 0.4
SO04	11	11.1 ± 0.3	8	8.4 ± 0.5	8	7.9 ± 0.6	7	7.0 ± 0.0
CA04	11	11.3 ± 0.7	8	8.3 ± 0.5	8	7.9 ± 0.3	7	6.7 ± 0.6
AR04	12	12.1 ± 0.3	9	8.7 ± 0.6	9	8.6 ± 0.6	8	7.8 ± 0.5
AP04	11	11.0 ± 0.0	8	8.2 ± 0.4	8	7.8 ± 0.4	7	6.7 ± 0.6
FA04	10	10.1 ± 0.3	7	7.4 ± 0.6	7	7.0 ± 0.4	6	6.0 ± 0.0
IS04	11	10.9 ± 0.4	8	8.0 ± 0.2	7	7.1 ± 0.3	7	6.8 ± 0.4
OR04	11	11.0 ± 0.0	8	7.8 ± 0.6	8	7.8 ± 0.4	7	6.7 ± 0.5
RE04	10	10.5 ± 0.5	7	7.4 ± 0.5	7	7.0 ± 0.0	6	6.0 ± 0.0
TH04	11	11.0 ± 0.4	9	8.9 ± 0.3	8	7.9 ± 0.3	7	7.0 ± 0.0

Table 5.1: Mean $\pm$ sd and median (Med) final number of phytomer per axis

Over most genotypes the final number of phytomers on tiller one is three less than the final number observed on the main stem and four and five less for tillers two and three respectively. However, this pattern is not always the case. Some genotypes are shown to have the same final number of phytomers on more than one of the three tillers. The linear relationship found between the mean final number of leaves on the main stem and tillers one has an r^2: 0.652 and rmse=0.294, tiller two an r^2:0.767, rmse=0.233 and tillers three an r^2: 0.692, rmse=0.255.

Delay Parameter

In ADEL-wheat it is assumed that the delay parameter for each tiller is the same for all final organ length (or width) models enabling them to be set as the same constants within all organ type models. The analysis of data collected from all three experiments however illustrate that both the final lamina and internode length models are similar but that the delay parameters for the final sheath length model are different.

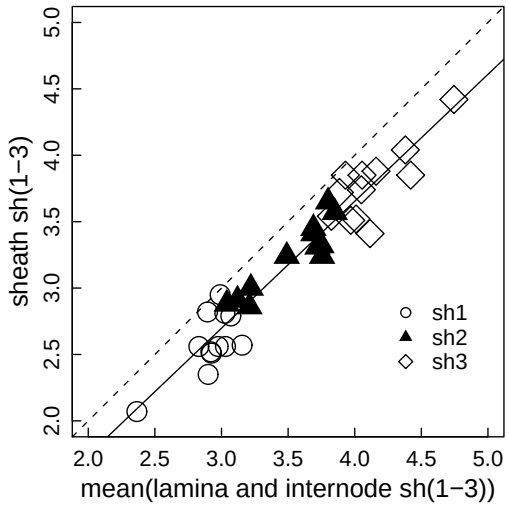

Figure 5.2: The mean delay parameter as estimated by final lamina and internode length models is shown against the mean delay parameter as estimated by the final sheath length model. A 1:1 line is shown by a dotted line.

As such, a delay parameter per axis for all final organ length models is not used. Instead a mean delay parameter is calculated using the delay parameter of the final lamina length model and

Genotype	sh1 $\pm$ rmse	sh2 $\pm$ rmse	sh3 $\pm$ rmse
SO99low	2.90 ± 0.03	3.70 ± 0.03	3.93 ± 0.03
SO99	2.99 ± 0.03	3.80 ± 0.03	3.89 ± 0.03
SO04	2.98 ± 0.03	3.21 ± 0.02	3.97 ± 0.03
SO05	3.08 ± 0.03	3.70 ± 0.02	4.16 ± 0.03
AR04	3.04 ± 0.06	3.22 ± 0.04	4.12 ± 0.08
AP04	3.03 ± 0.03	3.04 ± 0.03	4.16 ± 0.03
CA04	2.90 ± 0.04	3.04 ± 0.04	4.01 ± 0.07
CA05	2.93 ± 0.02	3.50 ± 0.03	4.38 ± 0.03
FA04	3.16 ± 0.18	3.75 ± 0.10	3.83 ± 0.08
IS04	2.84 ± 0.03	3.72 ± 0.04	4.06 ± 0.04
OR04	3.03 ± 0.02	3.85 ± 0.04	4.75 ± 0.02
RE04	2.93 ± 0.05	3.80 ± 0.04	4.43 ± 0.09
TH04	2.37 ± 0.05	3.13 ± 0.04	4.06 ± 0.05

Table 5.2: The shift parameter values used to model tiller day for each genotype with their associated error (rmse)

internode length models only (as listed in Table5.2 and used within lamina length and width and internode length models.

The delay parameters for the sheath length model are instead estimated using the relationship between sheath delay parameter value and internode and lamina length value, using equation 5.8 (see Figure 5.2, model fit is r^2 0.925).

$$sh_S = 0.956 * (mean(sh_L, sh_I) - 0.17) \tag{5.8}$$

where
sh_S= sheath shift
sh_L= lamina length shift
sh_I= internode shift

These delay parameters were set within the appropriate final organ length models and both the model parameters re-estimated and the quality of the fit of the model calculated. In general the fit of the model using the phytomer shift parameters calculated by equation 5.8 did not increase the error in the model fit (see Table 5.3). An average shift for all organ types, per genotype, as

$r^2 \pm$ rmse				
Genotype	Internode	Sheath	Lamina length	Lamina width
SO99low	0.995 ± 0.64	0.995 ± 0.44	0.960 ± 2.1	0.983 ± 0.07
SO99	0.995 ± 0.66	0.995 ± 0.45	0.996 ± 0.6	0.973 ± 0.07
SO04	0.978 ± 1.34	0.963 ± 0.95	0.914 ± 1.5	0.912 ± 0.13
SO05	0.999 ± 0.18	0.866 ± 1.74	0.874 ± 2.6	0.946 ± 0.10
AR04	0.979 ± 1.36	0.978 ± 0.84	0.922 ± 1.5	0.937 ± 0.13
AP04	0.979 ± 1.24	$-$	0.854 ± 1.7	0.901 ± 0.18
CA04	0.979 ± 1.26	0.948 ± 0.97	0.918 ± 1.6	0.928 ± 0.14
CA05	0.996 ± 0.54	0.960 ± 0.89	0.903 ± 1.8	0.933 ± 0.13
FA04	0.863 ± 5.40	0.943 ± 1.18	0.845 ± 2.2	0.880 ± 0.15
IS04	0.952 ± 1.39	0.967 ± 0.90	0.900 ± 1.7	0.914 ± 0.14
OR04	0.981 ± 1.40	0.984 ± 0.69	0.913 ± 1.6	0.937 ± 0.10
RE04	0.972 ± 1.75	0.963 ± 0.90	0.920 ± 1.3	0.930 ± 0.12
TH04	0.970 ± 1.58	0.960 ± 1.17	0.883 ± 1.9	0.876 ± 0.14

Table 5.3: The r^2 and rmse of the fit of the model using a mean delay parameter to model tiller delay

calculated using the method described, and is therefore used within the rest of this investigation.

Final Sheath Length

Figure 5.3 illustrates the observed (points) and modelled (line) final length of sheath for the range of genotypes. Data from a range of phytomer ranks is missing from the genotype Apache (AP04). As such, the model could not be fitted to this data set. Constraining the model delay parameters to be the weighted mean as estimated from the three organ length models (sheath and internode final length) the model was found not to converge when fitted to Recital (RE04) or Cap Horn (CA04) data and instead the best fit model was applied and the parameters estimated.

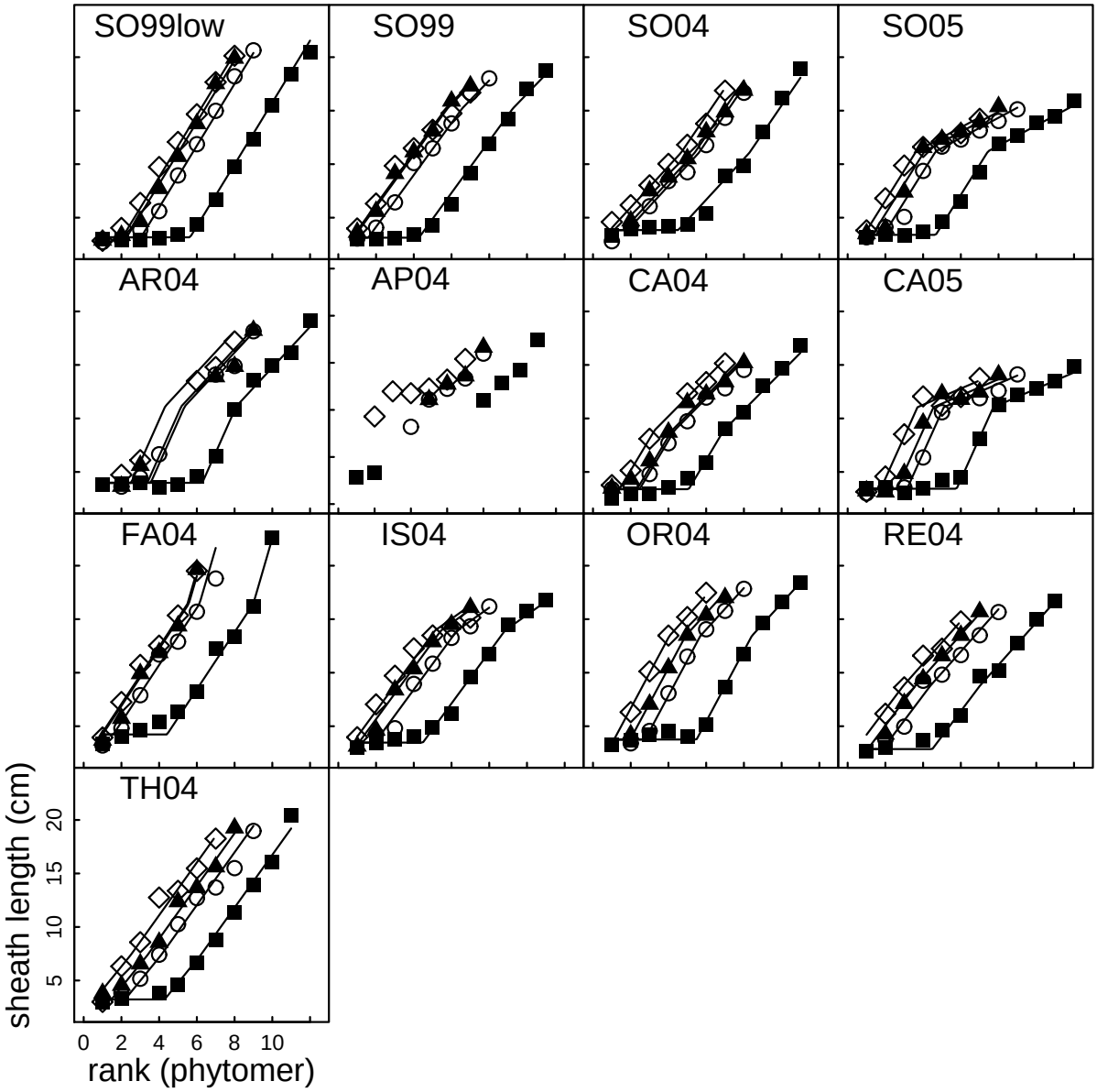

Figure 5.3: The observed (points) and modelled (line) final sheath length is shown over phytomer ranks. Main stem= square,Tiller one=circle, Tiller two=triangle and Tiller three=diamond

Genotype	Type	S_1	S_2	S_F	N_{S1}	N_{S2}	inc_{S1}	inc_{S2}
SO99low		3.16	–	21.54	5.64	–	2.50	–
	rmse	0.13	–	0.17	0.08	–	–	–
SO99		3.13	15.20	18.39	4.27	9.24	2.42	1.82
	rmse	0.21	1.49	0.30	0.12	0.66	–	–
SO04		3.84	11.06	18.08	4.51	8.29	1.91	2.59
	rmse	0.06	0.54	0.10	0.06	0.24	–	–
SO05		3.39	11.20	15.49	4.67	7.44	2.81	0.94
	rmse	0.12	0.33	0.20	0.10	0.17	–	–
AR04		3.98	11.13	18.56	6.28	8.09	3.96	1.90
	rmse	0.05	0.55	0.13	0.08	0.19	–	–
AP04		–	–	–	–	–	–	–
	rmse	–	–	–	–	–	–	–
CA04		3.39	8.90	16.13	5.07	6.93	2.95	1.77
	rmse	0.05	0.52	0.15	0.08	0.23	–	–
CA05		3.43	11.04	14.29	5.77	7.72	3.91	0.75
	rmse	0.06	0.14	0.10	0.05	0.06	–	–
FA04		4.23	16.42	22.56	4.41	8.98	2.66	6.07
	rmse	0.08	0.43	0.34	0.06	0.11	–	–
IS04		3.46	13.94	16.65	4.47	8.83	2.40	1.25
	rmse	0.04	0.24	0.09	0.03	0.11	–	–
OR04		3.75	13.44	18.43	5.48	8.42	3.30	1.93
	rmse	0.05	0.32	0.09	0.03	0.11	–	–
RE04		2.86	8.77	16.67	4.48	7.00	2.34	1.97
	rmse	0.13	1.42	0.14	0.10	0.65	–	–
TH04		3.22	7.38	19.20	4.28	6.20	2.16	2.46
	rmse	0.12	2.52	0.13	0.19	1.06	–	–

Table 5.4: Parameter values for the final sheath model are given per genotype with the rmse value.

Table 5.4 outlines the parameter values of the final sheath length model all genotypes.

Final Internode Length

Figure 5.4 illustrates the observed and modelled final length of internode over phytomer ranks. No final internode length data was collected on the tillers of Cap Horn (CA05) and Soisson (SO05) during experiment two.

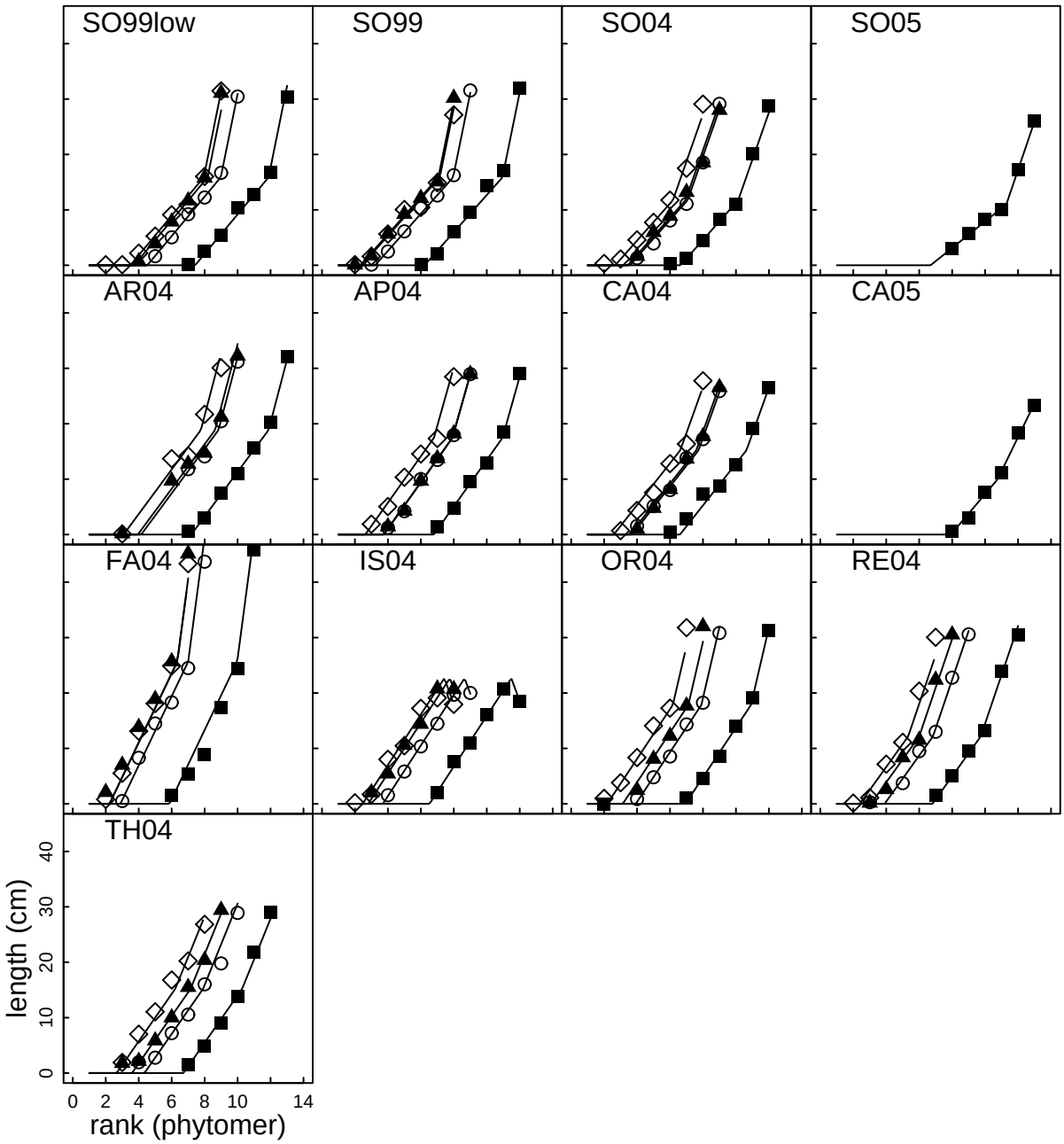

Figure 5.4: The observed (points) and modelled (line) final internode length is shown over phytomer ranks. Main stem= square,Tiller one circle, Tiller two triangle and Tiller three=diamond

Genotype	Type	I_2	I_{F+1}	N_{I1}	N_{I2}	inc_{I1}	inc_{I2}
SO99low		15.81	32.33	7.41	11.87	3.54	14.70
	rmse	0.47	0.37	0.08	0.04	–	–
SO99		15.94	31.34	6.21	10.94	3.37	14.60
	rmse	0.44	0.37	0.10	0.05	–	–
SO04		11.89	27.69	6.63	10.14	3.38	8.53
	rmse	0.30	0.15	0.05	0.05	–	–
SO05		10.99	26.03	6.68	11.28	2.39	8.76
	rmse	0.46	0.31	0.17	0.10	–	–
AR04		18.82	31.59	7.18	11.87	4.01	11.37
	rmse	0.51	0.24	0.11	0.05	–	–
AP04		17.36	28.47	6.78	10.94	4.17	10.56
	rmse	0.38	0.17	0.05	0.04	–	–
CA04		15.19	26.54	6.60	10.63	3.76	8.31
	rmse	0.55	0.23	0.07	0.09	–	–
CA05		9.97	23.75	7.92	10.74	3.52	6.12
	rmse	3.26	0.84	0.25	0.61	–	–
FA04		22.68	47.03	5.77	9.89	5.50	22.12
	rmse	1.50	1.26	0.18	0.13	–	–
IS04		22.75	18.54	6.52	11.48	4.58	−8.19
	rmse	0.27	0.28	0.03	0.05	–	–
OR04		17.80	31.88	6.94	10.90	4.49	12.83
	rmse	0.33	0.20	0.04	0.03	–	–
RE04		12.50	31.20	6.80	9.80	4.16	8.50
	rmse	0.89	0.28	0.09	0.11	–	–
TH04		15.24	27.93	6.71	10.26	4.28	7.33
	rmse	0.72	0.20	0.05	0.13	–	–

Table 5.5: Parameter values for the final internode model are given per genotype with the rmse value.

Table 5.5 outlines the parameter values of the final internode length model all genotypes.

Final Lamina Length

Figure 5.5 illustrates the observed and modelled final length of lamina over phytomer ranks. Table 5.2.1outlines the parameter values of the final lamina length model for all genotypes.

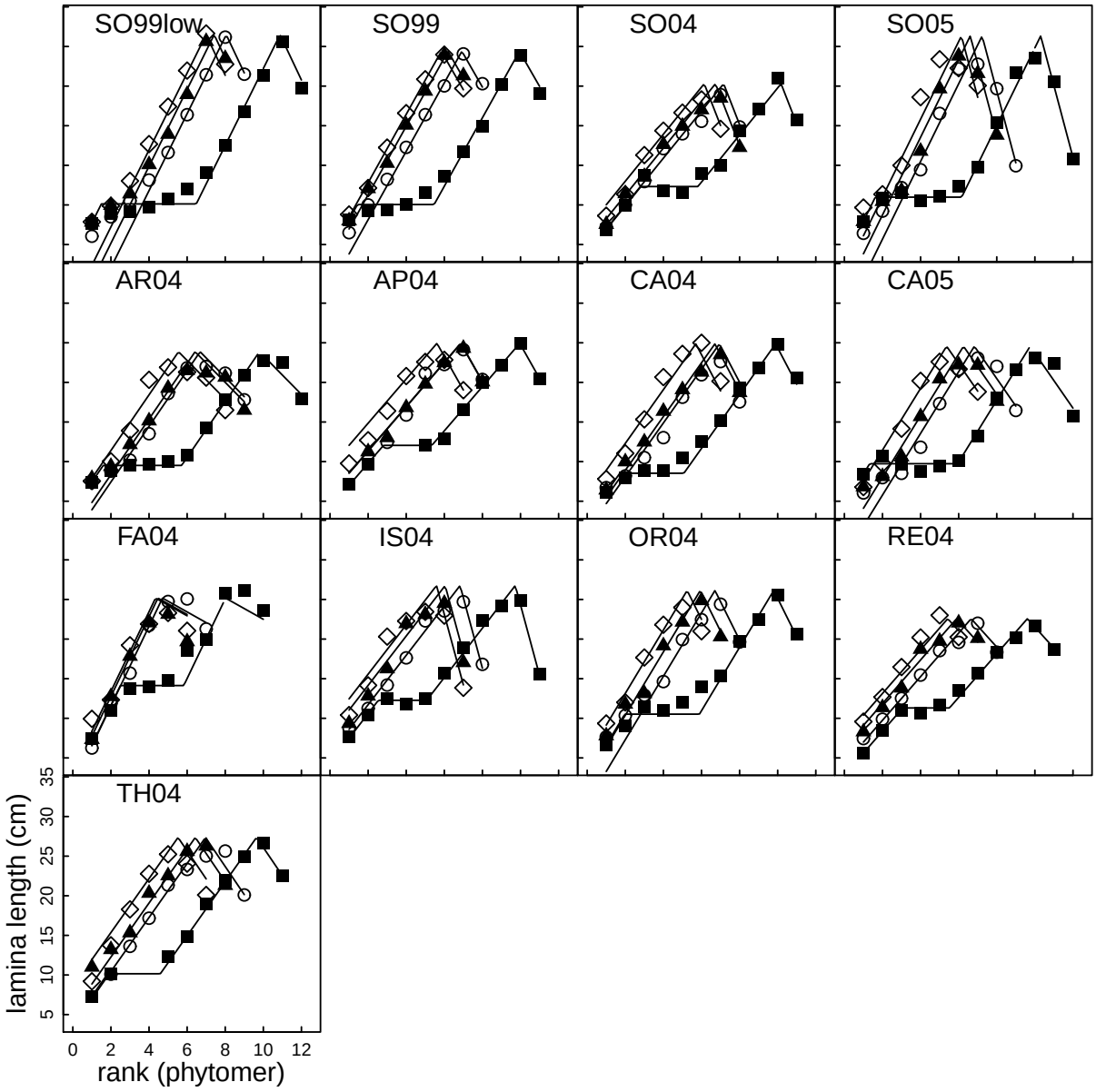

Figure 5.5: The observed (points) and modelled (line) final lamina length is shown over phytomer ranks. Main stem= square, Tiller one=circle, Tiller two=triangle and Tiller three=diamond

Genotype	Type	L_0	L_1	L_2	LF	N_{L0}	N_{L1}	N_{L2}	INC_{L1}	INC_{L2}
SO99low	mean	2.85	10.12	31.48	25.76	1.49	6.42	1.12	4.85	−5.09
	rmse	1.20	0.53	0.27	0.41		0.18	0.06		
SO99	mean	3.82	10.04	29.39	24.96	1.44	5.43	1.05	4.32	−4.19
	rmse	1.11	0.55	0.16	0.23		0.19	0.04		
SO04	mean	3.93	12.31	25.29	20.22	2.82	5.76	0.82	2.97	−6.16
	rmse	0.11	0.12	0.16	0.21		0.05	0.05		
SO05	mean	3.01	10.98	31.33	15.99	1.62	5.97	1.69	4.90	−9.05
	rmse	0.15	0.07	0.30	0.51		0.02	0.06		
AR04	mean	3.90	9.51	23.86	18.47	1.59	5.66	2.20	3.51	−2.44
	rmse	0.17	0.09	0.23	0.25		0.04	0.08		
AP04	mean	4.21	12.04	24.93	20.49	2.80	5.39	1.04	2.79	−4.25
	rmse	0.31	0.98	0.21	0.24		0.35	0.06		
CA04	mean	2.72	8.53	24.86	19.76	1.71	4.81	1.11	3.39	−4.58
	rmse	0.25	0.15	0.27	0.33		0.06	0.07		
CA05	mean	4.55	9.73	24.56	16.74	1.32	5.94	2.24	3.89	−3.47
	rmse	0.14	0.06	0.19	0.26		0.03	0.06		
FA04	mean	1.57	14.13	25.17	22.49	2.49	5.48	1.98	5.03	−1.34
	rmse	0.25	0.23	0.47	0.40		0.06	0.11		
IS04	mean	4.35	12.27	26.75	15.40	2.53	4.85	1.27	3.11	−8.90
	rmse	0.07	0.09	0.13	0.22		0.03	0.02		
OR04	mean	2.62	10.52	26.13	20.28	1.97	5.56	1.20	4.00	−4.84
	rmse	0.21	0.12	0.17	0.22		0.04	0.04		
RE04	mean	2.86	11.30	22.56	18.85	3.06	5.34	1.39	2.75	−2.66
	rmse	0.18	0.20	0.20	0.29		0.09	0.08		
TH04	mean	3.91	10.15	27.35	22.54	1.83	4.50	1.35	3.40	−3.54
	rmse	0.26	0.26	0.20	0.24		0.09	0.06		

Table 5.6: Parameter values for the final lamina length model are given per genotype with the rmse value.

Final Lamina Width

Figure 5.6 illustrates the observed and modelled final width of lamina for all genotypes. Table 5.7 outlines the parameter values of the model.

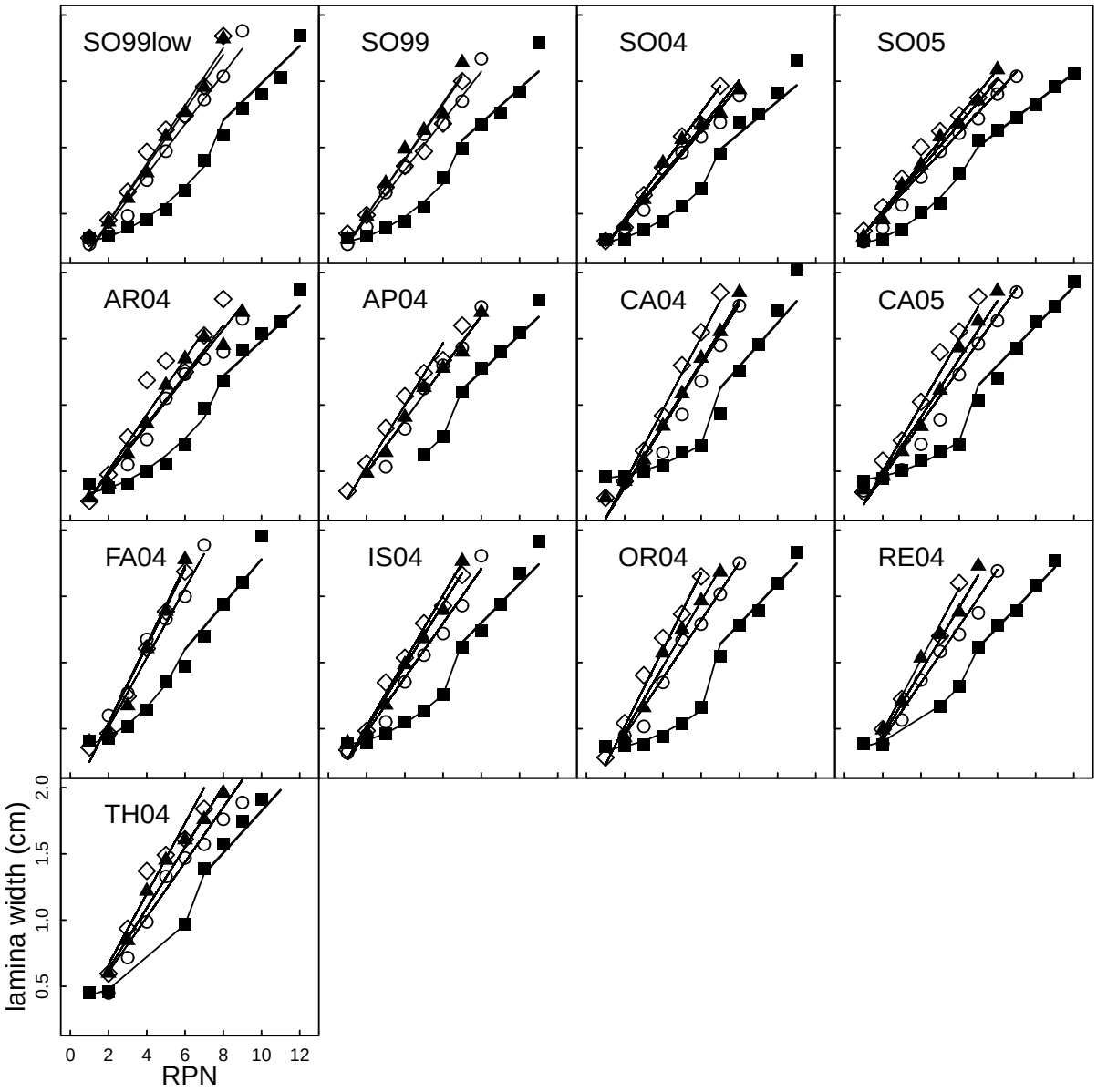

Figure 5.6: The observed (points) and modelled (line) final lamina width is shown over phytomer ranks. Main stem= square,Tiller one=circle, Tiller two=triangle and Tiller three=diamond

genotype	W_0	W_1	alpha
AR04	0.25	1.81	0.0138
IS04	0.25	1.74	0.0157
SO04	0.24	1.51	0.0127
RE04	0.21	1.71	0.0179
FA04	0.13	1.78	0.0348
AP04	0.25	1.70	0.0141
OR04	0.18	1.75	0.0140
TH04	0.43	2.05	0.0147
CA05	0.29	1.86	0.0151
SO05	0.33	1.57	0.0106
SO99	0.27	1.56	0.0126
SO99low	0.22	1.74	0.0135

Table 5.7: The estimated model parameters of the lamina width model per genotype

5.2.2 Parameter Correlations

It is one of the aims of this research to minimise the number of parameters required within the model. This section looks into the possibility of correlations between the parameter values by comparing the parameters looked at so far within this chapter.

Final phytomer number and Shift parameter

Comparison between the estimated delay parameters used in the final organ models and the difference in the final number of phytomers between the main stem and tillers (1,2 & 3) shows a linear correlation with r^2 0.692. Figures 5.7 illustrate the relationship between the difference in the median final number of phytomers between tillers and the main stem and the delay parameters used within the models (lamina length and width and internode length models).

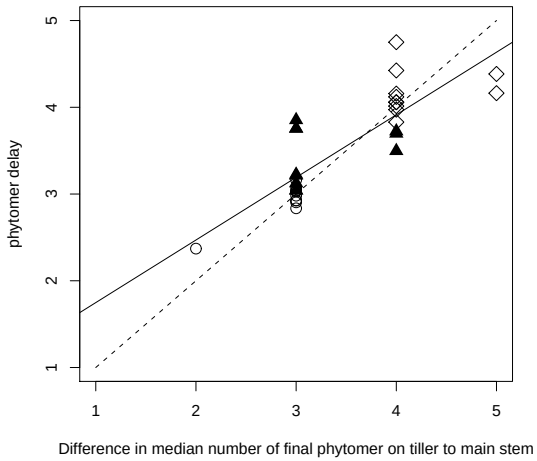

Figure 5.7: Delay parameter compared with the difference in median number of phytomers on axis compared to main stem. Shift 1=circle, Shift 2=triangle and Shift 3=diamond. The constant line is the linear model through the data and the dotted line represents the 1:1 relationship.

Increments

Correlations in the variations of model parameters between varieties were investigated. Correlations of increments were found to be poor with the highest r^2 value being 0.168 which corresponds to the correlation between the increment of sheath length and lamina length.

Break point in models

Comparison between the rank at which the break points within the model occur has been carried out. The break point between the juvenile and adult stage, i.e around phytomer 6 has been found for the majority of genotypes to differ consistently within organ type, with this parameter estimated by the final internode model to be at a higher rank and that estimated by the sheath length being at the lower rank. It must be noted however that the value of this parameter, as estimated by the sheath length model is lower than expected due to the constraints of the suggested model. If a curvilinear line was accepted over the lower phytomers of the sheath length model this initial break point would be higher and as such, closer in value to that estimated by the other two models.

The estimated parameter N_1 is compared between all organ length models. The most reasonable correlation was found between N_1 as estimated for the sheath length and internode length models, where a r^2 value of 0.727 (mean confidence interval of 0.269 and standard error of 0.120).

An alternative to investigating correlation between rank N_1, is to look at the number of phytomers that are extending between rank N_1 and N_2. It is generally accepted that in winter wheat 4-5 internodes extend however no such assumption has been made for any other organ types. The relationship between the number of phytomers between N_1 and N_2 as estimated using the final internode, sheath and lamina length models was investigated. The r^2 of the correlation between this number of phytomers was however found to be weak with the phytomer number, according to the sheath and internode model, having the highest r^2 of 0.568.

Correlation between the final number of lamina on the main stem and the estimated parameter N_1 for all organ length models (except lamina width) was investigated and the estimated parameter values of an assumed linear relationship and the fit of this model and the rmse can be found in

Organ Type	Intercept	Slope	r^2	rmse
internode	-0.133	0.619	0.631	0.337
sheath	-1.767	0.595	0.536	0.414
lamina length	1.950	0.309	0.394	0.425

Table 5.8: Estimated parameter values of an assumed linear relationship between N_F of the main stem and the estimated N_1 parameter per organtype per genotype. The fit (r^2)and rmse is also given

Table5.8.

Final organ length at different phases of the model

Comparing the relationship between estimated parameter values for NF (flag leaf length) and L_2 (length of lamina at rank N_2) a linear relationship is observed with 4-5 outliers (which correspond to the genotypes, Isengrain (IS04), Florence-Aurore (FA04), Soisson (SO05) and Caphorn (CA05) see Figure 5.5. From Figure 5.5 it can be observed that FA04, SO05, CA05 have two leaves on the downward slope of lamina length from N_2 to NF, with the only other genotype exhibiting this similar pattern being AR04. The pattern between rank N_2 and NF for genotype IS04 does show a greater decrease in length than noticed on other genotypes. As a result of these inconsistencies a constant difference between the values of the parameters LF and L_2 is not assumed.

5.2.3 Discussion

Model Fitting

Final number of phytomers on main stem and axes

In the three experiments carried out, total leaf number on main stem varied between 10 and 12, depending on year, density and genotype. Although this is a reduced range of final lamina number (main stem) of variation to that encountered in growing wheat worldwide, it corresponds

to what can be expected for winter wheat in France, under these conditions.

Phytomer delay

The pattern of final organ length on the tillers can be modelled as delayed main stems when considering final sheath and internode length. For lamina length and width only the later phytomers can be described by a delay parameter. The pattern over the early phytomers of final lamina width and length show no similarity to that found on the tillers. The growth of early lamina is thought to be dependent on environmental conditions and as such would explain, to some extent the variability found in the results and especially that between the same genotypes grown during different years (SO04 & SO05 and CA04 & CA05).

Overall the analysis of the data collected during the three experiments confirm over a range of cultivars and condition, the finding of (Fournier *et al.* 2003, Evers *et al.* 2005) that a shift parameter allows the pattern of final lamina, sheath and internode lengths along lateral axes to be derived from that along the main stem with a high accuracy. When calculated independently on lamina; sheath and internode, the value of the shift required to transpose from main stem to a given axis were similar for lamina and internode and slightly lower for sheaths. However using a unique shift value for all organ types did not reduce significantly the quality of fit of the model of final lengths of organs. In some cases the use of a single shift resulted in lack of convergence of the models of final organ size, however the best fit parameter values gave good r^2 values.

The value of the shift parameters when set to be genotype specific and not genotype and organ type specific, between main stem and tillers varied also between year or cultivars (min to max values of all genotypes shown, sh1= 2.37:3.16, sh2= 3.04:3.85, sh3=3.83:4.75). Our protocol does not enable the precise reason or reasons why these variations occur to be identified, but does illustrate the year to year variation for genotypes Soisson and Caphorn are in the same range as variation between genotypes in 2004. These variations are sufficient so that shift parameters should be fitted to experimental data when accurate simulation of final size of organs on tiller are required.

The shift calculated for an axis was not found to be highly correlated with the difference in mean leaf number between that axis and the main stem

Sheath length

Pattern of sheath length as a function of relative phytomer number could be described by a quasi-plateau followed by a broken line, thus requiring 9 parameters (S_1, S_2, S_F, N_{S1}, N_{S2}, N_{SF}, sh1, sh2, sh3). The plateau included phytomers below RPN = 4 to 6 and this value was correlated with total leaf number (n1 = 0.66*NF-2.56, r^2 = 0.48), that is, very close to the parameter N_{I1} for internodes. The slope of increase of length of sheath as a function of phytomer number was generally higher for two or three phytomers following the plateau, than for the 4 or five topmost phytomers. The difference being very marked in some cases (SO05 and CA05) and weak or un-existing in others cases (SO99 low). There is no strong idea about the why these differences occur. Finally, given that the phytomer shift for each axis is known, it appears that 6 parameters are sufficient to describe the pattern of sheath length of all axes.

Internode length

Internode length along the shoot could be described by a broken line function, with a total of 7 specific parameters, I_2, I_F, N_{I1}, N_{I2}, sh1, sh2, sh3, plus one axis parameter NF. Such parameterisation holds, where stem shortener were used (2004 and 2005) and not used (1999). The number of elongated internodes in wheat is usually 4 or 5 (ref). Defining the number of elongated internodes raises the question of the criteria for the minimum length of an elongated internode. Here the use of parameter N_{I1} allows for an objective estimate. N_{I1} was correlated with total leaf number (N_{I1} = 0.71 NF-1, 2; r^2 = 0.71) .

In wheat, the ear peduncle is generally significantly longer than the top most vegetative internode, suggests actually that some qualitative changes exist between conditions of extension of the vegetative internodes and that of the peduncle. So in the previous parameterisation in ADEL, position of break point N_{I2} was considered equal to total leaf number N_{I2}= NF. Results here shows that such qualitative change may also affects the top most vegetative internode. The fractional value of N_{I2} suggest actually that some qualitative change affect both the peduncle and, to a variable amount the topmost vegetative internode, probably depending on the time when the change occurs. The position of break point N_{I2} varied between NF_I-1 and NF_I , and the full range of variation could be observed even for a given variety (e.g. Soisson). However because the range of variation was restricted to NF_I-1 - NF_I a constant relation N_{I2}= NF_I -0.5

could be accepted in a simplified parameterisation.

Finally, given that the phytomer delay for each axis is known, it seems that 3 parameters N_{I2}, I_1, I_2 are sufficient to describe the pattern of internode length of all axes of a plant. More over, the small range of variation of N_{I2} makes the approximation N_{I2} = NF_I-1, probably acceptable in most cases.

Lamina length

Lamina length along the shoot could be described by a broken line function, with a total of 9 specific parameters, plus one axis parameter (NF). The pattern over the main stem and tillers was found to be similar only after rank N_{L1}. There are no strong ideas of the origin of the plateau in lamina length on the main stem between ranks N_{L0} and N_{L1} and this pattern has not been suggested by other authors. . The relationship between the length of the flag leaf and the length of the longest leaf was not found to be strong, with four main outliers. These outliers were generally the genotypes where two lamina were found to decrease in length between ranks N_{L2} and NF. The increment before and after the plateau gives a model with fewer parameters and also one that fits well to experiment data over three experiments and as such any error is accepted to be small. Finally, given that the phytomer shift for each axis is known, it appears that 9 parameters are sufficient to describe the pattern of lamina length of all axes.

Lamina width

The pattern of lamina width, as with lamina length, is not found to be the same over all phytomers between all axes. Similarity between tillers and the main stem phytomers above rank of phytomer that the internode start to extend (N_{I1}) exist in that a linear relationship with lamina width and rank is observed. A similar increase in lamina width per increase in rank however was not observed. It was considered that a normalised phytomer rank should be used instead of a relative phytomer rank used for the other final organ length models. A similarity between such phytomers on such axes is noticed using relative phytomer rank, but only for tillers 1-3. From the full results of (Ljutovac 2002) however, it was identified that tillers above rank 3 diverged from this pattern, necessitating the need of a normalised relative phytomer rank. The model suggested within this

chapter only considers three tillers, due to the survival and production rate of tillers four being so low. In order to keep parameter values low, an alternative model was suggested. This is a broken line function, with a total of 8 parameters. W_0, W_1, α, NF_i, sh1, sh2, sh3. There are 8 parameters as an additional parameter N_{I1} is required, but estimated within the internode length model. The model requires the lamina width at rank 1 and the final lamina rank and calculates the linear model accordingly. For the lower phytomers on the main stem a curvilinear relationship is assumed and requires an appropriate parameter to describe this relationship. Although this relationship would perhaps not hold if the plant was to produce more tillers, only three tillers were found to be produced and survive for a significant period of time in both experimental years and as such is deemed appropriate for the purposes of this study.

5.2.4 Conclusion

The idea of tillers being 'delayed mini-main stems' has been shown using the pattern of final organ length over all axes to be strong enough to enable accurate simulation of the pattern of all final organ lengths on all axes from that observed on the main stem, with the addition of one 'shift' parameter per axis. It was found however that for final lamina width and length that the pattern was not similar over the different axis for all phytomer ranks and that the similarity was apparent for all ranks of the tillers but only over higher ranks for the main stem. It is possible that the rank, is the same for lamina length and width, above which the pattern is the same for all axes, however the models applied to lamina width and length do not allow this comparison to be made with any accuracy.

It was observed that not all organ types start significant growth (i.e rank N_1) around the same time, although for lamina and sheath, increased growth per phytomer rank was noticed for most genotypes to be around rank 5-6 and for internode growth, one phytomer later. No significant correlations could however be found to enable this parameter to be estimated from the final number of phytomers.

The final models to be suggested, although in some cases increase the number of parameters required from that currently suggested in the ADEL-wheat model, do however encompass the pattern of final organ length as observed on a range of genotypes and for genotypes grown under different conditions.

5.3 Leaf Appearance

In an attempt to strengthen the idea that tillers are delayed main stems, as discussed within the final organ length section of this thesis (section 5.2.4), a comparison of LAR (Leaf Appearance Rate) between the MS and tillers and the thermal time at which the flag leaf on all axis becomes liguled is carried out. Also within this section a comparison of LAR between genotypes and also between the same two genotypes grown under different environmental conditions is carried out to investigate possible environmental and genotypic influences on leaf appearance rate.

5.3.1 Introduction

Integration of leaf appearance rate (LAR) enables the number of emerged leaves on the plant's main stem to be estimated; a useful measure of plant development (Streck *et al.* 2003). Accurate predictions of plant developmental stages are important in crop simulation models and for crop management. For crop management, knowledge of the timing of plant developmental events is important for the scheduling of field operations such as fertilizer applications, pest control and harvest (Streck *et al.* 2003). For crop simulation models, accurate prediction of developmental stage is important as partitioning of assimilates to different plant organs varies with developmental stage affecting important processes such as, dry matter accumulation, light interception, canopy photosynthesis, and yield (Amir and Sinclair 1991, Hodges and Ritchie 1991, McMaster *et al.* 1991, Streck *et al.* 2003). For these reasons the rate of leaf appearance has been the subject of many studies, particularly in wheat. As summarised by McMaster (2003) temperature is assumed to be the primary factor affecting leaf appearance rate with light to a lesser extent, however additional factors are also considered such as the effect of sowing data (Hay and Delecolle 1989, Cao and Moss 1991) and the correlation between the rate of day length change at crop emergence (Baker *et al.* 1980, Kirby *et al.* 1982).

In the crop models, CERES-Wheat (Ritchie and Otter 1991) CERES-Maize (Kiniry 1991) SHOOTGRO (McMaster 1992, Wilhelm *et al.* 1993, Wilhelm and McMaster 2003), MODWht (Rickman *et al.* 1996) SIRIUS (Jamieson *et al.* 1998b) and GRAAL (Drouet and Pages 2003) leaf appearance is simulated using the phyllochron approach. A phyllochron is most often defined as the thermal time (TT, °Cd), between the appearance of successive leaf tips (Rickman *et al.* 1996,

McMaster and Wilhelm 1997, Slafer and Rawson 1997) or the appearance of successive fully expanded leaves (collar emergence) or nodes (Campbell *et al.* 1998). It is commonly assumed that the phyllochron is constant with phytomer rank (constant phyllochron approach). However modifications to this model have been suggested. An extensive review on the phyllochron and the limitations of suggested approaches is given by (McMaster and Wilhelm 1995), however will not be discussed here as an in-depth analysis is not to be carried out with regards to the most appropriate model of LAR within this section.

The work carried out in this section is primarily interested in ascertaining the similarities in LAR between axis, currently assumed within most crop models and to further the idea that tillers behave as delayed mini-main stems. Similarities between the LAR of different genotypes is also to be investigated. This is of importance due to the discrepancy of results found between authors such as Frank and Bauer (1995) who have suggested that differences in LAR between genotypes do exist and also from studies carried out at Wageningen (Birch *et al.* 1998) which suggest that the differences are small and environmental differences have a more significant impact and that LAR should be based not of genotype of the plant but on environmental conditions.

5.3.2 Aim

- To establish whether the leaf appearance rate is the same for all leaves on all axis.
- To establish whether differences in LAR exist between varieties and between the same genotypes grown under different conditions.

5.3.3 Methodology

Plant measurements

The following data; number of liguled and non liguled lamina, the length of the visible leaf and its final length once liguled were extracted from the data collected on all genotypes using both non-destructive and destructive sampling techniques during experiments one and two. For more detail on the methodology used see chapter 4.

Meteorological measurements

In both experiments 1 and 1, air temperature was measured every hour, at 2 meters above ground by a Stevenson screen (located no more than 400 meters from the field site) and was used to calculate the thermal time. The sowing date is used as the base date from which degree days is calculated, for experiment one and two respectively the dates were the 16^{th} October 2003 and the 26^{th} October 2004. The accumulated TT was calculated as

$$TT = \sum (T - T_b) \tag{5.9}$$

with constraints

$$if T \leq T_b \, then \, T = T_b$$

where
T is the hourly mean air temperature divided by 24
T_b is the base temperature (0 °C), which has been reported to be the case for both spring and winter wheat (Baker *et al.* 1986, Cao and Moss 1989, Frank and Bauer 1997, McMaster and Wilhelm 1998).

During experiment 1, in addition to the air temperature, soil temperature at the depth of 3cm was also measured every hour within the canopy of one of the genotypes. Thermal time is calculated for experiment 1, using canopy temperature until the point of internode extension, which is assumed to be the date when the fourth leaf from the flag leaf becomes liguled (this assumes that there is a constant number of five internodes which extend per genotype). For experiment two only air temperature was recorded and thus this measurement only was used to calculate thermal time.

Experiment 1

Non-destructive sampling occurred weekly for genotypes Soisson and Isengrain (longer gaps were occasionally left between sampling dates) from the middle of February (2004) when the

plants had on average 6 visible and 5 liguled leaves up until the end of July (2004) when the flag leaf was present and most leaves were fully senesced. For the other genotypes, non-destructive sampling took place every two weeks from and to the same point of development as for genotypes Soisson and Isengrain. Data was collected from the main stem of twenty median plants per genotype and for all genotypes. For genotypes Soisson and Isengrain data was also collected on all tillers of ten of these twenty plants and for the other genotypes data was collected on the tillers of five of the twenty measured plants.

The first destructive sampling took place in December (2003) when on average 3 visible and 2 liguled leaves were present (except Soisson (SO04) where 4 visible and 2 liguled were present) and occurred at 4 separate dates up until the final measurement which occurred when the flag leaf had become liguled and the peduncle has completed growth. For genotypes, Soisson and Isengrain, data was collected on all axis of no more than twenty plants per sampling date and no more than thirteen for the other genotypes.

Experiment Two

Non-destructive sampling took place weekly for both genotypes, Soisson (SO05) and Caphorn (CA05). This sampling started in January (2005), when on average 5 visible and 3 liguled leaves were present on both genotypes and finished in May (2005) once the flag leaves on both genotypes had appeared. Data was collected from all axes of 30 tagged Soisson and Cap Horn plants. This number reduced during the sampling period to 15, whereby the 15 plants were identified as median plants. Data, however remained to be collected on the main stem only of the non-median plants throughout the sampling period.

Destructive sampling was carried out twice during the sampling period per genotype. The initial sampling date was in December (2004) when 3 visible and 2 liguled leaves were present and the final sampling date was once the flag leaf had liguled, which was in May (2004).

5.3.4 Data analysis

The appearance of each leaf and the thermal time of this event was not directly measured in either experiment 1 or experiment 2. Instead a developmental index is used per axis per genotype for each sampling date, of which the thermal time is known. Although the use of a developmental index is not sufficient to investigate the most appropriate model of leaf appearance, as it is an estimate of leaf appearance in the absence of direct measurements, it is assumed to be sufficient to explore the differences in LAR between axes and genotypes. This is due to the index giving an indication on the plant stage based on both the number of fully ligulated leaves and developing leaves thus giving a continuous index of development.

Choice of index

The decimal phytomer index (Ljutovac 2002, Hillier *et al.* 2005) is a modified Haun stage, which gives a more continuous index. In calculating this index sufficient data is required to determine the length of the visible leaf (per rank and axis) when the subsequent leaf emerges, however the quantity of such data was not available from either experiment one or two. As such, the Haun stage is the developmental index used within this analysis.

The Haun stage used in the following analysis was however modified slightly (see equation:5.10) so that

$$HS = L_n/L_{(nl)} + (n-1) \tag{5.10}$$

where:
n is the number of visible leaves on the axis
L_n is the length of the youngest visible leaf
$L_{(nl)}$ is the length of youngest visible leaf once liguled

In the rest of this section, where the Haun stage is mentioned it has been calculated using equation 5.10.

Calculation of Index

The method used to calculate Haun stage varied slightly depending on the sampling technique used to collect the data set. The median number of final leaves per axis per genotype was calculated from the final non-destructive data. The data collected on the axis of plants which developed to have the median number of final leaves were used in the analysis. Any data collected on any axis that did not develop to produce the median final number of leaves was excluded. The actual final length of the visible leaf once liguled could be used with non-destructively sampled data. For non-destructive data, the mean final length of the visible leaf once liguled had to be used per genotype as the actual final length was not known. Due to the sampling procedure used in Experiment 2, only the mean final length of the visible leaf once liguled was used to calculate the Haun stage per sampling date regardless of the sampling strategy used.

Calculation of LAR per axis and per genotype

A linear model is chosen to be the most appropriate to simulate the relationship between Haun stage and thermal time for all axis. The LAR which is estimated as the slope of this model is compared between axis and genotypes.

Estimation of thermal time when flag leaf is liguled

When the flag leaf has become liguled, the number of liguled leaves is equal to the number of visible leaves; the Haun stage, for the purpose of this analysis in such cases, is set to be the final number of leaves. This enables the Haun stage to increase over thermal time and then to plateau when the final number of leaves are present. By applying the LAR model as suggested from the initial analysis with an additional straight line model with gradient equal to zero, to simulate the plateau in Haun stage over thermal time, the point at which both models converge is accepted to be a good estimate of the thermal time once the flag leaf has become liguled. This is carried out per axis and genotype and compared between both axis rank and genotype.

5.3.5 Results

Model of LAR

Figure 5.8 shows graphically the relationship between thermal time and Haun stage per axis for all genotypes. The solid line represents the linear model simulating the rate of leaf appearance and the points represent the mean Haun stage. No data is available for genotypes Soisson (SO99low or SO99), from the experiment carried out by Ljutovac in 1999.

The linear model fits to all genotypes and axis with a high r^2 value with the lowest fit being 0.943 (rmse 31) on genotype Soisson (SO05) tiller three.

Comparison of LAR with axis

Each solid black line on Figure 5.9 represents the LAR on all axis for one genotype and is shown to be fairly constant for all tillers, with a slightly lower LAR estimated for the main stem and a slightly higher LAR estimated for tiller 3. Although these differences are not shown to be significant when the standard deviation is taken into account.

Synchrony of the appearance of the liguled flag leaf between axis

Table 5.9 contains the estimated thermal time at which the flag leaf becomes liguled for each genotype per axis. The standard deviation is shown to be higher when comparing per axis between genotypes than per genotype and between axis. No thermal time is calculated for tiller three of genotypes caphorn (CA04) or Recital (RE04) due to low data quantity.

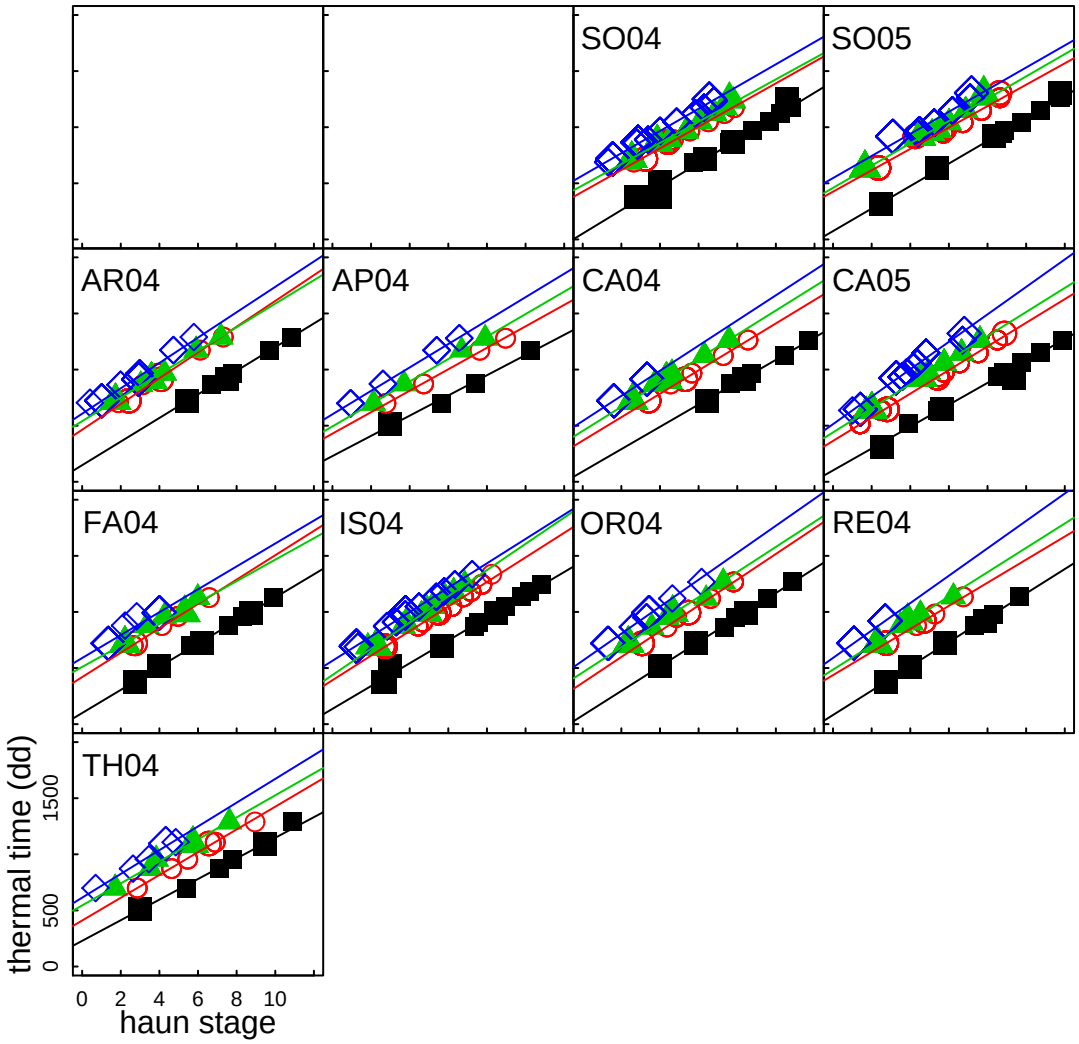

Figure 5.8: Thermal time (in degree days) against Haun stage for all axis for all genotypes. Larger points indicate destructive data and smaller points non-destructive data. The axes are distinguished by the colour and style of points; black square=main stem, red circle=tiller one, green triangle=tiller two and blue diamond=tiller three. The model of LAR is shown per axis using a continuous coloured line, the colour of the line distinguishing the rank of the axis.

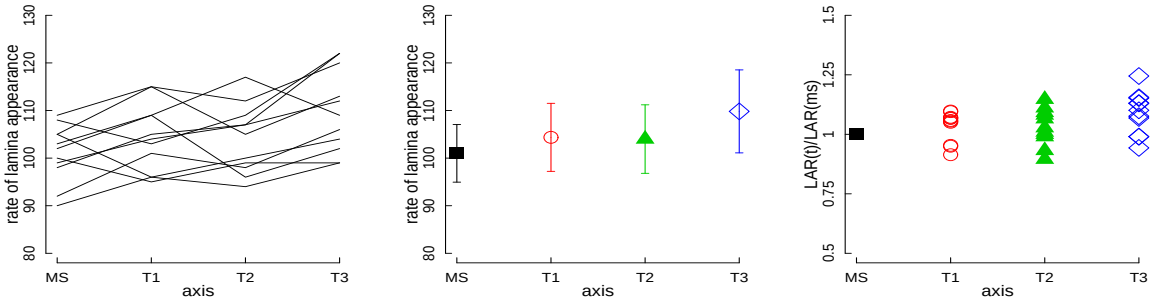

(a) (b) (c)

Figure 5.9: a)LAR per axis per genotype, with each line representing a genotype. b)Mean ± sd of LAR per axis with different axis represented by a different colour and design of point, see Figure 5.8 for key. c)LAR(t)/LAR(ms), against axis(t), where t = 1,2,3.

Genotype	MS	T1	T2	T3	Mean ± sd
SO04	1214	1201	1234	1265	1228 ± 28
SO05	1275	1286	1253	1304	1280 ± 21
AR04	1412	1509	1483	1528	1483 ± 51
AP04	1223	1287	1295	1332	1284 ± 45
CA04	1257	1261	1268	–	1262 ± 6
CA05	1263	1298	1257	1359	1294 ± 47
FA04	1120	1135	1091	1003	1087 ± 59
IS04	1243	1295	1242	1352	1283 ± 52
OR04	1262	1266	1277	1328	1283 ± 30
RE04	1127	1131	1167	–	1142 ± 22
TH04	1232	1333	1297	1140	1251 ± 85
mean ± sd	1239 ± 78	1273 ± 103	1293 ± 157	1265 ± 103	

Table 5.9: Estimated thermal time in degree days at which flag leaf becomes liguled per genotype, per axis. Mean and standard deviation given per genotype over all axis and per axis over all genotypes

Phytomer shift

A linear model with slope one is shown to have a reasonable fit and therefore relevant to represent the relationship between the Haun stage on the main stem and that on the tillers with the intercept of this model accepted to be the 'shift' in Haun stage per tiller This calculated shift (mutliplied by -1) is compared to the shift parameters as estimated within the final organ length analysis (the mean shift parameters calculated for all final organ length models, per genotype) (see section 5.2.4). Figure 5.10 shows the linear relationship between both these estimated shift parameters for all three axis when considering all genotypes.

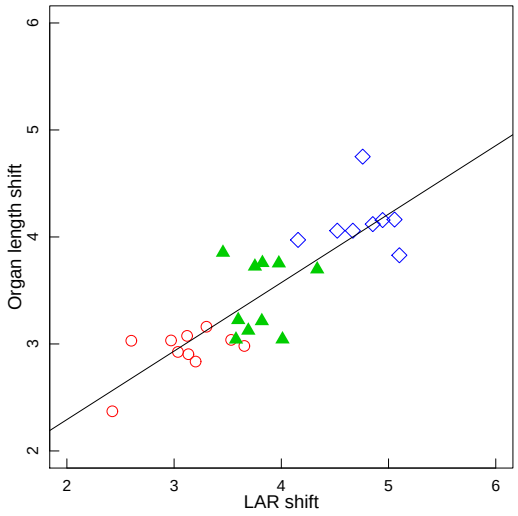

Figure 5.10: Shift parameters as estimated per genotype from the final lamina length model against the LAR shift, the fit of linear model (shown as a black continuous line) is r^2 0.78. Red circular points= tiller one, green triangles=tiller two and blue diamonds=tiller three

Table 5.10 containing the fit and rmse of this (r^2) model per axis per genotype and for all axis per genotype.

genotype	T1 r^2 (rmse)	T2 r^2 (rmse)	T3 r^2 (rmse)	all axis r^2 (rmse)
$SO04$	0.98 ± 0.22	0.98 ± 0.26	0.99 ± 0.20	0.99 ± 0.23
$SO05$	0.96 ± 0.41	0.95 ± 0.42	0.90 ± 0.42	0.95 ± 0.42
$AR04$	0.94 ± 0.43	0.98 ± 0.29	0.96 ± 0.27	0.97 ± 0.34
$AP04$	0.95 ± 0.57	0.96 ± 0.45	0.94 ± 0.44	0.96 ± 0.50
$CA04$	0.98 ± 0.24	0.68 ± 0.93	$-$	0.89 ± 0.65
$CA05$	0.99 ± 0.26	0.99 ± 0.20	0.89 ± 0.56	0.97 ± 0.37
$FA04$	0.996 ± 0.10	0.86 ± 0.53	-1.08 ± 0.87	0.87 ± 0.54
$IS04$	0.98 ± 0.25	0.86 ± 0.59	0.95 ± 0.39	0.95 ± 0.42
$OR04$	0.98 ± 0.23	0.70 ± 0.90	0.00 ± 1.09	0.79 ± 0.81
$RE04$	0.99 ± 0.10	0.81 ± 0.56	$-$	0.93 ± 0.41
$TH04$	0.90 ± 0.45	0.93 ± 0.50	0.93 ± 0.35	0.95 ± 0.45

Table 5.10: The r^2 of the fit and associated rmse of the fitted model using the relationship found between the mean shift parameter per genotype for final organ length models to model the shift in leaf appearance between the main stem and tiller leaves.

As can be observed from Table 5.10 the fit of the model to all axis is generally quite high but there are a few exceptions. The fit of the model to the LAR of genotypes Oratario (OR04) and Recital (RE04) tiller three is not calculated as these two genotypes have very little observed data on which to apply a model.

Comparison between genotypes

The mean LAR per genotype as calculated as the mean LAR of all four axis, MS, T1, T2, & T3 is very similar for genotypes grown in both experiments one and two (see Table 5.11) with the mean LAR for all genotypes from both experiments being 105 ± 6. The mean LAR over all axis of all genotypes fall within this acceptable range. No significant difference is noticed between the LAR over all axis of genotypes Soisson and Caphorn when grown under different conditions (SO04 & SO05 and CA04 & CA05).

Genotype	mean $\pm$ sd LAR
SO04	98 ± 4.8
SO05	98 ± 2.2
AR04	110 ± 5.3
AP04	98 ± 6.0
CA04	106 ± 5.4
CA05	108 ± 10.1
FA04	102 ± 5.3
IS04	109 ± 6.1
OR04	114 ± 4.7
RE04	110 ± 8.1
TH04	99 ± 5.9

Table 5.11: Mean $\pm$ standard deviation of LAR per genotype

5.3.6 Discussion

The sampling frequency differed between genotypes and consequently on some occasions more than one leaf emerged between sampling dates (using either sampling technique; destructive or

non-destructive. For some genotypes there is more than one occasion where the mean difference in Haun stage is greater than 1 between sampling data and that the maximum difference is less than 1 for one genotype only (and one axis of this genotype). Although different sampling periods have been used to characterise main stem Haun stage and LAR, ranging from daily (Haun 1973), every 2-days (Hotsonyame and Hunt 1997), every 3-5 days (Yin and Kropff 1996) to weekly (Cudney *et al.* 1989, Juskiw *et al.* 2001), the low sampling frequency of data collected in both experiment 1 and 2 does mean that a detailed response of LAR to the environment cannot be studied. However it should be noted that it does not hinder the completion of the aims of this section.

As expected a strong linear model was found between the Haun stage and thermal time of most axes per genotype as suggested by (Skinner and Nelson 1995). It was found that the LAR over all axes is similar with no significant differences between axis being noted. This along with the finding that the thermal time at which the flag leaf became liguled is similar on all axes per genotype adds to the idea that tillers are mini-main stems and that leaves which appear at the same thermal time have the same properties. The differences in thermal time of flag leaf ligulation were, for most genotypes (except TH04), over all axes, less than 60 degree days. The mean thermal time for the appearance of a leaf is assumed from this analysis to be 105 degree days and as such, the flag leaves on all axes becomes liguled well within the appearance time of one leaf which could be attributed to the way in which the thermal time of flag leaf ligulation was estimated.

Assuming that the LAR is the same on all axes, a shift parameter can be used to simulate the LAR over all tillers from the LAR on the main stem, a finding discussed when modelling final organ length. The relationship between the shift between the LAR on the main stem and the tillers and the phytomer shift as noted between the same axis when simulating final organ length was found, (r^2 : 0.78). Using this relationship enabled the LAR on all axes to be simulated from a model of LAR on the main stem only. Again it was found that the model fit to the observed data was high with the exception of a couple of genotypes. Utilising this relationship results in a reduction of parameters within the model, which is an overall aim of this thesis.

Differences in the mean LAR for all axes between genotypes grown under the same environmental conditions was found to be small, although the overall difference in temperature between growing seasons was also found to be small. In general no significant difference in the mean

LAR for all axes was found bewtween genotypes when the standard deviation around the mean value for all genotypes was taken into account.

Month	Experiment	
	One	Two
November	8.1	7.3
December	4.8	3.3
January	4.7	5.1
February	5.0	2.8
March	6.6	7.1
April	10.1	10.6
May	12.7	13.5
Mean	7.4	7.1

Table 5.12: Mean monthly air temperature (°C) during the growing season of both experiment one and two, and the overal mean temperature for both years between December and May.

.

5.3.7 Conclusion

Overall it is was found that LAR is similar between genotypes, which is consistent with the results of Birch *et al.* (1998). Slight differences in LAR between the same genotypes grown in different years (SO04 & SO05, CA04 & CA05) were noted but not thought to be important. Overall therefore it cannot be suggested that the adjustment of LAR is more appropriate per environmental conditions than with regards to genotype, which was the final conclusion of (Birch *et al.* 1998). From the results of this analysis it is suggested that LAR does not differ significantly between axes and can be assumed to be the same as the main stem. Synchrony between the appearance of the flag leaf on all axes was found to be good which also adds to the idea that tillers can be assumed to be delayed main stems as first discussed within the final organ length section of this thesis. Assuming that the tillers are delayed main stems, the delay, or shift parameters as estimated by the final organ length models were used, with some adjustment, to model LAR on the tillers from the model of LAR on the main stem. A good fit of this model to observed data, for most axes on most genotypes was found. This method reduces the overall number of parameters required by the model which is an ultimate aim of this thesis.

5.4 Tiller dynamics

5.4.1 Introduction

Tillering is an important adaptive feature of wheat which balances the assimilate sources and sinks within the plant and increases the yield per acre, yet as Lafarge *et al.* (2002) stated 'the prediction of tillering is poor or absent in existing sorghum crop models'

Accurate simulation of tillering is essential for the accurate prediction of crop LAI (Leaf Area Index) development (Hammer *et al.* 1987, Lafarge and Hammer 2002) and hence on crop water use patterns and adaptation to water limited environments (van Oosterom *et al.* 2008) and importantly, crop yield. Within agronomic practises, tiller density can be used as LAI is, to determine the optimum level of inputs such as fertilizers, fungicides and growth regulators at given stages of crop development and to account for variations within a field (Scotford and Miller 2004). Crop models from which tiller density can be predicted are therefore useful tools for agronomic decision making processes as well as for the analysis and design of ideotypes due to their increased ability to explain interactions between canopy architecture and crop performance (Evers *et al.* 2004). This thesis is focused on developing a crop model to be used within remote sensing studies. For such models, the ability to simulate the development and architecture of tillers is of importance as they alter either directly (microwave) or indirectly (optical) the remote sensing signal.

SHOOTGRO (McMaster 1992), I-wheat (Integrated Wheat Model) (Meinke *et al.* 1998) and ADEL-wheat have attempted to some degree to include environmental conditions to control tiller production. Within the SHOOTGRO model the percentage of each tiller that appears and aborts on plants of a cohort are controlled by water, nitrogen and light conditions. The Integrated Wheat Model (I-WHEAT) also takes into account water or nitrogen limitations, which result, as in the SHOOTGRO model, in accelerated tiller death. Currently within the ADEL-wheat model tillers are considered to be and generated just like the main stem. One difference being that they are derived by axillary bud modules which are temporary modules that abort if tillering is not authorised during a phase of latency. The mechanisms behind the plants decision to abort the bud or to allow it to grow into a tiller are not considered within the model, instead a number of buds giving rise to a tiller is set as a parameter along with the duration of latency (approx. 4

plastochrons for all axis) (Fournier *et al.* 2000).

It is important here to acknowledge the differences between tiller production, tiller cessation and tiller death. Tiller production controls the number of buds on the main stem that are produced into tillers. Tiller cessation is the point at which bud formation ceases, thus creating a maximum tiller number per plant and tiller death regulates the number of tillers that have been produced that will survive to produce a viable head.

Studies on wheat (Friend 1965) and other crops (Honda and Okajima 1970, Kirby 1972) have led to the suggestion that tiller production depends on resource availability, such as nitrogen and carbohydrate. Recently, however Kim *et al.* (2010b) have suggested that a supply demand ratio is a key factor controlling not only tiller production but their growth and survival. This ratio is described as a complex indicator of plant carbohydrate status that depends on both environmental and genotypic factors. Solar radiation and temperature being the main environmental factors that affect the Supply/Demand ratio. Solar radiation was also found by Evers (2006) to affect tiller dynamics, mainly cessation, and in response coupled the architectural model ADEL-wheat with a light model (nested radiosity)(Chelle and Andrieu 1998). This enabled the amount of PAR (photosynthetically active radiation) and R(red):FR(far red) sensed by the plant at each leaf to be estimated, allowing some control over tiller production and cessation to be included within the model. Tiller death was not formally included within this model. Coupling ADEL-model with a light model is computationally expensive and parameter heavy. This chapter seeks a more semi-empirical approach to including tiller dynamics.

Lafarge *et al.* (2002) found that tiller emergence ceased at an optimal LAI value and stated that it is probably associated with hormonal effects in response to changes in light quality (red:far-red ratio). Using the LAI values, which are already estimated within the model would require less parameters and also in a semi-empirical way would incorporate the light quality affects that are suggested to control tillering without the need of an additional light model.

Tiller death is thought to be associated with anthesis, an important reproductive stage, which occurs about 3 phyllochron after the appearance of the flag leaf ligule (Jamieson *et al.* 1998a). Significant tiller death is thought to occur at the transition from vegetative to floral state due to assimilates from the main culm leaf being exported towards the elongating internodes to the detriment of tillers (Lauer and Simmons 1985). The rate of reduction in number of tillers pro-

duced has been shown by Lafarge *et al.* (2002) to be linearly related to the ratio of realized to potential leaf area growth. This is an indicator of the source-sink balance in young plants and they suggest that this ratio provides a basis by which to predict the rate of decrease in the number of potentially fertile tillers. Any decrease in tiller number is further suggested to reduce the rate of potential leaf area growth until the balance point with realizable leaf area is reached. The model they suggest requires planting density, daily temperature and incident radiation as inputs and provides a means to simulate fertile tiller dynamics in sorghum for a wide range of conditions. It is suggested within this chapter that a developmental cue is used to indicate the start of tiller death eliminating the need to calculate incident radiation within the model.

In order to incorporate the differing survival rates according to tiller rank, a hierarchal approach is suggested, similar to that used by Kim *et al.* (2010a) and Lafarge *et al.* (2002).

In summary this section looks at incorporating a semi-empirical approach to modelling tiller dynamics by taking advantage of the observed correlations between LAI values (Lafarge *et al.* 2002), as mentioned, and appearance of flag leaf ligule (developmental stage). A hierarchical approach to tiller production and survival is also included to incorporate the differing production and survival chances per axis rank.

5.4.2 Data Collection

For a detailed description of how the data used in this analysis was collected refer to chapter 4. The presence of tillers was recorded using both destructively and non-destructively sampled plants from a range of winter wheat genotypes, over two growing seasons. In general tagged median plants were used to obtain measurements although exceptions do exist (see chapter 4). A tiller was marked as present if it had grown between sampling visits (one to two weeks apart) and absent if no growth had occurred. Only the presence of primary tillers ranked 1-3 are included in this analysis. Secondary tillers and primary tillers ranked 4 or above have been omitted due to the lack of these tillers reaching full maturity and the limited time frame at which they were found to be present during the plant's development. In order to calculate the green leaf area index of the plants the number of liguled and non liguled leaves was also recorded as well as the final lamina length and final maximum lamina width and percentage area senescence of the leaves. Final lamina length being the distance from the ligule to the tip and maximum width the

distance between the edge of the lamina at its widest point. Sensecence was estimated visually as the percentage area of leaf which had turned yellow or brown. The number of plants from which observations were made at each sampling date differed per genotype and year; for non-destructive sampling a minimum of five and maximum of ten plants per sampling date were measured and for destructive a minimum of ten and a maximum of thirteen plants.

Air temperature, at 2 m above ground, was recorded hourly by a Stevenson screen located no more than 400 m from the experimental plots in both experiment 1 and 2. In experiment 1 soil temperature was also measured at a depth of 2 m by thermocouples located within the canopy of one of the genotypes. These measurements were used to calculate thermal time.

5.4.3 Data Analysis

The sowing date is used as the base date from which degree days is calculated. For experiment 1 this was the 16^{th} October 2003 and for experiment 2, the 26^{th} October 2004. The accumulated TT was calculated as

$$TT = \sum (T - T_b) \tag{5.11}$$

with constraints

$$if\ T \leq T_b\ then\ T = T_b$$

where
T is the hourly mean air temperature divided by 24
T_b is the base temperature (0 °C), which has been reported to be the case for both spring and winter wheat by (Baker *et al.* 1986, Cao and Moss 1989, Frank and Bauer 1997, McMaster and Wilhelm 1998).

For experiment 1, soil temperature was used to calculate thermal time up until the point of internode extension, which is assumed to be the date when the fourth leaf from the flag leaf becomes liguled (this assumes that there is a constant number of five internodes which extend per genotype). For experiment 2 only air temperature was recorded and thus this measurement, only, was used to calculate thermal time.

Dynamic tiller model

The mean number of tillers per plant per genotype is calculated per sampling date and compared against thermal time. A model is suggested that is consistent with the observed pattern over all genotypes. The suggested model is fitted using the gnls function in the free statistical package R (R Development Core Team 2005), which performs numerical non-linear regression using a modified Newton-Raphson method. The model is fitted separately to data collected per genotype. For some genotypes data is absent over lower thermal time and in such cases the model is adjusted accordingly.

Tiller Hierarchy

The ratio of each tiller (per rank) present by the potential number is calculated per sampling date per genotype (as used in the GLAI (Green leaf area index) calculation). The maximum ratio observed throughout the growing season is given as the maximum potential number of each tiller rank to be produced and the ratio of tiller survival is assumed to be the ratio recorded on the final sampling date. The hierarchy of tiller production and survival is compared between the tillers 1, 2 and 3.

Parameter Correlation

In order to reduce the parameters required to model tiller dynamics model parameter correlation is explored as is the correlation of specific timings in terms of tiller dynamics and GLAI and the number of leaves on the main stem.

GLAI

Green leaf area index has been confirmed by previous studies to be associated with tiller dynamics. In order to compare the development of GLAI over time and tiller dynamics the GLAI is

estimated from the phenological data collected over experiment 1 and 2 using equation 5.12.

$$GLAI = A - A * S \tag{5.12}$$

where

$$A = L * W * FF \tag{5.13}$$

where
A = leaf area
S = fractional senescence
L = maximum lamina length
W = maximum lamina width
FF= form factor (This is assumed to be 0.76, see 6.1.7).

In order to obtain GLAI the mean GLAI per axis, for each sampling date, is initially calculated and then multiplied by the assumed plant density (250 p/m^2) and the percentage presence of each axis. The percentage presence of each axis being calculated as the number of each tiller rank present by the potential number present (i.e the number of sampled plants). The percentage presence of the main stem being assumed to be 100%. The sum of the GLAI over all axes is given as a good estimate of GLAI. A simple model of GLAI is suggested and fitted to all genotypes, using the gnls function within R. The GLAI over lower thermal time and until the maximum GLAI is also fitted using an exponential relationship in order to compare the GLAI more accurately at the thermal time of tiller cessation.

The rate of tiller death between the maximum number of tillers produced and the number of tillers surviving to produce a head is compared between genotypes. A comparison between this rate and changes in GLAI at this time are also compared.

Final Number of Main Stem Leaves

Tiller development is thought to be affected by the number of leaves on the main stem, with the decrease in tiller numbers reducing around the same time that the flag leaf ligule appears (Lafarge and Hammer 2002). In order to investigate such a relationship a linear relation is assumed between thermal time and leaf ligule appearance. From this linear relationship the thermal time at

which the flag leaf ligule appears is estimated (per genotype) and this thermal time is compared to the dynamic tiller model to investigate if a correlation between the two exists.

5.4.4 Results

Dynamic Tiller Model

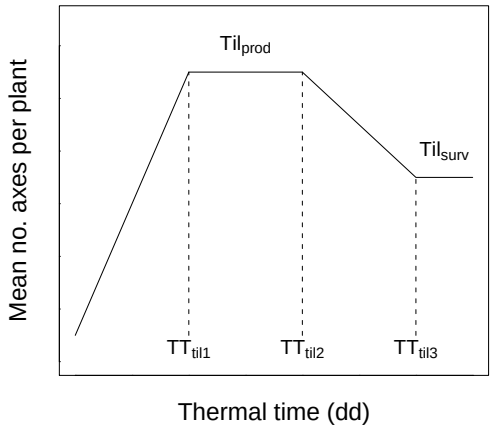

Figure 5.11: Schematic diagram of the tiller model over thermal time labelled with the model parameters.

Figure 5.11 is a schematic representation of the pattern, observed on all genotypes from both experiment 1 and 2, of the mean number of tillers per plant over thermal time. An initial increase in the mean number of tillers per plant is shown to occur over lower thermal time followed by a plateau. This plateau represents a mean maximum number of tillers per plant. At the end of this plateau, mortality of tillers occurs until a second lower plateau, which corresponds to the maximum number of axes per plant at the end of the plants development.

From this visual analysis the following model is suggested with five parameters, TT_{til1}, TT_{til2}, TT_{til3}, Til_{prod} and Til_{surv} (shown also on Figure 5.11).

$$\begin{array}{ll} \frac{Til_{prod}}{TT_{til1}-TT_{min}} * (TT - TT_{min}) & \text{for } TT \leq TT_{til1} \\ Til_{prod} & \text{for } TT_{til1} < TT \leq TT_{til2} \\ Til_{prod} + \frac{Til_{surv}-Til_{prod}}{TT_{til3}-TT_{til2}} * (TT - TT_{til2}) & \text{for } TT_{til2} < TT \leq TT_{til3} \\ Til_{surv} & \text{for } TT_{til3} < TT \end{array} \quad (5.14)$$

where
TT_{til1} is the thermal time at the beginning of Til_{prod} plateau
TT_{til2} is the thermal time at the end of Til_{prod} plateau
TT_{til3} is the thermal time at the beginning of Til_{surv} plateau
Til_{prod} is the maximum number of axes per plant
Til_{surv} is the number of axes per plant after rank TT_{til3}
TT_{min} is the thermal time from which tillers start to be produced which is set to be 350 degree days

Figure 5.12 shows the tiller dynamic model against observed data (black points). The model shown in green highlights where the model was found to converge with the data and gives an estimate of the parameter fit and the red, highlights where the best fit model was applied visually. For genotypes Apache (AP04), Arminda (AR04) and Caphorn(CA04) the model was altered to exclude the initial increase in tiller number before the maximum plateau. Table 5.13 contains the estimated parameter values of the fitted individual tiller model for each genotype and the ratio between the parameters Til_{prod} and Til_{surv}. This ratio is shown to vary greatly between genotypes, with 0.44 (CA05) being the lowest and 0.83 (FA04) the highest. The fit and rmse of the model is given per genotype in Table 5.13 to each genotype, the lowest being with AR04 with a r^2 of 0.9 and rmse 0.06, the degree days difference between the TT_{til2} and TT_{til3} within genotypes is small with the variation being less that 100 degree days between all genotypes.

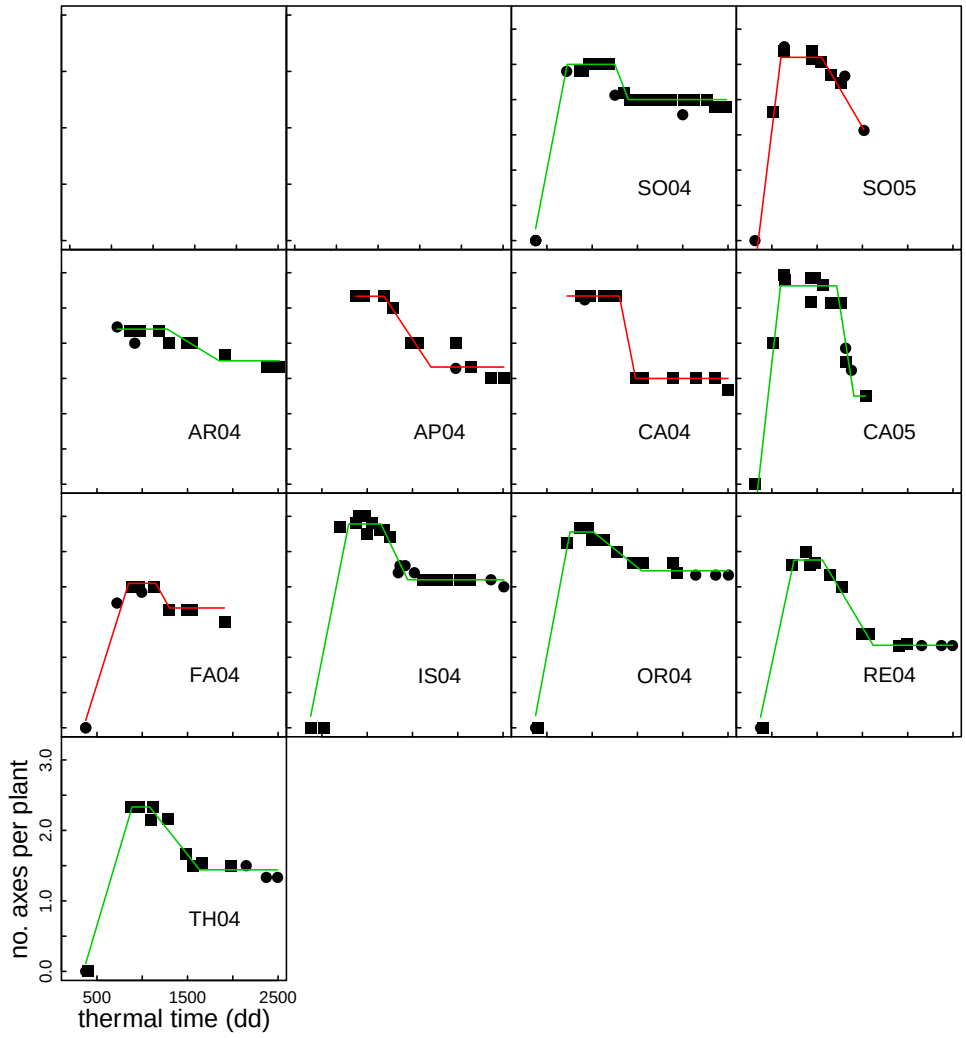

Figure 5.12: Mean number of tillers per plant per thermal time shown per genotype. Circular points are used to distinguish data collected using destructive sampling to that collected using non-destructive sampling. The green line represents the fitted model and the red line the best fit model.

Gen	TT_{til1}	TT_{til2}	TT_{til3}	Til_{prod}	Til_{surv}	Ratio	$Rate_{Death}$	$r^2 \pm$ rmse
SO04	732	1157	1379	2.45	1.97	0.80	-0.0022	0.99 ± 0.09
SO05	600	1050	1550	2.60	1.50	0.58	-0.0022	0.96 ± 0.16
CA04		1300	1480	2.67	1.50	0.56	-0.0065	0.99 ± 0.05
CA05	595	1216	1406	2.81	1.25	0.44	-0.0082	0.95 ± 0.18
AR04		1122	2349	2.14	1.67	0.78	-0.0004	0.90 ± 0.06
AP04		1185	1704	2.67	1.66	0.62	-0.0019	0.92 ± 0.13
FA04	850	1150	1300	2.05	1.70	0.83	-0.0023	0.97 ± 0.12
IS04	796	1152	1447	2.89	2.10	0.73	-0.0027	0.94 ± 0.26
OR04	756	1013	1547	2.78	2.23	0.80	-0.0010	0.98 ± 0.13
RE04	746	1058	1619	2.38	1.17	0.49	-0.0022	0.98 ± 0.11
TH04	888	1082	1633	2.33	1.44	0.62	-0.0016	0.98 ± 0.12
mean	745	1135	1583	2.52	1.65	0.66	-0.0028	
sd	106	82.63	280.95	0.28	0.33	0.13	0.0024	

Table 5.13: Tiller model parameter values are shown along with the ratio of Til_{prod}:Til_{surv} and the rate of tiller death between TT_{til3} and TT_{til2} and the fit of the model ($r^2 \pm$ rmse)

Tiller Hierarchy

The likelihood of each tiller (rank 1, 2 and 3) being 'allowed' to develop seems equal, see Table 5.14 for details, were it can be observed that there is no significant difference between percentage of tillers produced according to rank. However for tiller survival, tiller three is shown to have a significantly lower survival rate than both tiller one and two. The survival rate for tiller one and two is noted as being very similar.

genotype	Tiller production			Tiller survival		
	t1	t2	t3	t1	t2	t3
SO04	0.70	0.95	1.00	0.60	0.80	0.60
SO05	0.85	1.00	1.00	0.50	0.62	0.44
CA04	0.92	1.00	1.00	0.67	0.83	0.00
CA05	1.00	1.00	1.00	0.62	0.38	0.25
AP04	1.00	0.83	1.00	0.83	0.33	0.67
AR04	0.62	1.00	0.92	0.50	0.83	0.67
FA04	0.67	0.92	0.85	0.67	0.83	0.17
IS04	1.00	1.00	1.00	0.80	0.80	0.50
OR04	1.00	1.00	1.00	1.00	0.83	0.50
RE04	0.83	0.85	0.85	0.67	0.67	0.00
TH04	0.83	0.83	0.77	0.46	0.77	0.31
$mean \pm sd$	0.86 ± 0.14	0.94 ± 0.07	0.94 ± 0.09	0.67 ± 0.16	0.70 ± 0.19	0.37 ± 0.25

Table 5.14: The ratio of tillers emerged and survived per axis and per genotype is shown. The mean and standard deviation ratio of tillers emerged and survived is given per axis for all genotypes

These results are also displayed graphically in Figure 5.13 with the percentage of each tiller present (to potential number) displayed against thermal time in degree days. In general, for all genotypes, an increase is observed over lower thermal time followed by a decline in ratio until a plateau of final ratio is achieved. This final plateau is less obvious with the data collected on genotypes Soisson (SO05) and Caphorn (CA05) during experiment 2 due to the measurements finishing earlier in the growing season than compared to experiment 1. From Figure 5.14 the percentage of tiller 2s present is shown to be slightly greater than tiller 1, which is slightly greater than the percentage of tiller 3's, as mentioned. However when each genotype is considered separately (see Figure 5.13 this pattern is not found to be consistent between genotypes.

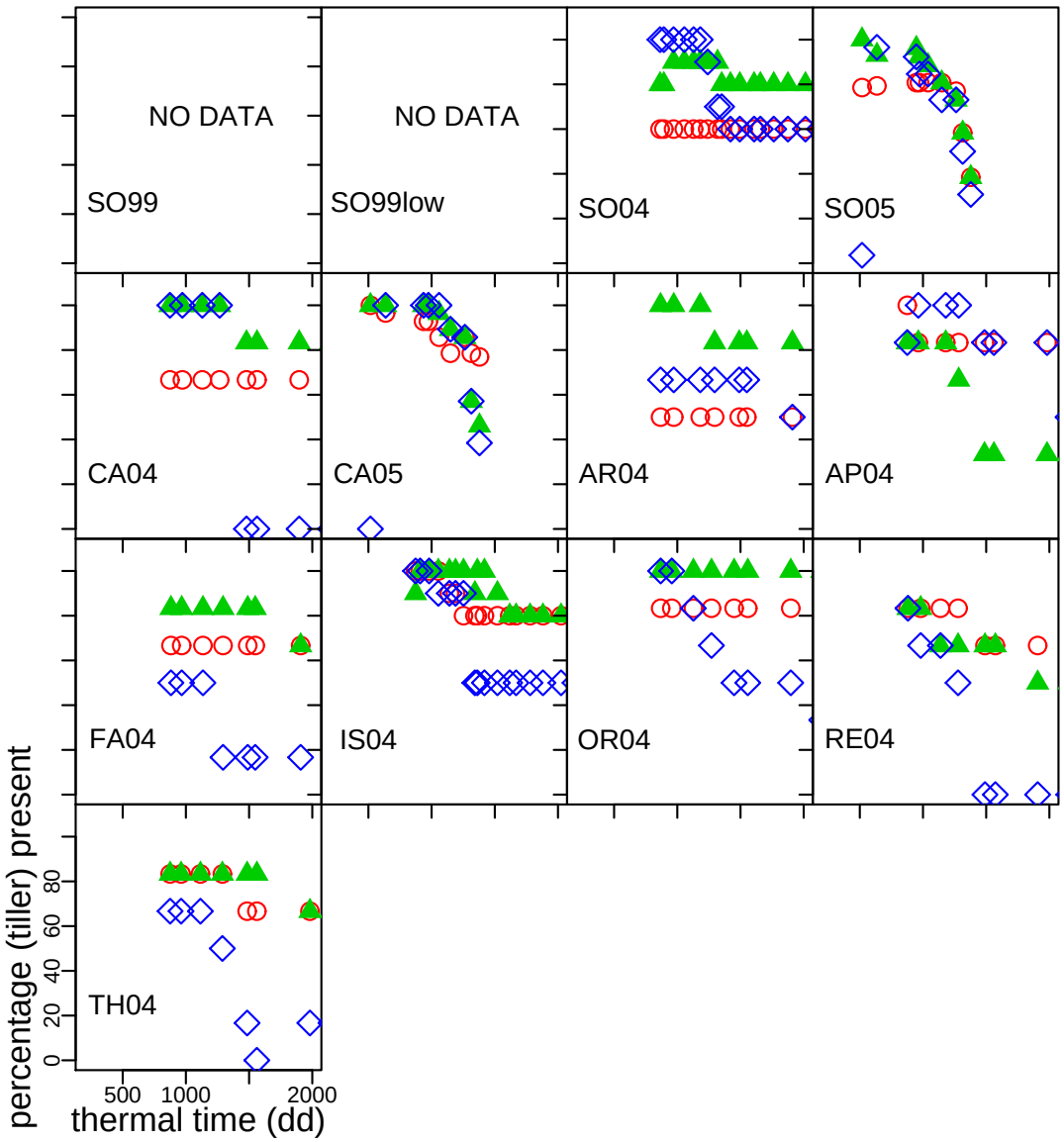

Figure 5.13: The percentage presence of each tiller over thermal time and per genotype. Red circles are Tiller 1, Green triangle, Tiller 2 and blue diamonds Tiller 3.

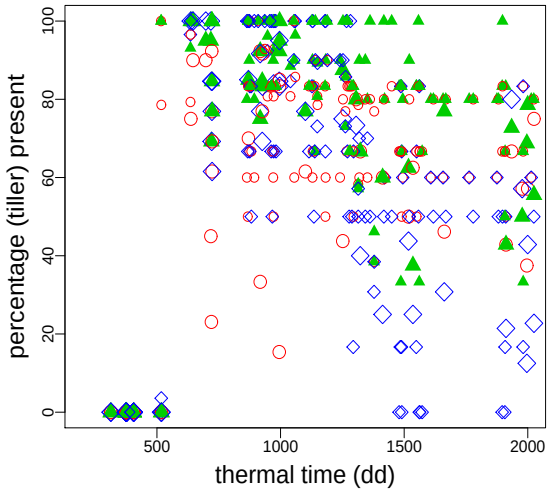

(a)

Figure 5.14: The percentage presence of each tiller present over thermal time for all genotypes.Red circles are Tiller 1, Green triangle, Tiller 2 and blue diamonds Tiller 3.

Model parameter correlations

Correlation between the parameters of the dynamic tiller model are investigated. Figure 5.15 illustrates the lack of correlation found between the different model parameter values between genotypes. From this it was assumed that no significant correlations exist.

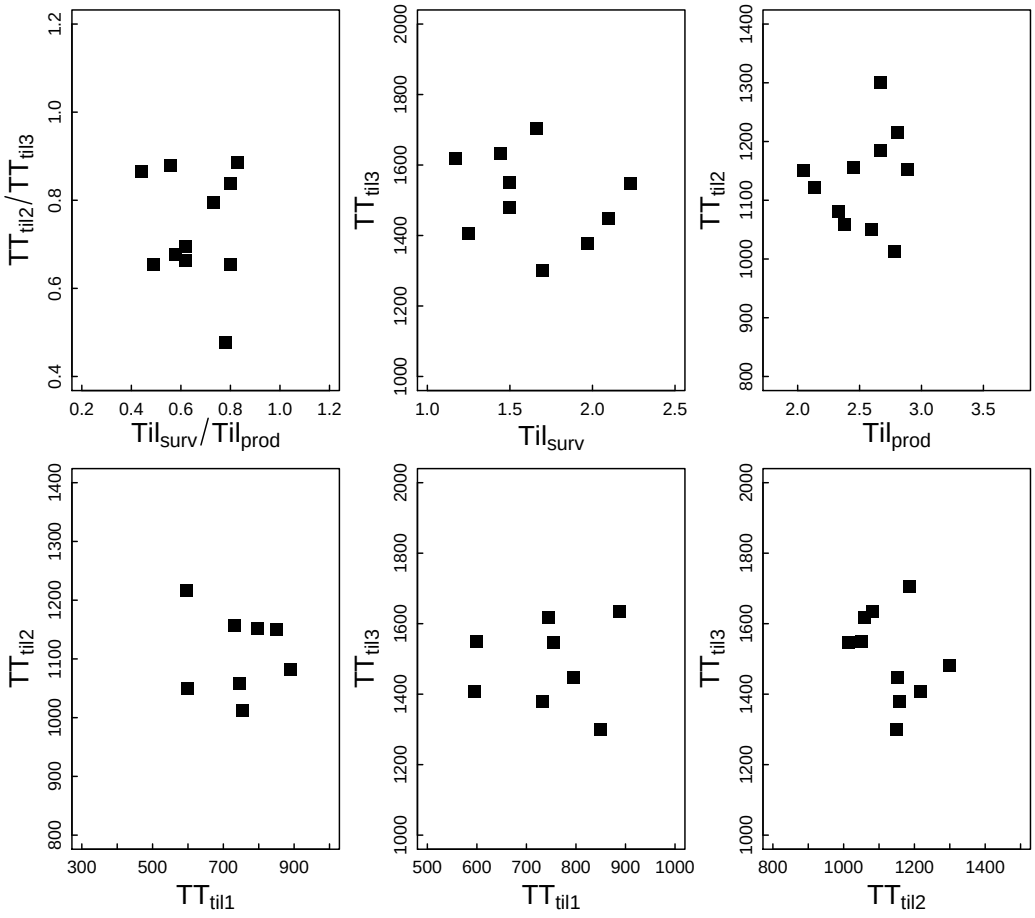

Figure 5.15: Comparison is shown between the estimated parameter values from the tiller dynamic model.

GLAI

GLAI was calculated as explained for each genotype and is displayed over thermal time in Figure 5.16. It is shown in these figures to increase exponentially over lower thermal time until a maximum GLAI is reached. After this point GLAI reduces significantly over a short period of time before reducing at a much slower rate. This is a stable pattern observed on all genotypes. Figure 5.16 enables to some extent a visual comparison of the fitted tiller model with the progression of GLAI over thermal time. There are two genotypes where the GLAI data is of good quality over the transition points of the GLAI model, which are Soisson (SO04) and Caphorn (CA04).

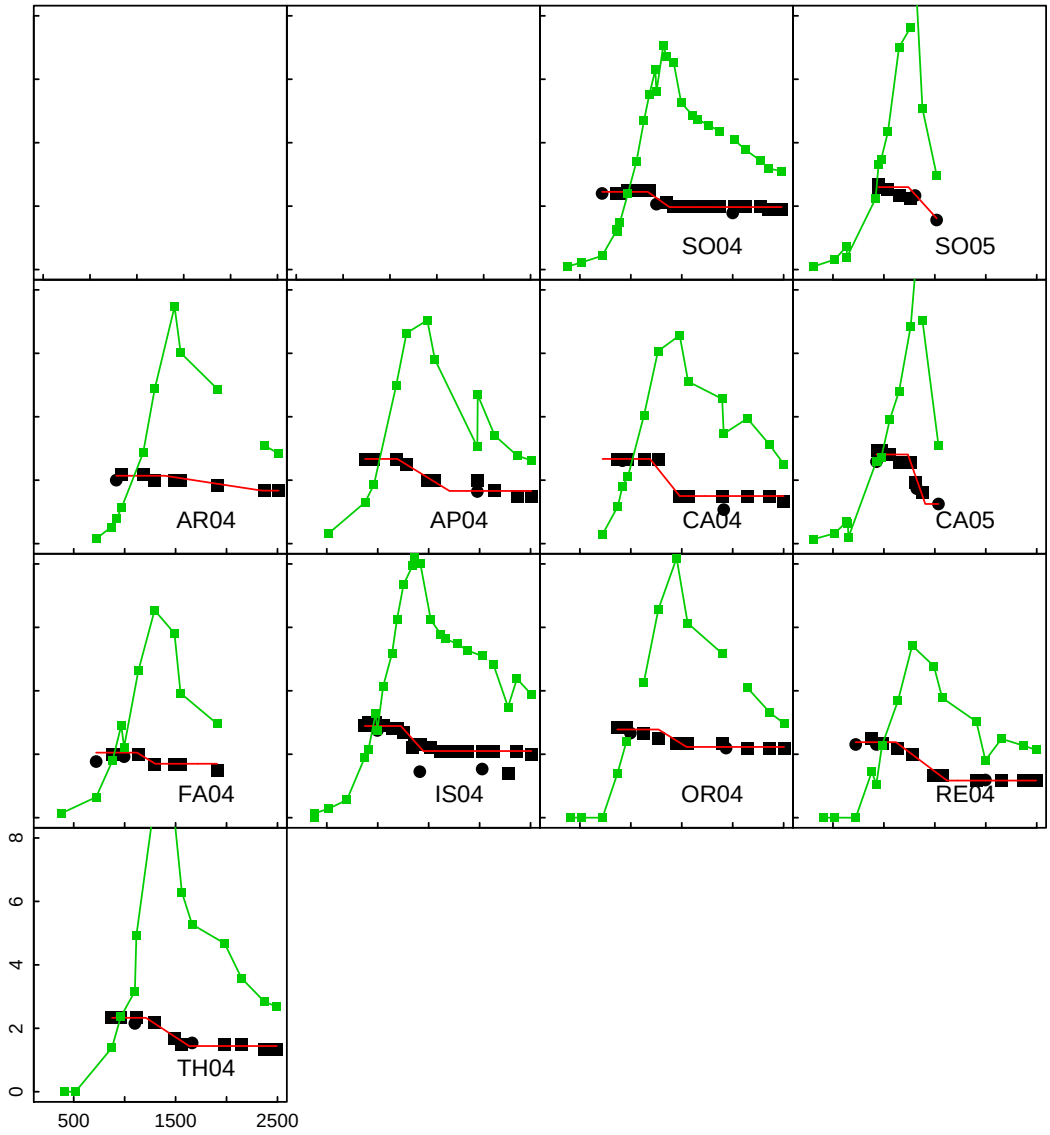

Figure 5.16: GLAI and tiller dynamic model per genotype.The x axis is thermal time and the y axis is the GLAI for the green points and line and number of axes per plant for the black points and red line

Gen	TT_{til1}	a	b	GLAI
SO04	732	0.017	0.0048	0.57
SO05	600	0.029	0.0046	0.46
CA04	$m745$	0.037	0.0039	0.68
CA04	$m745$	0.010	0.0053	0.52
CA05	595	0.031	0.0045	0.45
AR04	$m745$	0.007	0.0049	0.28
AP04	$m745$	0.065	0.0034	0.82
FA04	8504	0.030	0.0044	1.25
IS04	796	0.028	0.0045	1.01
OR04	756	0.090	0.0032	1.01
RE04	746	0.043	0.0038	0.73
TH04	888	0.031	0.0044	1.54

Table 5.15: The parameter values of the initial exponential part of the GLAI model per genotype. The genotypes where TT_{til1} is not known the mean TT_{til1} for all genotypes is used and indicated by a m

Tiller Cessation

From observations of the pattern of the data an exponential model is assumed the most appropriate model of GLAI progression over lower thermal time until maximum GLAI. Only this part of the GLAI progression over thermal time was modelled due to the data being insufficient to apply a full model and also only being interested, in terms of the tillering model, of the GLAI at the point when tiller production ceases. Using this model the GLAI at TT_{til1} can then be estimated and compared. It must be noted however that the quality of data over the period of thermal time where significant changes in GLAI amount occur, is for most genotypes patchy. This increases the error when trying to compare changes in tiller dynamic model with changes in GLAI over thermal time.

$$GLAI = aexp^{bTT} \tag{5.15}$$

where a and b are parameters and
TT is Thermal time

The genotypes from which the observed and modelled tiller dynamic data shows good correlation are SO04, SO05, CA05, RE04. Using only the data collected on these genotypes a mean value

of 0.55 ± 0.13(see Table 5.15) is found for the GLAI value at which tiller cessation occurs.

It is also of interest to investigate any corresponding relationship of GLAI and the parameters involved in tiller death, or rate of tiller death, as one affects the other. It would seem from the genotypes of good data, that GLAI 6-6.5 occurs about the same thermal time that tillers no longer die and those that are present remain to produce heads. A ratio of the GLAI at TT_{til2} to that at TT_{til3} has been calculated for genotypes Soisson (SO04) and Isengrain (IS04) to be 1.34 and 1.32 respectively. These genotypes were used due the quality of data. The rate of tiller death has been quantified per genotype and can be found in Table 5.13.

It can be seen from this table, and also from observing the graphs of tiller number, that the maximum number of tillers produced and the maximum number of tillers surviving is similar for genotypes AR04, FA04 and SO04. Considering the GLAI of these genotypes compared to that of other genotypes. There is a greater difference between the maximum number and final number of tiller with no obvious difference in leaf size (length and width) or GLAI, that would suggested that smaller leaves mean more tillers survive. It must be noted however that the maximum number of tillers is arbitrary as secondary tillers were not noted and neither were tillers of rank 4, due to their observed short lifespan during data collection. Perhaps these genotypes produced more tillers of rank 4 which would have meant the tiller death rate was comparable to that noticed on other genotypes.

Number of Leaves on the Main Stem

Although the thermal time of leaf appearance was not directly measured, it has been estimated using the methodology as set out in the analysis section to investigate a possible relationship between the onset of tiller death and the number of leaves on the main stem. Table 5.16 contains the thermal time estimated when the appearance of ligules of all leaves on the main stem has occurred (using the linear relationship observed in section 5.3.7 and the thermal time that tillers start to reduce in number (TT_{til2}).

For all genotypes the parameter TT_{til2} is similar to the thermal time at which the penultimate leaf or final leaf is estimated to become liguled. Instead of this parameter (TT_{til2}) being estimated within the model it is fixed to be the thermal time the penultimate leaf becomes liguled. Figure 5.17 illustrates the dynamic tiller model which uses the estimated thermal time the penultimate leaf becomes liguled in replacement of the TT_{til2} parameter. The fit of the model is shown

Gen	TT_{NFL}	TT_{til2}	TT_{NFL-1}	TT_{NFL-2}	TT_{til3}	TT_{til3}-TT_{til2}
SO04	1274	1250	1167	1060	1400	150
CA04	1308	1250	1188	1069	1450	200
AP04	1285	1210	1192	1099	1539	329
AR04	1504	1200	1394	1284	1300	100
FA04	1233	1150	1121	1010	1300	150
IS04	1333	977	1227	1121	1545	568
OR04	1386	1018	1273	1159	1411	393
RE04	1222	1074	1118	1014	1501	427
TH04	1310	1170	1209	1108	1520	351

Table 5.16: Estimated thermal time at which the final and penultimate leaf ligule appears on the main stem and tiller dynamic model parameters per genotype

Gen	NFL	NFL-1
SO04	0.808±0.10	0.901±0.07
SO05	0.645±0.21	0.800±0.15
AR04	0.722±0.09	0.799±0.08
AP04	0.898±0.14	0.921±0.13
CA04	0.954±0.13	0.933±0.16
CA05	0.343±0.47	0.923±0.16
FA04	0.748±0.09	0.482±0.13
IS04	0.555±0.31	0.686±0.26
OR04	0.652±0.13	0.792±0.11
RE04	0.955±0.11	0.979±0.08

Table 5.17: The $r^2 \pm$ the rmse of the tiller dynamic model fitted using the thermal time estimated that the ligule appears on the flag leaf (NFL) and the penultimate leaf (NFL1)

to be good, where data is sufficient (see Table 5.17 which also shows the fit of the model using the thermal time the flag leaf becomes liguled (NFL)). It must be noted that all the other model parameters were fixed to the values as suggested from the free fitting of the model.

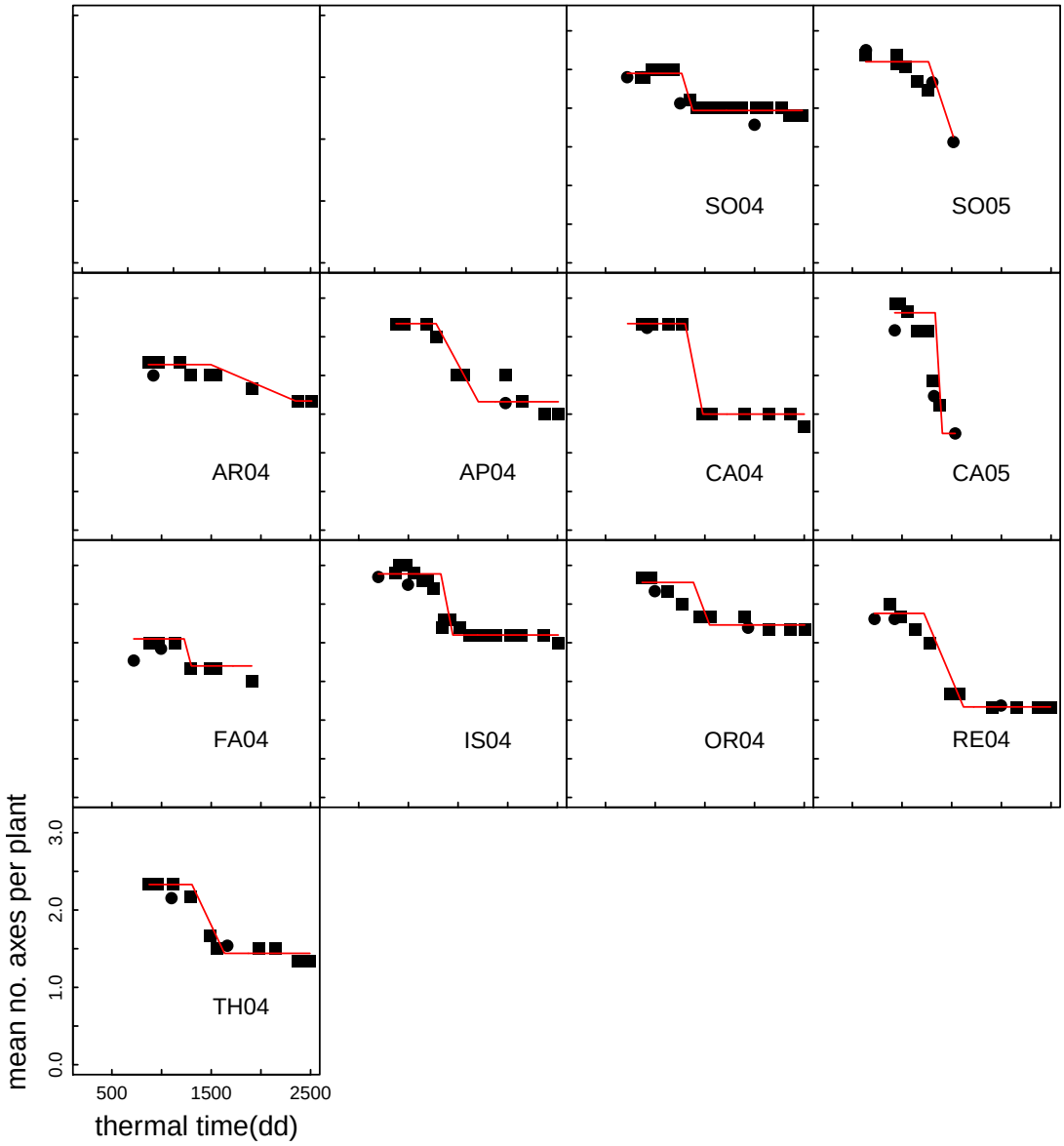

Figure 5.17: The (observed) mean number of axes per plant over thermal time, per genotype is shown using black points. The red line represents the modelled number of axes per plant. The model uses the thermal time of penultimate ligulation as parameter TT_{til2}

5.4.5 Discussion

Dynamic Tiller Model

Tiller number has been shown to increase over lower thermal time until reaching and maintaining a maximum tiller number. This number of tillers is shown to be maintained for a significant amount of time before decreasing over a short period of time (in degree days) until reaching a final number which then go on to produce a head. This pattern was found to be consistent over all genotypes and between two genotypes over different growing seasons and was also noted by Kim *et al.* (2010b) and Kim *et al.* (2010a) when investigating tillering in response to environment and genetics. The suggested model was found not to converge on all data however this is most likely due to insufficient data rather than a reflection of the suitability of the model. When the suggested model is fitted to the tiller data from each genotype, using both visual estimation and the best fit estimation the fit of the model for all genotypes has a r^2 above 0.9. No significant correlation was found between tiller model parameters that would help reduce the parameters required to describe the tiller dynamics.

Tiller Hierarchy

Tiller hierarchy has been shown, in this chapter, to differ between genotypes. However when the data is grouped from all genotypes the general pattern is that tiller 2 and tiller 1 are, in general, equally dominant, and more dominant than tiller 3. Tiller dominance was noted by Evers (2006) to be in accordance with appearance of tillers, i.e tiller 1 is more dominant over tiller 2 etc. Lafarge *et al.* (2002) found with Sorghum that tiller dominance was inversely related (for the first three tillers) to tiller appearance. Reasons for this hierarchy are suggested by Lafarge *et al.* (2002) who concluded that tiller dominance is probably dependent on assimilate availability from the main stem, and on early perception of inter-plant competition, and that subsequent development is affected by assimilate availability at the time of tiller emergence, probably defined by the area of the subtending leaf and the developmental stage of the main stem as well as the external environment. Peterson *et al.* (1982) noticed that tiller emergence in wheat was highly reduced if its subtending leaf or other one above it was excised. Hence the rate of emer-

gence and subsequent fertility and tiller from lower axis were probably affected by the small area of the subtending leaves that led to low tiller leaf area development, as previously suggested by Cannel (1969). The results of this experiment show that all tillers had a similar probability of being produced regardless of rank but that tiller 3 had a reduced chance of surviving to produce a head, with tiller rank one and two having a similar good chance of producing a head. The implication of the hierarchy suggested from the analysis is that a simple improvement of the tillering sub module within the ADEL-wheat model is required. Currently it is assumed that the last tiller to have emerged is preferentially 'killed' at a certain thermal time. Instead a probability of survival is given to each tiller according to its rank.

Parameter Correlation

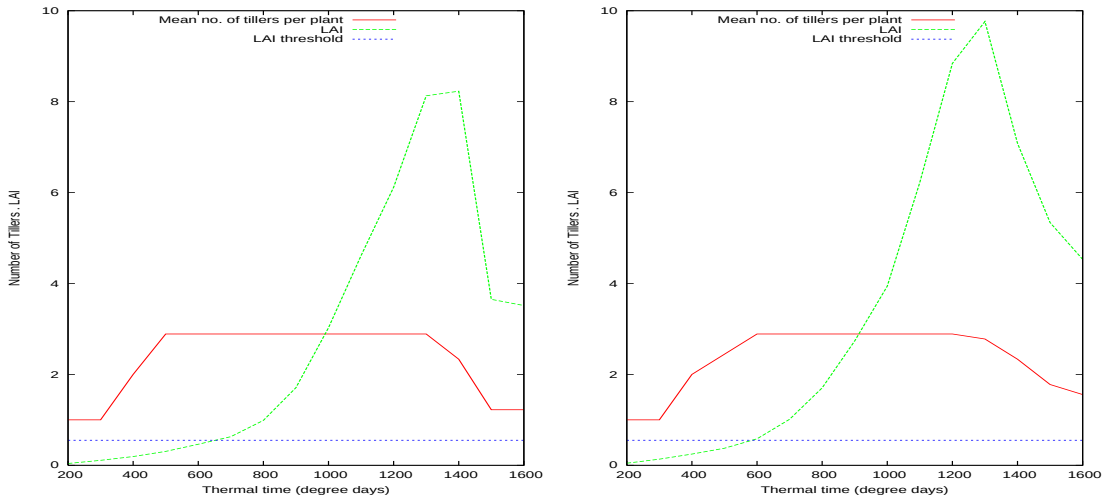

(a) Caphorn (b) Soisson

Figure 5.18: The number of tillers as estimated from the ADEL-wheat model is shown against thermal time (red) along with the LAI model as estimated from the ADEL-wheat model (Green). The LAI threshold value (blue) is also included. The graph on the left represents the output of the model parameterised to simulate a field of Caphorn plants and the right the output of the model parameterised to simulate a field of Soisson plants.

No correlation was observed between the parameters of the suggested tiller dynamics model. It was observed however that there is a constant GLAI value at which tiller cessation occurs. This is a simple and computationally inexpensive way to model Supply/Demand ratio and light quality effects which can be used to model more accurately tiller death. Lafarge *et al.* (2002) found the optimal LAI to be around 0.6, in this experiment it was found to be 0.55. It must be noted that only tiller appearance of the first 3 tillers was used in this analysis and as such the maximum number of tillers ($Till_{prod}$) is artificially low for some genotypes, which would have produced a tiller 4. The number of tiller 4's present however was observed during data collection to be low, for any one genotype. Also, the amount of time a tiller 4, if produced, survived, was not deemed great enough for this to present a large error. The difference between GLAI and LAI would also account for a lower value being observed.

The development of GLAI over thermal time is shown here to be an important consideration within the tiller dynamic model. The original Sirius model (Jamieson *et al.* 1998b) and its later version (Jamieson and Semenov 2000) describe GAI development (which includes all green area of the plant) as a function of thermal time (Jamieson *et al.* 1995) with no reference to current leaf number (N). Initial GAI growth in thermal time was shown to be exponential, followed by a linear phase and then capped at a maximum level. GAI was then shown to remain constant until anthesis and then decrease quadratically. Two parameters describing the shape of the initial exponential growth, and a third describing the grain filling period in thermal time were suggested to describe GAI development. The exponential parameters in this case are semi empirical and require careful calibration against experimental canopy data for each wheat cultivar. GLAI is considered within the chapter and so is lower than GAI which also takes into account the stem. Within this experiment, the onset of GLAI is also shown to increase exponentially until a maximum is achieved, however the difference to other observations is that this is not maintained. Instead a steep decrease is noted followed by a slower decrease. As only leaf area was taken into account this is suggested to be why GLAI was not shown to maintain itself at its maximum for a period of time.

Implementing a LAI threshold within the model was of interest. Incorporating the tiller dynamic model within the ADEL-wheat model and comparing the LAI and tiller number estimates over thermal time it is evident that the estimate of thermal time at which tiller production ceases and the thermal time at which LAI reaches the threshold value of 0.55 did not match for CA05 and was more than a 100 degree days out. This causes an over estimation of maximum tiller number.

However, for genotype Soisson the thermal time at both these events was similar and if this threshold was included would result in a good estimate of maximum tiller number.

Implementation of a tiller dynamic model whereby the maximum number of tillers is not set and tiller cessation is instead controlled by GLAI or LAI is logical. However, as senescence is not formally considered within the model this would also cause some error if it was implemented. It is also important to note that the number of tillers being calculated within the model is the number of initiated axes. However the field data from which tiller number is estimated uses the number of tillers present (visible). If the GLAI of initiated axes was instead used it would result in a greater delay. Perhaps by including tiller number of tillers greater than 2 cm long when estimating GLAI from the model would have given a better cut off point for tiller cessation, however due to the way in which tiller data was collected, it can only be suggested that this is looked into in more detail with additional data and that it may give a better way of modelling tillers rather than using a set maximum number of tillers.

As this model did not work sufficiently well for both genotypes it was considered more appropriate to allow the model to create tillers until a maximum number of tillers was achieved, after which the tiller number would be maintained until the signal for tiller death.

It is important however to understand, the measurements of GLAI are not LAI as used within the model and as senescence is not within the scope of this thesis cannot be estimated. However it shows that there is promise in using LAI as an indicator to cease tillering and thus implementing a semi empirical model of tiller cessation into the model. Furthering of this idea is highly recommended

Tiller Death

The relationship found between the time that flag leaf becomes liguled and tiller death is not in agreement with the observation by Lawless *et al.* (2005) that tiller cessation occurs once the flag leaf on the main stem is liguled. Instead it was observed that the thermal time that the penultimate leaf becomes liguled corresponds with tiller cessation. Ligule appearance was not measured directly. Instead it was estimated using the linear relation between leaf appearance and thermal time and thus it is recognised that errors will have occurred, although these are assumed

small.

5.4.6 Conclusion

A dynamic model of number of tillers over thermal time has been successfully applied to observed data from a range of genotypes over two growing seasons, which describes number of tillers per plant using five parameters.

Tiller production is set using an equal hierarchy so that each tiller has an equal chance of being produced. Tiller survival is shown not to be equal between tillers. Tillers 1 and 2 are instead shown to be equally likely to survive and produce a viable ear, with tiller 3 being the most likely tiller to die before producing a viable ear and so at the point of tiller death, T3 has a set probability of surviving as 37% and T1 and 2, 69% (the mean of the T1 (67) and T2(70)).

Parameter reductions are suggested by assuming that the thermal time at which the penultimate leaf becomes liguled on the main stem is the time at which tiller death commences. A rate of death can then be applied specific to each genotype until the number of surviving tillers is obtained (Til_{surv}). It is also suggested that further exploration into incorporating an LAI threshold trigger for the onset of tiller cessation takes place so to remove the need of setting the parameter describing a maximum tiller number.

Chapter 6

Architecture

6.1 2D Lamina Shape

Lamina of different relative phytomer rank from a range of winter wheat genotypes have been collected over two growing seasons. Using a software called Lamina2Shape (Dornbusch and Andrieu 2009) developed at INRA-grignon the width at equal increments from the base of each lamina has been estimated. This data has allowed the idea of a constant leaf shape model to be investigated. Analysis within this chapter focuses on the potential difference in leaf shape between genotypes, phytomer and axis rank and difference between lamina of two genotypes grown under different environmental conditions. A modified version of the leaf shape model currently implemented within ADEL-wheat is suggested and tested.

6.1.1 Leaf Shape and Area

Leaf area and shape are important parameters to be considered when modelling plant growth and development. The amount of light intercepted by a crop, its photosynthate production and the amount of nitrogen stored is determined either directly or indirectly by leaf area. The spatial distribution of leaf area is determined by the 3D structure of the plant, such as the orientation of the stems and of the leaves themselves, but also by the shape of the leaves. Together, leaf area and shape can alter the micro-climate within the canopy and thus the growth and development of the crop. Within studies that focus on, for example the spread of foliar disease, both leaf area and shape are therefore extremely important.

Within optical remote sensing knowledge of leaf area and its distribution within the canopy is required to enable the total amount of radiation absorbed and reflected to be estimated accurately. For microwave remote sensing experimental research has demonstrated that the microwave backscatter coefficient is also sensitive to crop biomass and in addition affected by the shape and dimensions of the plant leaves and stems (Bracaglia *et al.* 1995, Paloscia *et al.* 1999, Macelloni *et al.* 2000)). The simulation of leaf shape is therefore also an important consideration within crop models in remote sensing studies.

Leaf area is frequently estimated from mathematical models of leaf shape (Stewart and Dwyer 1999). Leaf shape models describe the geometric outline of the leaf as the relation between leaf

width to the distance from the base of the blade (ligule) or from it's tip (Fournier and Andrieu 1998). Leaf area can either be estimated by integrating this model or using a simple model suggested by Montgomery (1911) where leaf area= max_{width}* max_{length}* form factor (ff). The form factor being a shape characteristic. Currently within ADEL-wheat leaf shape is modelled using an adapted version of the Prevot model (see equation 6.1).

$$W^* = a(L^*)^2 + bL^* + 0.66 \tag{6.1}$$

where
W^*= w/W
L^*= u/L
a = -2.5
b = 1.84
u = distance to the base (ligule) of the lamina
L = total lamina length
w = width at point u
W = maximum width
0.66 = relative width at base (ligule) of the lamina

Fournier and Andrieu (1998) re-expressed this model to describe leaf shape as a function of the distance from the leaf tip instead of leaf base (ligule). This is a useful addition for dynamic architectural models, as it enables the width of the leaf portion emerging from the cell division zone to be calculated at any stage of growth. The relative width at the base of the lamina is set as 0.66 but recently Dornbusch *et al.* (2010) suggested 0.6 to be a more appropriate value. Within ADEL-WHEAT the co-efficient a is set as -2.3 rather than -2.5 as suggested by Prevot. This relates to a form factor of 0.748.

It is generally assumed that the relative width at the ligule and the form factor is constant for all ranks of phytomer. For maize the original form factor suggested by Montgomery (1911) was 0.75, however values ranging from 0.65 to 0.85 have been suggested by Sanderson *et al.* (1981) with the most widely used value being 0.73 (McKee 1964). For spring wheat it has been found to vary with phosphorus conditions (Rodriguez *et al.* 1998) and temperature but is unaffected by light intensity (Bos and Neuteboom 1998). Differences in the value of the factor therefore

occur between plant types and also environmental conditions however as mentioned one common assumption to date has been that form factor is the same for all leaves on all axes. Recent research by Dornbusch *et al.* (2010) however highlights architectural differences in lamina of grasses growing within the juvenile and adult phases. This chapter aims to suggest the most appropriate leaf shape model for use within remote sensing studies by taking into account differences in lamina shape between phytomer rank and genotype and considering the potential effect on a remote sensing signal.

6.1.2 Method

2D leaf data was collected throughout the growing season of Experiment 1 and 2. Most of the plants sampled in both these experiments were tagged so that phytomer and axis rank could be identified directly. Of those plants not tagged, the phytomer and axis rank were estimated from phenological measurements taken from the tagged plants. All leaves collected were required to have no or very little senescence. The leaves once removed from the plant were grouped per relative phytomer rank and placed as flat and as vertical as possible with the base of the blade (ligule) at the top of a clean piece of paper and the tip at the bottom. This was then scanned, using a computer scanner and gimp software. The removal and scanning of the leaves from the plants were made as much as was possible on the same day to avoid measurements being taken from wilted plants. When time was limited the plants were kept over night wrapped in moist paper towels in a fridge and any remaining measurements made the following morning.

Experiment 1

At least ten lamina of all ranks from the main stem of all genotypes were attempted to be collected throughout the growing season and additionally, for genotypes Soisson and Isengrain, from the tillers as well. Due to time restraints some ranks of lamina for different axes and genotypes were not sampled. For a summary of the data that was collected see Table 6.1

All of the plants, from which lamina were removed and scanned, had been destructively sampled. It must be noted that although all these measurements were made on the same plants relating the

$Experiment1$	$Axis$	1	2	3	4	5	6	7	8	9	10	11	12
$Soisson$	MS						$*$	$*$	$*$	$*$	$*$	$*$	
	$T1$		$*$	$*$		$*$	$*$	$*$	$*$				
	$T2$			$*$	$*$	$*$	$*$	$*$					
	$T3$		$*$	$*$	$*$	$*$	$*$	$*$					
$Isengrain$	MS							$*$	$*$	$*$	$*$		
	$T1$					$*$	$*$	$*$	$*$				
	$T2$			$*$	$*$	$*$	$*$	$*$					
	$T3$		$*$	$*$									
$Caphorn$	MS					$*$	$*$	$*$	$*$		$*$	$*$	$*$
$Recital$	MS					$*$	$*$	$*$	$*$		$*$	$*$	$*$
$Arminda$	MS					$*$	$*$	$*$				$*$	$*$
$Apache$	MS										$*$	$*$	
$Thesee$	MS							$*$	$*$	$*$	$*$	$*$	
$Florence - Aurore$	MS					$*$	$*$	$*$	$*$	$*$	$*$		
$Oratario$	MS					$*$	$*$	$*$	$*$	$*$	$*$	$*$	
$Experiment2$	$Axis$	1	2	3	4	5	6	7	8	9	10	11	12
$Soisson$	MS			$*$	$*$	$*$	$*$	$*$	$*$	$*$	$*$	$*$	$*$
	$T1$	$*$	$*$	$*$	$*$	$*$	$*$	$*$	$*$	$*$			
	$T2$	$*$	$*$	$*$	$*$	$*$	$*$	$*$	$*$				
	$T3$	$*$	$*$	$*$	$*$	$*$	$*$	$*$					
$Caphorn$	MS		$*$	$*$	$*$	$*$	$*$	$*$	$*$	$*$	$*$	$*$	$*$
	$T1$	$*$	$*$	$*$	$*$	$*$	$*$	$*$	$*$	$*$			
	$T2$	$*$	$*$	$*$	$*$	$*$	$*$	$*$	$*$				
	$T3$	$*$	$*$	$*$	$*$	$*$	$*$	$*$					

Table 6.1: Lamina per rank, axes and genotype of which scans were collected.$*$denotes scans were acquired.

data sets is not possible as the plant number was not written on the lamina as they were scanned. The frequency of sampling differed between genotypes. Soisson and Isengrain were sampled at four stages during the growing season whereas the rest of the genotypes were sampled at a maximum of three dates which corresponds to the frequency of destructive sampling.

Experiment 2

Blades of all ranks from all axes were collected from both genotypes; Soisson and Caphorn. The sampling frequency was dependent on the progression of senescence, so that if the lamina of the last phytomer rank to have been scanned started to senesce the remaining liguled lamina were scanned as soon as possible. Due to the reduction in the number of tagged plants available for destructive sampling, as described in the methodology chapter, destructive sampling was initially carried out on un tagged plants, later on in development destructive sampling was carried out on half the plants on which non-destructive measurements were being made and then finally on the remaining non destructively sampled plants. Using non-tagged plants early on in development required the ranks of phytomer and axis to be identified, this was carried out by referring to the non destructive measurements on the same genotype.

6.1.3 Measurements

Lamina2Shape (Dornbusch and Andrieu 2009) developed by INRA-grignon was used to calculate leaf width at increments from the base of the leaf to the tip. An overview of the software is given here however for a more detailed description see Dornbusch and Andrieu (2009). The software initially creates a binary image of the scanned lamina. However any white marks left on the leaves from the tagging process of Experiment 1, cause the binary image of the leaf to have gaps where the tag is present, so these marks are at first identified and edited. The binary images of all lamina are smoothed so that the shape of the lamina is maintained but the edges are more continuous and less jagged. A smooth binary image of each leaf allows for the midrib to be easily identified and the maximum width at increments from the leaf base to be estimated. The data obtained per blade is the width at each increment from the base of the leaf, the maximum length and total area. Maximum width is obtained by extracting the maximum width from the

width measured at each increment from the base of the lamina.

6.1.4 Data Analysis

The 2D leaf shape software calculates the width of the leaf at increments from the base of the lamina and so is initially rearranged so that the width data is from the tip of the leaf instead. Random noise is added to each data point (lamina width at increments from tip). The maximum noise added is equal to the length of one pixel and is included to make sure the data is more continuous. Initially, maximum length and maximum width of the scanned lamina is compared to the same data collected using destructive and non-destructive sampling, on the same genotypes and during the same experiment. As only median plants are to be used, the maximum length and width of the scanned lamina are compared to the same data collected within the field. Where the maximum length or width are within the standard deviation (*2) of the same data obtained from destructive and non destructive sampling, the scanned lamina are used in the rest of this analysis, those that fall outside this limit are disregarded. Phytomer rank of lamina is altered within this analysis so that rank 0 represents the flag leaf and rank 1 the penultimate leaf and so on. This is carried out to allow easier comparison between lamina of genotypes with different final number of leaves.

The idea of a constant leaf shape model is investigated by comparing the form factor of the lamina over the different phytomer rank, axis and genotypes. The form factor of each lamina is calculated using eqn 6.2. The leaf area used is that which is estimated from the image software.

$$Formfactor = Area/(L_{Max}W_{Max}) \tag{6.2}$$

where L_{Max} and W_{Max} are maximum lamina length and width respectively.

The idea of a constant leaf shape model is further investigated by comparing the normalised length along the midrib that maximum width occurs and the normalised width at the base of the lamina (ligule) for lamina of different phytomer rank over different axis and for a variety of genotypes. This data is obtained by normalising the length (along the midrib) and the width of the lamina and applying a spline from which the two data points of interest are extracted.

The constant leaf shape model as currently implemented within ADEL-wheat is re parameterised using the findings from this analysis and the fit of this model is compared against rank, axis and genotype. Leaf area and form factor are estimated from this model (via integration of re parameterised model) and compared to observed values (as obtained from the Lamina2Shape software).

Further analysis is carried out which highlights the possibility of re-expressing the currently implemented 2D leaf shape model. This model has the advantage of requiring form factor as its only parameter. The fit of this model is compared against phytomer rank and genotype.

6.1.5 Results

Form Factor

The form factor of all ranks over all axis for all genotypes from experiment 1 and 2 are displayed in Figure 6.1.

The rank is given as the number from the last phytomer (flag leaf), with the flag leaf given a value 0 and the penultimate leaf a value 1 etc. The results from a t-test/anova suggest that there is no significant difference in form factor over rank or between genotypes. However from Figure 6.1 it does seem that winter leaves and flag leaves may have a different form factor to other lamina. The mean form factor for all lamina is 0.773 (confidence interval of 0.002) and the mean when excluding the winter and flag leaves (so ranks 2-8) is 0.780 (confidence interval of 0.002). No consistent difference in form factor is noted between axis (see Figure 6.2). A difference however is observed in form factor between the same genotypes, Soisson and Caphorn, grown under different environmental conditions (experiments 1 and 2) (see Figure 6.2 and Figure 6.3). In experiment 2 the lamina of both genotypes Soisson and Caphorn are shown, in general, to have a higher form factor than that measured in experiment 1. Lamina from tillers were only collected from genotype Soisson over both experiments and thus this observation for Caphorn is based on main stem data only.

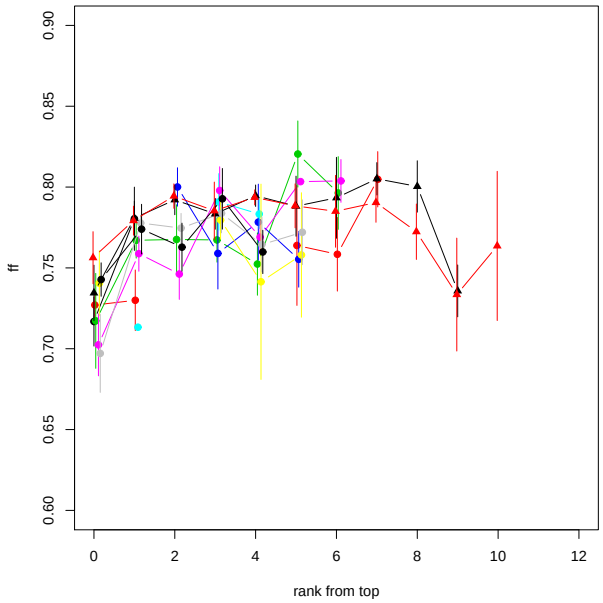

Figure 6.1: Form factor (ff) of leaves against leaf rank, which is given as number from flag leaf, with flag leaf being rank 0. Each colour represents a different genotype. Triangular points distinguish genotypes from experiment 2 (2005) from those from experiment 1 (2004) which are shown with circular points. Main stem data is shown only.

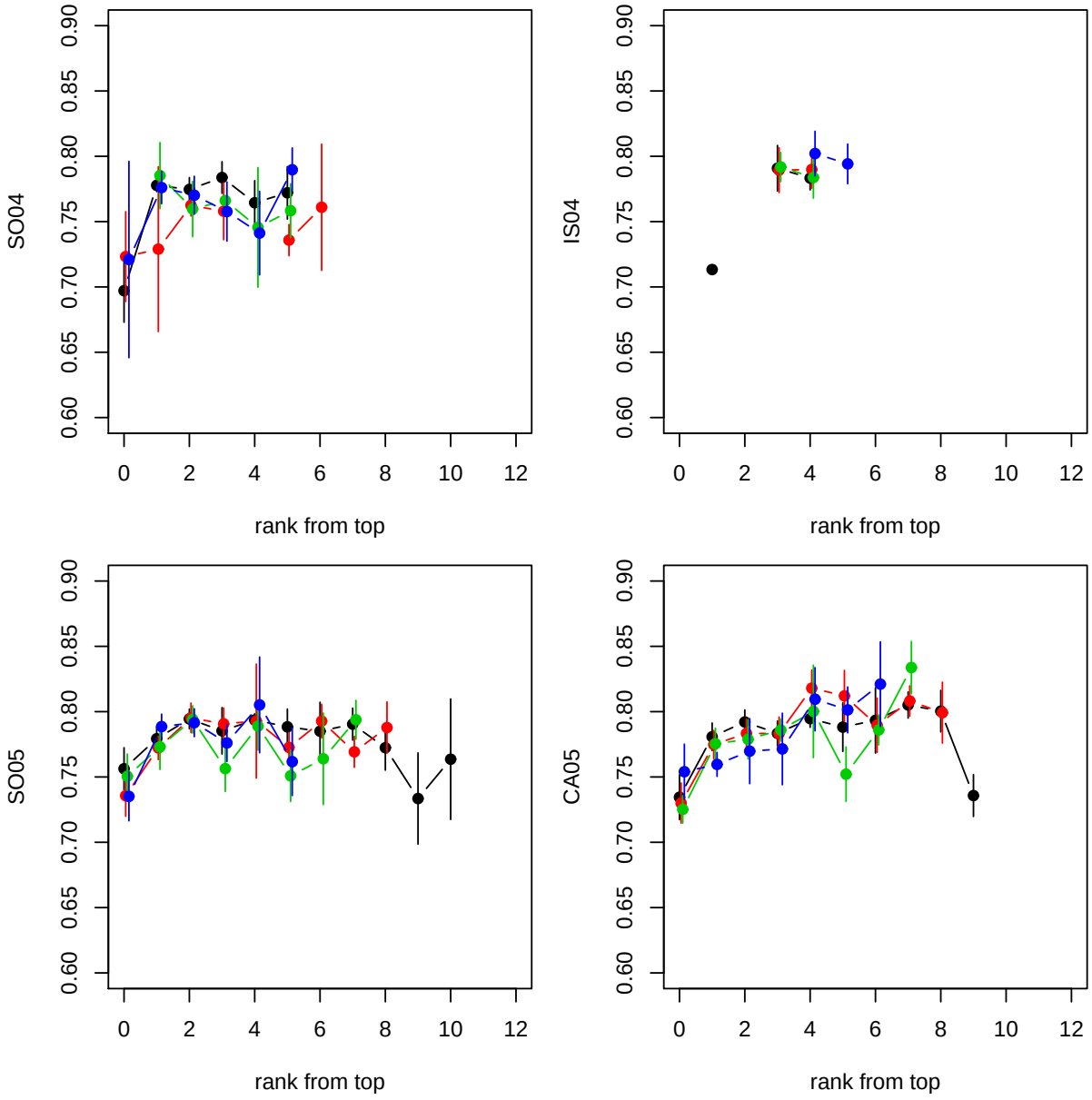

Figure 6.2: Form factor of leaves of genotypes Soisson and Isengrain from experiments 1 (04) and Soisson and Caphorn from experiments 2 (05). Main stem in shown in black, tiller 1 in red, tiller 2 in green and tiller 3 in blue.

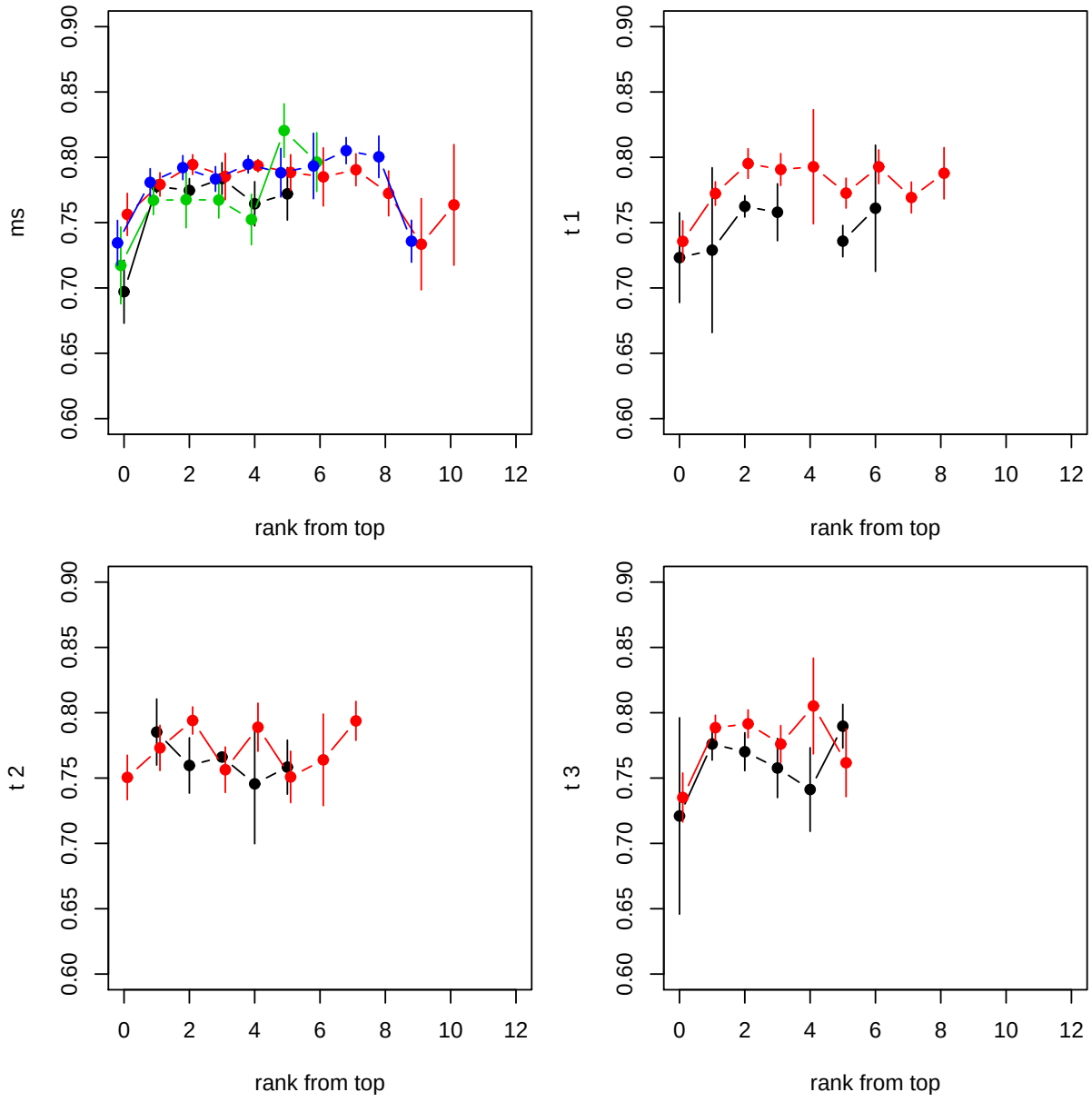

Figure 6.3: Form factor of leaves of genotypes Soisson and Caphorn from experiments 1 (04) and 2 (05). SO04 is shown in black, SO05 red, CA04 green and CA05 blue.

Normalised lamina length at maximum lamina width

Figures 6.4 illustrate for different genotypes and different ranks, normalised lamina width against normalised lamina length.

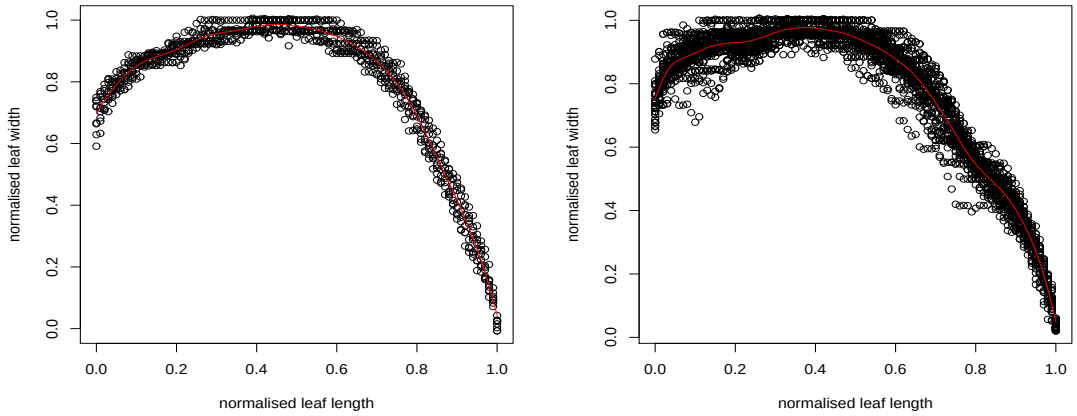

(a) FA04 Rank 3 from top

(b) SO04 Rank 2 from top

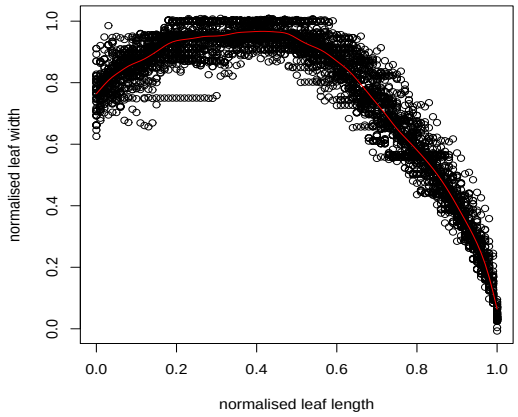

(c) SO04 Rank 4 from top

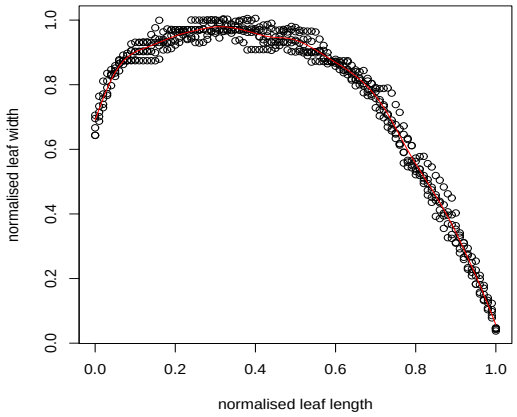

(d) CA04 Rank 2 from top

Figure 6.4: Spline (in red) through the normalised width against normalised length from base of leaf for different genotypes and ranks.

The maximum width of the leaf is observed to occur at a fairly constant normalised length from the tip of the leaf, the mean being 0.35 ± 0.08 for all genotypes and ranks and axis and from both experiments. If flag leaves are considered on their own the mean is 0.33 ± 0.06 which is

within the general mean. If lamina of ranks 2-4 are considered sepearately the mean is 0.35 $\pm$ 0.09 and if lamina of ranks 6-8 the means is 0.38 $\pm$ 0.07, again both of these are within the the general mean.

Normalised lamina width at the base is shown in Figures 6.5 to increase the lower the phytomer rank, with flag leaves having the smallest normalised base width. The variation in normalised base width seems consistent over rank, axis and genotype, with the mean over all genotypes, ranks and axis being 0.74 $\pm$ 0.06, for flag leaves on their own, it is 0.633 $\pm$ 0.04 and for ranks 2-4 0.73 $\pm$ 0.04 and for ranks 6-8 0.79 $\pm$ 0.05. Flag leaves have a range of normalised base width that is lower than that of the more general mean value.

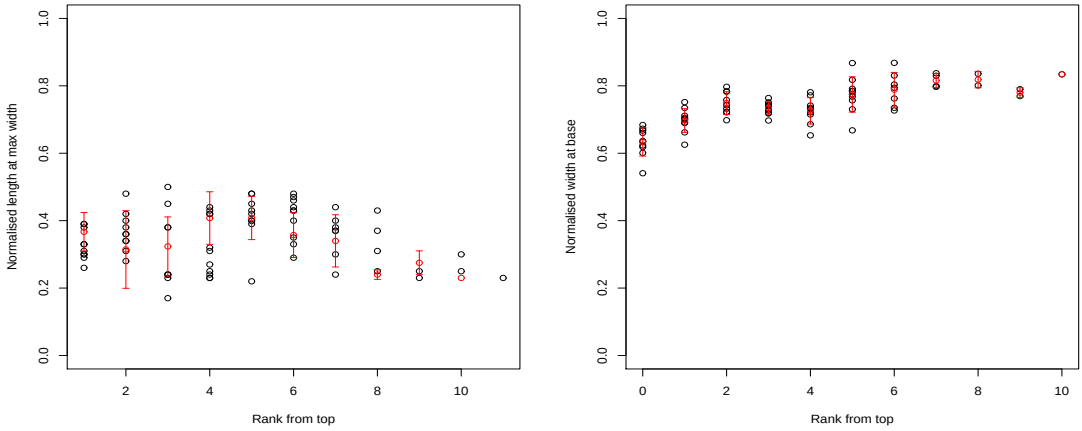

(a) Normalised length at max width (b) Normalised base width

Figure 6.5: Mean sd of normalised length and maximum width and normalised width at base of leaf (ligule) for all genotypes, all ranks from both experiment one and two

Parameterisation of 2D leaf Model

Accepting the difference noted in normalised lamina base width of flag leaves and the small error of assuming a constant normalised lamina base width for all leaves, the rest of the data suggests that a constant model is appropriate for modelling 2D leaf shape.

Rank	Axis	CA05	SO05	CA04	SO04	IS04	AP04	RE04	OR04	FA04	AR04	TH04
1	0											
2	0		0.63									
3	0	0.94	0.83									
4	0	0.69	0.91									
5	0	0.66	0.84	0.75				0.90	0.69	0.92	0.73	
6	0	0.68	0.75	0.40	0.79			0.92	0.40	0.87	0.87	
7	0	0.67	0.65	0.81	0.91	0.84		0.91	0.94	0.96	0.75	0.79
8	0	0.73	0.65	0.82	0.78	0.80			0.86	0.80		0.79
9	0	0.81	0.82		0.90	0.86			0.94			0.92
10	0	0.79	0.76	0.93	0.92	0.93	0.87	0.98	0.97			0.92
11	0	0.88	0.85	0.96	0.87		0.96		0.94		0.89	0.98
12	0	0.97	0.94	0.95							0.97	

Table 6.2: The r squared of the fit of the quadratic model to main stem leaves

Currently the leaf shape model within ADEL is an adapted version of the prevot model. It requires three parameters; a, b and c. Using the observations from experiments 1 and 2 the parameters are set to -2.3, 1.59, 0.73 respectively. This relates to the maximum width occurring at 0.36 normalised length from the tip and the width at the tip being zero and the normal width at the ligule being 0.73.

This model was fitted to all leaves from all genotypes over both experiments, see Figure 6.6.

The fit of the model to main stem leaves is summarized in table 6.2 and the fit and rmse is shown per rank from top for all leaves in Figure 6.7

The fit of the leaf shape model is shown to be good for all ranks of all genotypes with the lowest r^2 value being 0.63 for early leaves on SO05 where the sampling quality and quantity would have been lower compared to other leaves measured.

Checking the re parameterised model

Comparison between the area of the leaf estimated by integrating the leaf shape function and that estimated by the leaf shape software can be observed in figures 6.8. This comparison is only

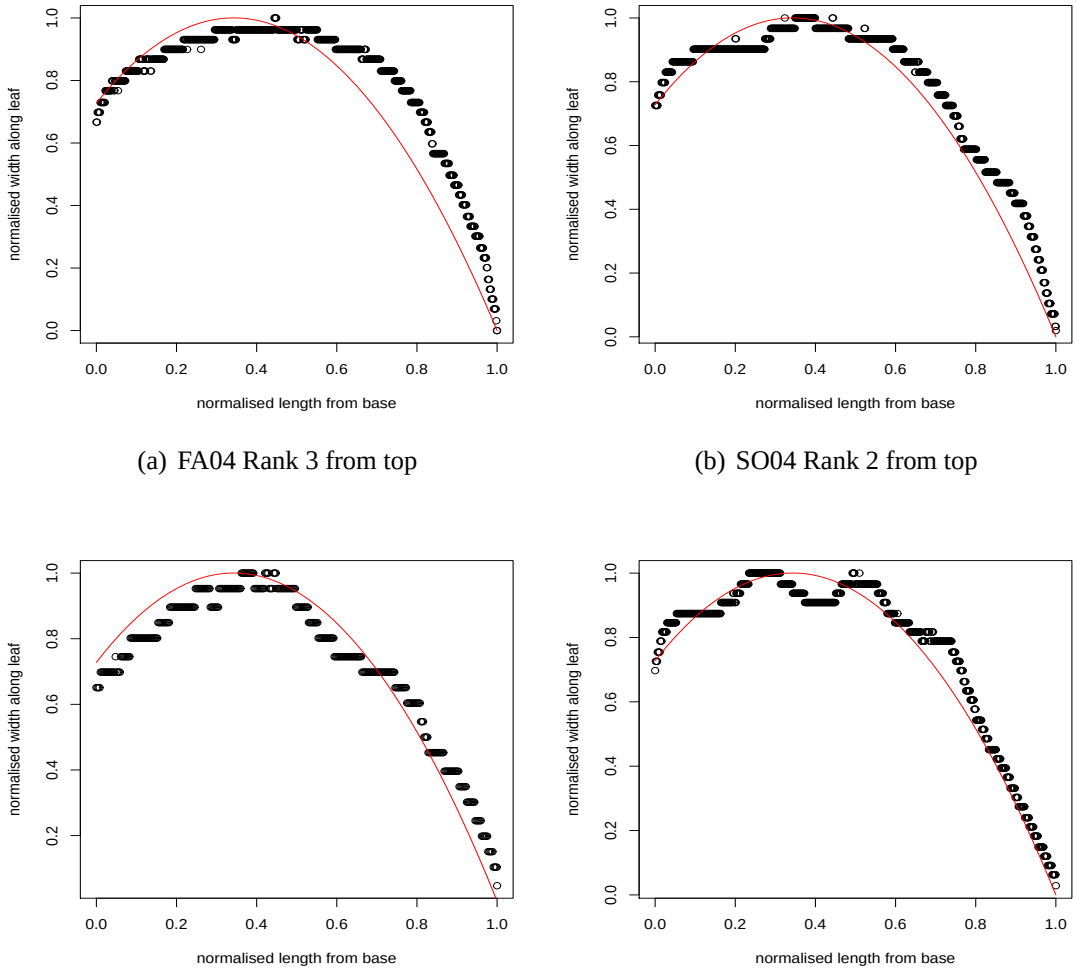

(a) FA04 Rank 3 from top

(b) SO04 Rank 2 from top

(c) SO04 Rank 4 from top

(d) CA04 Rank 2 from top

Figure 6.6: Suggested lamina shape model shown in red. The black points represent the normalised width against normalised length from the base of leaf. This is shown for genotype Florence Aurore on a phytomer rank 3 lamina, for Soisson on a pyhtomer rank 2 and also rank 4 lamina (experiment 1) and of a lamina of phytomer rank 2 of genotype Caphorn (experiment 1).

carried out for 2004 data and not 2005 due to an error in the software calculating area within the software during the 2005 experiment.

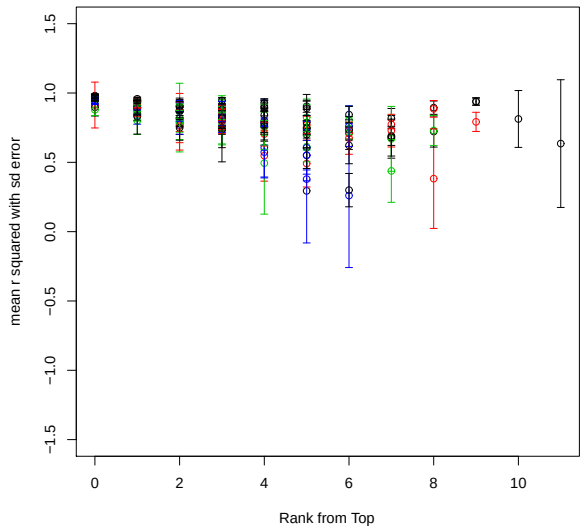

Figure 6.7: Mean fit of the suggested leaf shape model is shown per rank of lamina, with rank 0 representing the flag leaf and the penultimate leaf rank 1 etc. The mean fit is shown for all genotypes with the axis from which the lamina are growing distinguished by colour. Black is main stem, red tiller 1, blue tiller 2 and green tiller 3

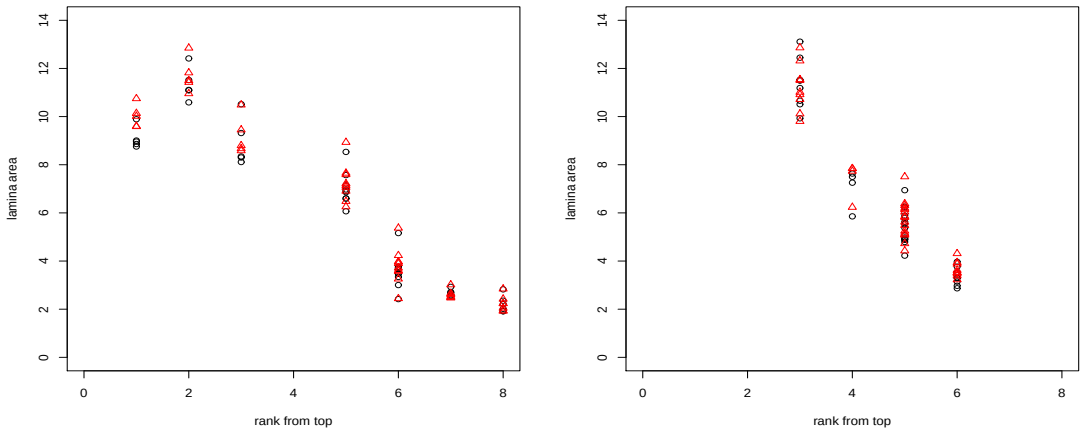

(a) CA04 (b) FA04

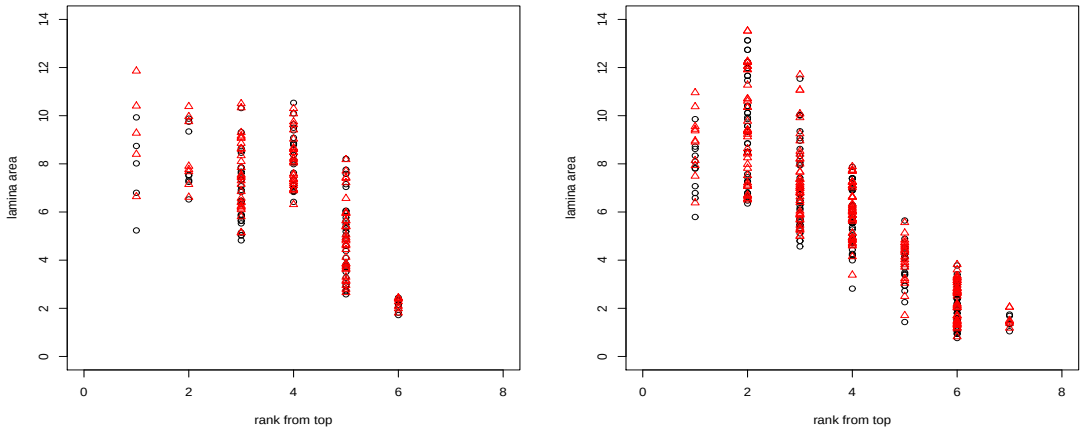

(c) IS04 (d) SO04

Figure 6.8: Comparison of area of leaf as estimated from the integration of the quadratic shape function (red triangles) and the area as estimated from the image processing data (black circles).

As can be see from figures 6.8 the difference between observed and modelled leaf area are not significant.A KS test was also carried out with the results showing that the data sets are similar. (Soisson: D=0.1034, P=0.1669, Isengrain: D=0.0926, P=0.7435, Florence-Aurore: D=0.1579, P=0.7307, Caphorn: D=0.1064, P=0.9564).

The estimated form factor using this leaf shape model is 0.75 (it is constant as the model is constant). This is different from that noticed in the initial analysis which suggested a higher form factor of 0.78. Comparison of the constant (modelled) form factor of 0.75 (as suggested from the constant leaf shape model) and the form factor (observed) as estimated from the leaf shape software can be observed in figures 6.9

The modelled form factor as estimated using the constant model is adequate for all leaves. Due to the observations that flag leaves although found not to be significantly different, did differ in shape to the rest of the leaves per plant, it was considered to have the difference in shape of the flag leaf to be a percentage of the previous leaves. However the difference between the shape of the flag leaf and previous leaves is not consistent between genotypes, instead the the small error, within remote sensing applications, is assumed acceptable in order to keep the number of parameters of the model low. This is further confirmed by the area of the leaves as estimated using the form factor of the constant model and that estimated by the leaf shape software being adequate for all ranks including the flag leaf.

Re express 2D Leaf Model

A further improvement in terms of reduction of the number of parameters and inclusion of more intuitive parameters is suggested. The adapted Prevot model currently used within the ADEL wheat to simulate leaf shape is suggested to be re arranged and expressed using form factor (ff).

This model is obtained by assuming a constant leaf shape described by a simple quadratic and omitting the constraint of set normalised leaf width at the base of the leaf.

$$y = ax^2 + bx$$

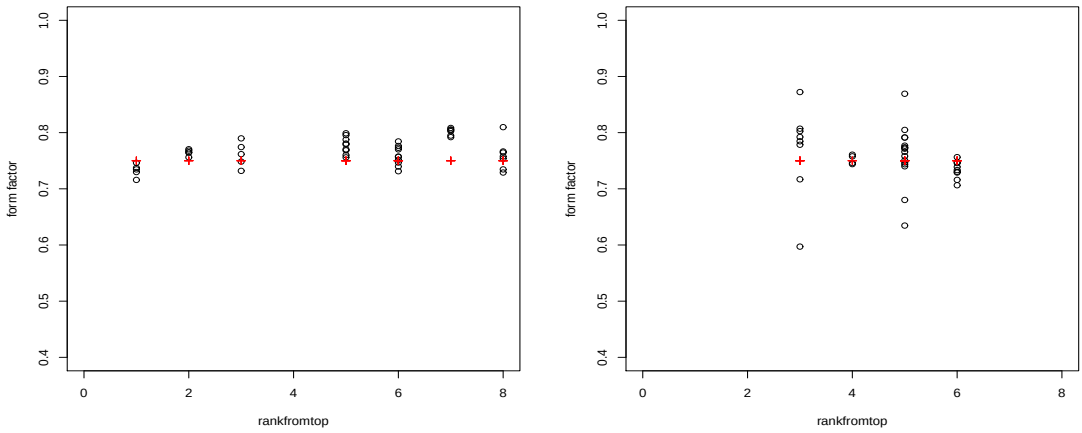

(a) CA04

(b) FA04

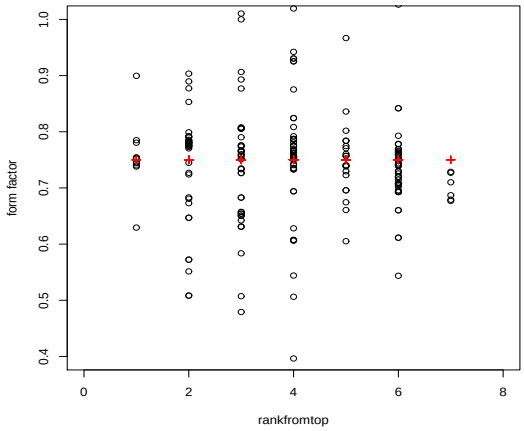

(c) SO04

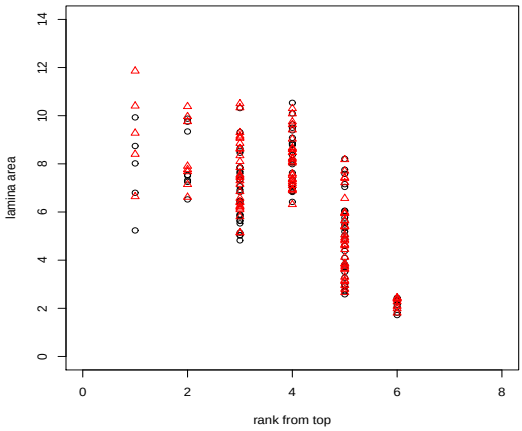

(d) IS04

Figure 6.9: Comparison of the form factor of lamina as estimated from the integration of the quadratic shape function and the form factor as estimated from the image processing data.

where:
x = length from the base of the leaf
y = width of leaf

Considering the differential of y at the length from the base of the lamina where maximum width occurs (x_{max}):

$$\begin{aligned} y^{'} &= 0 \\ &= 2ax + b \\ x_{max} &= \frac{-b}{2a} \end{aligned}$$

and that the area under the curve is the form factor (ff):

$$\frac{a}{3} + \frac{b}{2} = ff$$

and considering the two constraints 1. The base of the leaf cannot be negative or bigger than one due to being normalised:

$$0 < \quad c \quad < 1$$

and 2. The normalised length along the leaf at maximum width must be less than 0.5 or larger than 0 otherwise the base of the leaf would be negative, which cannot be true, (as stated above):

$$0 <= \quad x_{max} \quad < 0.5$$

Taking into account these constraints and using mathematical, the constant leaf shape model can be expressed in terms of form factor.

$$= \frac{-3 + 6ff(1-x)^2 \pm sqrt(3)sqrt(-((-3+4ff)(1-3x)^2(-1+x)^2) + 3(4-3x)(1-x))}{2} \tag{6.3}$$

where:
x = length from the base of the leaf
y = width of leaf

There are two possible descriptions of leaf shape from this model due to the positive and negative component (see Figure6.10). It is also of interest to note that the form factor is itself limited. It would have to be greater than 2/3 (0.67) and less than or equal to 0.75. This is due to the constraints of the base width, in that it must be greater than 0 or less than 1 (due to it being normalised) and that the length from the base along the leaf where the width of the leaf is maximum must be 0.5 or lower with these constraints.

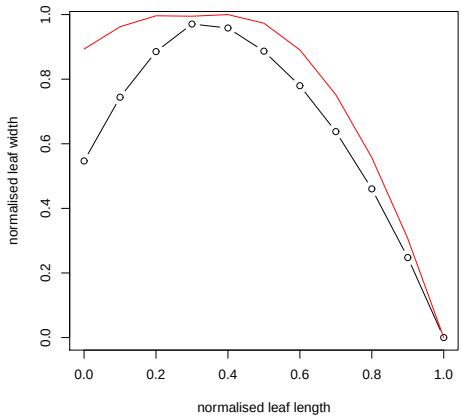

Figure 6.10: The leaf shape shown with two solutions. The black is calculated using the negative root and the red line the positive root of the equation.

It may be possible to include an additional parameter to enable a higher form factor than 0.75 as was observed with the experimental data. This would be achieved by using a power function. See Figures 6.11.

The fit of this model to observed data was found comparable with the re- parameterised constant leaf shape model already implemented within ADEL-wheat(see figures 6.12).

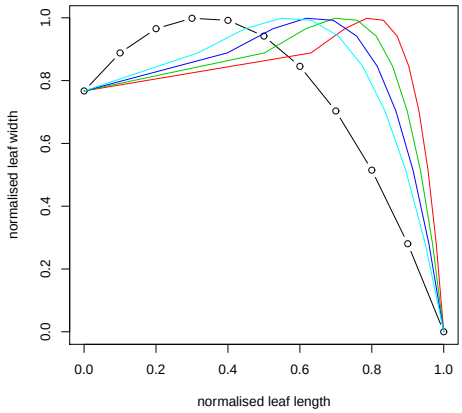

Figure 6.11: The black line with points is the shape function using form factor 0.7499, The red is the shape function with the same form factor (0.7499) with a the normalised length along the leaf raised to a power of 0.2, green line = 0.3, blue line =0.4 and turquoise line=0.5

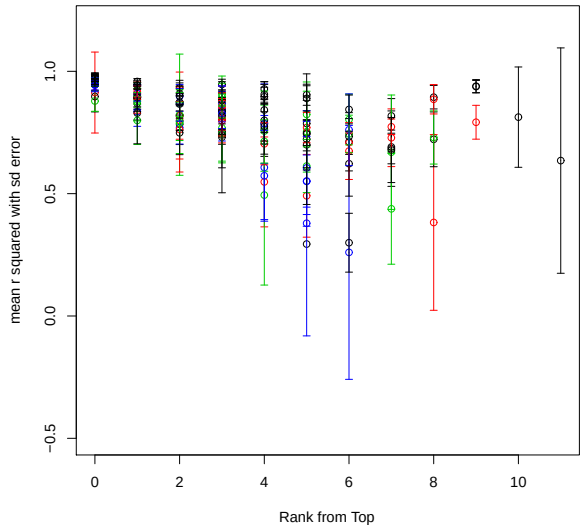

Figure 6.12: Mean fit of the new suggested leaf shape model is shown per rank of lamina, with rank 0 representing the flag leaf and the penultimate leaf rank 1 etc. The mean fit is shown for all genotypes with the axis from which the lamina are growing distinguished by colour. Black is main stem, red tiller 1, blue tiller 2 and green tiller 3

6.1.6 Discussion

The overalnew l aim of the work for this thesis is to re-parameterise the ADEL-wheat model so that it is generic and requires a small number of parameters. This analysis of form factor, as used to estimate leaf area, has shown that any differences in form factor between rank of leaves and genotype are small and the addition of parameters to describe leaf shape and area for leaves of different rank or genotype not required.

However, although statistically proven not to be significant, there does seem to be a difference in the form factor of winter leaves. The implications of this are that a lower form factor is assumed to be appropriate for such leaves and using the current model the area of these early leaves will be possibly overestimated. This in turn with affect the green leaf area which is the switch (at 0.55 GLAI) to initiate tiller cessation and must be considered when looking at model outputs if queries are raised around such areas in the model output.

It is interesting to note that environmental conditions do seem to have an affect on form factor with a difference noted between the form factor of Soisson leaves in experiment 1 and 2 (SO04 and SO05 respectively). Differences in leaf length and width were also observed for this genotype between years, with SO05 having longer and slightly wider leaves than SO04 leaves. To investigate environmental effects on form factor further data would have to be collected to confirm this.

implementing into ADEL-wheat

The model currently implemented within ADEL-wheat is appropriate as a generic model. This is a simple quadratic model that assumes a constant shape over rank, axis and genotypes and different environmental conditions.

$W^* = aL^{*2} + b(L^*) + c$
L* is the normalised length of the leaf from the base
W* is the normalised width of the leaf at length L

Lamina Area = W*L*0.748
where
W= Max Lamina Width
L= Max Lamina Length

However to reduce parameter inputs into the model it is instead suggested that the model is re expressed in terms of form factor. The form factor being set to 0.75.

$$W* = \frac{-3 + 6FF(1 - L*) \pm sqrt(3)sqrt((3 - 4FF)(1 - 3L)^2(1 - L)^2 + 3(4 - 3L)) * L}{2} \tag{6.4}$$

6.1.7 Conclusion

From the results collected from experiments 1 and 2 the form factor has been shown to be similar for all leaves of all genotypes on all axis for two different growing seasons. The simple quadratic model currently implemented in ADEL-wheat is considered to be the most appropriate for the modelling of 2D leaf shape with small alterations to the parameter values to allow variations between genotypes and axis and rank as found in the two experiments. It was considered that the flag and winter leaves should have different parameterisations as the form factor was found to be lower than other leaves, although not significantly. The extra parameterisation was deemed unnecessary as the lamina area and shape was found to be estimated accurately with the constant model.

6.2 3D Lamina Shape

The 3D geometry of individual plants and their spatial arrangements in a canopy strongly affect the quantity and quality of radiation intercepted, scattered and emitted within the canopy. This in turn not only affects the micro environment and the plants growth and development but also the remote sensing signal. The 3D structure of the plant is therefore an important consideration within crop models to be used within remote sensing studies. Various aspects of the plants architecture must be considered; the angle of the main stem and tillers, the curvature of the leaves within the canopy and the phyllotaxy of the leaves along the main stem and tillers. The difference of these characteristics, between genotypes and the affect on the remote sensing signal are therefore of particular interest within this chapter. Currently within ADEL-wheat, 3D Architecture is simulated by considering such characteristics, however the individual models are based on data obtained from one genotype of winter wheat only. This chapter looks at the current models already in place and investigates whether they are appropriate for a variety of genotypes.

Figure 6.13 illustrates the different models used to describe midrib curvature within ADEL-wheat. Different models are used to describe the ascending part of the leaf and the descending. A parabola is used to describe the ascending model and an ellipse the descending. A ratio between parabola length and ellipse length is used to describe the amount ascending and descending, with 1 being a leaf that is described using only a parabola model.

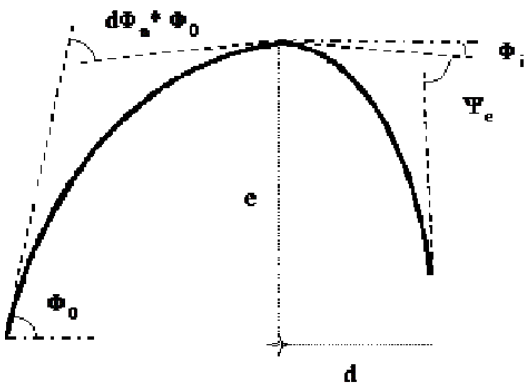

(a)

Figure 6.13: Parameterisation of the blade midrib curvature with models. The ascending part is a parabola and the descending part is an ellipse. Reproduced from (Fournier et al. *2000) pg 88.*

There are two parameters, Φ_o and Φ_n used to describe the parabola model. Φ_o describes the tangent of the inclination angle (from the horizontal) and Φ_n is normalised by this angle and describes the angular curvature at the tip of the parabola also from the horizontal. The normalising of this angle means that leaves cannot be simulated where the tip angle (from the horizontal) is more than the base inclination angle, which would give a leaf curving in towards the stem. It addition it means that leaves are not able to have an inclination angle less than the horizontal, so no negative angles.

There are three parameters, d, e and ε and Φ_i used to describe the ellipse model. d is the length of the horizontal ellipse axis, e the length of the vertical ellipse axis, ε whose absolute value is the ellipse eccentricity and Φ_i which is the top tangent(See Figure 6.13).

An additional parameter is also used to describe midrib curvature which is P_{cass}. This parameter gives the proportion of the length of the leaf that is described using the parabola model.

Whilst the leaf is emerging, it is simulated to have an erectophile characteristic and only takes on the parameterised 3D shape once the sheath appears, as illustrated in Figure 6.14. The parameterisation of the model which describes how the leaf emerges is left untouched as 3D measurements were only collected on leaves once the ligule was formed.

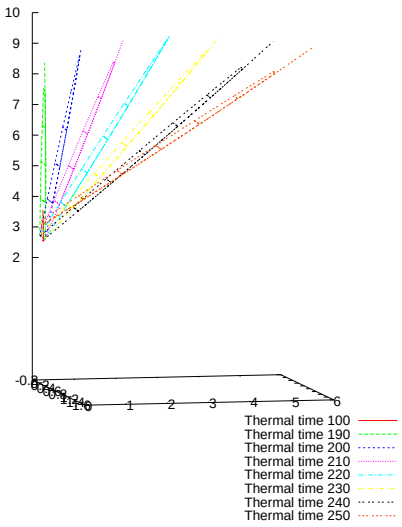

(a)

Figure 6.14: Illustration of the architecture of an emerging leaf.

Currently within ADEL-wheat the lower leaves are expected to be purely ascending and as such only the parabola model is applied. The higher leaves are assumed to be a mixture of purely ascending leaves and leaves that have ascending and descending parts, this is modelled using the P_{cass} parameter as mentioned.

Within this chapter a modification to this midrib curvature model is suggested whereby only a parabola model is used to describe the 3D shape of all leaves. In order to suggest such modifications data on the 3D structure of the plants is required. There are several methodologies used to measure the 3D dimensions of a plant. A review of the different methodologies has been made by (Rakocevic *et al.* 2001) and specifically for functional structural crop models (Heijden *et al.* 2007) with a brief review given in this thesis in Chapter 1.

A magnetic contact digitiser (rather than use of string or sound) was decided the most appropriate to collect the 3 Dimensional data for this research. It was decided to be the most suitable as the orientation angle can be measured and an accuracy of a few millimetres can be expected within small canopies (Rakocevic *et al.* 2001). Although the measurements are laborious, plant organs can be distinguished and recorded during measurements, which is not always possible using non contact digitisers. The data obtained can also be processed using a selection of software removing the need to solve the complex problem of reconstructing the plant structure from a scatter diagram of spatial points.

6.2.1 Methodology/Data Collection

Method

Digitising was mostly carried out in the field, however on one occasion plants were removed from the field and measured in a greenhouse due to the wind. A digitiser and Polhemus software was used. Points were recorded up the main stem with the position of liguled leaves recorded with their rank, where known or their rank from the top leaf if not. Points were also taken along each non senescing lamina of the main stem, with points recorded at the base of the lamina (collar) and then at 1-2 cm intervals along the leaf until the tip.

Experiment One

The architecture of the tillers and angle from the main stem was measured for tagged plants of genotype Soisson (SO04) and Isengrain (IS04), with only non-senescing lamina being measured. Ideally at each sampling date a sample set of twenty plants for genotypes Soisson and Isengrain were measured and at least 13 plants for the other genotypes. This however was not always possible due to weather conditions and as such sampling was not at regular intervals for all genotypes although it was attempted to be so that all ranks of leaves would be digitised, especially for genotypes Soisson and Isengrain. Table 6.3 documents the number of plants measured per genotype at each sampling date and whether the tillers were measured or not. On the last sampling date, the plants of some genotypes were removed from the field and digitised within the laboratory, this was due to the wind moving the plants whilst measurements were being taken. The data collected on tiller angle cannot therefore be used for analysis of main stem or tiller angle.

	SO	***IS***	***AR***	***CA***	***FA***	***OR***	***RE***
Date 1	**20**	**20**	**15**	**13**	**8**	**13**	**13**
Date 2	**19**	**20**	**12**	**13**	**13**	**13**	**13**
Date 3	**15**	**16**	**8**	**6**	**13**	**13**	**12**
Date 4	**14**	**16**					

Table 6.3: Number of plants per sampling date per genotype digitised. Main stem and tillers digitised on Soisson (SO)and Isengrain (IS) and main stem only for other genotypes

Experiment Two

Digitisation of both genotypes (Soisson (SO05) and Caphorn (CA05)) was intended to occur at the beginning of the six week sampling period and at the end, however due to weather conditions only one set of data was obtained for genotype Soisson (two were obtained for Caphorn). Due to abnormalities in the condition of the field, the tagged plants due to be digitised were not representative of the rest of the field. Instead representative plants were chosen away from these affected sites and non tagged plants digitised from the top of the plant down. This enabled each lamina to be digitised and its rank recorded as flag leaf, flag leaf -1 etc. Tillers were also digitised, however the rank could not be identified with a high degree of accuracy and so instead identified as 'non main stem'.

6.2.2 Data Analysis

The original data from the Polhemus software was re-organised so that blade and stem data could be extracted along with rank of leaf and rank of axis effectively, to allow for analysis and plotting of the data. The x,y,z coordinates of each digitised point on the plant was related back to the x y z co-ordinates at the base of the main stem of the plant, which was set to 0 0 0.

Main Stem and Tiller Angle

In order to ascertain the angle of the main stem, a spline was forced through the extracted Polhemium data from the main stem. The direction vector was obtained from this spline data and the difference between the vertical assumed to represent the angle of the main stem. The same method was applied to the tiller stem data and the angle relative to the main stem obtained. In ADEL wheat the tiller is assumed to become more vertical the further from the base of the tiller. This is modelled according to the appearance of internodes along the tiller. The position and appearance of internodes along the tiller were not recorded within the data obtained in experiment one or two and as such the model cannot be fully validated.

Midrib curvature

Leaf architectural data is obtained from the co-ordinates measured with the Polhemus software. It is initially assumed that each leaf lies within one plane any possible twisting of the leaf is ignored. For each leaf the most appropriate plane is estimated using a function that interpolates between consecutive points and a spline fitted. In addition the distance from the leaf base to the tip is normalised and the inclination angle at regular small intervals calculated. It is this data that is used to compare leaf architecture. Phytomer rank from top, so flag leaf is rank 1, is used to compare the architecture of leaves from different plants. The architecture is also compared between genotypes, of which the analysis focuses on two main genotypes, Soisson and Caphorn. Soisson leaves are generally more planophile and Caphorn more erectophile and it is due to these architectural differences that these two genotypes are being compared. Comparisons are also made between the leaves of different axis and between leaves of the same genotype grown under differing environmental conditions.

Within the ADEL-wheat model the leaf curvature is modelled using two models, a parabola and an ellipse model, with the lower earlier leaves being described using only a parabola model. Within this analysis this parabola model is considered appropriate for all leaves. This is due to the lack of significant differences found in architecture between ranks of leaves when comparing the two parameters required to describe the model; inclination angle at the base and at the tip. These parameters are estimated from the fitted quadratic model and compared between genotypes, rank and axis.

Phyllotaxy

In order to consider the phyllotaxy of the leaves up the stem, the main stem is rotated to the vertical position and the angle between the successive leaves when looking down the stem from the tip are calculated. Due to senescence not all leaves are digitised at one time per plant. The angle between successive leaves is therefore analysed with only two or at the most four leaves. The analysis of this data is as such, not in depth, but gives some idea of the possible phyllotaxy differences between genotype and if the current model is sufficient. The direction of each leaf is initially ascertained from the results of the splineMe function which forces the leaf into one appropriate plane. The angle between the plane each subsequent leaf falls in is then calculated

and comparisons over rank and genotype are made.

6.2.3 Results

Main Stem Angle

The direction vector of the main stem for all digitised plants of all genotypes was obtained once a spline had been forced through the extracted Polhemium data. The angle of the main stem is not assumed to be vertical in this analysis. Table 6.4 displays the angle in degrees the main stem lies from the vertical for each genotype data and Table 6.5 the mean angle from the vertical the main stem is at each sampling date for two genotypes, Soisson (SO04) and Isengrain (IS04). Only the main stem data where the error of the fitting of the spline through the points collected on the main stem were 0.9 or above were used in this calculation.

Genotype	Mean $\pm$ sd
SO04	5.2 ± 10.33
IS04	2.8 ± 5.61
CA04	2.3 ± 2.67
RE04	4.0 ± 3.71
AR04	5.1 ± 8.51
OR04	4.2 ± 5.55

Table 6.4: The mean $\pm$ st dev of the main stem angle in degrees from the vertical

Date	Thermal time	SO04	IS04
		mean $\pm$ sd	mean $\pm$ sd
1	700	24.2 ± 20.03	27.8 ± 17.22
2	900	4.6 ± 3.22	5.2 ± 5.65
3	1250	0.8 ± 1.43	0.1 ± 0.12
4	2000	0.2 ± 0.12	0.1 ± 0.12

Table 6.5: The mean main stem angle in degrees from vertical and sd per sampling date for Soisson (SO04) and Isengrain (IS04)

From the results it can be observed that the deviation of the main stem from a purely vertical stem is small, with the largest mean distance from the vertical being 5.16 ± 10.33 degrees for genotype Soisson and the smallest of 2.27 ± 2.67 degrees for Caphorn. It is interesting to note that the Caphorn and Recital plants have a far lower deviation when compared to genotypes Soisson and Arminda. It is also of interest that the main stem deviates less from the vertical the later on

in development which is suggested to be due to the strengthening of the main stem due to the extension of the internodes. Currently within the ADEL model the main stem is parameterised at angle 10 which from this analysis seems quite high and an average value of 4 for a generic model seems more appropriate.

Tiller Stem Angle

A low rmse was found when a linear spline is fitted to the tiller stem data and so it is assumed acceptable to consider the tillers to be straight. The angle between the main stem and the three tillers (rank 1, 2 & 3) was found to vary according to sampling date, with the tillers measured at earlier sampling dates (closer to emergence) having a greater angle from the main stem compared to those measured later on (further from emergence) (see Table 6.6).

$Axis$	$Date$	$IS04$ $Angle$ $Mean \pm sd$	$IS04$ $No.of$ $Leaves$	$IS04$ $No.of$ $Nodes$	$SO04$ $Angle$ $Mean \pm sd$	$SO04$ $No.of$ $Leaves$	$SO04$ $No.of$ $Nodes$
1	1	30.3 ± 11	$3,2$	0	37.6 ± 20	$4,3$	0
	2	9.4 ± 6	$6,5$	5	6.6 ± 4	$5,4$	4
	3	4.3 ± 4	$6,6$	5	4.1 ± 4	$9,8$	8
	4	4.6 ± 4	$6,6$	8	4.7 ± 4	$9,9$	9
2	1	28.1 ± 13	$3,2$	0	35.4 ± 21	$3,2$	0
	2	10.3 ± 7	$5,4$	4	7.5 ± 4	$5,4$	4
	3	5.1 ± 3	$5,5$	8	6.0 ± 3	$8,8$	8
	4	5.4 ± 3	$5,5$	8	5.9 ± 3	$8,8$	8
3	1	27.6 ± 10	$2,1$	0	37.2 ± 19	$2,1$	0
	2	9.1 ± 6	$4,3$	3	6.9 ± 4	$4,3$	3
	3	4.3 ± 3	$4,4$	7	3.9 ± 2	$7,6$	6
	4	NA	$4,4$	7	NA	$7,7$	7

Table 6.6: Mean $\pm$ SD of the angle each tiller (1-3) is from the main stem for genotype IS04 (Isengraina) and SO04 (Soisson) at the four sampling dates. The number of leaves generally found at each sampling date is given as number of visable leaves, number of leaves with ligules and the highest phytomer number of extending internodes

The model currently implemented within ADEL, takes change in tiller angle into account. It does this by adjusting the tiller angle relative to the main stem, according to the number of internodes extended on the stem (n_r) as summarised below.

inc = -INCT for n_r=1
inc = 3/4 INCT for n_r=2
inc = 1/6 INCT for n_r=3
inc = 1/12 INCT for n_r=4

where:
inc is the inclination between successive internodes
INCT the absolute angle between vertical and most basal internodes
n_r the rank of the internode

This model suggests that the inclination of the tiller becomes more erectophile as the tiller develops, which is confirmed by the data collected in experiment one and two (see Table6.6). The value of the parameter INCT cannot be validated due to the presence of internodes on tillers not being recorded during the digitisation. However by utilising the destructive data, the number of extending (although not fully extended) internodes can be associated with this tiller angle data, which is shown in Table 6.6. It must be noted that the destructive data was not taken on the same date but within a few days of digitising. Tiller inclination angle is shown (see Table 6.6 to decline substantially between date 1 and 2, such as the extension of internode rank 2 and 3 as suggested within ADEL if INCT is 60 (see below).

inc is 45, for n_r=2
inc is 10, for n_r=3
inc is 5, for n_r=4

The final angle is shown in Table 6.6 to also be approximately 5 and as such, it is suggested that INCT should remain as 60.

No comparison on tiller angle can be made between experiment one and two meaning that environmental differences in growing conditions cannot be compared, as data on tillers was not

recorded on genotype Soisson in experiment two.

Midrib Curvature

Figure 6.15 illustrates two leaves, one from genotype Caphorn and the other from genotype Soisson. Figure a, shows the leaves using its x y coordinates once a spline has been fitted to the original x, y, z data. This spline forces the leaf into one plane. Figure b, shows the same leaves but described using inclination angle over the normalised leaf length. From observing the characteristics of leaf curvature using the x y coordinates and the pattern of inclination angle over normalised leaf length it is suggested that a quadratic model (see equation 6.5) fitted to inclination angle data is the most appropriate model to describe midrib curvature. Figure 6.15 b shows this quadratic model using a solid line.

$$IA = aL + b(L)^2 \tag{6.5}$$

where
L is the normalised length along the leaf from the base and
IA is the inclination angle.

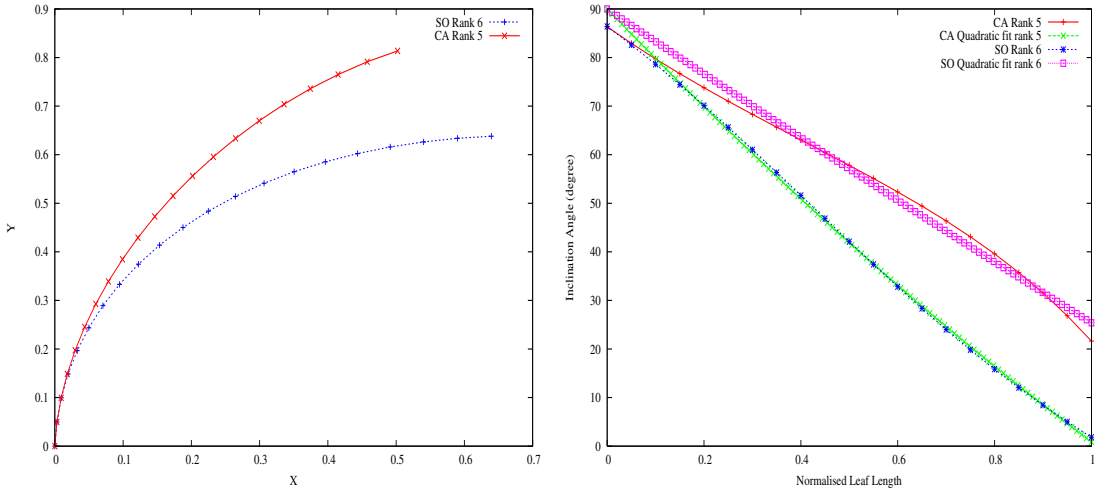

(a) Reconstruction (b) Model

Figure 6.15: The original x,y coordinates of two leaves are shown in Figure a. Figure b, shows the same two leaves when described using inclination angle along the normalised leaf length and the fitted quadratic model.

The quadratic model was applied to all measured leaves and the fit in terms of r^2 found to be high for all leaves regardless of rank, axis, genotype or growing conditions, with an acceptable r^2 for all leaves of above 0.8. The rmse of the fit of the model was also compared over phytomer rank, see Figure 6.16. Within this figure data from experiment one and two is distinguished by colour, as well as between leaves from different axis. The rmse of Soisson leaves is shown to have a slightly greater deviation over lower rank of leaves compared to Caphorn. The variation of rmse between the two years is shown to be similar for both genotypes. No significant distinction between rank, axis or genotypes however could be made in terms of the fit of the model and is thus suggested to be a relevant model for all leaves.

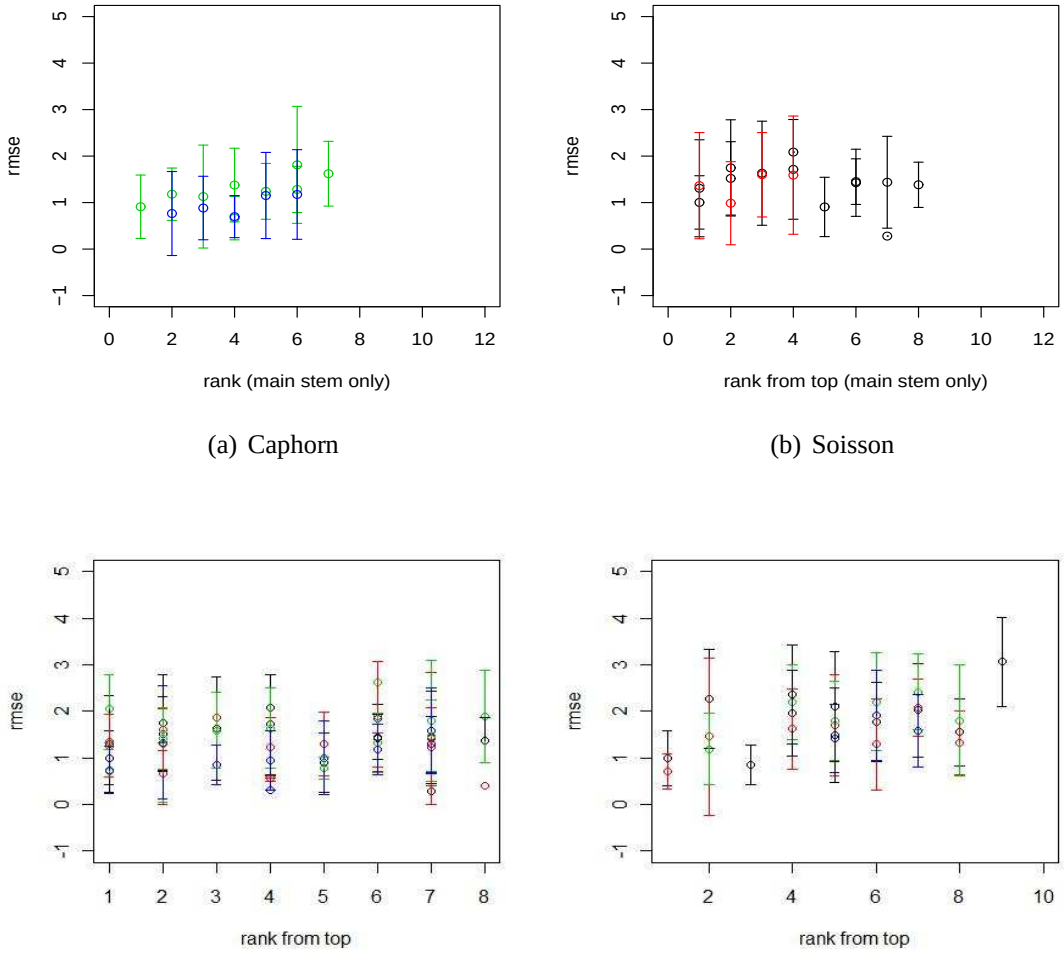

(a) Caphorn (b) Soisson

(c) Soisson (d) Isengrain

Figure 6.16: Figures a and b, The rmse of the fit of the quadratic model to midrib curvature of leaves of differing ranks (main stem only) for genotypes Caphorn and Soisson. Data obtained (per genotype) from experiment one and two is distinguished by colour (Soisson black = experiment one, red = experiment two, Caphorn, green = experiment one and blue = experiment two. Figures c and d, The rmse of the fit of the quadratic model to midrib curvature of leaves of differing ranks with data from axis distinguished by colour. Black = main stem, Red = tiller one, Blue = tiller two and Green= tiller three. The two genotypes shown are Soisson and Isengrain

The parameters a and b of the quadratic model are compared for all leaves. Only the leaves where the model has been fitted with a low rmse (<2) are included in this analysis. Figure 6.17 illustrates the value of the a and b parameters of the fitted quadratic model per leaf rank for genotypes Soisson and Caphorn (using main stem data only and those where the model fitted with a rmse of < 2). The values are shown to remain fairly constant over all ranks and between genotypes. A difference between data obtained from experiment one and two for each genotype is noted with the parameter A being consistently lower for both genotypes grown in experiment two. The deviation from the mean of this parameter is also shown to be much reduced, although the sample size was also reduced in experiment two. Although this difference is noted no significant difference is shown and as such the data collected during 2004 and 2005 experiments for both genotypes will be considered as one data set from here onwards.

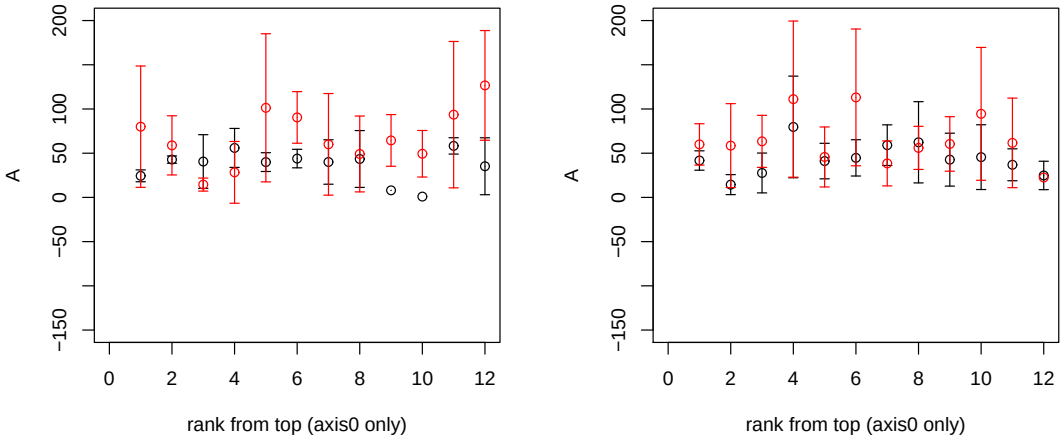

(a) SO (a)

(b) CA (a)

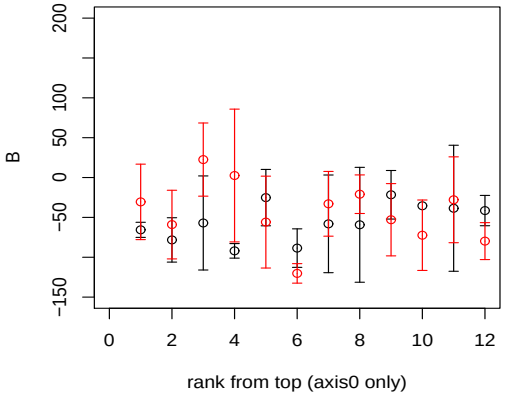

(c) SO (b)

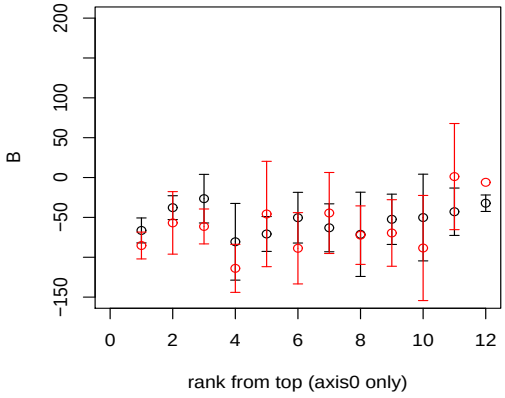

(d) CA (b)

Figure 6.17: Estimated parameters a and b when the inclination model is applied to leaves of genotype Soisson and Caphorn, measured over the two experiments. Red indicates measurements from experiment 1 and black from experiment 2.

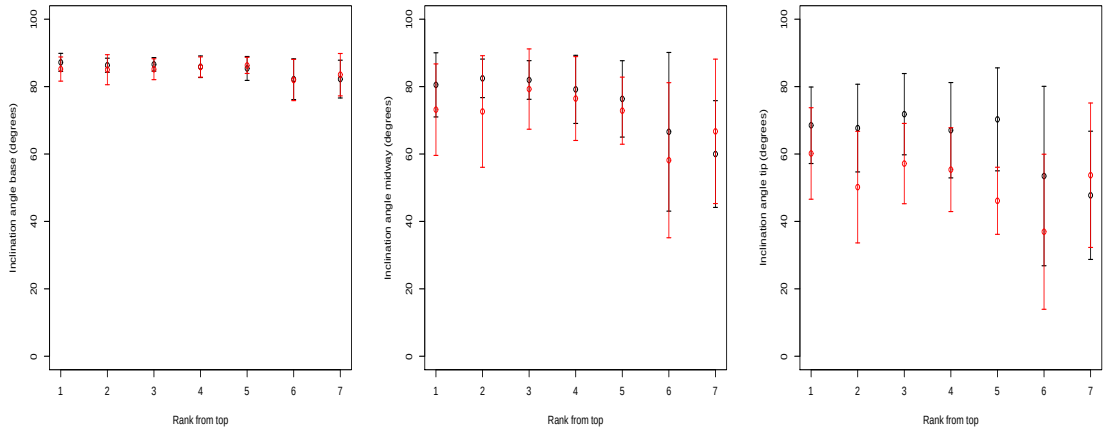

(a) Base (b) Middle (c) Tip

Figure 6.18: The mean and standard deviation of the inclination angle per rank from top, at the base, middle and tip of the leaves on the main stem. The red circles represent Soisson (data collected over experiment 1 and 2) and the black squares, Caphorn (data collected over experiment 1 and 2).

It is assumed that the quadratic model is appropriate for all leaves. No correlation between the parameters a and b were found and no significant difference can be observed between the architecture of winter leaves and higher leaves.

Currently within the ADEL wheat model the parabola model is expressed using inclination at the base of the leaf and tip to describe the curvature of the leaves. Using the fitted quadratic model, these two parameters were estimated, assuming the base of the leaf is 0.1 normalised length from the base. In addition the inclination angle at the middle of the leaf was also estimated.

Within ADEL-wheat these two parameters are set as angles from the azimuth rather than from the main stem and as such the inclination angles will be described within this analysis as such. Figure 6.18 displays the base, middle and tip angles for leaves of Caphorn and Soisson (using data from experiment one and two) per phytomer rank from top (flag leaf is rank 1).

The inclination angle at the base of the leaves is shown for both genotypes to be very close to the angle of the stem. The deviation from the mean base inclination angle is shown to be greater for the leaves of lower phytomer rank. The inclination angle midway along the leaf is shown to be stable over phytomer rank. An increased deviation from the mean middle inclination angle over

the lower ranks is however also noticeable for both genotypes. A slight although not significant difference is observed between the two genotypes, with Caphorn having a consistently greater mid leaf inclination angle, with the exception of rank (from top) 6 when compared to mid leaf inclination angle from leaves of genotype Soisson. The difference between genotypes is more obvious when comparing tip inclination angle, with Soisson having consistently lower inclination angles compared to Caphorn for leaves of all phytomer ranks. This difference is not significant and neither is the slight difference noted in lower leaves for both genotypes, with the inclination angle being lower, see Figure 6.18. The base inclination angle is shown here to be very close to the direction of the main stem.

When the ADEL wheat model was initially parameterised a strong relationship was found between the inclination angle at the base and that found at the tip. The inclination angle at the base (0.1 normalised length from the base) of the leaf is shown to be close to 90 degrees. No useful correlation is found between this angle and the angle at the tip of the leaf. Instead a comparison between the inclination angle at normalised length of 0.1 along the midrib from the base of the leaf, to the inclination angle at the mid point and at the tip of the leaf was investigated. A stronger relationship is found to exist when looking at the inclination angle at 0.1 normalised length along the leaf and the inclination angle at the middle of the leaf but not at the tip (see figure 6.2.3).

When digitising the leaf the initial data points collected represent the leaf along the main stem, which has resulted in this observed high inclination angle. As a result it is suggested not to be appropriate as the parameter base inclination angle required within ADEL wheat to simulate leaf curvature. Instead it is assumed that ‘base inclination angle’ should be the estimated inclination angle midway along the leaf.Further analysis is suggested to find the most appropriate length from the base to be used within the model however was not carried out here due to time restraints and low confidence in the data collected.

Instead, it is assumed that the parabola model is sufficient to model all leaves and that the parameter base inclination angle Φ_0 is better described using the inclination angle midway along the leaf. These parameters are described using a distribution function within the ADEL-model.

In order to calculate these distributions the following histograms of these two parameters include data obtained from leaves where the inclination of the leaf is above zero as it is assumed that leaves with lower inclination angle are senescent or broken and as such not representative of a

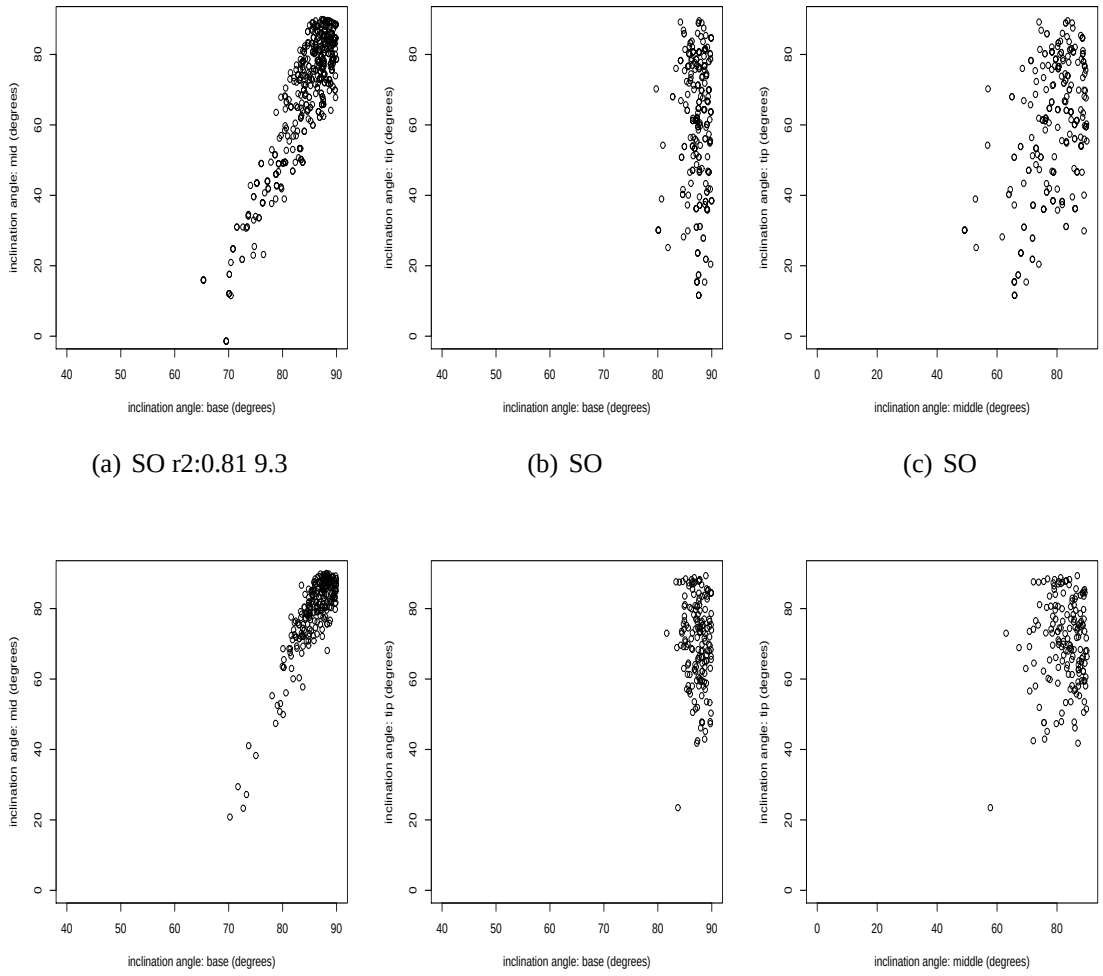

(a) SO r2:0.81 9.3 (b) SO (c) SO

(d) CA r2: 0.78 5.9 (e) CA (f) CA

Figure 6.19: Correlation of the inclination angle near the base (0.1), middle of the leaf and at the tip for lamina of Soisson and Caphorn (experiment 1 and 2 data)

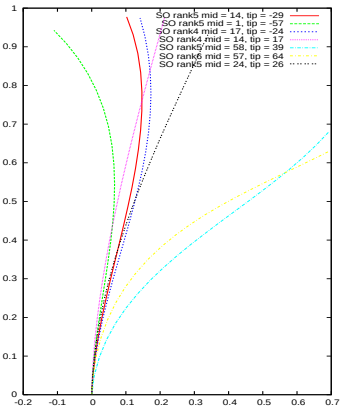

(a)

Figure 6.20: Reconstruction of the curvature of Soisson laminae are shown to illustrate negative tip angles.

median leaf. Leaves which have an inclination angle at the tip which is greater than that measured midway along the leaf are also ignored, thus ignoring leaves which bend towards the main stem.

There are occurences when leaves are estimated to have a negative tip inclination angle (from the vertical) (see Figure 6.20). Most of these leaves are from the genotype Caphorn which has erectophile leaves. It is assumed that these results are due to the errors accepted with digitising. Most of these leaves have an inclination angle of negative 10 degree or less at the tip and those with this tip angle have a similar angle found for the inclination angle at the middle of the leaf. Instead of disregarding these leaves the difference in angle from the stem, so in this example -10 degrees, is instead assumed to be 10 degrees.

The tip angle is currently parameterised within the model as a normalised value of the inclination angle. This assumes that the tip angle cannot be more than the base angle (i.e leaves folding towards the stem) and also that leaves cannot have a tip angle less than zero. It must be noted that during this analysis it was observed that some leaves have negative inclination angles and as such cannot be included within suggested parameterisation. No obvious pattern or reason was found to connect the appearance of leaves with negative tip inclination angles, when considering phytomer rank or axis. It was found however that if only leaves with a low rmse (rmse <1) are used within the analysis the leaves with negative tip inclination angle are omitted altogether. It is therefore deemed acceptable to assume that these leaves instead have a zero tip angle. If instead negative tip angles were allowed and as such tip angle was no longer normalised by the

inclination angle at the base (in this case middle of the) leaf, it would result in two separate distributions being used to describe base and tip midrib angle which would result in unrealistic leaves being described.

It is suggested here that further analysis, which cannot be completed within the time frame of this thesis, is carried out into the presence of negative tip angles, but that it should be assumed here that normalising the tip angle to the base angle (the middle angle in this analysis) is appropriate and the error created with assuming all negative tip angles are zero, is small. The following histograms show the distribution of the parameter: dphin values (tip angle normalised by base angle(middle angle in this analysis)) for both Soisson and Caphorn and the Cumulative frequency. The cumulative frequency is used within the parameterisation of the midrib curvature within the model.

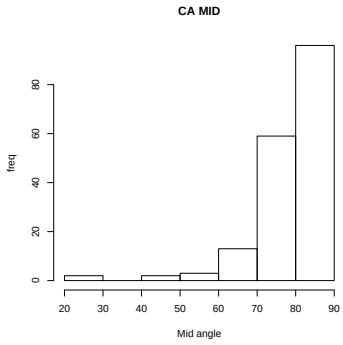

(a) Caphorn

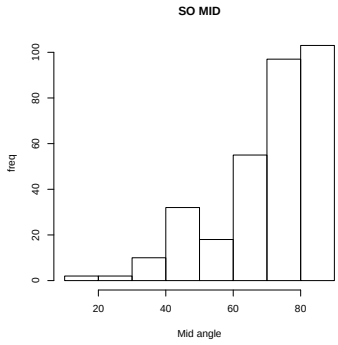

(b) Soisson

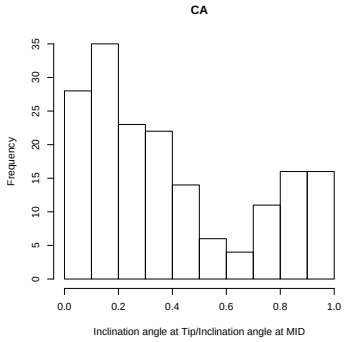

(c) Caphorn

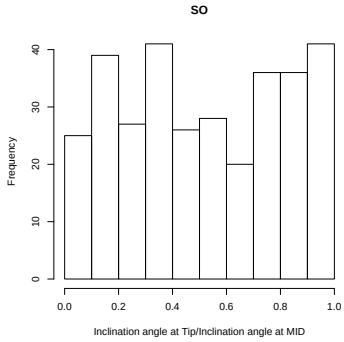

(d) Soisson

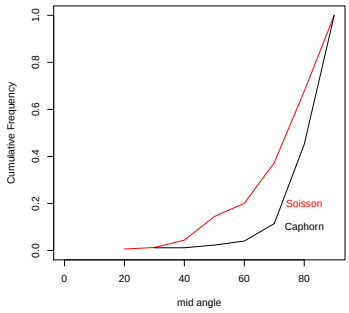

(e) Inclination Angle

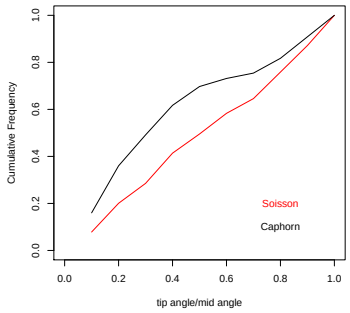

(f) Tip Angle

Figure 6.21

6.2.4 Phyllotaxy

The range of observed angles between subsequent blades was found to be relatively large, however the angle between subsequent leaves of genotype Isengrain are shown to be clustered around 100 degrees and those of Soisson around 85 degrees. No significant difference in angle between subsequent leaves is noticed with rank of leaf. It can be suggested from looking at these two genotypes in particular that leaves are more likely to have a spiral phyllotaxy for all leaf rank, rather than an opposite which would have a a difference in degree at 180. This contradicts the parameterisation currently in place within the ADEL-wheat model where the bottom leaves (8 ranks below flag leaf) are suggested to be more opposite (180 degrees) and the top leaves a more spiral phyllotaxy.

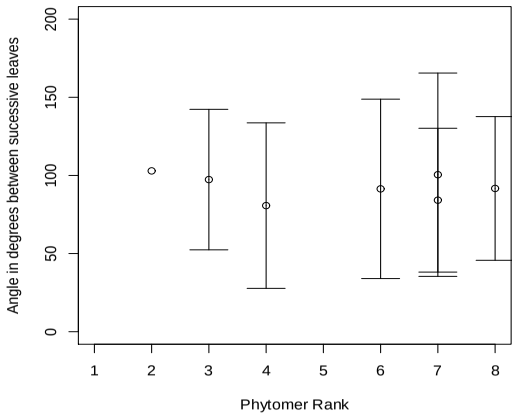

(a) IS

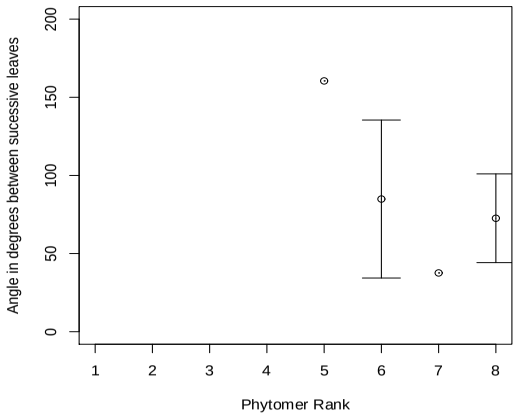

(b) SO

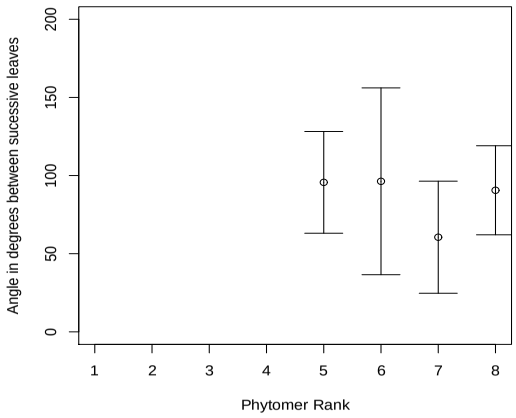

(c) CA

*Figure 6.22: Mean and Standard Deviation(*2) of the angle between subsequent lamina of genotypes Isengrain (IS), Soisson (SO) and Caphorn (CA)*

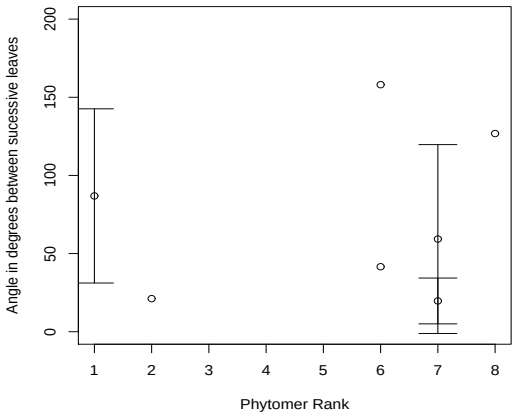

(a) IS T1

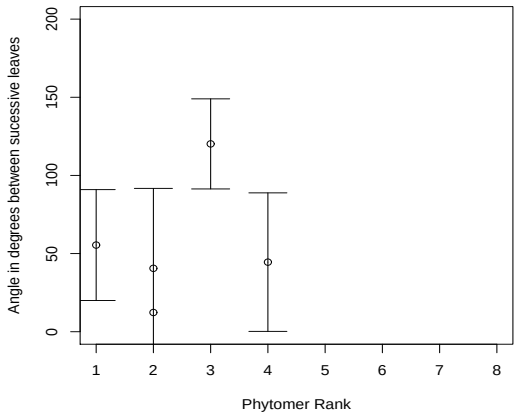

(b) IS T2

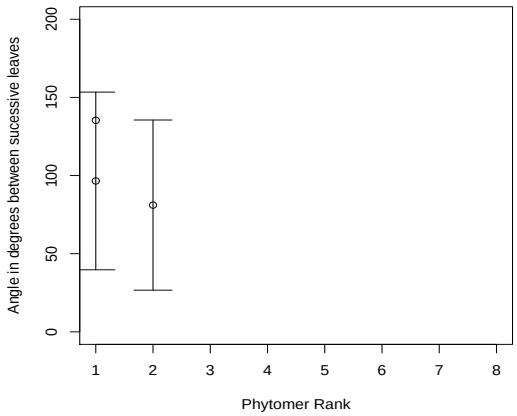

(c) IS T3

*Figure 6.23: Mean and Standard Deviation(*2) of the angle between subsequent lamina on the three tillers (Tiller 1 (T1), Tiller 2 (T2) and Tiller 3 (T3)) of genotype Isengrain.*

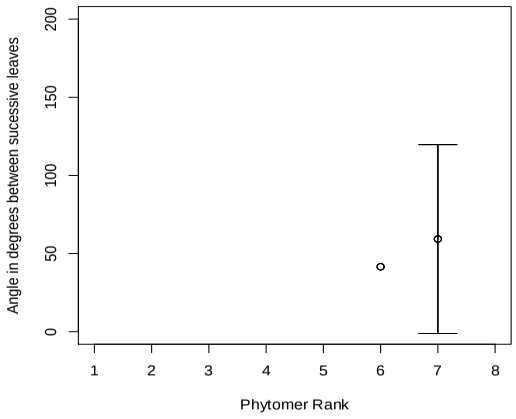

(a) SO T1

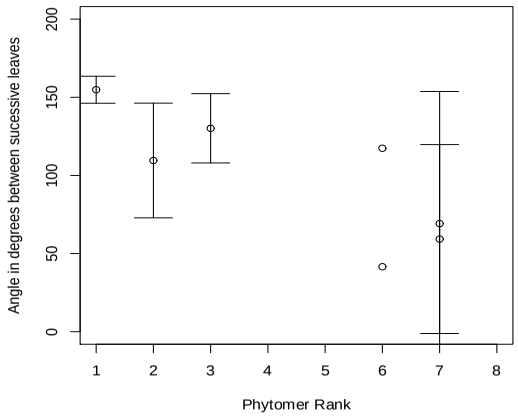

(b) SO T2

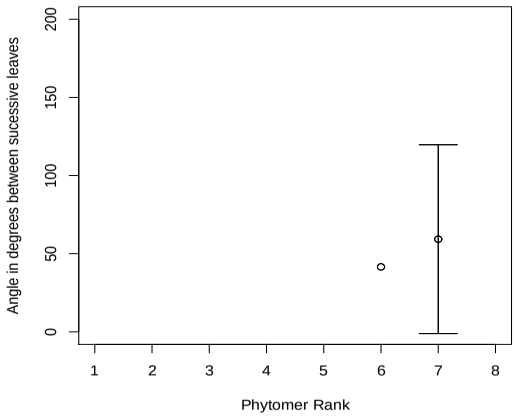

(c) SO T3

*Figure 6.24: Mean and Standard Deviation(*2) of the angle between subsequent lamina on the three tillers (Tiller 1 (T1), Tiller 2 (T2) and Tiller 3 (T3)) of genotype Soisson.*

6.2.5 Discussion

Main stem and tiller angle

The angle of the main stem was found to vary very slightly from the vertical, with the angle becoming closer to the vertical the further on from development. It was found for Soisson, over the earliest date that data was obtained, that variation from the vertical was much greater than for any other genotype included in the analysis. This seemed counter intuitive, Soisson plants were no taller, or the leaves of no greater area, which may have given some reason for this observation. Soisson does however have more planophile leaves which may have the effect of 'pulling' at the main stem causing this variation.

No difference could be observed in tiller angle over rank, although it is suggested that additional data should be obtained to confirm this finding. In addition data is suggested to be obtained that spans different growing seasons which did not occur within this research. Most published literature focuses on tiller production rather than angle from the main stem and so meaningful comparison with published data is limited.

Midrib curvature

Midrib curvature was found not to vary significantly between different years and as such different growing conditions. There was also little difference noticed over rank, however early ranks (less than rank 4) were not measured. This makes it hard to agree or disagree with the parameterisation in place for winter leaves within ADEL-wheat, which assumes that bottom and middle leaves are mainly ascending only and top leaves are made up of ascending and descending parts. No differences could be found between middle and top leaves in terms of error if a parabola model only was applied to the data. There was however a greater variation in rmse of the fit of the parabola model over lower ranked leaves of Soisson compared with Caphorn leaves of similar rank. Again this may be a result of the Soisson leaves being more planophile than Caphorn leaves. It is accepted that the data obtained from the digitisation does contain a lot of noise making comparisons and observations on midrib curvature and the effect of rank, genotype and growing conditions problematic.

Phyllotaxy

Phyllotaxy was found to differ between the genotypes Isengrain and Soisson with subsequent leaves of genotype Isengrain shown to be clustered around 100 degrees and those of Soisson around 85 degrees. Within ADEL-wheat it is assumed that the phyllotaxy changes with rank of leaf however no significant difference in angle between subsequent leaves is noticed with rank of leaf. One observation is that the leaves are more likely to have a spiral phyllotaxy for all leaf rank, than opposite which contradicts the parameterisation currently in place within the ADEL-wheat model where the bottom leaves (8 ranks below flag leaf) are suggested to be more opposite and the top leaves more spiral. Due to the data quality and quantity it is decided that the parameterisation of phyllotaxy remain as to that already suggested within the ADEL-wheat model. It is suggested that in order to carry out a more in depth study of phyllotaxy that at least two leaves are digitised per sampling date to enable more data on angles between leaves.

6.2.6 Conclusion

In general the confidence with the data collected is low, making new assumptions and changes to the current parameterisation within ADEL-wheat difficult. However some changes have been made such as the main stem angle from the vertical. This has been reduced from 10 degrees to 5 degrees. This is not perfect and a parameter which allows a variation in angle is suggested to be a useful further development in the model. The data collected on tiller angle did not include internode location and rank and as such no in depth analysis into the straightening of the tillers in relation to the internode ranks could be made. A significant change was made to the leaf midrib curvature. It is suggested that a simple parabola model is sufficient to model all leaves over all ranks. A warning is given however that no data was recorded on leaves of rank 4 and lower, however within the ADEL model it is suggested that base and middle leaves are more similar in architectural traits that upper leaves. Data was obtained on middle leaves and as such lower leaves are assumed to be similar to the data obtained on such leaves. In summary it is accepted that the data obtained from the digitisation does contain a lot of noise making comparisons and observations on midrib curvature and the effect of rank, genotype and growing conditions problematic. An additional problem that could not be overcome in the time frame of this thesis is the inability to parametrise a leaf to have an inclination angle (from the horizontal)

greater than 80. Much time was spent on this problem with no clear solution. Although many of the leaves were shown to have inclination angle much higher they are given a maximum of 80 degrees due to the limitation of the model.

Chapter 7

Model Checking

7.1 Canopy Cover

Canopy cover is one way in which the output of the ADEL-wheat model can be validated and so for this purpose canopy cover photographs were taken throughout experiment 2 of the two canopies; Soisson and Caphorn. This chapter outlines the method used to obtain the photographs and the analysis applied to estimate percentage cover. The estimated percentage cover (from canopy cover photos) and associated error is given over thermal time.

7.1.1 Experiment 1

Ten horizontal, hand held, canopy cover photographs were taken on the 21^{st} February (2004) over two canopies, Soisson and Isengrain. The photos were taken parallel to the crop row with at least two inter rows present. Random locations within each plot were chosen at each sampling date. To avoid shadowing they were taken at an overcast part of the day.

7.1.2 Experiment 2

Canopy cover measurements were made weekly from 4^{th} January 2005 to 28^{th} April 2005. At each sampling date ten hand held horizontal photographs were taken of both canopies; Caphorn and Soisson. Each of the ten photographs were taken at the same location, with each location being marked by a numbered orange picket.

7.1.3 Date Analysis

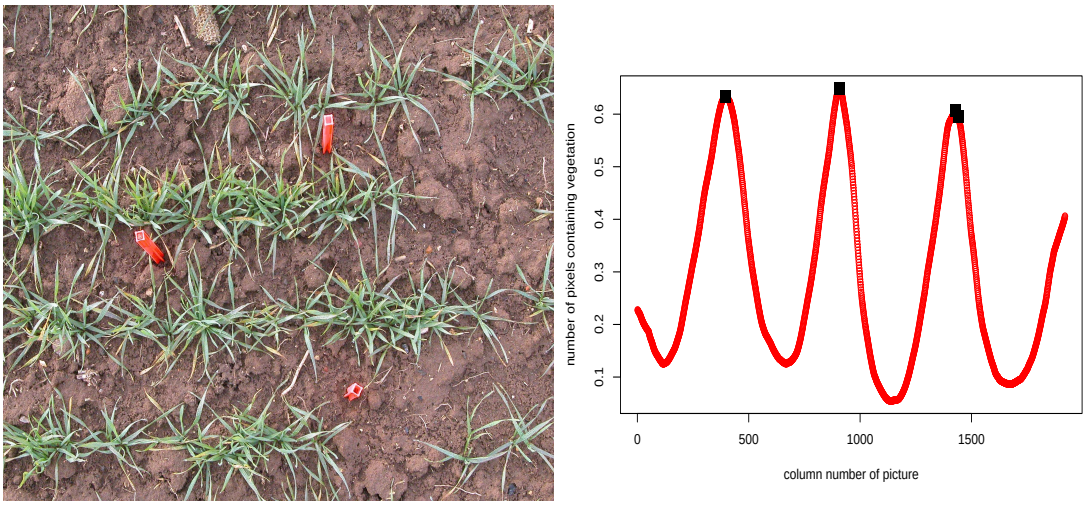

Figure 7.1: a. The initial canopy cover photograph taken on 9th February 2005 over the Caphorn canopy. b. The total value of the photograph columns where vegetation is one and soil is zero with a smoothing function added and estimated local maxima shown.

The images were taken in NEF or TIFF format and initially converted to JPG. These images were then transformed from RGB (red, green, blue) colour space to HSI (hue, saturation, intensity). A despeckle function was then carried out on all images to counteract any possible compression issues when converting from the original format of NEF or TIFF to jpg (a value of median 5 was used). The hue band was used to distinguish vegetation from soil. The threshold values used were kept constant for all photographs. For each sample set of photographs obtained per day, the threshold values were checked to be appropriate. In order for the percentage cover to be calculated using the same number of rows and interows over all images a method was used whereby the sum of cover per image column was initially calculated. A smoothing function was then applied to this data and the local maxima extracted. This local maximum represented a row of plants (see Figure 7.1). A row spacing is set using this data and 3 times this is given as the area to be used to estimate percentage cover. If, on visual inspection, the calculated row spacing looked to be incorrect it was over overridden and a more plausible row spacing given based on that calculated from other photographs taken on the same day. The percentage cover was calculated within this set area and also within the whole photograph giving a mean best and total percentage cover estimate respectively.

Various methods were also applied to images where the above methods were giving unrealistic estimated. Such methods were developed to estimate canopy cover of some photographs taken on and around February 14th (2004); experiment 2, which were being incorrectly estimated using the method just described.

The chosen alternative method involved initially reducing image resolution which results in smoothing the images in addition to applying a medium filter. Then using band 1 and band 2, hue and saturation, a scatter plot was used to identify three distinct regions, which were soil and yellow and green vegetation. Using the boundaries for these categories, an Iso Cluster analysis was performed using only one iteration. Where this method is used it is referred to within this chapter as the Iso Cluster method.

7.1.4 Results

Figure 7.2 shows two original canopy cover images and the analysis of each image using method 1 and the Iso Cluster method.

The Iso Cluster method is found not to work on one of the images (right). This image was taken on the 8th March 2005 and the other image was taken on the 17th January 2005. Images taken later in the sampling year were found to be underestimated, on some dates by more than 15%, using the Iso Cluster method.

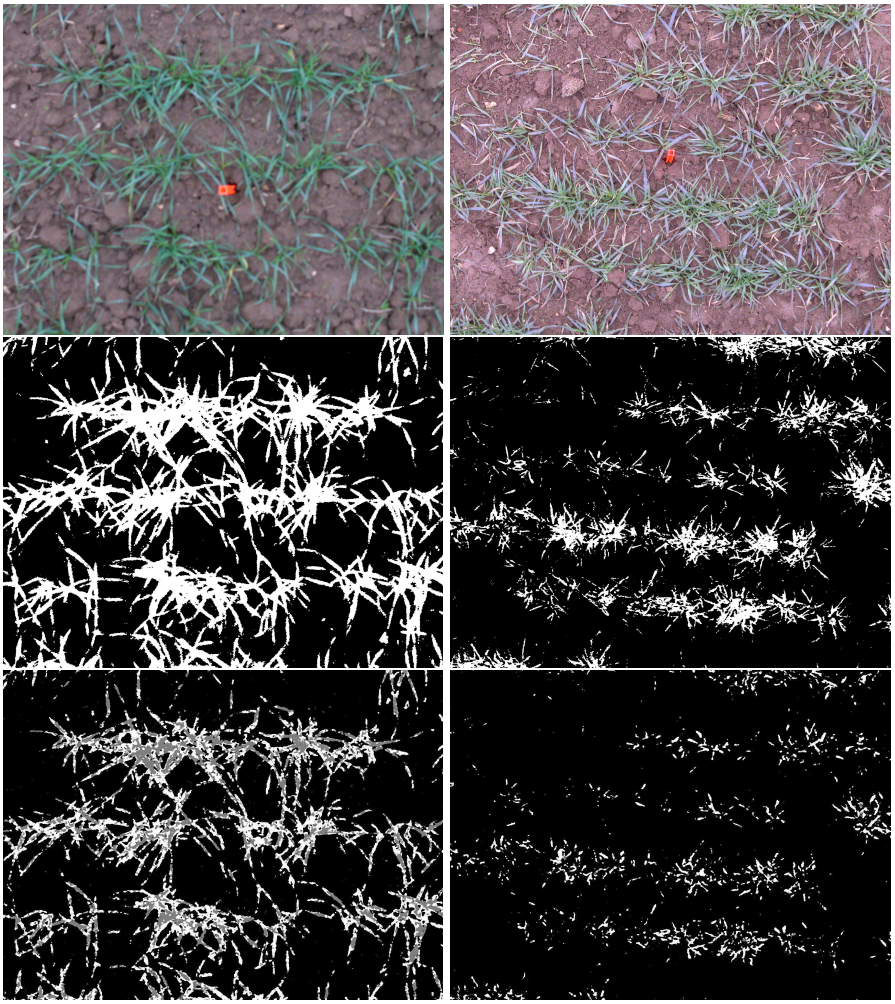

Figure 7.2: The top figures show examples of observed canopy cover. The figures underneath show these observed images when the simple technique are used to estimate canopy cover and at the bottom when the the shrinking and Iso Cluster method is used.

From varying the thresholds and methods it was considered that the best option was to apply method 1 to all images and omit the problem data captured on certain dates. Figure 7.3 illustrates the estimated canopy cover using method one for all data. The photographs that give unexpected canopy cover are those taken between the 14th February and the 3rd March (632 and 646 degree days respectively)

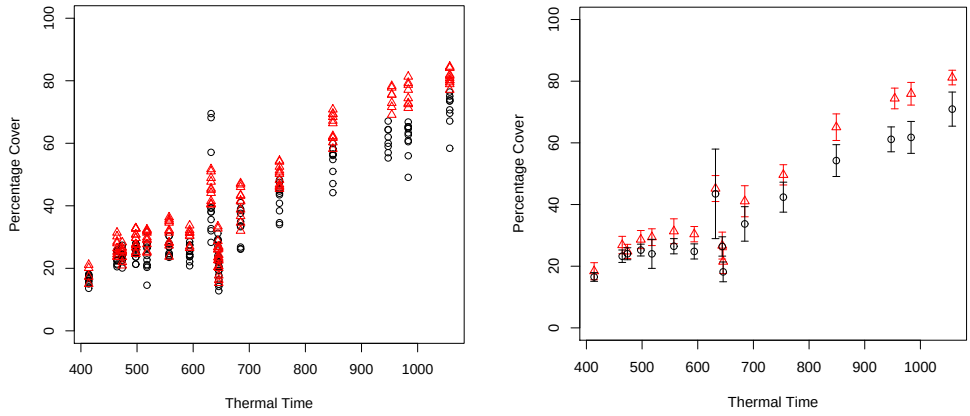

Figure 7.3: Canopy cover as estimated from method 1 over all all sampling dates. Soisson is shown using triangles, and Caphorn is shown using circles.

Figures 7.3 show the original data and the analysis of each image using method 1.

As can be observed the data obtained on the 14th February was being over estimated and that on the 3rd March under estimated. The data on the 21st February however seems to be reasonably estimated in relation to images before and after this date.

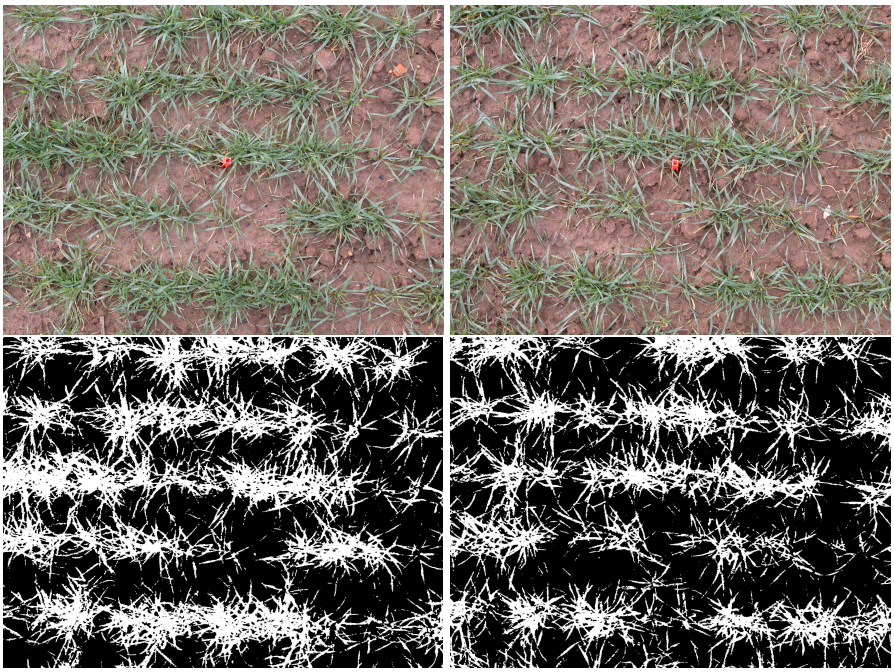

Figure 7.4: Two canopy cover photographs taken on the 14th February are shown underwhich are two classified images (using method 1) of these photographs

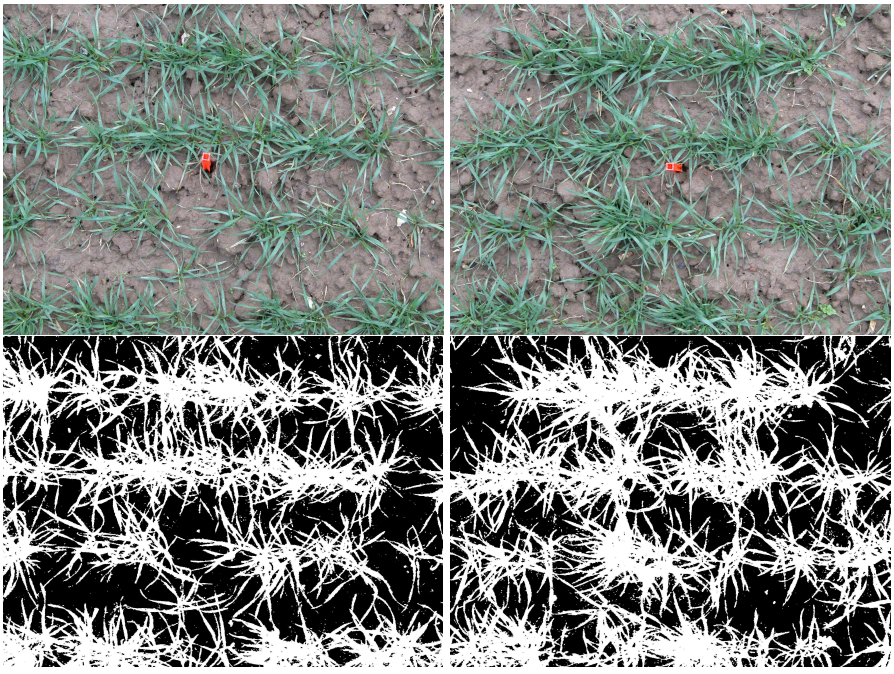

Figure 7.5: Two canopy cover photographs taken on the 21st February underwhich are two classified images (using method 1) of these photographs

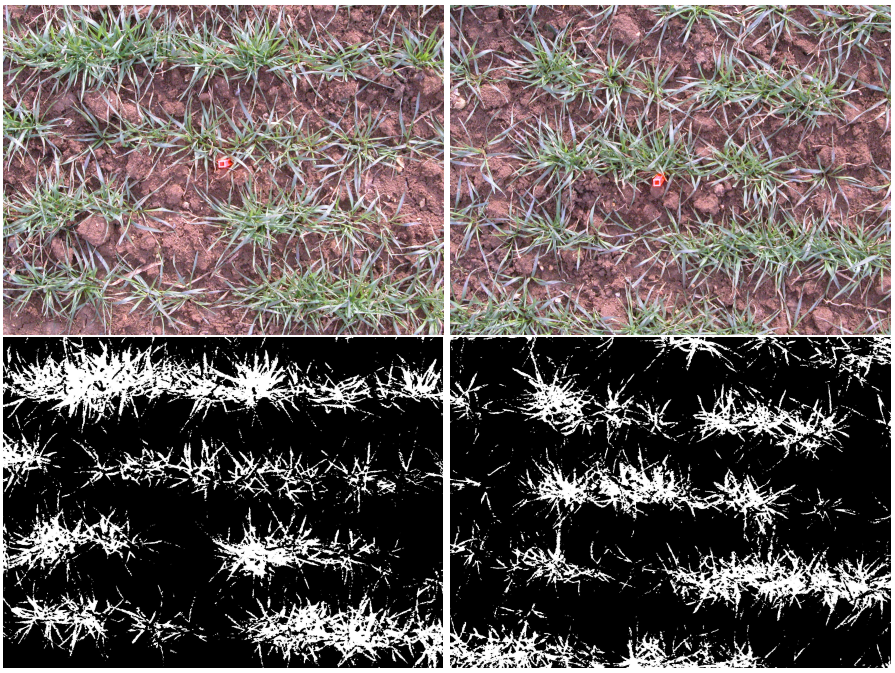

Figure 7.6: Two canopy cover photographs taken on the 3rd March underwhich are two classified images (using method 1) of these photographs

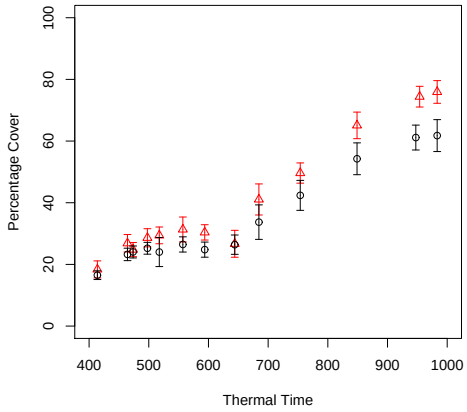

Figure 7.7: Percentage cover as estimated using method 1 with 14st February and 3rd March data omitted. Caphorn shown using circles and Soisson using triangles

It is observed that the canopy cover percentage over thermal time of the Soisson is greater than that of Caphorn. Soisson is expected to show a more planophile leaf angle distribution and Caphorn a more erectophile leaf angle distribution which would explain this difference. Alternatively the difference could be due to LAI which would link to the final lamina length and/or width and or tiller density. Similarity between the LAI of both genotypes indicates that LAI is unlikely to be an influential factor creating the observed differences in canopy cover between these two genotypes. If instead lamina length and width are compared, the lamina of genotype Soisson (experiment 1) are found to have thinner leaves after rank 6 (inflexion point on lamina length model) compared to the leaves of Caphorn (experiment 1) with early leaves having similar width and length. Comparison of lamina dimension between the same genotypes but as measured in experiment 2, show a similar pattern as those of experiment 1,with two exceptions. The higher ranking leaves of Caphorn are slightly thicker and Soisson and Caphorn are shown to have much shorter leaves later on after the plateau (rank 6 and greater) than compared to Soisson and Caphorn from experiment 1. It is unlikely that these differences, especially as LAI is shown not to differ significantly between genotypes to be causing the observed difference.

A difference is observed between the tiller model of Caphorn and Soisson (experiment 2 only), with Caphorn shown to have a higher number of observed tillers than Soisson but slightly less that survive to produce a head (ks-test D=0.333 P=0.401, which confirms this difference). The difference observed between tiller number dynamic between the two genotypes could therefore be considered to be having an influence on the observed canopy cover differences between the two genotypes.

From considering the LAI and leaf width and length of both genotypes the difference in cover is suggested not to be influenced by these factors. The difference in the tiller model may have an effect on the canopy cover however the architectural difference is considered more likely to be the cause of difference.

7.1.5 Discussion

The method of extracting three rows of crop from the photographs of the observed canopy cover images, from which percentage canopy cover is estimated is presented here as an interesting idea. However from the small sample set it was shown not to greatly affect the estimated final

percentage cover when compared to estimating cover over the entire image.

The profile of the distribution of vegetation over the image, used within the method to extract three rows is considered a useful visual representation of the canopy and is utilised within the following chapter when looking at the effect the different model parameters have on its ability to model canopy cover.

The Iso Cluster method did not significantly decrease the error or help give a more reasonable estimate of cover for some of the images which were hard to classify. The advantage of the Iso Cluster method was that it calculated the senesced material and green material. However for the purposes of this work, only the overall percentage cover was required and it is concluded that either method presented is suitable to calculate the percentage cover.

When looking at the progression of canopy cover over time in experiment 2, there is a plateau (around 500 - 620 thermal time) of canopy cover. This corresponds to the plateau in lamina length over phytomer rank and helps to explain why this plateau in canopy cover is observed.

7.1.6 Conclusion

The progression of canopy cover is estimated for two genotypes, Caphorn and Soisson, grown during experiment 2. Different methods were used to estimate percentage cover from the photographs. The extraction of three rows of canopy from the image and estimating cover from these cropped images was presented as a fair method of estimating vegetation cover. The Iso Cluster method was also applied to some images, however the estimates of cover were deemed not to increase the estimated cover.

7.2 Structural Validation

The ADEL-wheat model is parameterised using the results discussed in previous chapters of this thesis. It is parameterised to represent two genotypes, Soisson and Caphorn which have differing architectural characteristics. The observed (from canopy cover photographs) and modelled (model simulated images of) canopy cover are compared. In addition the profile of modelled and observed canopy cover images are also compared. Suggestions are made and new simulations run to investigate why at some thermal times the model is not accurately predicting canopy cover.

It is important to understand the effect different parameters have on the modelled canopy cover. This is because modelled canopy cover is an important output of this model when coupled with a canopy reflectance model. If this canopy cover is modelled inaccurately it will inevitably create an unreliable modelled canopy reflectance and reduce the usefulness of this combination of models in predicting canopy reflectance.

Within this chapter parameters that effect the canopy cover have been grouped into three categories; phenological and architectural parameters and physical proprieties of how the data is collected for example, the distance from the canopy to the lens of the camera, which is referred to as boom length in this chapter. The effect on canopy cover of the placement of plants within the field is also investigated, which in this chapter is referred to as jittering. This is considered as the plants within a field do not grow in exact lines, instead the plants are jittered around the crop row. Another term used within this chapter is clumping. This is used to take into account the fact that some plants do not grow or die during development leaving gaps in the crop rows. This is also attempted to be simulated within this chapter and its effect on canopy cover investigated.

Thorough analysis has been carried out into the effect these parameters or setting values have on the canopy cover of the two genotypes mentioned, Caphorn and Soisson.

7.2.1 Methodology

The architecture of genotypes Soisson and Caphorn differ with Soisson being more planophile and Caphorn more erectophile. The parameterisation for these genotypes has been based on the

data collected in 2005 (experiment 2) (see table 7.1 for list of model parameters). The model outputs have been compared with observed data collected throughout the growing season, such as number of tillers, LAI, final organ lengths and canopy cover. Differences are noted between modelled and observed canopy cover. These differences effect the radiometric signal and therefore it is important to gain an understanding of why they have occurred. The rest of this chapter gives consideration to the perspective effect, leaf architecture, phyllochron (rate of leaf emergence), boom length (distance from canopy to camera lens) and the non-uniform spacing of the plants within the field (jittering and clumping, which is explained later in this chapter) as possible reasons why differences between modelled and measured canopy cover have occurred. Four models are suggested, two for each genotype which, within the next chapter are coupled with a canopy reflectance model and the modelled and observed radiometric data compared. Initially a ks-test is used as a comparison test to indicate similarities or differences between the two genotypes (Caphorn and Soisson) in terms of final organ length, number of tillers, LAI and percentage canopy cover. It is then used to compare modelled and observed final organ length for the two genotypes.

Phenological parameters

The parameters shown at the top of the table 7.1 describe as they suggest the final number of leaves that are to be produced on the different axes, MS (main stem), T1 (tiller one), T2 (tiller two) and T3 (tiller three). The stem angle is the angle in degrees the main stem deviates from the vertical. The tiller total is the maximum number of tillers that can be produced on each plant and the ShiftT1 (T2 and T3) is the delay in phytomer between each tiller and the main stem. NL1, NL2, L0, L1 and LF are all parameters that describe the lamina length over phytomer rank. NL1 is the phytomer rank at the end of the modelled plateau in lamina length noticed over the early phytomer. NL2 is the number of phytomer before the last phytomer that the lamina length starts to decline in length. L0 and L1 and LF are the lamina length in cm. LO is the length at phytomer rank 1, L1 is the length of the lamina during the plateau in length and LF the length of the final lamina. S1, S2, N1S, N2S and SF are all parameters used to describe the sheath length over phytomer rank. S1 and S2 describe the sheath length at rank NS1 and NS2 respectively. NS1 is the rank at the end of the plateau, and NS2 is the phytomer rank at the the end of the first increment in length phase and the beginning of the second. N1I, N2I, I2 and IF are the parameters that describe the length of the internodes over phytomer rank. N1I is the phytomer rank at which the internodes start to elongate and NSI is the phytomer rank at the end of the first increment phase and beginning of the second. I2 is the internode length at rank N2I and IF, the length of the final internode. The next three parameters describe the lamina width model. W0 is the lamina width at

Parameter	Description	Caphorn	Soisson
$Total\ Leaves\ MS$	12	12	
$Total\ Leaves\ T1$	9	9	
$Total\ Leaves\ T2$	8	8	
$Total\ Leaves\ T3$	7	7	
$Stem\ Angle$	4	4	
$Tiller\ total$	3	3	
$Shift\ T1$	2.9	3.1	
$Shift\ T2$	3.5	3.7	
$Shift\ T3$	4.4	4.2	
$NL1$	5.94	5.97	
$NL2$	2.24	1.69	
$L0$	4.55	3.01	
$L1$	24.56	31.33	
LF	16.74	15.99	
$S1$	3.43	3.39	
$S2$	11.04	11.20	
$N1S$	5.77	4.67	
$N2S$	7.72	7.44	
SF	14.29	15.49	
$NI1$	7.92	6.68	
$N2I$	10.74	11.28	
$I2$	9.97	10.99	
IF	23.73	26.03	
$W0$	0.29	0.33	
$Walpha$	0.0151	0.0106	
$W1$	1.86	1.57	
$PHYLL$	107	98	

Table 7.1: Phenological parameters used to model Caphorn and Soisson

phytomer rank 1, Walpha is the curved model parameter describing the lower mains stem lamina and W1 is the lamina width of the final lamina.

x	u R(0,1)	Phi_O(x,u)
<0.1	–	$30 + 50 * u$
$>0.1<0.45$	–	$70 + 10 * u$
>0.45	–	80

Table 7.2: Values are shown that are used to estimate the inclination angle of the lamina of Caphorn (Phi_O).

x	u R(0,1)	$DPhi_n$(x,u)
<0.16	–	$0.1 * u$
$>0.16<0.36$	–	$0.1 + 0.1 * u$
$>0.36<0.49$	–	$0.2 + 0.1 * u$
$>0.49<0.62$	–	$0.3 + 0.1 * u$
$>0.62<0.70$	–	$0.4 + 0.1 * u$
$>0.70<0.73$	–	$0.5 + 0.1 * u$
$>0.73<0.75$	–	$0.6 + 0.1 * u$
$>0.75<0.81$	–	$0.7 + 0.1 * u$
$>0.81<0.91$	–	$0.8 + 0.1 * u$
>0.91	–	$0.9 * 0.1 * u$

Table 7.3: Values used, along with the inclination angle from the base, to model the parameter $DPhi_n$ for Caphorn. $DPhi_n$ is the inclination of the tip of the lamina. The values in this table describe the ratio of the lamina tip angle in relation to the inclination angle $DPhi_o$

Geometry parameters

PCASS is a parameter which describes the ratio between the parabola and ellipse model which simulates the curvature of the lamina midrib and is set to 1 for both genotypes. The other geometry parameters are shown in Tables 7.2 which gives the distribution of parameter values of the inclination angle for the midrib of Caphorn lamina and Table 7.3 which gives the ratio of the inclination angle, which is used along with the inclination angle at the base to describe the angle at the tip of the lamina and Table 7.5 which gives the distribution of parameter values of the inclination angle for the midrib of Soisson lamina and Table 7.4 which gives the ratio of the inclination angle, which is used, along with the inclination angle at the base to describe the angle at the tip of the lamina. *Caphorn midrib curvature parameters*

x	u R(0,1)	$DPhi_n$(x,u)
<0.1	–	$0.1 * u$
$>0.1<0.2$	–	$0.1 + 0.1 * u$
$>0.2<0.3$	–	$0.2 + 0.1 * u$
$>0.3<0.4$	–	$0.3 + 0.1 * u$
$>0.4<0.5$	–	$0.4 + 0.1 * u$
$>0.5<0.6$	–	$0.5 + 0.1 * u$
$>0.6<0.65$	–	$0.6 + 0.1 * u$
$>0.65<0.76$	–	$0.7 + 0.1 * u$
$>0.76<0.87$	–	$0.8 + 0.1 * u$
>0.87	–	$0.9 + 0.1 * u$

Table 7.4: Values used, along with the inclination angle from the base, to model the parameter $DPhi_n$ for Soisson. $DPhi_n$ is the inclination of the tip of the lamina. The values in this table describe the ratio of the lamina tip angle in relation to the inclination angle $DPhi_o$

x	u R(0,1)	Phi_O(x,u)
<0.14	–	$20 + 30 * u$
$>0.14<0.2$	–	$50 + 10 * u$
$>0.2<0.37$	–	$60 + 10 * u$
<0.68	–	$70 + 10 * u$
>0.68	–	80

Table 7.5: Values are shown that are used to estimate the inclination angle of the lamina of Soisson (Phi_O).

Soisson midrib curvature parameters

7.2.2 Phenology

The two genotypes chosen to be the focus of this chapter are Caphorn and Soisson, as mentioned this is to do with their architectural differences. Below are graphs which show the phenological characteristics of these two genotypes, the observed and modelled final organ length measurements. Before comparing these differences for each genotype it is relevant to compare the two genotypes. A more detailed comparison can be found in the Phenology chapter (section 5), however when KS-tests were carried out it was found the biggest statistical difference between the two genotypes in terms of final organ length is between sheath length and the least difference with lamina length (lamina width ks-test D=0.278, P=0.161, lamina length ks-test D=0.352, P=0.013, sheath length ks-test D=0.117, P=$6.1x10^{-5}$, internode length ks-test D=0.167, P=1). In general the lamina of Caphorn are shorter but slightly wider than those of Soisson, with Soisson having a slightly longer final internode length. The number of tillers present is shown to differ between the genotypes, with Caphorn having a higher number of observed tillers than Soisson but having slightly less that survive than Soisson (ks-test D=0.333 P=0.401, which confirms this difference). The accumulation of these differences can be expected to be seen more clearly when calculating LAI. This was carried out using green leaf area and the estimated number of tillers present on the plant. The LAI is shown to be similar between the two genotypes (ks-test D=0.167, P=0.958). The difference is also expected to be seen when comparing the canopy cover between the two genotypes (ks-test D=0.338, P=0.295, which confirms the difference). As can be observed the pattern of canopy cover over low thermal time shows an initial increase followed by a plateau for approximately 300 degree days before a notable increase in cover until about between 1000 and 1100 degree days. The peak of canopy cover is shown to reach about 70 % for Caphorn but about 10 % higher for Soisson. A ks-test was caried out on the observed and modelled canopy cover for both genotypes , CA: D=0.375, p=0.215, SO: D= 0.438, p=0.066,the results of which indicate a difference between the observbed and modelled. To investigate this further the ks-test was carried out on data before thermal time 600 and after, the results being for Soisson before thermal time 600, D=1 and p= 0.016, and after D=0.546 nad P=0.075, and for Caphorn , before thermal time 600, D= 1 and p=0.0159 and after D=0.546 and p =0.075. It can be seen from these results a larger difference between observed and modelled is apparant over lower thermal times for both genotypes compared to higher thermal times.

Comparisons between observed and modelled outputs of final organ length over phytomer rank (sheath, lamina length and width and internode length) and number of tillers, LAI and percentage

canopy cover over thermal time (degree days) is also shown below. The graphs show that all final organ lengths (lamina length and width, internode and sheath length) are being simulated well within the model and that modelled LAI is also similar in pattern and absolute value over thermal time to that observed (CA: D=0.175 and P=0.919, SO: D=0.152, P=0.983). The modelled number of tillers is shown to be similar to that observed from 600 degree days onwards but with the modelled number of tillers, at earlier thermal times, being an over estimation (CA:D=0.296, P=0.507, SO: D=0.500 and P=0.077).

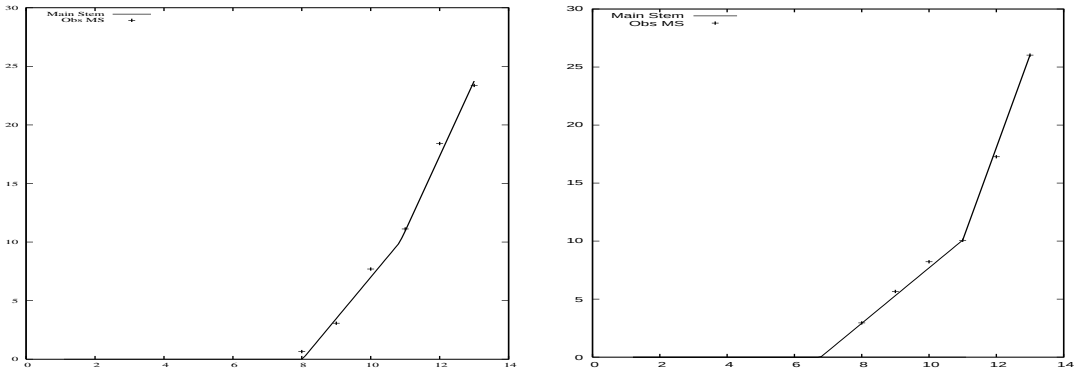

(a) CA05 Internode Length (b) SO05 Internode Length

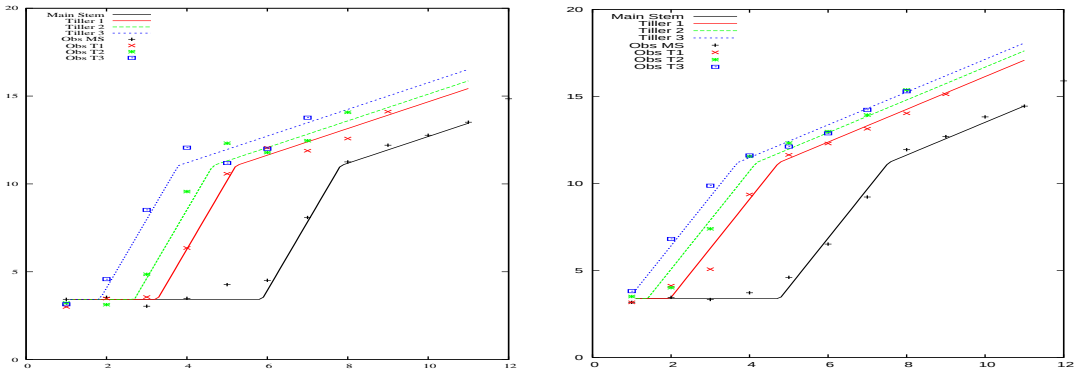

(c) CA05 Sheath Length (d) SO05 Sheath Length

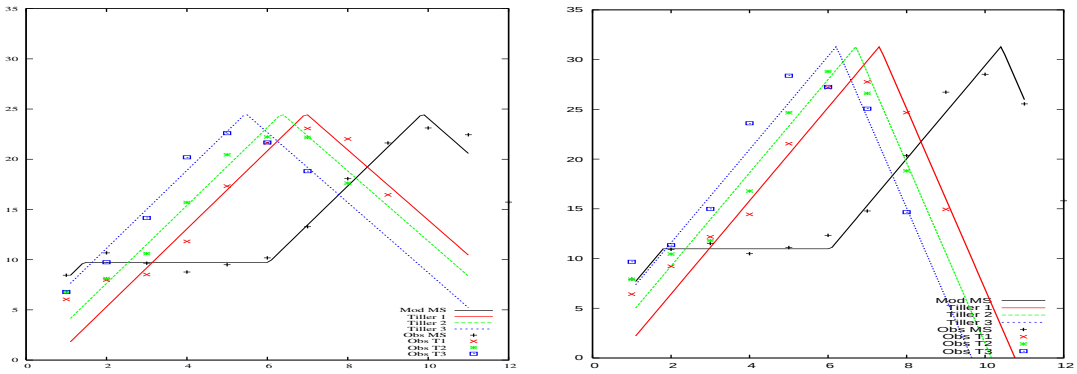

(e) CA05 Lamina Length (f) SO05 Lamina Length

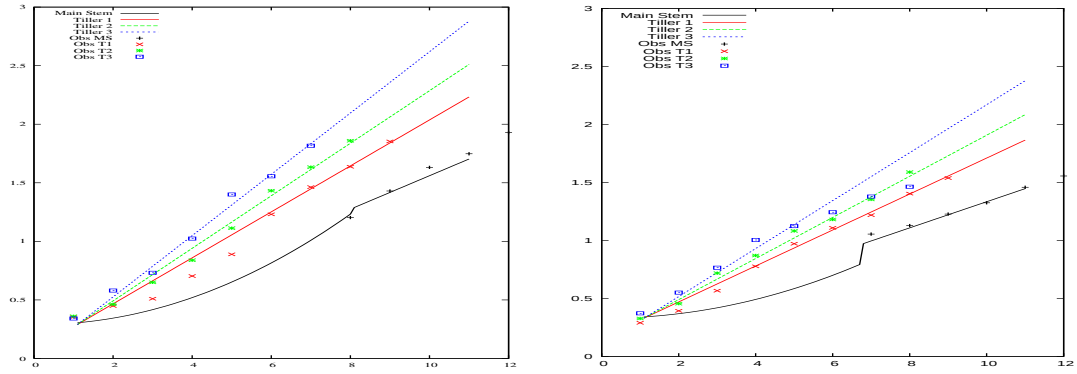

(g) CA05 Lamina Width (h) SO05 Lamina Width

Figure 7.8: The modelled final organ length as estimated from ADEL-wheat is shown using solid lines (main stem= black, Tiller one= red, Tiller two= green, Tiller three= blue). The points, also distinguished by axis rank by the same colour code, shows the suggested modelled final organ length as suggested within section 5.2.4.

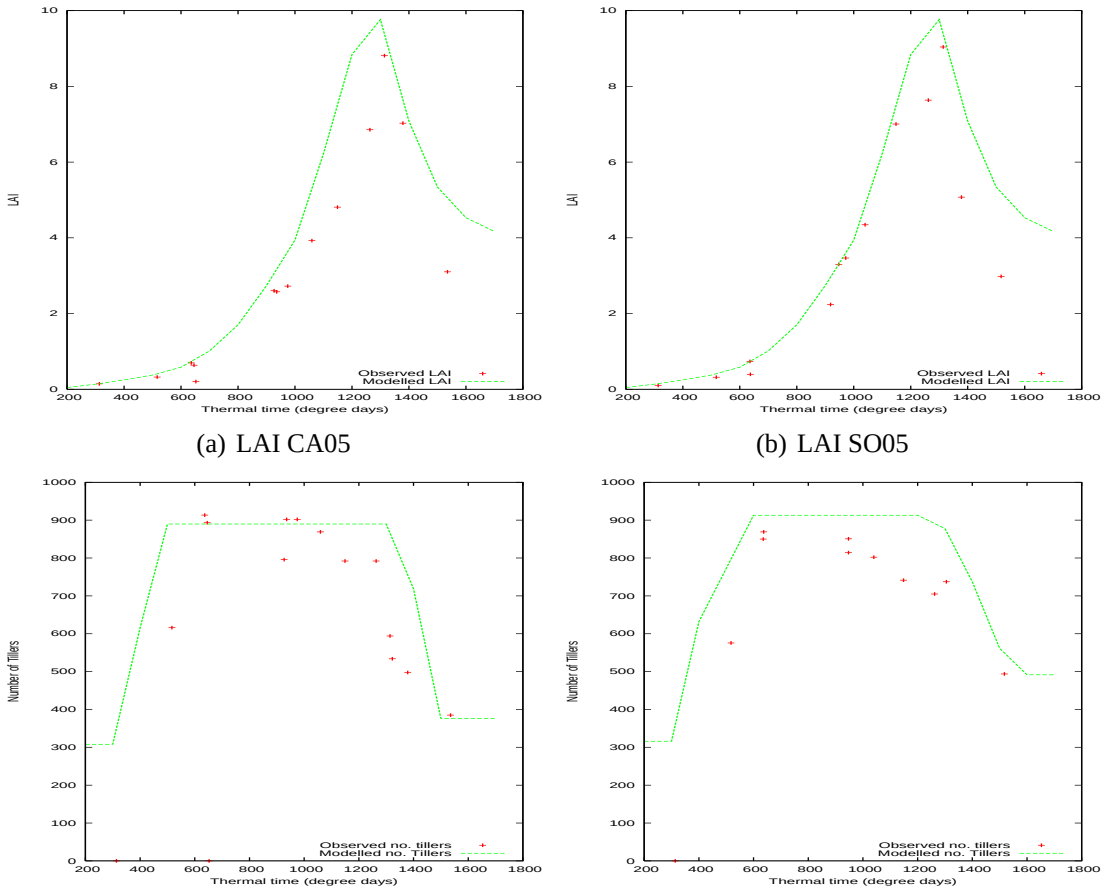

(a) LAI CA05 (b) LAI SO05

(c) No.Tillers CA05 (d) No.Tillers SO05

Figure 7.9: The modelled LAI and tiller number dynamics as estimated from ADEL-wheat is shown using solid (green) lines. The points (red) show the observed LAI and tiller number dynamics as suggested within section 5.4.6.

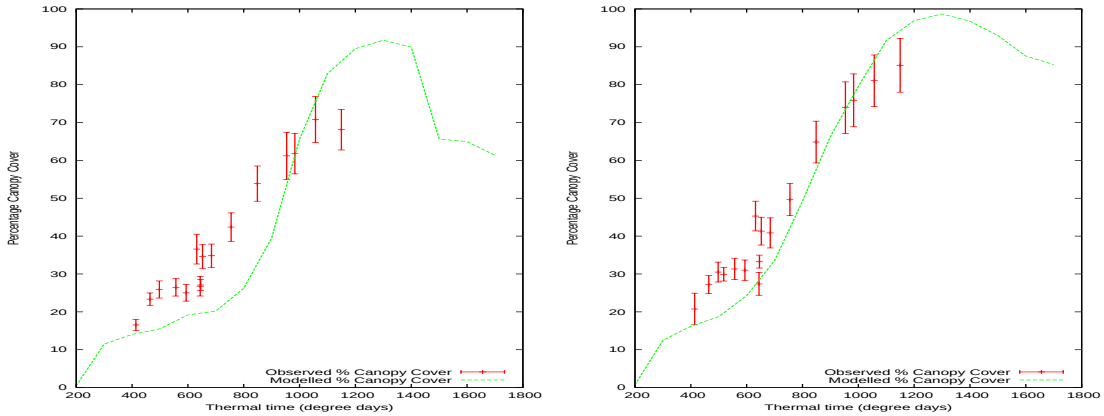

(a) Canopy Cover CA05 (b) Canopy Cover SO05

*Figure 7.10: The modelled canopy cover percentage as estimated from ADEL-wheat is shown using solid lines (green). The points (red) show the observed mean and standard deviation (*2) of the canopy cover percentage estimated from photographs taken of the canopy.*

Differences over early development can be observed in Figures 7.10 between modelled and observed percentage canopy cover for both genotypes. For both genotypes the difference between modelled and observed, before thermal time 600, is approximately 10-15%, with the observed canopy cover being higher than the modelled. After thermal time 600, the modelled canopy cover for Soisson is close to the observed value, howeover for Caphorn the difference increases to approximately 20-25% between thermal time 600-1000. The modelled canopy cover is then shown to be similar to that observed between thermal time 1000 to 1200 and then over estimated around thermal time 1200.

In order to investigate these differences the profile of the observed and modelled canopy have been produced. The output image from the model of the canopy cover is classified into soil and vegetation. A classification is used similar to the method used to estimate cover from actual photos. Three rows of canopy were identified and limits of DN value were associated with soil giving an image consisting of 0 (vegetation) and 1 (soil). The profile of the vegetation per image column is subsequently calculated (see Figure 7.11). The y axis values of these plots are ratio of soil:vegetation with 1 representing a row on the image containing only soil and 0 being a row containing only vegetation. The high plateau on these plots represent the soil gaps between the rows of plants. As can be observed these plateaus reduce in absolute value with development (thermal time) as more vegetation becomes present between the rows. The sharper low peaks represent the rows of vegetation (winter wheat) and these peaks are shown, as expected, to decrease in intensity (soil to vegetation) throughout the development of the crop .

Comparing the profiles of both genotypes (see Figure 7.11), at the same thermal times, differences can be observed between the two genotypes. At thermal time 400 the profiles are at their most similar (ks-test D=0.089, P=0.0302) however by thermal time 600 a difference has already emerged (ks=test D=0.2891, P $<2.2\text{x}10^{-16)}$). The width of soil plateau is shown to have reduced for the genotype Soisson when compared to Caphorn. The biggest difference is shown to be at thermal time 800 (ks-test D=0.59, P $<2.2^{-16}$), here the soil plateau is shown to reduce by 10% for Soisson but remain similar for Caphorn. The vegetation peaks are shown to be similar in absolute value (around 50% maximum vegetation) for both genotypes. At Thermal time 1000 the soil plateau reduces for Caphorn to a similar intensity to that found for Soisson (around 80%), however for Soisson the soil plateau has become more of a peak (ks-test D=0.426, P $<2.2\text{x}10^{-16}$). These differences can be in part explained by the more planophile structure of Soisson plants causing the leaves of the plant to spread out more into the gaps between the crop rows.

Below are some figures (Figures 7.12 and 7.13) which show the profile of both the observed and modelled canopy cover images at thermal times 400 and 600 for both genotypes. Comparison over lower thermal time is focused on due to the observed differences between modelled and observed estimations of cover at these thermal times.

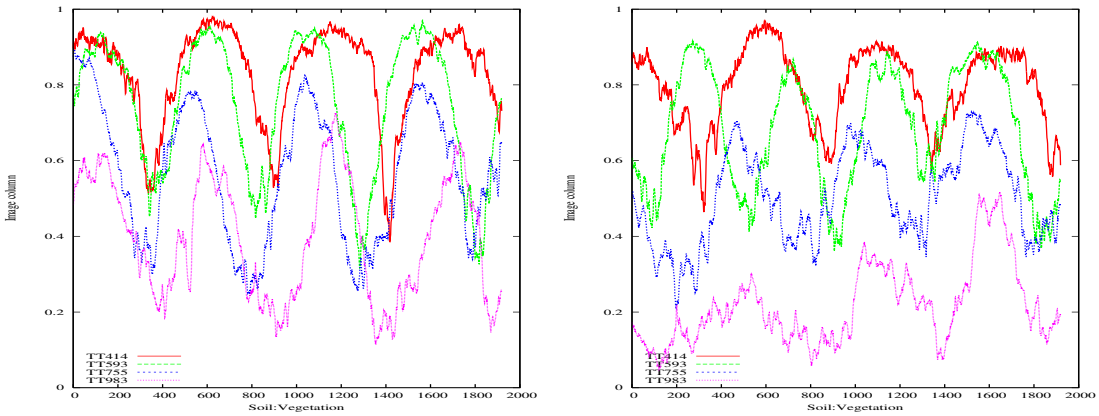

(a) Profile CA05 (b) Profile SO05

Figure 7.11: The soil:vegetation profile over modelled canopy cover images for different Thermal Times for both genotypes; Caphorn and Soisson

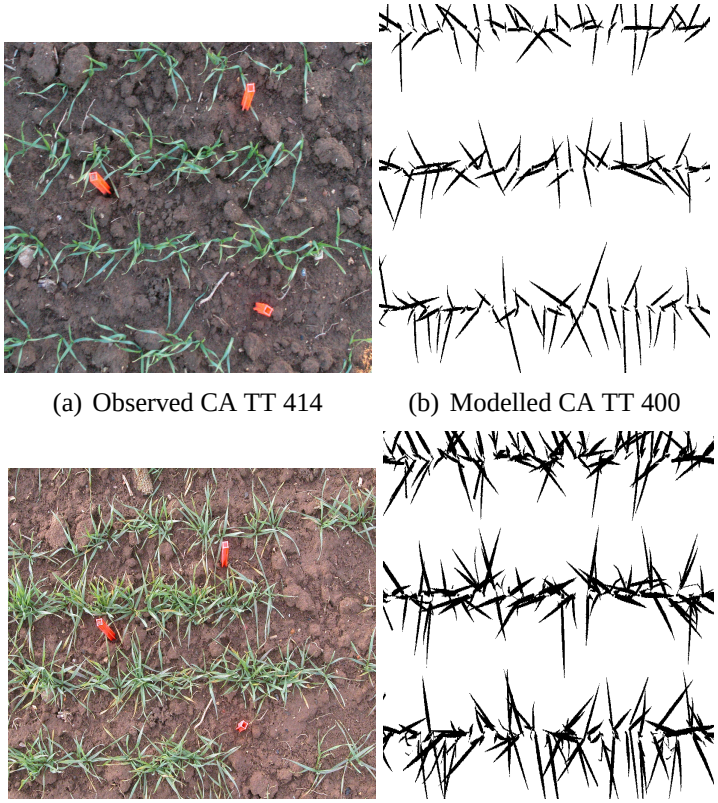

(a) Observed CA TT 414 (b) Modelled CA TT 400

(c) Observed CA TT 594 (d) Modelled CA TT 600

Figure 7.12: Observed canopy cover of Caphorn at thermal times 414 and594 as well as the modelled canopy cover at thermal times 400 and 600.

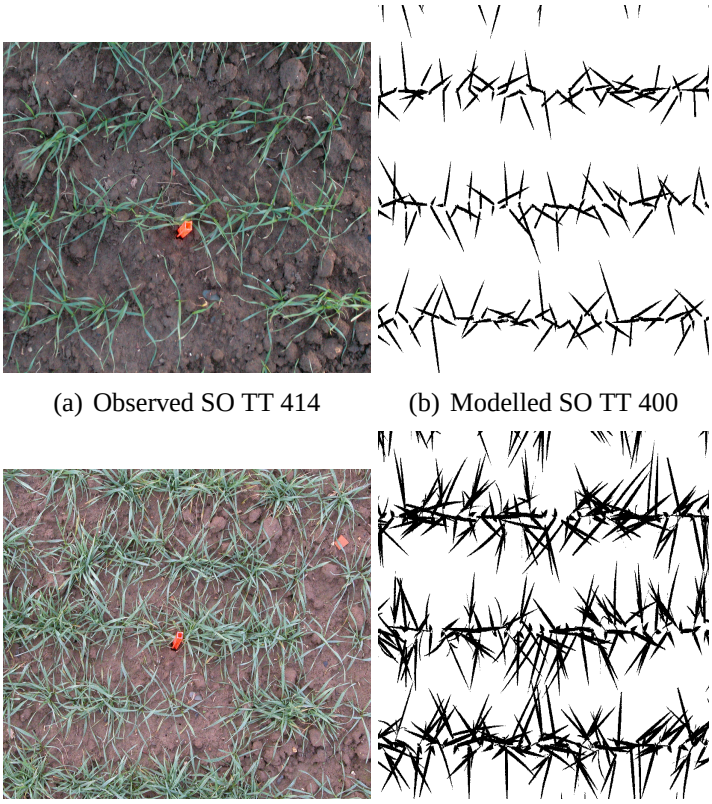

(a) Observed SO TT 414 (b) Modelled SO TT 400

(c) Observed SO TT 594 (d) Modelled SO TT 600

Figure 7.13: Observed canopy cover of Caphorn at thermal times 414 and594 as well as the modelled canopy cover at thermal times 400 and 600.

7.2.3 Perspective Effect

Two important considerations have to be taken into account within this modelled process, the first is that the field was on an incline and the second is experimental error means that the lens axis was not always accurately perpendicular to the soil surface. If the cover is measured with these errors it can result in a perspective effect which is proposed to artificially increase the measured canopy cover, until a certain point in development where it would become insignificant due to high cover of the crop. This error is proposed initially to explain why the observed and modelled canopy cover differs over lower thermal time. Figure 7.14 illustrates the perspective effect well. Instead of seeing only the top of the orange pickets within the photo you are seeing almost the whole of it, suggesting the photographs were not taken directly above the crop.

Figure 7.14: A photograph taken of a canopy with orange pickets to illustrate the perspective effect on the canopy cover images.

In order to ascertain what effect these combined errors have on the modelled canopy cover, simulations are run using the suggested model for Soisson and Caphorn but assuming the viewing angle from the top is not 90 degrees and allowing for a 5% error. The resulting modelled canopy cover is shown in Figures 7.15. Comparison between the observed canopy cover and the modelled canopy cover at different thermal times, when the perspective effect is included in the simulation and when it is not is shown in Figures 7.16 for a caphorn canopy and in Figures 7.17 for a soisson canopy.

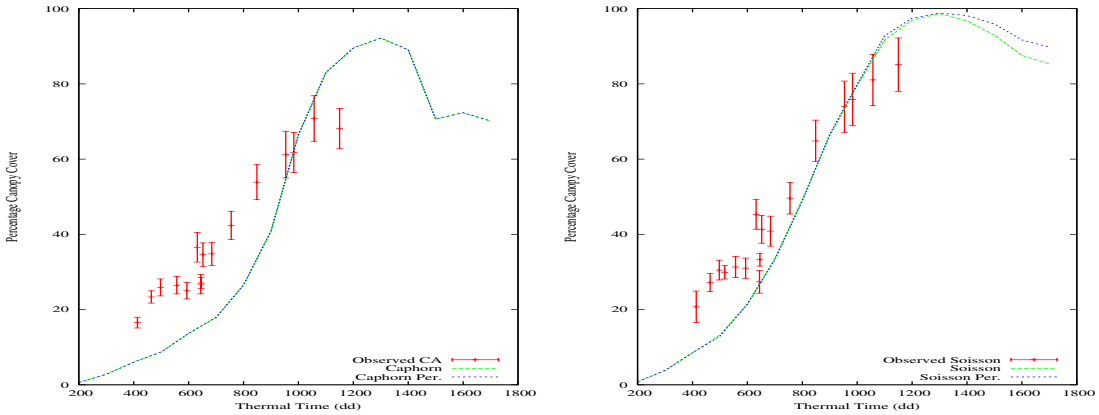

(a) CA (b) SO

Figure 7.15: The modelled canopy cover for Soisson and Caphorn over thermal time including the perspective effect.

It can be observed that by modelling the perspective effect it does not have an effect on canopy cover until later on for Caphorn canopies only.

It was also expected that by modelling the perspective effect the canopy cover over certain thermal times would be increased, however there is little evidence to suggest it does affect the canopy cover, although the expected difference not observed. It is decided that for the purposes of this thesis that the perspective effect should be included within the rest of the simulations due to its presence within the observed canopy cover photos.

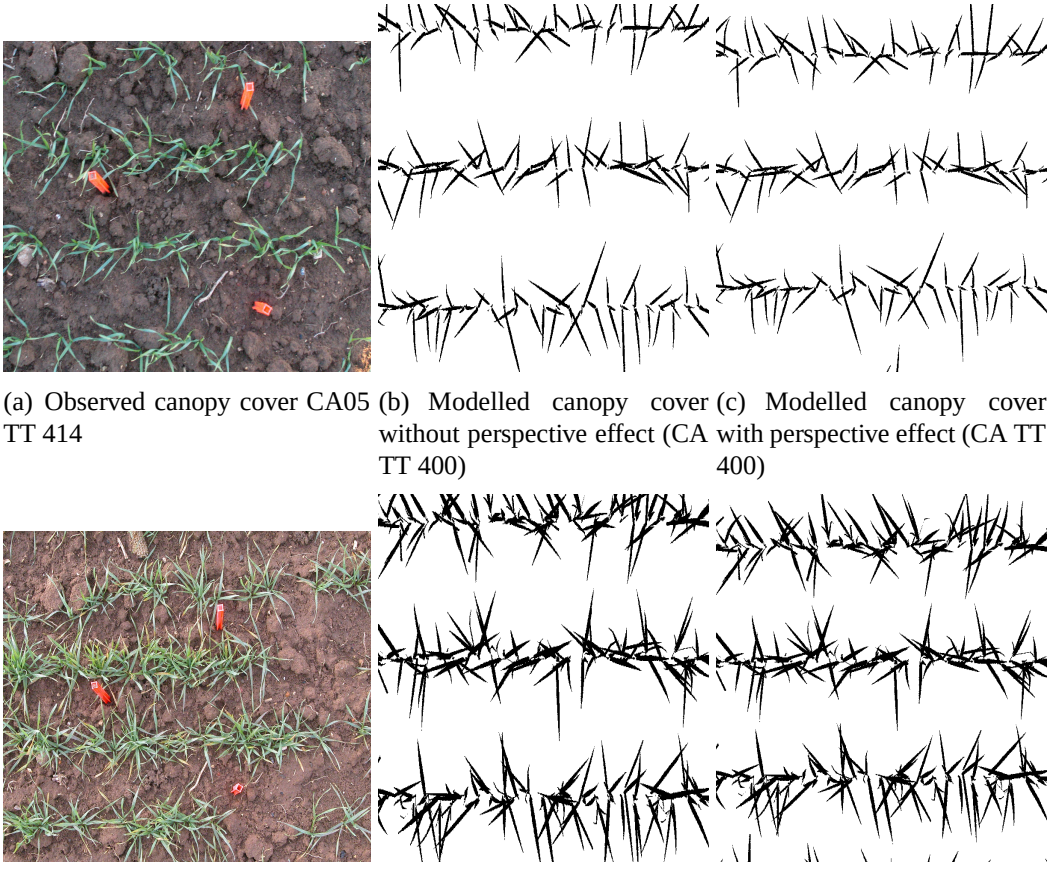

(a) Observed canopy cover CA05 TT 414

(b) Modelled canopy cover without perspective effect (CA TT 400)

(c) Modelled canopy cover with perspective effect (CA TT 400)

(d) Observed canopy cover CA05 TT 594

(e) Modelled canopy cover without perspective effect (CA TT 600)

(f) Modelled canopy cover with perspective effect (CA TT 600)

Figure 7.16: The observed canopy cover of Caphorn at Thermal times 414 and 594 are shown and next to them comparison is made between the modelled (using ADEL-wheat) canopy cover at thermal times 400 and 600, when considering the perspective effect and when not considering it within the simulation process.

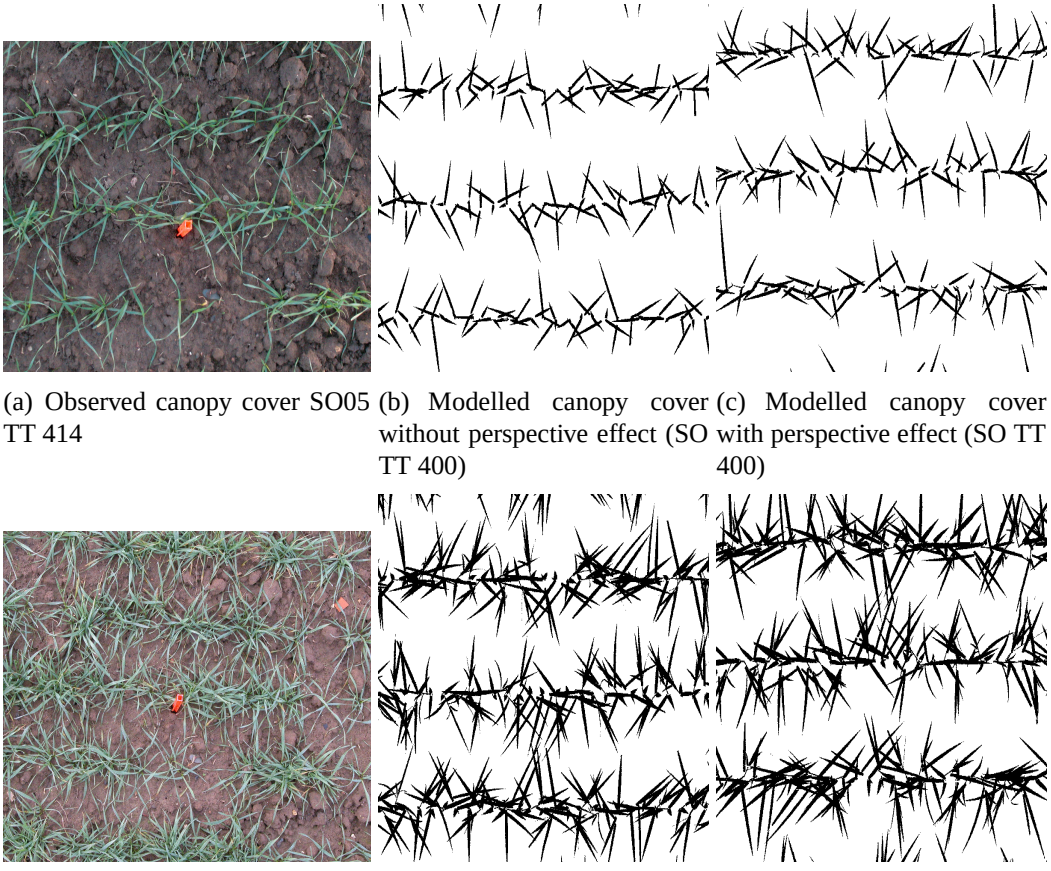

(a) Observed canopy cover SO05 TT 414

(b) Modelled canopy cover without perspective effect (SO TT 400)

(c) Modelled canopy cover with perspective effect (SO TT 400)

(d) Observed canopy cover SO05 TT 594

(e) Modelled canopy cover without perspective effect (SO TT 600)

(f) Modelled canopy cover with perspective effect (SO TT 600)

Figure 7.17: The observed canopy cover of Soisson at Thermal times 414 and 594 are shown and next to them comparison is made between the modelled (using ADEL-wheat) canopy cover at thermal times 400 and 600, when considering the perspective effect and when not considering it within the simulation process.

7.2.4 Phyllochron

The main inconsistency in terms of canopy cover for Caphorn seems to lie with the thermal time at which canopy cover increases significantly. The modelled canopy cover suggests this significant increase in canopy cover over thermal time, to be at thermal time 800 and the observed data a thermal time of 600.

In response to this observation further investigation into the phyllochron rate is carried out. The phyllochron rate for Caphorn is suggested to be 107 compared to that for Soisson which is estimated at a lower 98. The mean leaf appearance rate for all genotypes measured in both experiments is 105 ± 6. The calculated 107 leaf appearance rate for Caphorn falls within this observed range.

Reducing the leaf appearance rate of Caphorn to be the same as Soisson has the effect of reducing the thermal time at which the canopy cover increases after the plateau. This has the effect of reducing the observed difference in modelled and observed canopy cover between thermal time 600 and 900. The modelled over estimate of canopy cover from TT1000 onwards does still persist (see Figure 7.18).

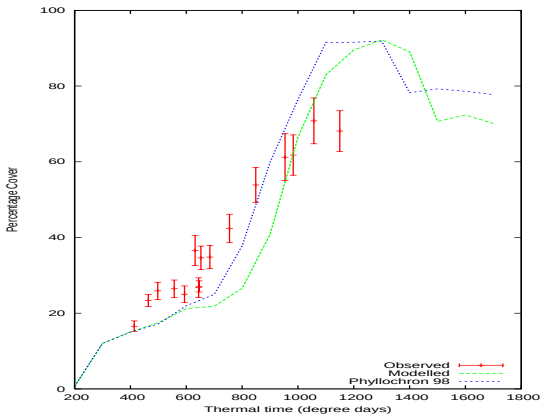

(a) phyll 98 plan

*Figure 7.18: Modelled (green)and observed canopy cover of Caphorn (mean $\pm$ sd(*2), red points) is shown. The canopy cover estimated with the ADEL-model with the phyllochron rate reduced to 98 (blue) is also shown for comparison.*

From the Figures7.19 it can be observed, for Caphorn, that at thermal time 600 the soil:vegetation

ratio reduces when the phyllochron is reduced to 98. This is shown to be higher than Soisson at the same thermal time. A ks-test shows that at thermal time 400 the profile of soil:vegetation profile is most similar between Caphorn with phyllochron rate at 98 and 107(ks-test D=0.084 P=0.032), however differences become more statistically noticeable at thermal time 600 with a ks-test; D=0.220, P=1.13x10^{-12} and at thermal time 800, D=0.456, P=2.2x10^{-16} and finally at thermal time 1000 D=0.423, P=2.2x10^{-16}) The profile of Caphorn with a phyllochron of 98 (Figure 7.19) becomes similar in absolute values to that of Soisson with a much lower soil intensity and higher vegetation intensity at thermal time 800. This is only seen by a slight decrease in D value when the ks-test is carried out. (SO thermal time 800 and CA thermal time 800 Phyllochron change (98) D=0.425 , SO thermal time 800 CA thermal time 800 D=0.627, P=2.2x10^{-16}) Visually the effect on the canopy cover is illustrated well here and highlights the importance and effect the phyllochron rate can have on the modelled canopy cover.

Planophile Winter Leaves

The LAI and the final organ lengths are shown to be modelled closely to the observed which leads to a suggestion that modelled canopy cover for both genotypes is underestimated over lower thermal times not due to leaf shape being misrepresented but instead the architecture of the lower leaves. Digitising of the leaves started once the plants had four or more leaves on the main stem. This was in response to adverse weather conditions which made measuring the plants with the invasive measuring technique adopted hard to complete without damaging the plants. The data collected therefore did not include these earlier leaves. From observing the pictures taken of the plants during this early development it can be suggested that the architecture of these leaves is perhaps more planophile than the parameterisation of the model allows. Within the original ADEL-wheat model the leaves were assumed to be purely ascending up until the higher leaves. However the inclination angle with the higher probability, from the stem, was assumed to be 20-30 degrees which is more planophile than the data from experiment 1 and 2 of this research suggests. Considering the absence of data for the lower leaves (except that collected on some tillers over lower ranks which are assumed to had a high associated error) it is suggested to investigate the effect of assuming the earlier leaves have a more planophile architecture. The modelled outcome of this is shown in Figure 7.20. For these simulations it is assumed that the leaves of rank -1NG, which is rank 4 and before are allocated the largest angle from the stem that was measured within the experiment.

The obvious effect is that canopy cover is increased over the lower thermal time as can be observed in figures7.20. The actual view of the canopy from above is shown along with the observed, modelled and the modelled canopy assuming a more planophile architecture of lower leaves. The canopy cover photos are shown from thermal times 400 and 600, which is when the canopy cover photos were taken within the field (see figures 7.21 and figures 7.20).

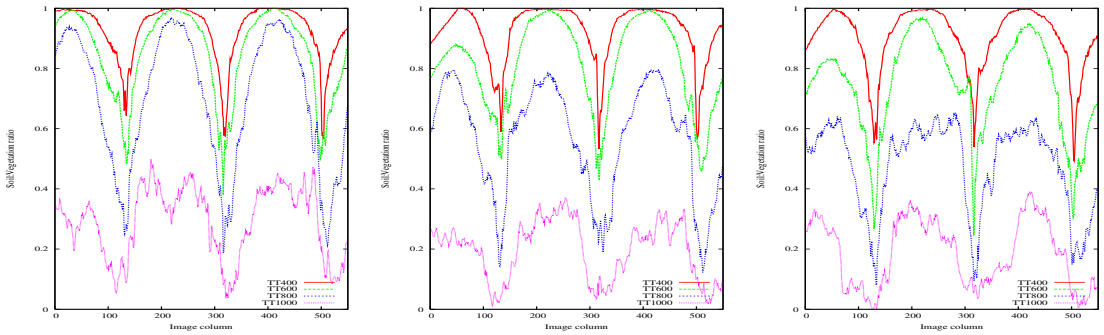

(a) Profile CA05 with phyllochron rate 107 (b) Profile CA05 with altered phyllochron rate 98 (c) Profile SO05 with phyllochron rate 98

Figure 7.19: The ratio of soil:vegetation profile for modelled canopy cover at thermal times of 400, 600, 800 and 1000 are shown for simulation of caphorn canopies assuming a phllochron rate of 107 and 98. For comparison the ratio of soil:vegetation profile for modelled canopy cover at the same thermal times of a soisson canopy (phyllochron 98) is also shown.

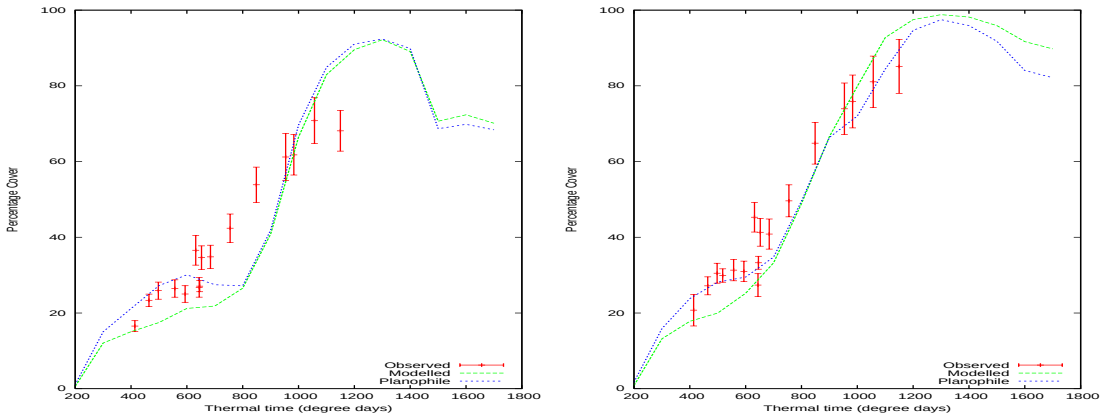

(a) CA (b) SO

*Figure 7.20: The mean and standard deviation (*2) of the observed canopy cover over thermal time for genotypes Caphorn (CA) and Soisson (SO) is shown in red. The modelled canopy cover for both genotypes is shown in green. The modelled canopy cover assuming the lower leaves are more planophile is shown in blue.*

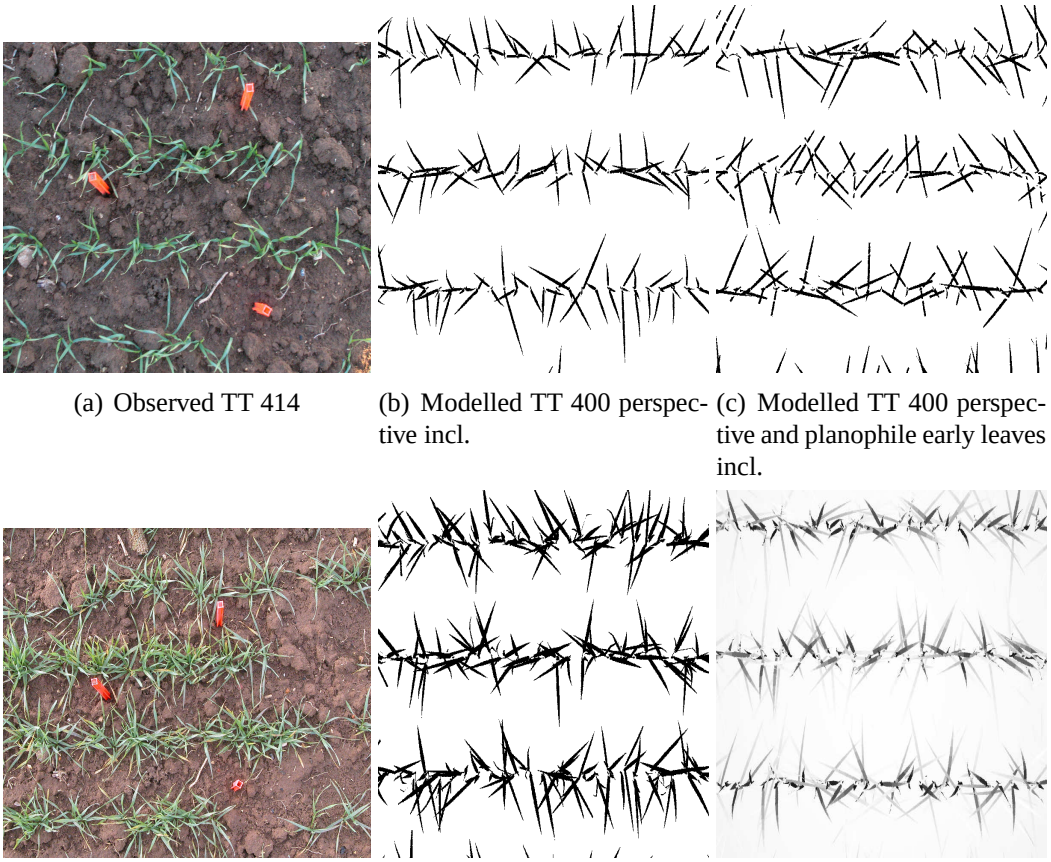

(a) Observed TT 414

(b) Modelled TT 400 perspective incl.

(c) Modelled TT 400 perspective and planophile early leaves incl.

(d) Observed TT 594

(e) Modelled TT 600 perspective incl.

(f) Modelled TT 600 perspective and planophile incl.

Figure 7.21: Modelled and observed canopy cover images of Caphorn with and without planophile early leaves

7.2.5 Phyllochron and Planophile

In this section the idea of changing the phyllochron for Caphorn and making the early leaves more planophile is explored. From comparing the modelled and observed canopy cover over thermal time differences in percentage cover are noticeable (see Figure 7.22). Figures 7.23 compare the observed canopy cover and the modelled canopy cover assuming these changes in phyllochron rate and architecture of winter leaves as well as the modelled canopy cover without these changes. Visually the difference in the spread of leaves over the gaps between the crop rows, as a result of the more planophile architecture of the winter leaves, is shown with these outputs from the different model simulations.

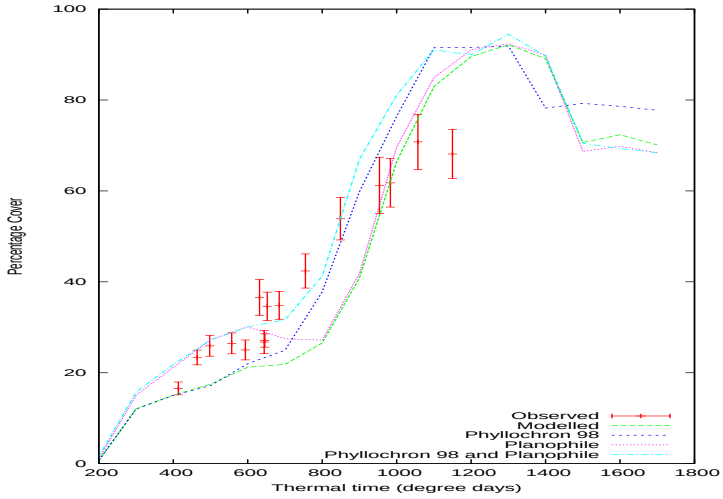

(a) plan

*Figure 7.22: Modelled (green) and observed canopy cover (mean ± standard deviation (*2), red) is shown. As well as the modelled canopy cover of caphorn assuming a lowered pyllochron of 98 (blue), planophile early leaves (pink) and a combination of phyllochron rate of 98 and early planophile leaves(turquoise).*

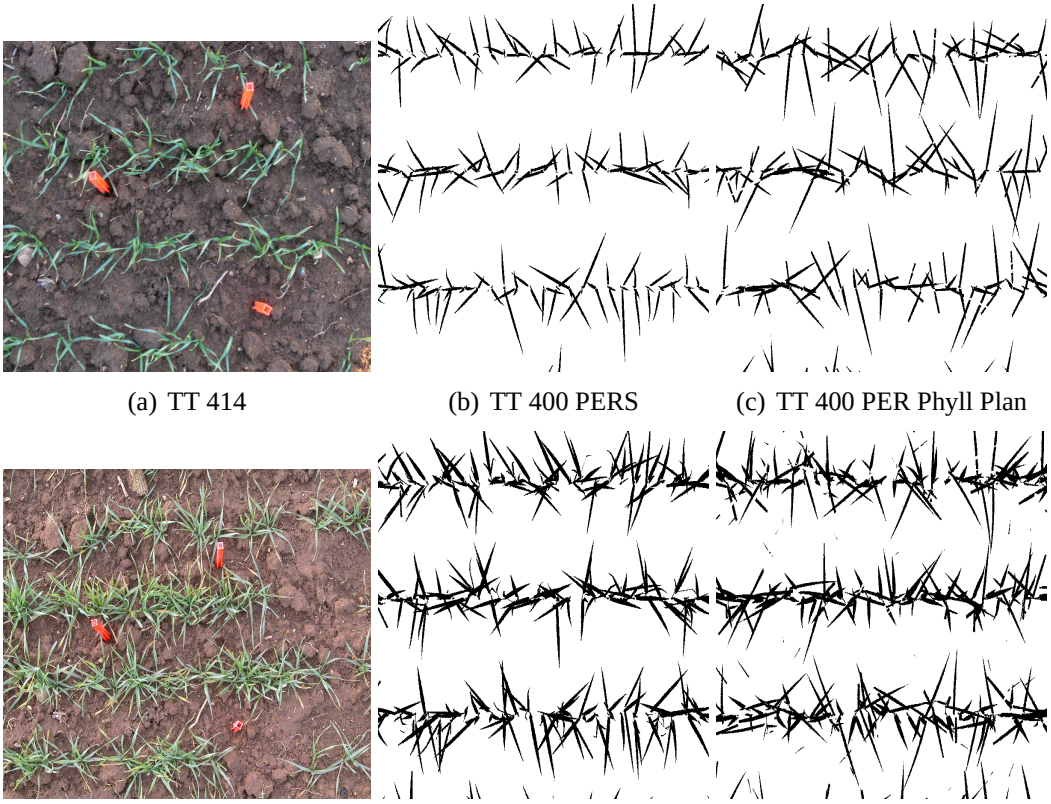

(a) TT 414 (b) TT 400 PERS (c) TT 400 PER Phyll Plan

(d) TT 594 (e) TT 400 PERS (f) TT 600 PERS Phyll Plan

Figure 7.23: Modelled and observed canopy cover images of Caphorn with and without planophile early leave and a reduced phyllochron rate of 98.

7.2.6 Boom Height

The canopy cover photos were taken by myself and Dr. Jon Hillier and Alain Fourtine. Due to the difference in height the photo may have been taken at the effect on canopy cover estimates at differing heights needs to be ascertained. This was modelled by altering the assumed boom height of the camera from the canopy, 100 cm, 150 cm and 200 cm.

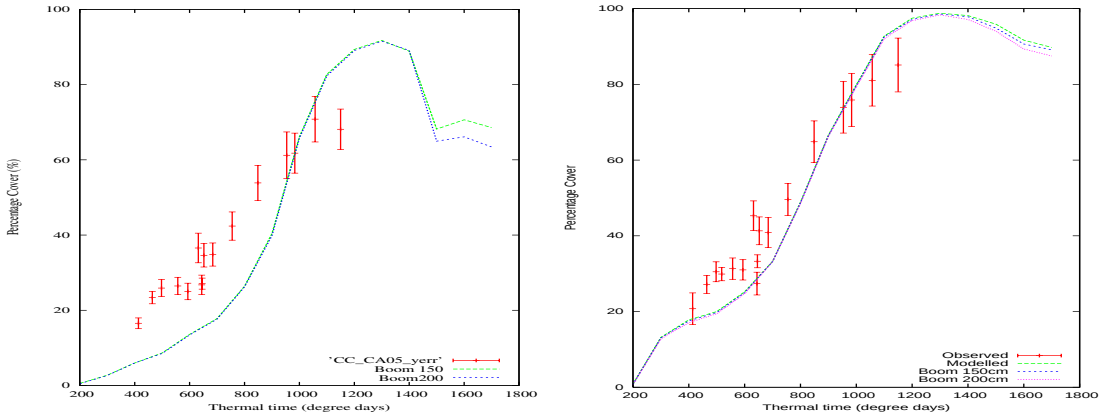

(a) CA Boom 150 and 200 (b) SO Boom 150 and 200

*Figure 7.24: Modelled canopy cover when the boom height is varied between 150cm (green) and 200cm (blue) with observed canopy cover as measured in the field (red) (mean ± standard deviation(*2)).*

It can be see in Figures 7.24 that these differences in boom length does not alter the estimated percentage canopy cover.

7.2.7 Tiller Angle

Another source of the differences observed between observed and modelled canopy cover may be due to the tiller angle being incorrectly simulated. Figures 7.25 are the estimated canopy cover when the tillers are assumed to be 40 degrees instead of the 60 degrees.

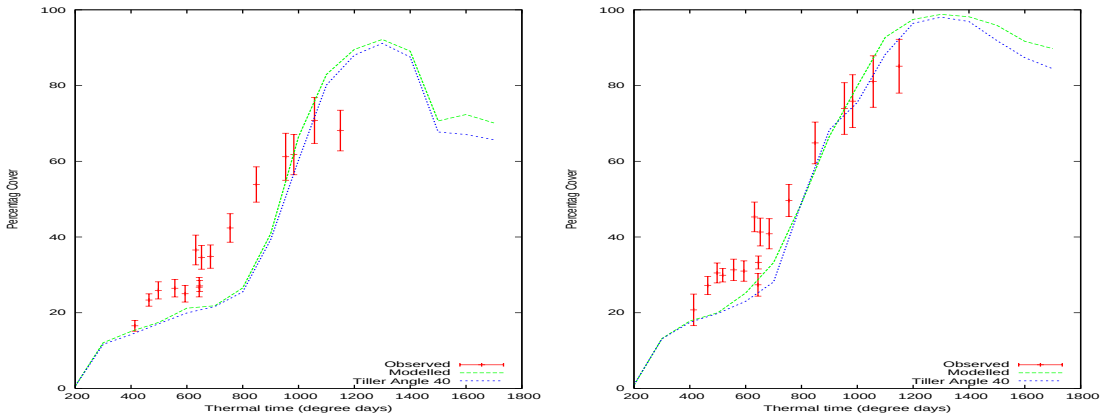

(a) CA (b) SO

*Figure 7.25: Modelled canopy cover when the tiller angle parameter is 40 (blue) and 60 (green) with observed canopy cover as measured in the field(red)(mean $\pm$ standard deviation(*2)).*

7.2.8 Clumping

It is visible from the observed canopy cover images that the field is patchy with plants missing along some rows. Although within the model it is possible to remove plants the model does not allow for the plants on the edge of these gaps to adjust their development as would be seen in the field. However, although the edge effect of these bare areas will not be incorporated into the modelled output it is thought important to look, within this analysis, at the effect of removing some plants. Due to the irregular pattern of clumping it is hard to numerically ascertain the extent of lost plants and so a qualitative assessment is made.

Below are some real canopy cover photos for lower thermal times of Caphorn and Soisson canopies along with some modelled canopy covers with some plants removed (see Figures 7.27, 7.28, 7.29, 7.30, 7.31, 7.32, 7.33 and 7.34). This was carried out by removing 2, 3 or 4 plant numbers out of the possible 10 that are then cloned. Where two plants were removed it is referred to as clump2 and where 3 were removed clump3 and so on. The simulated modelled canopy cover is shown over thermal time in Figures 7.26.

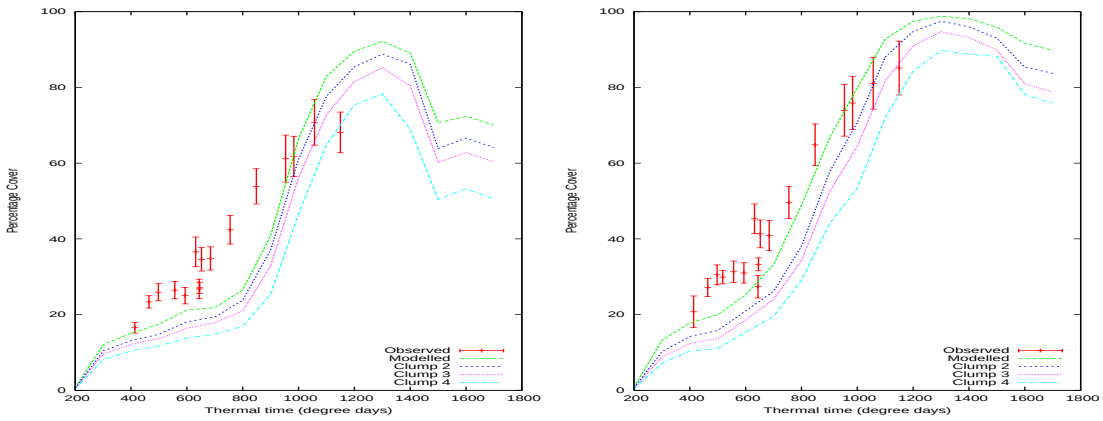

(a) CA CLUMP (b) SO CLUMP

*Figure 7.26: Modelled canopy cover within differing numbers of plants removed that can be cloned within the ADEL-wheat model (Clump2, 2 plants removed(blue), Clump3, 3 plants removed (red) and Clump4 (turquoise), 4 plants removed) with observed canopy cover as measured in the field(red)(mean ± standard deviation(*2)).*

(a) TT 414 observed (b) TT 400 modelled

Figure 7.27: Observed canopy cover image of Caphorn at thermal time 414 is shown as well as a modelled image of a Caphorn canopy at thermal time 400

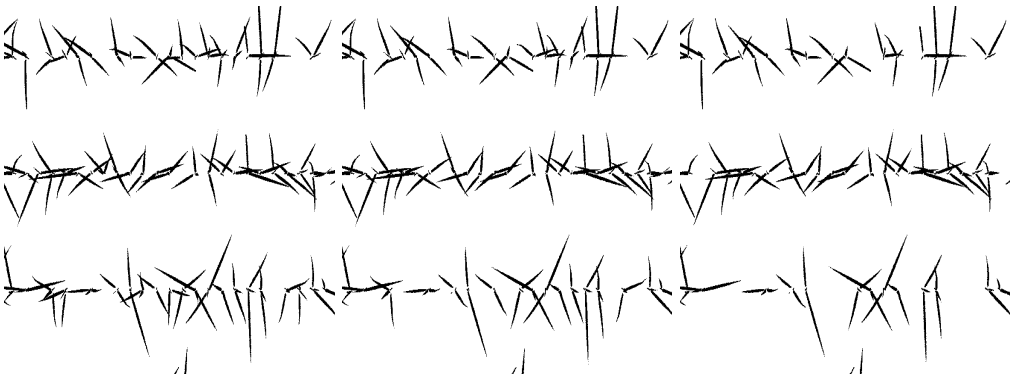

(a) TT 400 Clump2 (b) TT 400 Clump3 (c) TT 400 Clump4

Figure 7.28: Modelled Caphorn canopy cover of images at TT400 considering 'CLUMP' 2 3 and 4 .

(a) TT 594 (b) TT 600

Figure 7.29: Observed canopy cover image of Caphorn at thermal time 594 is shown as well as a modelled image of a Caphorn canopy at thermal time 600

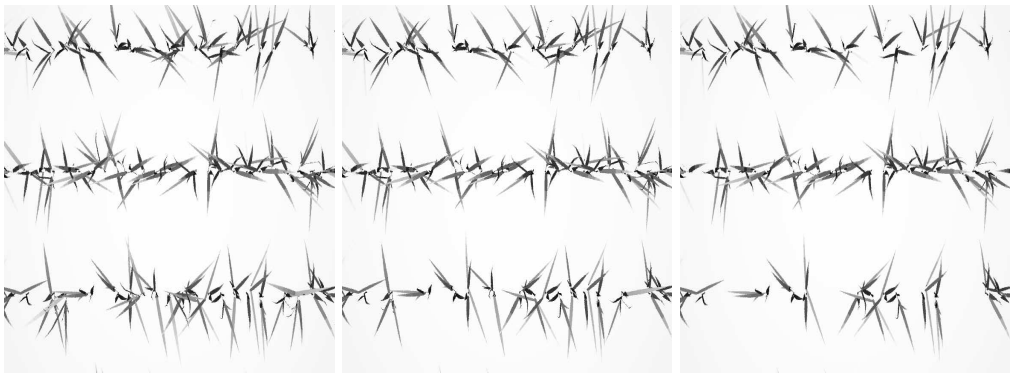

(a) TT 600 CLUMP2 (b) TT 600 CLUMP3 (c) TT 600 CLUMP4

Figure 7.30: Modelled Caphorn canopy cover of images at TT600 considering 'CLUMP' 2 3 and 4

(a) SO TT 414 (b) SO TT 400

Figure 7.31: Observed canopy cover image of Soisson at thermal time 414 is shown as well as a modelled image of a Soisson canopy at thermal time 414

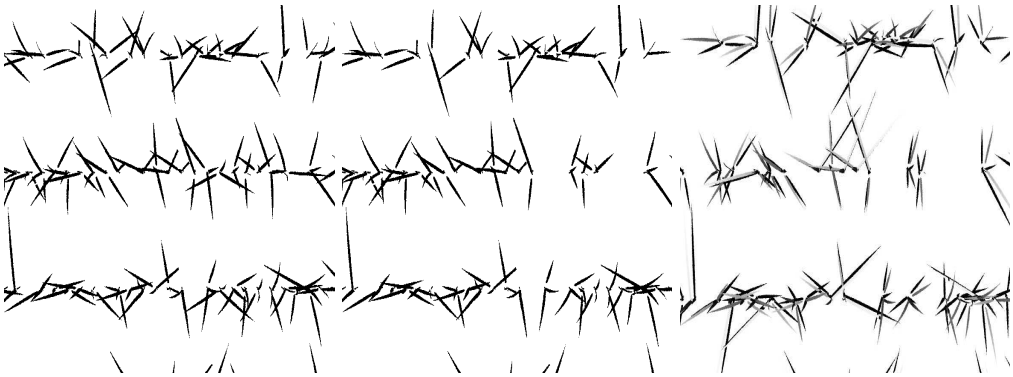

(a) SO TT CLUMP 2 (b) SO TT CLUMP 3 (c) SO TT CLUMP 4

Figure 7.32: Modelled Soisson canopy cover images at TT400 shown considering 'CLUMP' 2 3 and 4

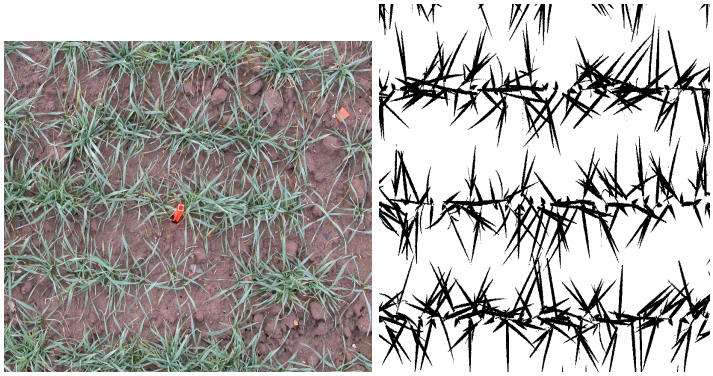

(a) SO TT 594 (b) SO TT 600

Figure 7.33: Observed canopy cover image of Soisson at thermal time 594 is shown as well as a modelled image of a Soisson canopy at thermal time 600

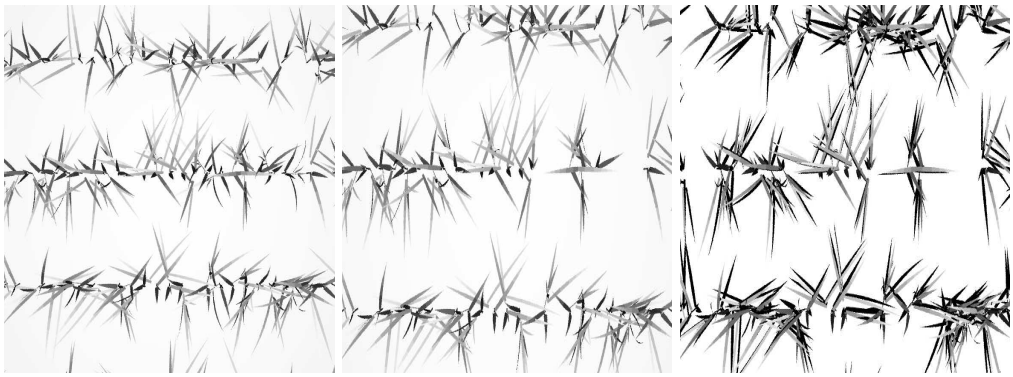

(a) SO TT 600 CLUMP2 (b) SO TT 600 CLUMP3 (c) SO TT 600 CLUMP4

Figure 7.34: Modelled Soisson canopy cover images at TT600 shown considering 'CLUMP' 2 3 and 4

7.2.9 Jitter

The observation between modelled and observed canopy cover images is that the modelled rows of plants is quite uniform whereas the plants in the rows in the field do not always fall within a straight line. In order to incorporate this within the modelled canopy, the plants are jittered about the row. This is achieved by altering the x and y coordinate of the placement of each plant. Three different simulations are run each with a different amount of variation from the regular grid placement initially adopted. Figure 7.35 illustrates the estimated canopy cover when the plants are 'jittered'. The difference in percentage cover is shown to be smaller for the Soisson canopy compared to Caphorn. Figures 7.35, 7.36, 7.37, 7.38, 7.39, 7.40, 7.41, 7.42 give a visual idea of how much the plants are jittered within the model simulation of the canopy and the spatial effect on the horizontal canopy distribution for both genotypes; Soisson and Caphorn over thermal times

(a) TT 414 (b) TT 400 PERS

Figure 7.35: Observed canopy cover image of Caphorn at thermal time 414 is shown as well as a modelled image of a Caphorn canopy at thermal time 400

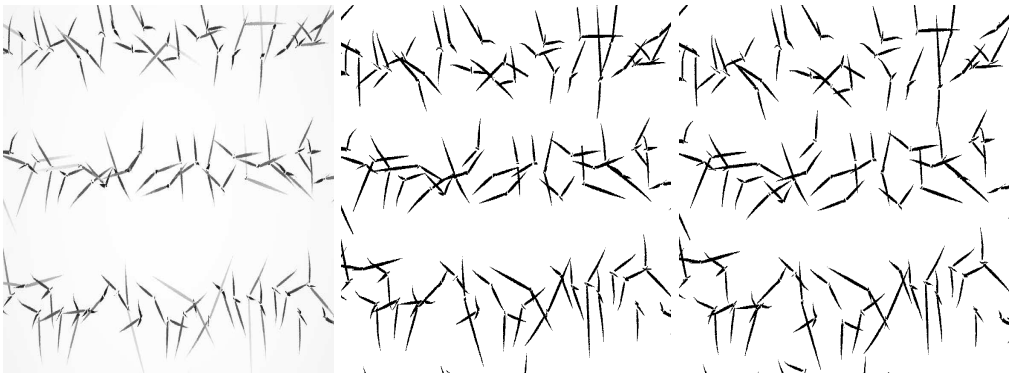

(a) TT 400 Jitter 2 (b) TT 400 Jitter 3 (c) TT 400 Jitter 4

Figure 7.36: Modelled canopy cover images of a Caphorn canopy with plants that have been 'jittered' by 2, 3 and 4 at TT400

(a) TT 594 (b) TT 600

Figure 7.37: Observed canopy cover image of Caphorn at thermal time 594 is shown as well as a modelled image of a Caphorn canopy at thermal time 600

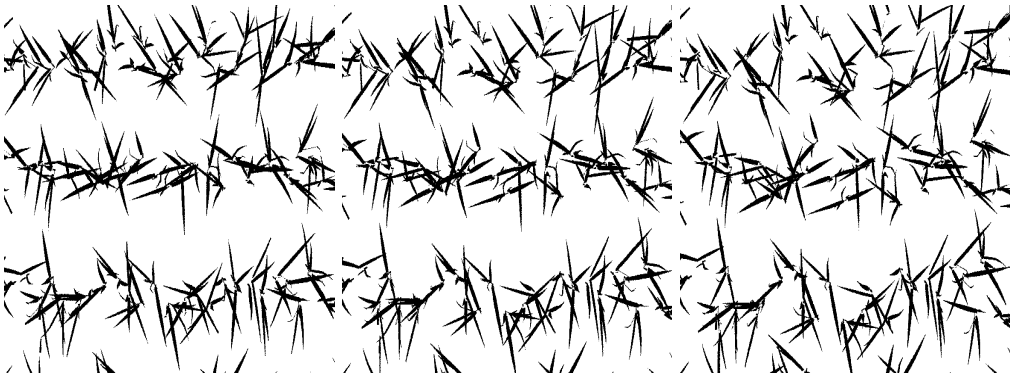

(a) TT 600 JITTER2 (b) TT 600 JITTER3 (c) TT 600 JITTER4

Figure 7.38: Modelled profile of soil:vegetation ratio for Caphorn canopies at thermal times 600 which have been 'jittered' 2 3 and 4.

(a) SO TT 414 (b) SO TT 400

Figure 7.39: Observed canopy cover image of Soisson at thermal time 414 is shown as well as a modelled image of a Soisson canopy at thermal time 400

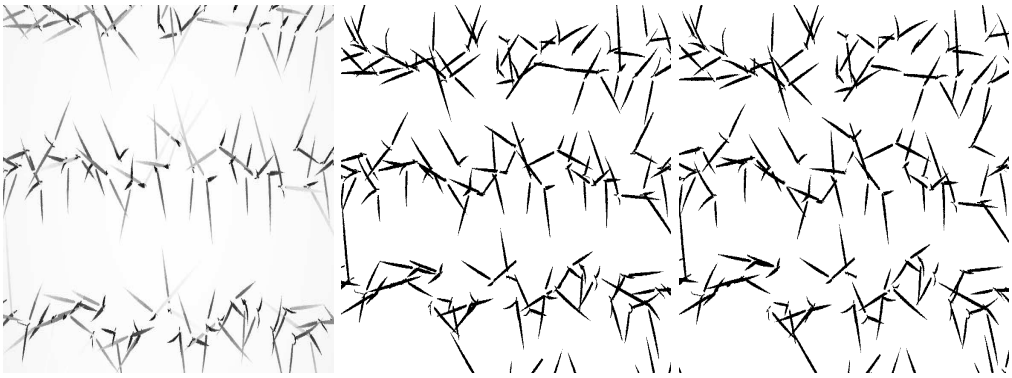

(a) SO TT JITTER 2 (b) SO TT JITTER 3 (c) SO TT JITTER 4

Figure 7.40: Modelled profile of soil:vegetation ratio for Soisson canopies at thermal time 400 which have been 'jittered' 2 3 and 4.

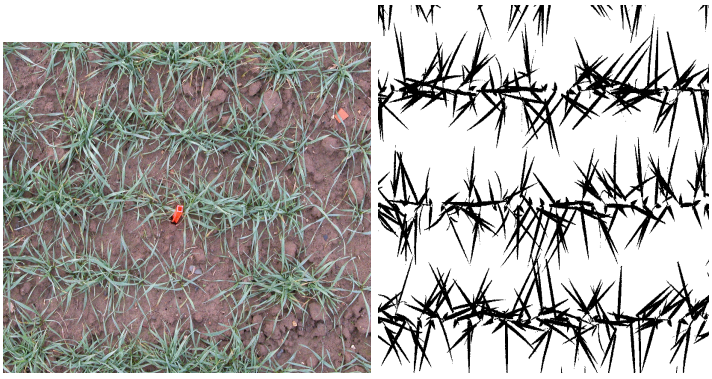

(a) SO TT 594 (b) SO TT 600

Figure 7.41: Observed canopy cover image of Soisson at thermal time 594 is shown as well as a modelled image of a Soisson canopy at thermal time 600

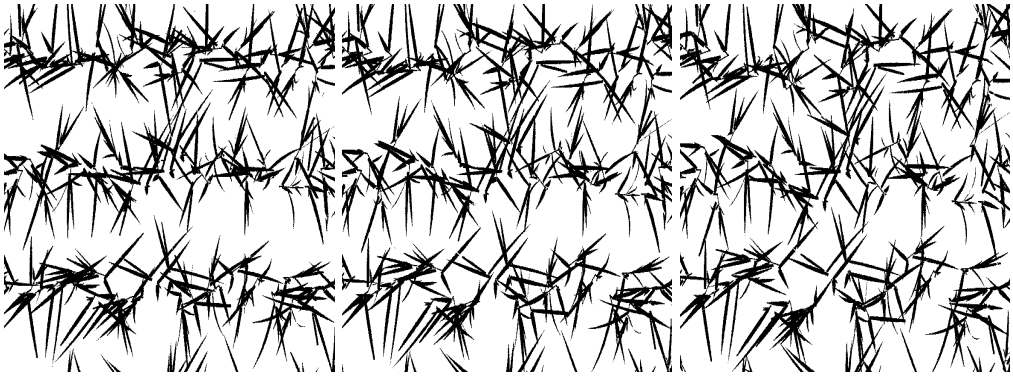

(a) SO TT 600 JITTER2 (b) SO TT 600 JITTER3 (c) SO TT 600 JITTER4

Figure 7.42: Modelled profile of soil:vegetation ratio for Soisson canopies at thermal times 600 which have been 'jittered' 2 3 and 4.

7.2.10 Discussion

This chapter is designed to investigate how some of the parameters and assumptions within the model affect its ability to predict what is observed within the field. It is found that the modelled final organ lengths are not significantly different to the observed measurements in the field which corresponds to the modelled LAI also being a close match to that observed. The observed and modelled number of tillers is also found to be close except over early thermal time where it is over estimated for both genotypes. It is accepted that the assumptions made within the tiller model need to be considered within further research. However if initial tiller number is reduced so that it is a closer match with that observed it would further lower modelled canopy cover over lower thermal time and as such increase the difference between observed and modelled canopy cover. It must also be mentioned again that observed tiller numbers did not include tiller four and as such reduces potential cover later on in development. However these tillers were small and most that were produced did not survive to produce a head.

When comparing the modelled and observed canopy cover, an important parameter for remote sensing studies, it is shown not to being modelled accurately. As observed and modelled phenology is shown to be a good match alternative causes of this difference in canopy cover have been investigated.

The difference between assuming a perspective and orthogonal camera when modelling the canopy cover was expected to have a notable effect on the canopy cover, however this was not the case. Also when looking at the profile of the canopy cover images with and without the perspective effect there were only very small differences observed. It is considered that this should be investigated more thoroughly than was able within this thesis.

The phyllochron for Caphorn is estimated from the observations to be 107 which is 9 higher than Soisson at 98. The effect of reducing the phyllochron rate of the Caphorn simulations to 98 had an obvious effect on the thermal time when the canopy cover increases significantly. By including this lower phyllochron the difference between the modelled and observed canopy cover improves for canopy cover between thermal time 600 and 1000 after which the change in phyllochron creates an over estimation of cover. The phyllochron was estimated using data from both experiments 1 and 2, for both genotypes and as such includes environmental effects. From looking at published research the phyllochron rate is usually expected to be 100 and as

such 98 is a good estimate. It was found that the mean for all genotypes measured within this experiment is also 105 ± 6. Therefore the phyllochron for Caphorn is higher, however including the standard deviation of the estimates it did fall within the range found. The main point raised from this investigation is the importance of the phyllochron rate when estimating canopy cover and that a small difference in the value of this parameter can create a significant differences in the progression of canopy cover over time.

The architecture of the leaves is assumed to create a notable difference in canopy cover. It is shown that the canopy cover of Caphorn, an erectophile plant is lower than Soisson a planophile plant. Accurate architectural data was hard to obtain for both genotypes. The lack of data collected on early leaves was disappointing, although was unavoidable considering the conditions in the field and the equipment being used to measure architecture. The effect of assuming early leaves are more planophile than that estimated from the data collected from older leaves had a positive effect on reducing the difference between observed and modelled canopy cover over lower thermal time.

An additional investigation was carried out into the combined effect of a lower phyllochron rate and a more planophile structure for early leaves on the Caphorn genotype only. Both these changes were modelled and the difference in the canopy cover over thermal time compared to the observed. The result was favourable, with observed and modelled becoming a closer match until thermal time 900 after which the canopy cover is shown to be overestimated by a significant 15 -20 %.

It must be noted that senescence has not been included within the model and that an improved model of senscence could perhaps reduce this error. Improving the initial estimation of cover does however seem to create a greater error in the estimation of cover in the later part of the development of the canopy.

Other parameters were altered such as tiller angle which was changed back to the original value of 60 degrees. This was found to have no significant effect on canopy cover. Also changing the boom height did not have a significant effect on the modelled canopy cover.

The location of the plants within the field were also investigated. In reality some seeds do not germinate which causes gaps in the rows, this was especially noticeable within experiment 2. The

plants also do not grow in an exact line and instead are described within this thesis to be jittered about a row. The model however assumes all plants to be placed in a grid like pattern within a field. Both these observations were attempted, to be incorporated with the model separately. They are included using arbitrary values so removing a different number of plants thus creating gaps in the field (clumping) and the second to misaligned the plants about their row, so that they do not form a perfect straight line (jittering). No quantitative assessment was made into how many plants should be removed or how by how much the plants deviate from straight rows, instead it was based on a visual assessment. This is a lot to do with the variation found within each image and the effect being relatively small on the canopy cover when modelled using these arbitrary quantities.

By removing some plants the obvious effect on the modelled canopy cover was that it was reduced and by including the jittering of plants about the row, the canopy cover was increased, although only very slightly. This would not be the case within the field. If a plant dies the plant next to it will spread out and use the extra light and space. This mechanism is not included in the model meaning that the effect of removing plants has to be analysed with caution. The effect of jittering is shown to have a limited effect on the overall canopy cover, which is also not realistic within the field. Less overlapping of the leaves of the plants would be expected and again extra tillers or leaves may be produced due to the extra light the plants would receive due to reduced competition.

Overall the investigations within this chapter have provided a good amount of information into the important considerations within the modelling process.

7.2.11 Conclusion

Final organ length models are shown to be simulated accurately within the model which also creates a good simulation of LAI. The dynamic model of tillering is shown to create a reasonable model of tillering although further work is discussed into making this model more accurate. The main limitations of the model are when simulating tiller number over lower thermal time, where it is currently over estimating the number of tillers. At this thermal time canopy cover is shown to be under estimated by the model and as such by improving the tiller dynamic model and reducing the number of tillers this effect would not be improved.

From the observations on the modelled and observed physiology of the plant additional features of the model are investigated as possible causes for the discrepancy between modelled and observed canopy cover.

The phyllochron rate has been shown to have a significant effect on canopy cover when it was altered when simulating a canopy of Caphorn plants. These observations highlight the importance of describing this parameter accurately when modelling crop development and indicates it to be an area where additional research would be beneficial. McMaster and Wilhelm (1995) also concluded, after comparing equations predicting the phyllochron of wheat and finding that no equation adequately predicted the phyllochron, that much opportunity exists to improve the prediction of phyllochron.

Leaf architecture was shown to have a positive effect on increasing the canopy cover over lower thermal time, when the younger leaves were simulated to have a more planophile architecture. As with the phyllochron rate the parameterisation of the midrib curvature was found to influence the canopy cover estimation from the model. The midrib curvature model presented within this thesis is much simplified from the original model and includes what are thought to be more meaningful parameters. The model was however parameterised using data collected on rank 4 and above leaves. The architecture of lower leaves being assumed the same as the older leaves. A greater emphasis is needed on the parameterisation of leaf architecture, is suggested.

The placement of the plants within the field and the loss of some plants has also been highlighted as something that should be considered when using a crop model. Parameters that were found to have limited effect on canopy cover and spatial arrangement were tiller angle and final organ lengths, also the distance of the camera from the canopy was not found to create a possible range of error if incorrectly estimated.

7.2.12 Alternative models

It is suggested that two models for each genotype are used to simulate radiometric data that will be compared to that observed within the field. One model which is parameterised using field data and one that is parameterised according to some of the findings and assumptions made from this chapter.

Caphorn alternative model

The alternative model for Caphorn was chosen to include the lower phyllochron rate of 98, planophile early leaves, a clumping of the plants (clump 3) and a jittering of the plants (jitter 3). As can be observed in Figure 7.43 the match between observed and modelled cover is improved until thermal time 800 after which the model over estimates canopy cover compared to that observed.

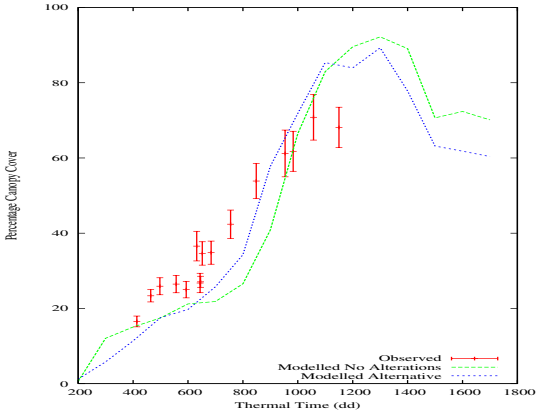

(a) CA

*Figure 7.43: Mean and Standard Deviation(*2) of the observed canopy cover of caphorn is shown in red. The modelled canopy cover over thermal time is shown in green. The adapted model to incorporate a lower phyllochron rate of 98, planophile early leaves, a clumping of plants (3) and a jittering of plants (4) is shown in blue.*

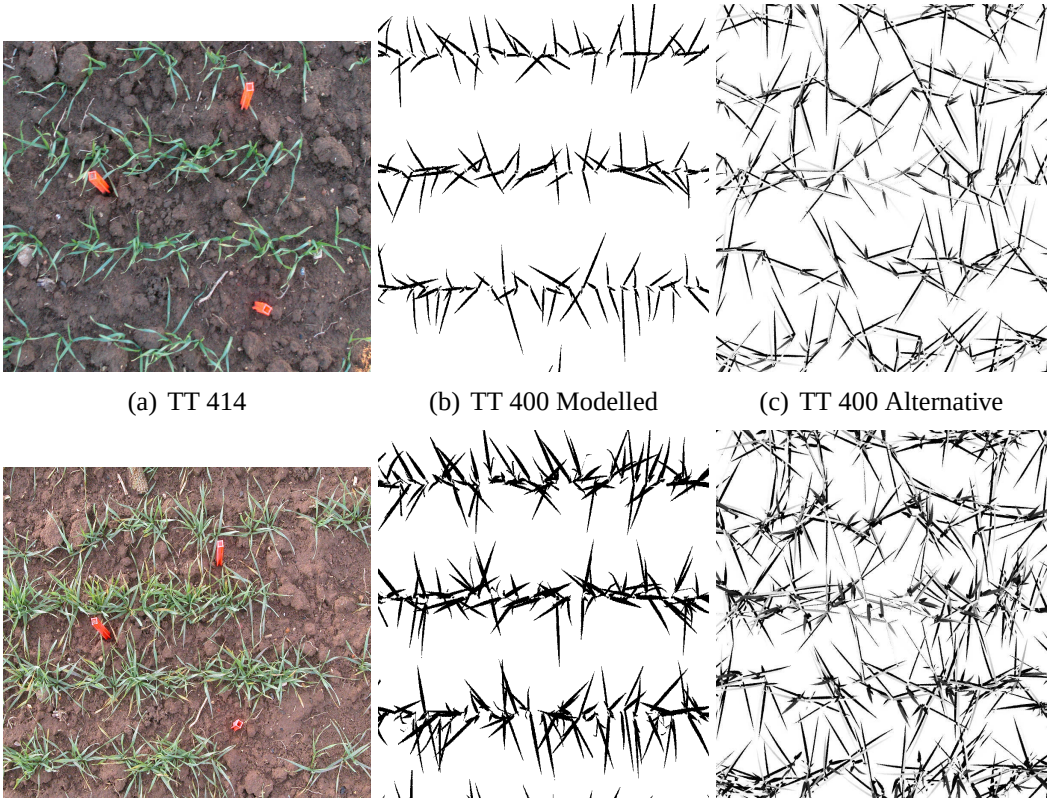

(a) TT 414 (b) TT 400 Modelled (c) TT 400 Alternative

(d) TT 594 (e) TT 600 Modelled (f) TT 600 Alternative

Figure 7.44: Observed canopy cover images of Caphorn at thermal times TT414 and TT594. Modelled canopy cover images of Caphorn ('modelled') and Modelled canopy cover images of Caphorn using the alternative model.

Soisson alternative model

The alternative model was chosen for Soisson to include planophile early leaves and the same 'jitter' and 'clumping' parameters as used within the Caphorn alternative model. As is the case for the modelled output of the alternative Caphorn model, the canopy cover is improved until thermal time 800 and after which an over estimation is observed.

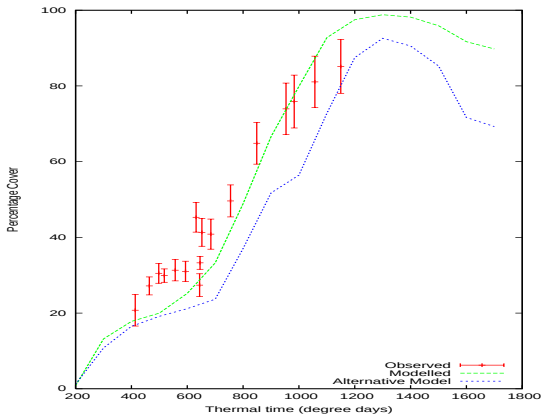

(a) SO

*Figure 7.45: Mean and Standard Deviation(*2) of the observed canopy cover of Soisson is shown in red. The modelled canopy cover over thermal time is shown in green. The adapted model to incorporate more planophile early leaves, clumping of plants (3) and a jittering of plants (4) is shown in blue.*

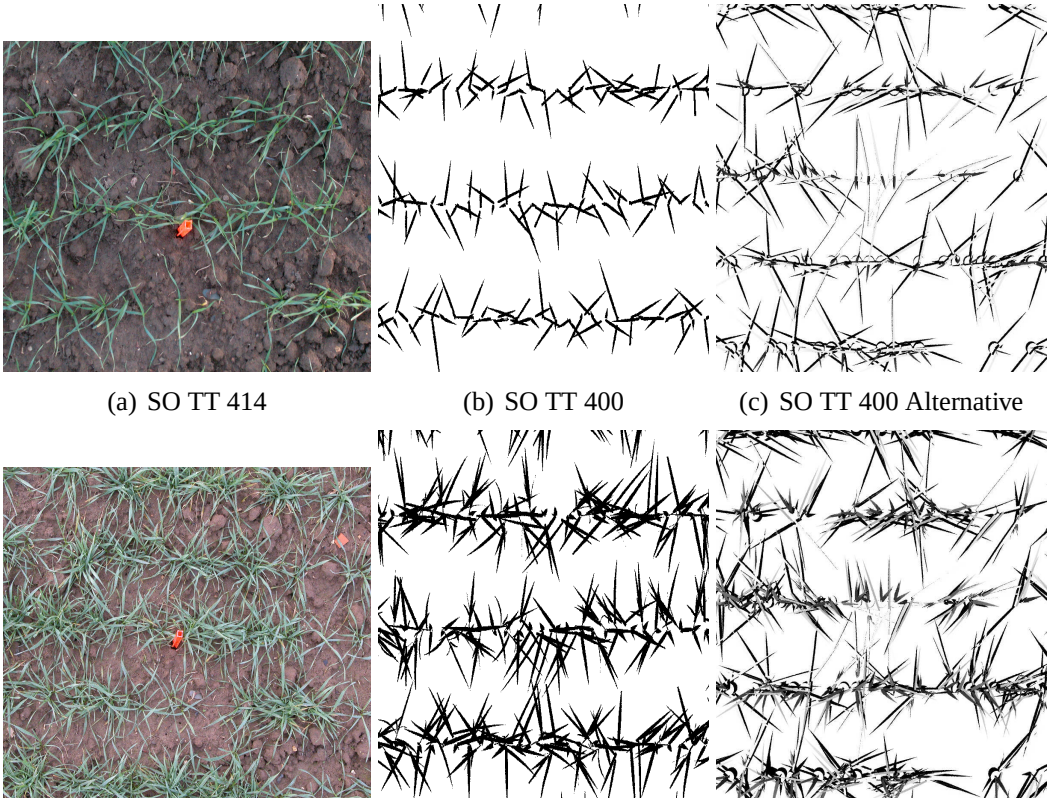

(a) SO TT 414 (b) SO TT 400 (c) SO TT 400 Alternative

(d) SO TT 594 (e) SO TT 600 (f) SO TT 600 Alternative

Figure 7.46: Observed canopy cover images of Soisson at thermal times TT414 and TT594. Modelled canopy cover images of Soisson ('modelled') and Modelled canopy cover images of Soisson using the alternative model.

7.2.13 Conclusion

From this chapter many different variables have been compared and their effect on the modelled canopy cover. Tiller angle and boom height have been shown to have no noticeable effect. The most easily observed effects were noticed when considering lower leaves to have a more planophile structure and the phyllochron of the Caphorn to be reduced from 107 to 98. Inclusion of a factor of jittering and clumping of the plants within the canopy are also shown to affect the cover and especially the profile of the cover. An expected result of the perspective effect increasing the canopy cover over some thermal time range was not observed. Two models for each genotype have been created, one parameterised solely on data collected within the experiment 2 and one which has been altered according to findings and discussions made within this chapter, per genotype.

7.3 Radiometric Validation

This chapter is focused on comparing the modelled and observed canopy reflectance. Spectral data was obtained using a GER1500 (8 degrees FOV and range 350 -1050 nm) as well as NIR and RED measurements from above the canopy of Soisson, by a Skye instrument SKR1800 2-channel radiometer (Skye Instruments, Llandrindod Wells, UK). This instrument has 2 channels and a hemisperical field of view. A second Skye instrument was placed over the field of Caphorn however this occurred very late on in development and also for a limited period. Two models of Caphorn and two of Soisson are run to simulate the field conditions and coupled with a brdf model to simulate the reflectance from these simulated canopies. Is is the reflectance that is compared with measured and also observed and modelled NDVI throughout development. Discussion is given as to the important parameters that effect the radiometry signal and the differences between the reflectance of the two canopies

7.3.1 Introduction

A leaf reflects approximately 10-30 % of total light falling on it in the green part of the spectrum and absorbs 70-90 % of the blue green light which it uses for photosynthesis. This occurs in the palisade layer of the leaf which contains the chloroplasts which in turn contain the chlorophyll. The mesophyll layer reflects about 60 % of the NIR part of the spectrum. The peak reflectance being in the NIR not the green part. In wavelengths longer that 1.3 nm water controls more of the spectral response of a leaf.

A canopy is made up of many leaves, some higher, some lower and some creating shadows. Canopy reflectance is therefore a combination of leaf reflectance and re-reflection off different layers of leaves. The geometry of the crop canopy will strongly influence the bidirectional reflectance distribution function (BRDF) while factors such as transmittance of the leaves, number of leaf layers the actual arrangement of leaves on the plant and the nature of the background and illumination angle are also important factors (Gibson and Power 2000).

In the region of the spectrum from just below 0.7 mm, vegetation response increases by an order of magnitude (Collins 1978). This is at the far red part of the visible spectrum and is

where chlorophyll absorption decreases and infrared reflection increases and is know as the red edge effect. As plants approach maturity it is expected that the position of the chlorophyll absorption edge or spectral response curve shifts towards longer wavelengths (know as the red shift)(Campbell 1995)

The differences seen in the radiometric signature of different plants are mainly seen in the pattern of NIR reflectance. NIR is also useful at aiding in the identification of deteriorating leaves. This is due to the cells dying causing a lower NIR reflectance and an increase in the visible spectrum.

An aim of this thesis has been to re-parameterise a 3D architectural model of winter wheat to be of use within remote sensing studies. As mentioned within the introduction and review chapters the output of this model is coupled with a canopy reflectance model to give a modelled canopy reflectance.

Within this chapter two models of each genotype, Caphorn and Soisson are coupled with the canopy reflectance model. One of each of these models is parameterised using only the field data collected in experiment 2 (see chapter 4 for more details of data collection methods) and the other parameterised using the field data but with the alterations as discussed in the previous chapter.

Soil and leaf reflectance are required for the canopy reflectance model simulations. Initially in this chapter the measured soil and leaf reflectance is shown and the limitations of this data examined.

The observed spectral reflectance of the canopy is shown over both canopies and over a range of sun angles and the differences discussed. These images are simulated by coupling the crop model and the canopy reflectance model and their differences investigated.

The observed NDVI is calculated throughout development using the data collected by the SKYE instrument and compared with the simulated NDVI for both canopies for Caphorn and Soisson. Comparisons are made between the observed and modelled values.

7.3.2 Soil and Leaf Reflectance

For more detail into the data collection methods used for soil and leaf reflectance please refer back to Chapter 4

7.3.3 Results

Leaf and Soil Reflectance

As can be seen within Figure 7.47 there is a slight difference between the reflectance of the leaves of Soisson and Isengrain. It can be observed for both genotypes that the higher rank of lamina have a higher reflectance although the differences overall are small as well as the sample set from which the comparisons are being made. The leaf reflectance data used within the canopy reflectance model is shown within this plot as is the data currently used with ADEL-wheat. One method considered is to calculate a mean leaf reflectance using both the measured Soisson and the Isengrain leaf reflectance. However, this would give a leaf reflectance that is not necessarily real. This goes with the same observation for phenology, when the mode plant was used rather than the mean plant. It has to be considered here due to the low sampling set and the difficulty in obtaining the measurements that the data presented may not be Representative of actual leaf reflectance. However, when compared to the leaf reflectance already used within the ADEL-model, this data is shown to lie within the variation found for both Isengrain and Soisson. It is decided that this reflectance pattern should be left unchanged within the model.

Variation in the measured soil reflectance at different dates during the crops development (see Figure 7.48). The effect of this variation on the modelled radiometric output would have been useful to quantify but was not carried out within the time frame of this thesis and is instead left as a recommendation for future work. The reading taken on the 11th April is considered to be the most representative reading of a bare soil. This is due to the lack of the red edge effect which the other measurements show. The red edge effect being the increase in reflectance around 700 nm.

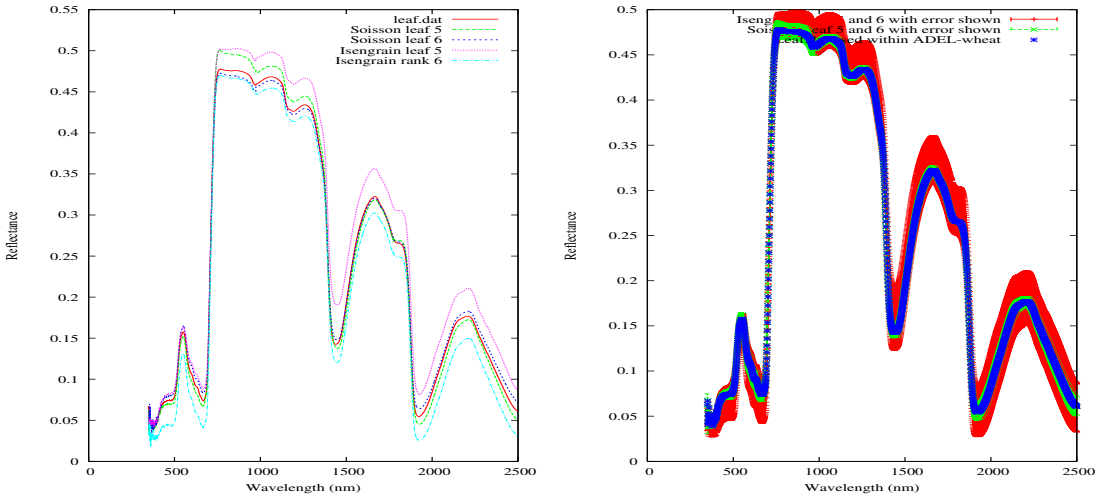

(a) leaf, no error shown (b) leaf with error shown

Figure 7.47: Measured leaf reflectance using an ASD clip attached to an ASD FSPro spectroradiometer (Analytical Spectral Devices, ASD Inc. Boulder, Colorado) on leaves of two ranks (phytomer rank 5 and 6) of both Soisson and Caphorn (distinguished by colour, see label) during experiment 1.

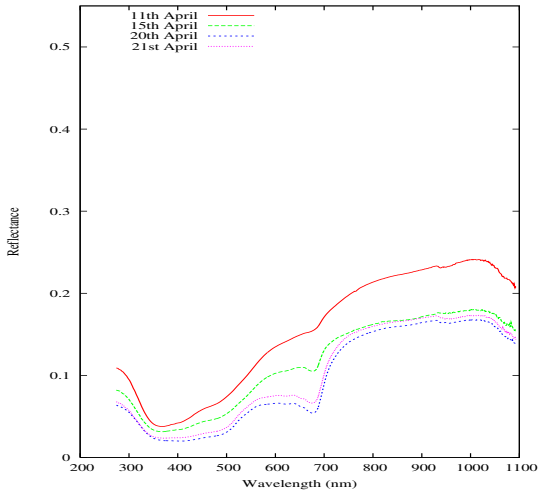

(a) Soil

Figure 7.48: Measured soil reflectance taken using the GER1500 (8 degrees FOV and range 350 -1050 nm) taken at approximately 1 m from the ground on the 11th (red), 15th(green), 20th (blue) and 21st (purple) of April.

Reflectance with varying sun angle

The effect of changing the sun angle on each sampling day was measured by taking GER1500 reflectance data at different times in the day. However, as there was only one GER1500 and the weather was so changeable no truley comparative data sets were taken over both genotypes under the same sun angles. The figures below (figures 7.49) show the modelled and measured reflectance over both Soisson and Caphorn canopies at different sun angles on April the 11th (2005, experiment 2).

Comparing visually the observed reflectance data between the genotypes Caphorn and Soisson it can be seen that Soisson has a higher observed reflectance than Caphorn. However the opposite is noticed with the modelled reflectance estimating the reflectance to be higher for Caphorn than Soisson.

On this sampling data the canopy cover for Caphorn and Soisson was 60% and 80% respectively. It would therefore be expected that the reflectance over the Soisson canopy would be higher.

Comparing the two modelled reflectance data for genotype Caphorn it can be visually observed that the alternative model predicts a closer reflectance pattern to that observed compared to the one based solely on field measurements. Referring back again to the canopy cover at this thermal time (970) the estimated cover for the models based solely on field data is closer to the observed cover than that estimated using the model parameterised with adaptations. So although the alternative model is modelling the canopy cover closer to that observed the reflectance pattern is not improved.

Comparing the two modelled reflectance data for genotype Soisson found the main difference to be over the lower wavelengths where the reflectance was increased with the alternative model. The alternative model assumed the earlier leaves to be more planophile leaves. When referring back to the observed and modelled LAI and canopy cover at thermal time 970, they are found to be relatively close and so this difference in modelled and observed reflectance is unexpected.

NDVI

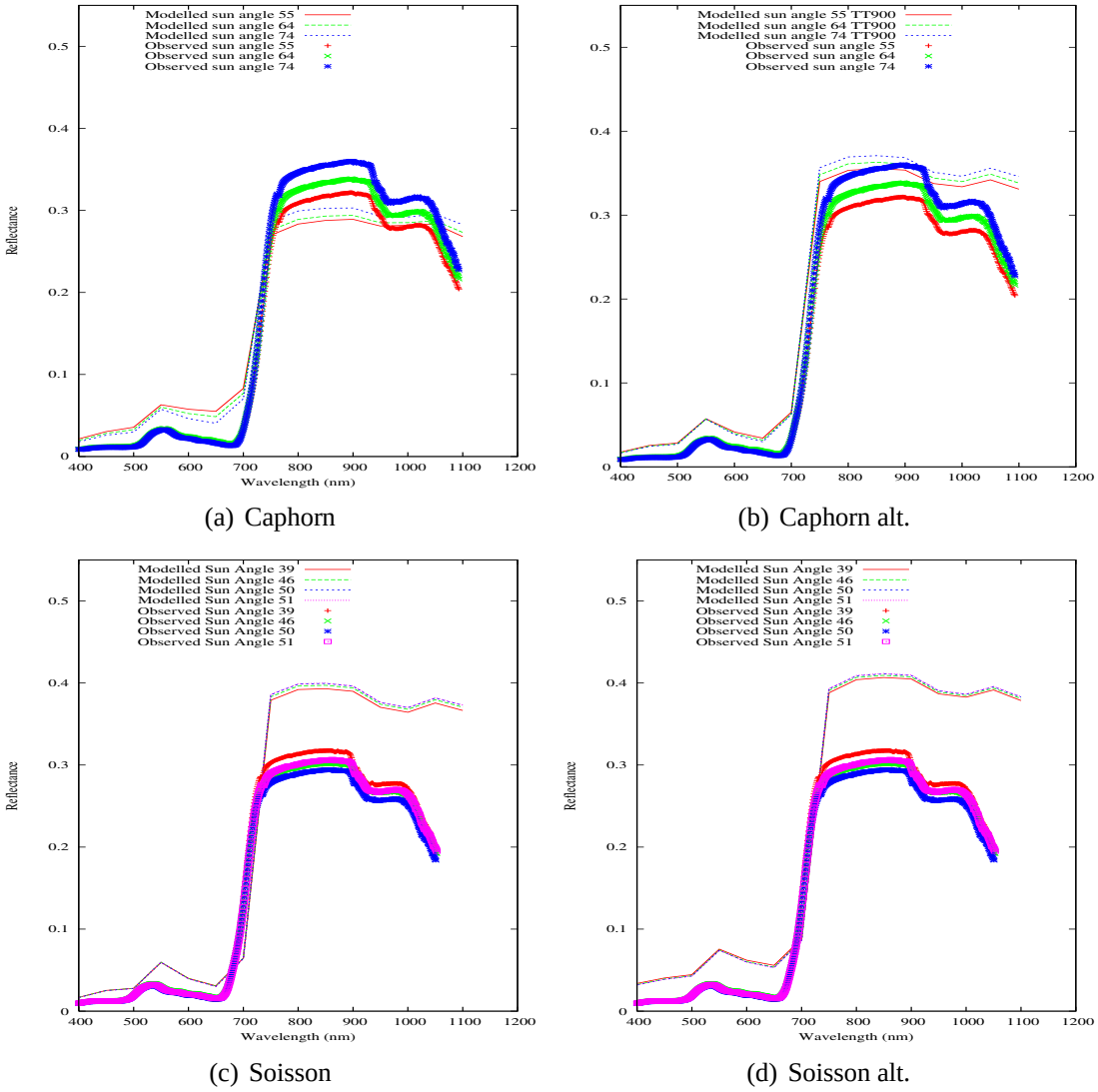

(a) Caphorn (b) Caphorn alt.

(c) Soisson (d) Soisson alt.

Figure 7.49: The effect of sun angle on observed reflectance over Soisson and Caphorn on 11th April 2005, TT 972

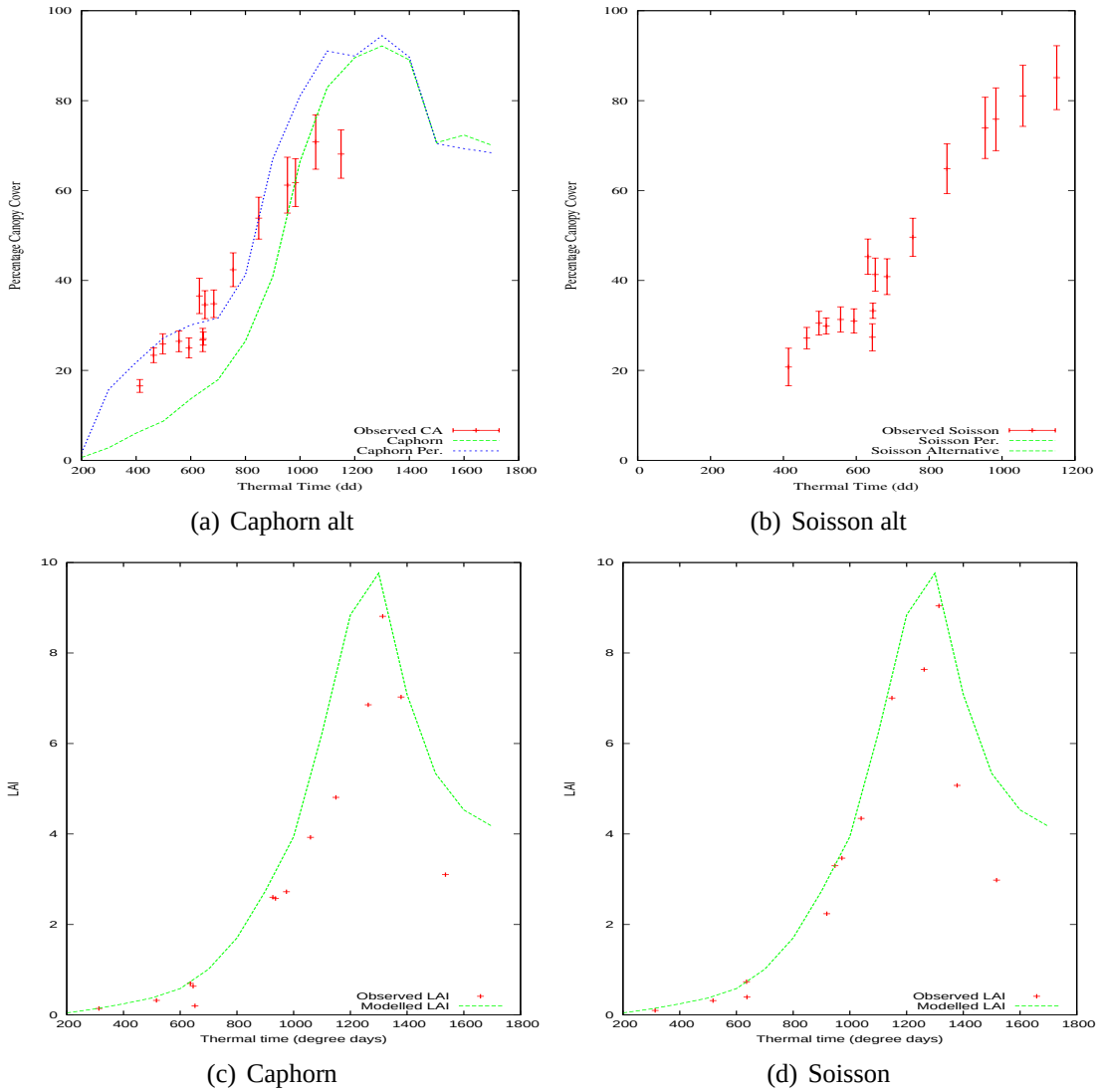

(a) Caphorn alt (b) Soisson alt

(c) Caphorn (d) Soisson

Figure 7.50: Observed and modelled canopy cover and LAI is shown separately for genotypes Caphorn and Soisson.

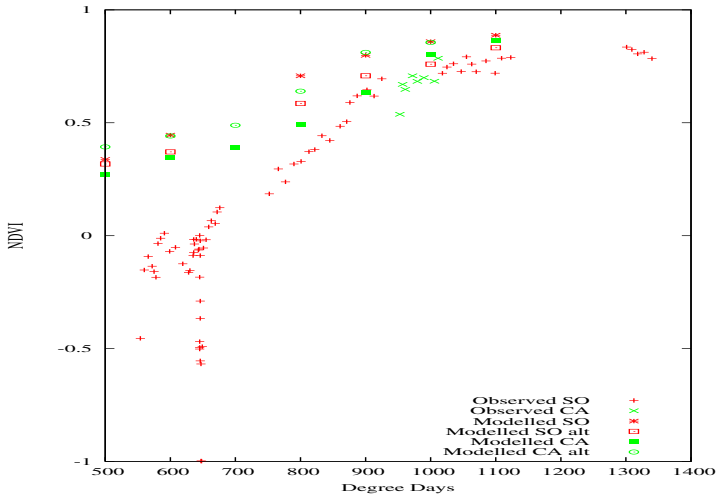

(a) NDVI

Figure 7.51: Observed NDVI over thermal time is shown in red for Soisson and in green Caphorn. The Modelled NDVI over thermal time is shown for both models of Soisson (red) and Caphorn (green).

The estimated NDVI values for all four models are compared with NDVI values measured in the field. The NDVI measured at solar noon was used and it is this NDVI value that was estimated using the models. In general the observed and modelled data is best matched later on in development, after thermal time 1000. The lack of match between the observed NDVI and the modelled NDVI before thermal time 700 is likely to be a result of the level of frost and snow which would have caused the NDVI to be zero or below. Considering the alternative model of Caphorn which estimated canopy cover closer to that observed it is expected that the modelled NDVI estimated from the output of this model will also be closer to the observed NDVI when compared to that from the model parameterised using only field data from experiment 2. However, considering these observations with those from Figure 7.51 it can be visually inferred that the Caphorn model based solely on field measurement gives a closer match of NDVI to those observed, the opposite of that observed with canopy cover. This discrepancy is found to also be true for Soisson.

Discussion

Leaf Reflectance

The variation in observed leaf reflectance between phytomer rank for both genotypes was small although not necessarily negligible and the same is true for the difference between genotypes. The sampling set was however too small in order to make a conclusive statement regarding the difference in leaf reflectance especially when considering the work of Pinter *et al.* (1985a) who found that single-leaf spectra measured in the laboratory with a spectrophotometer revealed no cultivar-related differences when measurements were taken over six winter wheat genotypes. However this was inter related differences and perhaps from the results obtained within this experiment that age of leaf affects the reflectance. This would not be hard to believe as the spectral reflectance of vegetation in the 400-700 nm region is primarily given by the abundance of chlorophyll and other pigments absorbing most of the incident radiation (Thomas and Gausman 1977, Broge and Mortensen 2002) and as a leaf ages the levels of these pigments change. The differences however may be negligible however a reduction in reflectance in lower leaves or older leaves could be incorporated within the model with relative ease. It has been assumed that the leaf reflectance data already within the ADEL-wheat should not be changed due to its similarity with the measured reflectance from experiment 2 and the lack of confidence with the data collected. A mean reflectance was not used as it would be unreal, in the same way the the

mode plant was used when choosing plants to measure.

Soil Reflectance

The variation in measured soil reflectance has been highlighted. The effect of this variation on the modelled radiometric output would have been useful to quantify and is a recommendation for future work. The measurement of soil reflectance required a small patch of the field to be cleared. This required manual cutting and removing of plants within a reasonable area of the field to enable a non contaminated reflectance measurement to be obtained. Some small amounts of vegetation would have been left and so would have affected the readings obtained. Within the readings taken after the 11th April the increase in reflectance at 700 nm is observed, this corresponds to the red edge effect which is suggestive that vegetation is present within the readings. The reading taken on the 11th April does not have such a visible red edge effect and is considered to be less contaminated and so has been incorporated within the model.

Reflectance with Varying Sun Angle

Pinter *et al.* (1985a) who found no difference in single leaf spectra measurement suggested this lack of difference along with the observed major differences in reflectance observed between six different genotypes of winter wheat at every time period despite their apparent similarities in green leaf area and green biomass supported the contention that the reflectance's were strongly influenced by canopy architectural features. They reinforced this conclusion with planophile canopies exhibiting the least amount of variability due to changes in sun angle and erectophile canopies showing the most. This is shown visually when comparing the observed and modelled reflectance between Soisson and Caphorn models. Although this pattern is noticed within the modelled data, it was suggested by Pinter *et al.* (1985b) that soil evaporation tends to be higher in open than in closed canopies which leads to the soil surface drying out faster when the mean leaf inclination angle is increased for the same foliage area. It is this soil surface drying which is associated with increased spectral reflectance (Irons *et al.* 1989) and so it would be premature to congratulate the model for simulating this effect appropriately.

NDVI

The estimated NDVI values for all four models are compared with NDVI values measured in the field. In general the observed and modelled data is best matched later on in development, so after Thermal time 1000. The lack of match between observed and modelled before thermal time 700 is likely to be a result of the level of frost and snow which would cause the NDVI to be zero or below. However there is a general lack of agreement between the observed and modelled NDVI between thermal time 650 and 1000 from all models even when the canopy cover estimates from the model are close to those observed.

7.3.4 Conclusion

The results of this chapter give more questions than answers and highlight the lack of correlation between modelling the canopy cover accurately and the radiometric signal. There is evidence to suggest that especially where there is an erectophile canopy more emphasis must be placed on soil reflectance. There is also some importance given to the differences in leaf reflectance over phytomer rank. Within the field NDVI values of two genotypes were not obtained at one time which makes it hard for a true comparison to be made. It would seem from the data available that the NDVI of both canopies does not differ greatly. It is instead suggested to focus more on the effect the architectural properties of the model have on reflectance by looking at the full reflectance data of the canopy and over varying sun angle.

Chapter 8

Conclusion

Within this thesis, work has been presented on a new development of an existing 3D structural crop model which has been parameterised using measured field structural and radiometric data. The result of coupling the crop growth model to a 3D simulation model is presented as well as how this coupling can be used to explore the impact of structure on the remotely sensed signal. To my knowledge this coupling of both structural and radiometric aspects with the aim to optimise crop model structure has not been attempted before and allows us to directly explore the effects of model structure on a remotely sensed signal in the optical domain.

Extensive field work spanning two growing seasons was carried out measuring the phenological and structural differences that occurred during the growth and development of different genotypes of winter wheat, this database has already been used within published research papers, highlighting it's usefulness for the furthering of agricultural research.

As mentioned, analysis of this data has aided in re parameterising an existing 3D model (ADEL-wheat). Within ADEL-wheat, the phenology of the plant is initially considered before calculation of the architectural properties of each organ. As a result this thesis has been divided up into two categories: Phenology and Architecture.

8.0.5 Phenology

Final Organ Length

A respected idea within crop modelling is that tillers can be considered as delayed main stems. This allows additional stems to be parameterised by one delay parameter rather than a full description of all organs on each tiller. Here, results showed that the pattern of final organ length over all axes was not consistent with the idea that tillers can be considered as delayed main stems. The pattern of final lamina width and length was shown to be different over the different axes for all phytomer ranks. The new models of final organ length proposed here in some cases increase the number of parameters required from that currently suggested in the ADEL-wheat model. However the resulting flexibility allows the modified models to encompass the observed patterns of final organ length across different genotypes and under different growing conditions. This results in a more flexible and general description of organ length.

It was observed that not all organ types start significant growth (i.e rank N_1) around the same time, although for lamina and sheath, increased growth per phytomer rank was noticed for most genotypes to be around rank 5-6 and for internode growth, one phytomer later. No significant correlations could however be found to enable this parameter to be estimated from the final number of phytomers.

Leaf Appearance

Although leaf appearance was not measured within the field, by using a leaf number index it was possible to compare leaf appearance over the different genotypes and also over two growing seasons. This work was important as it enabled the idea of tillers being treated as delayed main stems to be looked into over a variety of genotypes and from two genotypes grown in different environmental conditions.

Measured data showed that the leaf appearance rate (LAR) appears to be similar between genotypes, which is consistent with the results of Birch *et al.* (1998). Slight differences in LAR between the same genotypes grown in different years (SO04 & SO05, CA04 & CA05) were noted however the results were inconclusive as to whether the adjustment of LAR is more appropriate per environmental conditions than with regards to genotype (as found by (Birch *et al.* 1998)). From the results of this analysis it is suggested that LAR does not differ significantly between axes and can be assumed to be the same as the main stem. Synchrony between the appearance of the flag leaf on all axes was found to be good which also adds to the idea that tillers can be assumed to be delayed main stems as first discussed within the final organ length section of this thesis. Assuming that the tillers are delayed main stems, the delay, or shift parameters as estimated by the final organ length models were used, with some adjustment, to model LAR on the tillers from the model of LAR on the main stem. A good fit of this model to observed data, for most axes on most genotypes was found. This method reduces the overall number of parameters required by the model which is one aim of this thesis. Leaf appearance rate is an important consideration within the model as highlighted in the previous chapter. Further research into the effects on LAR are suggested that would enable a less empirical model of LAR to be implemented into the model. This would require data to be collected on the same genotypes over different growing seasons, and ideally include the thermal time of each leaf appearance.

Tillering

Tillering was not formally included within the ADEL-wheat model and instead a maximum tiller number was used which would trigger leaves to be cut off the plant at a given LAI threshold. A new dynamic model of tiller number over thermal time has been successfully applied using observed data from a range of genotypes over two growing seasons, requiring five parameters.

Tiller production is set using an equal hierarchy so that each tiller has an equal chance of being produced. Tiller survival is shown not to be equal between tillers. Tillers 1 and 2 instead are illustrated to be equally likely to survive and produce a viable ear, with tiller 3 being the most likely tiller to die before producing a viable ear and so at the point of tiller death, T3 has a set probability of surviving of 30% and T1 and 2, 70%

Parameter reductions are suggested by assuming that the thermal time at which the penultimate leaf becomes liguled on the main stem is the time at which tiller death commences. A rate of death can then be applied specific to each genotype until the number of surviving tillers is obtained (Til_{surv}). It is also suggested that further exploration into incorporating an LAI threshold trigger for the onset of tiller cessation takes place so to remove the need of setting the parameter describing a maximum tiller number.

8.0.6 Architecture

2D Leaf Shape

From the results collected from experiments 1 and 2 the form factor has been shown to be similar for all leaves of all genotypes on all axis for two different growing seasons. The simple quadratic model currently implemented in ADEL-wheat is considered to be the most appropriate for the modelling of 2D leaf shape. It was also found that the model could be re-expressed resulting in the need for one parameter only, this parameter being the form factor. The idea of using a separate parameterisation for flag and winter leaves was tested, as their form factor was found to be lower than other leaves. However the resulting differences were not significant so the additional parameterisation was deemed unnecessary. The lamina area and shape was found to

be estimated accurately with the constant model over all genotypes, ranks and axes.

3D Leaf Shape

Changes have been made to the main stem angle from the vertical which has been reduced from $10°$ to $5°$. Ideally however, parameterisation of main stem angle would allow for the variation in angle noted over the growing season, the trend of which was the angle from the vertical reduced throughout the plants development, thought to be due to the presence of internodes.

A new parameterisation of the base inclination angle for tillers was also proposed to be changed to $60°$ from $40°$. The data collected on tiller angle did not include internode location and rank which meant an in depth analysis into the straightening of the tillers in relation to the internode ranks could not be made.

In general, uncertainty in the measurements of midrib curvature was high, giving a low confidence with the 3D data on midrib curvature. However a simple parabola model was proposed to be sufficient to model the midrib curvature of all leaves over all ranks and axes. A warning is given however that no data was recorded on leaves of rank 4 and lower, however within the ADEL-wheat model it is suggested that base and middle leaves are more similar in architectural traits that upper leaves. Data was obtained on middle leaves meaning that lower leaves are assumed to be similar to the data obtained on such leaves. In summary it is accepted that the data obtained from the digitisation contains a lot of noise making comparisons and observations on midrib curvature and the effect of rank, genotype and growing conditions problematic. An additional problem that could not be overcome in the time frame of this thesis is the inability to parameterise a leaf to have an inclination angle (from the horizontal) greater than $80°$. Much time was spent on this problem with no clear solution. Although many of the leaves were shown to have inclination angle much higher they are given a maximum of $80°$ degrees due to the limitation of the model.

Canopy Cover

Modelled canopy cover was compared to observed canopy cover as a way of understanding how the model was predicting the canopy development and structure. In order to compare the data it was necessary to analyse the canopy cover photographs. A method of extracting three rows of crop per image was considered a fair way to calculate percentage cover over a range of photographs taken on different days and over different locations over the canopy. It was found however, that from the small sample set of images obtained, that using only three rows compared to estimating cover from the entire photographs did not greatly affect the final percentage cover.

This method was also extended to the output from the model. It enabled a profile of the distribution of vegetation at each thermal time step to be created. It also enabled a greater insight into why modelled and actual canopy cover differ by enabling an alternative visual comparison between modelled and actual canopy cover.

The Iso Cluster method did not significantly decrease the error or help give a more reasonable estimate of cover for some of the images which were hard to classify. The initial method, method 1, worked just as well as calculating the percentage cover. The advantage of the Iso Cluster method was that it calculated the senesced material and green material. However for the purposes of this work, only the overall percentage cover was required and it is concluded that either method is suitable to calculate the percentage cover.

When looking at the progression of canopy cover over time in experiment 2, there is a plateau (around 500 - 620 thermal time) of canopy cover. This corresponds to the time in which there is a plateau in lamina length over phytomer rank and would explain this plateau in canopy cover.

Validation

It is found that the modelled final organ lengths are not significantly different to the observed measurements in the field. Modelled LAI is also found to be a close match to that observed. The observed and modelled number of tillers is also found to be close except over early thermal time where it is over estimated for both genotypes. Assumptions made within the tiller model should be considered as part of future research. However if initial tiller number is reduced further to be

a closer match with that observed it would reduce the modelled canopy cover over lower thermal time and therefore increase the difference between observed and modelled canopy cover. It must also be mentioned again that observed tiller numbers did not include tiller 4 which reduces potential canopy cover later on in development. However these tillers were small and most that were produced did not survive to produce a head.

The focus of this chapter was to determine why canopy cover, an important parameter for remote sensing studies, was not being modelled accurately. As phenology is shown to be modelled accurately, alternative causes of this difference are needed to be investigated, such as architectural simulation.

When the perspective effect was included within the model it was expected to have an effect on the canopy cover, however none was observed in overall canopy cover. Also when looking at the profile of the canopy cover over the images with and without the perspective effect there were only very small differences observed.

The phyllochron rate was shown, when it was lowered for the simulation of a Caphorn canopy, to alter the timing at which the canopy cover increased significantly after the noticeable plateau in cover. This had a positive effect on lowering the difference between observed and modelled canopy cover until a thermal time of around 1200 when it created an over estimation of cover. There is no definitive phyllochron rate for winter wheat crops within published research, however it is usually stated to be around 100. The measured rate of 107 is therefore slightly higher however was within the mean and standard deviation for all genotypes measured during experiment 1 and 2. The main point raised from this investigation is the importance of the phyllochron rate when estimating canopy cover as it highlighted that a small difference in the value of this parameter can create a significant differences in the progression of canopy cover over time.

The architecture of the leaves is assumed to create a noticeable difference in canopy cover. It is shown that the canopy cover of Caphorn, an erectophile plant is lower than Soisson a planophile plant. Accurate architectural data was hard to obtain for both genotypes. The lack of data collected on early leaves was disappointing, although unavoidable considering the conditions in the field and the equipment being used to measure architecture. The effect of modelling early leaves to be more planophile than estimated from the field data (collected from older leaves) had a positive effect on reducing the difference between observed and modelled canopy cover over

lower thermal time.

An additional investigation was carried out to the combined effect of a lower phyllochron rate and a more planophile structure for early leaves on the Caphorn genotype only. Both these changes were modelled and the difference in the canopy cover over thermal time compared to the observed. The result was favourable, with observed and modelled becoming a closer match until thermal time 900 after which the canopy cover is shown to be overestimated by a significant 15-20 %.

It must be noted that senescence has not been included within the model and that an improved model of senescence could perhaps reduce this error. Improving the initial estimation of cover does however seem to create a greater error in the estimation of cover in the later part of the development of the canopy.

Other parameters were altered such as tiller angle which was changed back to the original value of 60 degrees. This was found to have no significant effect on canopy cover. Also changing the boom height did not have a significant effect on the modelled canopy cover.

The location of the plants within the field were also investigated. In reality some seeds do not germinate which causes gaps in the rows, this was especially noticeable within experiment 2. The plants also do not grow in an exact line and instead are described within this thesis to be jittered about a row. Both these observations were attempted, to be incorporated with the model separately. No quantitative assessment was made into how many plants should be removed or how much are the plants deviate from straight rows, instead it was based on a visual assessment. By removing some plants the obvious effect on the modelled canopy cover was that it was reduced and by including the jittering of plants about the row, the canopy cover was increased, although only very slightly. This would not be the case within the field. If a plant dies the plant next to it will spread out and use the extra light and space. This mechanism is not included in the model meaning that the effect of removing plants has to be analysed with caution. The effect of jittering is shown to have a limited effect on the overall canopy cover, which is also not realistic within the field. Less over lapping of the leaves of the plants would be expected and again extra tillers or leaves may be produced due to the extra light the plants would receive due to reduced competition.

Overall the investigations into 3D architecture have provided a good amount of information into the important considerations within the modelling process. It has also highlighted the need to look at the overall canopy cover as well as the spatial arrangement of the crop within the field. The limitation of the classification method used to create what has been referred to as the profile of the canopy cover image is accepted however it does help in highlighting the effect different variables have on canopy cover. It also brings to attention the usefulness of this when looking at the effects certain parameters or model considerations on canopy cover.

Validation: Radiometry A variation in leaf reflectance was observed between phytomer rank. The sampling set was however too small to make a conclusive statement regarding the difference in leaf reflectance especially when considering the work of Pinter *et al.* (1985a) who found that single-leaf spectra measured in the laboratory with a spectrophotometer revealed no cultivar-related differences when measurements were taken over six winter wheat genotypes. However this was inter related differences. If however it is considered that the spectral reflectance of vegetation in the 400-700 nm region is primarily given by the abundance of chlorophyll and other pigments absorbing most of the incident radiation (Thomas and Gausman 1977, Broge and Mortensen 2002) then as the leaf ages the levels of these pigments change and so does its reflectance. Incorporating an age related reflectance function within the model is a suggested further enhancement of this model.

Soil Reflectance

The variation in measured soil reflectance has been highlighted. The effect of this variation on the modelled radiometric output would have been useful to quantify and is a recommendation for future work.

Reflectance With Varying Sun Angle

Pinter *et al.* (1985a) who found, no difference in single leaf spectra measurement, suggested this lack of difference in reflectance observed between six different genotypes of winter wheat at every time period, despite their apparent similarities in green leaf area and green biomass, supported the contention that the reflectance's were strongly influenced by canopy architectural

features. They reinforced this conclusion by showing that planophile canopies exhibit the least amount of variability due to changes in sun angle and erectophile canopies showing the most. This is shown visually when comparing the observed and modelled reflectance between Soisson and Caphorn models. Although this pattern is noticed within the modelled data, it was suggested by Pinter *et al.* (1985b) that soil evaporation tends to be higher in open than in closed canopies which leads to the soil surface drying out faster when the mean leaf inclination angle is increased for the same foliage area. It is this soil surface drying which is associated with increased spectral reflectance (Irons *et al.* 1989) and so it would be premature to congratulate the model for simulating this effect appropriately.

NDVI

The estimated NDVI values for all four models are compared with NDVI values measured in the field. In general the observed and modelled data is best matched later on in development, so after Thermal time 1000. The lack of match between observed and modelled before thermal time 700 is likely to be a result of the level of frost and snow which would cause the NDVI to be zero or below. However there is a general lack of agreement between the observed and modelled NDVI between thermal time 650 and 1000 from all models even when the canopy cover estimates from the model are close to those observed.

8.1 Summary

The validation of the structural model outputs has proved to be tricky. This is a result of the subtlety of the changes in structure, and their various impacts on canopy cover and the remote-sensed signal. Limitations of radiometric measurements can often overwhelm variations due to structure. There is evidence to suggested a lack of correlation between modelling the canopy cover accurately and the radiometric signal and that especially where there is an erectophile canopy more emphasis must be placed on simulating soil reflectance accurately. There is also some importance given to the differences in leaf reflectance over phytomer rank. Within the field, NDVI values of two genotypes were not obtained at one time which makes it hard for a true comparison to be made. It would seem from the data available that the NDVI of both canopies does not differ

greatly. It is instead suggested to focus more on the effect the architectural properties of the model have on reflectance by looking at the full reflectance data of the canopy and over varying sun angle.

Further Work

This research has led to healthy number of questions. The combination of the 3D model and the canopy reflectance model is suggested and hopefully highlighted within this thesis as an efficient tool that can be utilised in answering some of these questions. There are many ways in which the 3D Architectural model could be improved. One of the ways would be to implement a senescence model. Extensive data on senescence was collated over Experiment 1 and 2 however time restraints meant a model was implemented within the course of this thesis. This model would enable a better simulation of the canopy over middle to late development. It would also then allow a LAI threshold to work efficiently in ceasing tiller development. Currently the new tiller model implemented uses a maximum tiller number to cease tiller development, however it was shown that a threshold value of LAI could be more appropriate. The 3D curvature of leaves is simplified within this thesis yet the suggested model did not allow for the leaves with inclination angle of more than 80° (from the horizontal). There is a need to understand at which point along the leaf blade that the angle of inclination is calculated and then it would be of interest to see how the inclination angle of leaves changes with age of leaf. In regards to the age of the leaf, the reflectance of leaves was found to differ over rank, which is a likely response to the change in pigments in the leaf as it ages. This could be investigated further and as suggested would be simple to implement into the model.

Summary

One aim of this work is to build a useful database of information on wheat growth and development. This has been successfully achieved. It holds information on many genotypes over one experimental period and information for two genotypes over two growing seasons. The database includes phenological and architectural data which can help feed into continuing research with wheat growth and development. It also gives feedback on the drawbacks and advantages of certain measurement techniques which should also aid in future experimental research. This

database has already proven useful to other applications of crop research and has contributed to two published papers ((Dornbusch *et al.* 2011, Dornbusch *et al.* 2010)) and no other published work can be found that details such an extensive database of information from the same growing season on winter wheat genotypes.

The crop model that this thesis is focused on is ADEL-wheat which is considered to be a dynamic 3D model of winter wheat and as mentioned simulates explicitly the structure of the crop at the plant level. There is no published work available on the coupling of a radiative transfer model with a 3D dynamic Architectural crop model in relation to wheat. This thesis aimed to investigate the idea of this combination of models and to illustrate its potential use within remote sensing studies to understand more about the how the structure of the canopy affects the radiometric signal. Despite the difficulties and limitations of validating the structural model via radiometric measurements, some conclusions were possible regarding the impact of new model developments of canopy architecture on the remote sensing signal. Two 3D-Architectural models exist of genotypes of winter wheat with differing architectural properties, grown under the same environmental conditions. They have with some success been coupled with a radiative transfer model and simulations of reflectance compared with actual reflectance. Additional time is required to now utilise the power of this tool to unpick in greater detail the properties affecting the reflectance and start to answer some of the questions raised.

References

ADAM, B., 1999, POL95-software to drive a Polhemus Fastrak 3 SPACE 3D digitiser, Technical report, UMR PIAF INRA-UBP, Clermont-Ferrand.

AMIR, J., and SINCLAIR, T., 1991, A model of the temperature and solar radiation on spring wheat growth and yield. *Field Crops Research*, **28**, 47–58.

ANDRIEU, B., BARET, F., JACQUEMOUD, S., MALTHUS, T., and STEVEN, M., 1997, Evaulation of an Improved Version of SAIL Model fo Simulating Bidirectional Reflectance of Sugae Beet Canopies. *Remote Sensing Environment*, **60**, 247–257.

ANDRIEU, B., and SINOQUET, H. ., 1993, Evaluation of structure description requirements for predicting gap fraction of vegetation canopies. *Agricultural and Forest Meteorology*, **65**, 207–227.

ATZBERGER, M., 2004, Object-based retrieval of biophysical canopy variables using artificial neural nets and radiative transfer models. *Remote Sensing Environment*, **93**, 53–67.

BACOUR, C., BARET, F., BEAL, D., WEISS, M., and PAVAGEAU, K., 2006, Neural network estimation of LAI, fAPAR, fCover and LAIxCab, from top of canopy MERIS reflectance data:principles and validation. *Remote Sensing Environment*, 313–325.

BAKER, C., GALLAGHER, J., and MONTEITH, J., 1980, Daylength change and leaf appearance in winter wheat. *Plant cell and environment*, **3**, 285–287.

BAKER, J., PINTER, P., REGINATO, R., KANEMASU, E., and KANEMASU, E., 1986, Effects of temperature on leaf appearance in spring and winter wheat cultivars. *Agronomy Journal*, **78**, 605–613.

BANK, W., 1994, *World Population Projections 1994-1995* (John Hopkins University Press).

BARET, F., and BUIS, S., 2008, Estimating Canopy Characteristics from Remote Sensing Observations: Review of Methods and Associated Problems., In *Advances in Land Remote Sensing*, edited by S. Liang (Springer Science), pp. 173–201.

BARET, F., and GUYOT, G., 1991, Potentionals and limits of vegetation indices for LAI and APAR assessment. *Remote Sensing of Environment*, **35**, 161–173.

BARILLOT, R., LOUARN, G., ESCOBAR, G., ABRAHAM, J., HUYNH, P., and COMBES, D., 2011, How good is the turbid medium-based approach for accounting for light partitioning in contrasted grass legume intercropping systems. *Annals of Botany*, **108**, 1013–1024.

BARNES, E., QI, J., and PINTER, P., 2001, Integration of Remote Sensing and Growth Models to Assist in Precision Crop Management.

BASTIAANSSEN, W., and ALI, S., 2003, A new crop yield forecasting model based on satellite measurements applied across the Indus Basin. Pakistan,. *Agriculture, Ecosystem, Environment*, **94**, 321–340.

BAUER, A., FRANK, A., and BLACK, A., 1984, Estimation of spring wheat leaf growth rates and anthesis from air temperature. *Agronomy Journal*, **76**, 829–835.

BIRCH, C., VOS, J., and KINIRY, R., 1998, Towards a robust method of modelling leaf appearance in plants, volume Australuan Society of Agronomy.

BLOOMENTHAL, J., 1985, Modelling the Mighty Maple. *Proceedings of SIGGRAPH; Computer Graphics*, **10**, 305–3111.

BOS, H., and NEUTEBOOM, J., 1998, Morphological Analysis of Leaf and Tiller Number Dynamics of Wheat (*Triticum aestivum* L.): Responses to Temperature and Light Intensity. *Annals of Botany*, **81**.

BOS, H., TIJANI-ENIOLA, H., and STRUIK, P., 2000, Morphological analysis of leaf growth of maize: responses to temperature and light intensity. *Netherlands Journal of Agricultural Science*, **48**, 181–198.

BRACAGLIA, M., FERRAZZOLI, P., MCDONALD, K., and GUERRIO, L., 1995, A fully polarimetric multiple scattering model for crops. *Remote Sensing of Environment*, **54**, 170–179.

BRISSON, N., GARY, C., JUSTES, E., ROCHE, R., MARY, B., RIPOCHE, D., ZIMMER, D., SIERRA, J. NAD BERTUZZI, P., BURGER, P., BUSSIE´ ERE, F., CAMBIDOCHE, Y., CELLIER, P., DEBAEKE, P., GAUDILL´ ERE, J., H´ ENAULT, C., MARAUX, F., SEGUIN, B., and SINOQUET, H., 2003a, An overview of the crop model STICS. *European Journal of Agronomy*, **18**, 309–332.

BRISSON, N., WERY, J., and BOOTE, K., 2003b, *An Introduction to crop Models*.

BROGE, H., and MORTENSEN, J., 2002, Deriving green crop area index and canopy chlorohpyll density of winter wheat from spectral reflectance data. *Remote Sensing of Environment*, **81**, 45–57.

BROGE, N., and LEBLANC, E., 2001, Comparing prediction power and atability of broadband and yperspectral vegetation indices for estimation of green leaf area and canopy chlorophyll density. *Remote Sensing of Environment*, **76**, 156–172.

CAMPBELL, J., 1995, Introduction to Remote Sensing, In *Introduction to Remote Sensing* (Guilford Press).

CAMPBELL, J., ROBERTSON, M., and GROF, C., 1998, Temperature effects on node appearance in sugarcane. *Australian Journal of Plant Physiology.*, **25**, 815–818.

CANNEL, R., 1969, The tillering pattern in barley varieties. II. The effect of temperature, ligt intensity and daylength on the frequency of occurrence of the coleoptile node and second tillers in barley. *Journal of Agricultural Science*, **72**, 423–435.

CAO, W., and MOSS, D., 1989, Temperature effect on leaf emergence and phyllochron in wheat and barley. *Crop Science*, **29**, 1018–1021.

CAO, W., and MOSS, D., 1991, Phyllochron change in winter wheat with planting data and environmental changes. *Agronomy Journal*, **83**, 396–401.

CHANTER, D., 1981, The use and misuse of linear regression methods in crop modelling, In *Mathematics and plant physiology*, edited by D. Rose, and D. Charles-Edwards (CRC press,Boca Raton,FL,USA), pp. 253–266.

CHELLE, M., and ANDRIEU, B., 1998, The nested radiostiy model for the distribution of light within plant canopies. *Ecological Modelling*, **111**, 75–91.

COLLINS, W., 1978, Remote Sensing of crop type and maturity. *Photogrammetric Engineering and Remote Sensing*, 43–55.

COLOMBO, R., BEKKINGEN, D., FASOLINI, D., and MARINO, C., 2003, Retrieval of leaf area index in different vegetation types using high resolution satellite data. *Remote Sensing of Environment*, **86**, 120–131.

COMBAL, B., 2002, Retrieval of canopy biophysical variables from bi-directional reflectance data. Using prior information to solve the ill-posed inverse problem. *Remote Sensing Environment*, 1–15.

CUDNEY, D., JORDAN, L., CORBETT, C., and BENDIXEN, W., 1989, Developmental rates of wild oats (*Avena fatua*) and wheat (*Triticum aestivum*). *Weed Science*, **37**, 521–524.

DANSON, F., ROWLAND, C., and BARET, F., 2003, Training a neural network with a canopy reflectance model to estimate crop leaf area index. *International Journal of Remote Sensing*, **24**, 4891–4905.

DAUZAT, J., CLOUVEL, P., LUQUET, D., and MARTIN, P., 2008, Using Virtual plants to analyse the light-foraging efficiency of a low-density cotton crop. *Annals of Botany*, **101**, 1153–1166.

DE VISER, P., MARCELIS, L., and VAN DER HEIJDEN, G., 2003, 3D digitization and modeling of flower mtutants of Arabidopsis thaliana. (University Press, Beijing), pp. 218–226.

DELECOLLE, R., and GUERIF, M., 1988, Introducing spectral data into a plant process model for improving its prediction ability. *Proceedings 4th Int.Colloq.Spectral Sig. in Rem. Sens., Sussois, France*, **Jan, ESA-SP287**, 125–127.

DESJARDINS, R., SIVAKUMAR, M., and KIMPE, C. D., 2007, The contribution of agriculture to the State of Climate: Workshop summary and reccomendations. *Agriculture and Forest Meteorology*, **142**, 314–324.

DIBELLA, C., FAIVRE, R., RUGET, F., and SEGUIN, B., 2005, Using VEGETATION satellite data and the crop model STICS-Prairie to estimate pasture production at the national level in France. *Physics and Chemistry of the Earth, Parts A/B/C*, **30**, 3–9.

DISNEY, M., KALOGIROU, V., LEWIS, P. NAD PRIETO-BLANCO, A., HANCOCK, S., and PFEIFER, M., 2011, 3D radiative transfer modelling of fire impacts on two-payer savanna. *Remote Sensing of Environment*, **115**, 1886–1881.

DISNEY, M., LEWIS, P., and NORTH, P., 2000, Monte Carlo Ray Tracing in Optical Canopy Reflectance Modelling. *Remote Sensing Reviews.*, **18**, 163–196.

DISNEY, M., LEWIS, P., and SAICH, P., 2006, 3D modelling of forest canopy structure for remote sensing simulations in the optical and microwave domains. *Remote Sensing of Environment*, **100**, 114–132.

DORNBUSCH, T., and ANDRIEU, B., 2009, Lamina2Shape - An image processing tool for an explicit description of lamina shape tested on winter wheat (Triticum aestivum L). *Computers and Electronics in Agriculture*, **70**, 217–224.

DORNBUSCH, T., BACCAR, R., WATT, J., HILLIER, J., BERTHELOOT, J., FOURNIER, C., and ANDRIEU, B., 2011, Plasticity of winter wheat modulated by sowing date, plant population desnity and nitrogen fertilisation: Dimension and size of leaf blades, sheaths and internodes in relation to their position on a stem. *Computers and Electronics in Agriculture*, **121**, 116–124.

DORNBUSCH, T., WATT, J., BACCAR, R., FOURNUER, C., and ANDRIEU, B., 2010, A Comparative Analysis of Leaf Shape of Wheat, Barley and Maize Using an Empirical Model. *Annals of Botany*, **107**, 865–873.

DORNBUSCH, T., WERNECKE, P., and DIEPENBROCK, W., 2007, A method to extract morphological traits of plant organs from 3D clouds as a database for an architectural plant model. *Ecological Modelling*, **200**, 119–129.

DOURADO-NETO, D., TERUEL, D. A.AND REICHARDT, K., NIELSEN, D., FRIZZONE, J. A., and BACCHI, O., 1998, Principles of crop modeling and simulation: I. uses of mathematical models in agricultural science. *Scientia Agricola*, **55**, 46 – 50.

DROUET, J., and PAGES, L., 2003, GRAAL: a model of growth, architecture and carbon allocation during the vegetative phase of whole maize plant. Model description and parameterization. *Ecological Modelling*, **165**, 147–173.

ESPANA, N., BARET, F., and ARIES, F., 1999, Radiative transfer sensitivity to the accuracy of canopy structure description: The case of a maize canopy. *Agronomie*, **19**, 241–254.

EVERS, J., 2006, *Tillering in Spring Wheat: A 3D Virtual Plant Modelling Study.*, Ph.D. thesis, Wageningen.

EVERS, J., VOS, J., FOURNIER, C., ANDRIEU, B., CHELLE, M., and STRUIK, P., 2004, A 3D approach for modelling tillering in wheat (*Triticum aestivum* L.), In *FSPM04*.

EVERS, J., VOS, J., FOURNIER, C., ANDRIEU, B., CHELLE, M., and STRUIK, P., 2005, Towards a generic architectural model of tillering in Gramineae, as exemplified by spring wheat (*Triticum aestivum*). *New Phytologist*, **166**, 801–812.

FANG, H., and LIANG, S., 2005, A hybrid inversion method for mapping leaf area index from MODIS data: experiments and applications to broadleaf and needle leaf canopis. *Remote Sensing Environment*, **94**, 405–424.

FAO, 2002, *World Agriculture: towards 2015/2030. Summary Report* (Rome: FAO02).

FAOSTAT, 2007, *Food and Agriculture Organisation of the Uniter States* (USA: FAO).

FIELD, C., RANDERSON, J., and MALMSTROM, C., 1995, Global net primary production: combining ecology and remote sensing. *Remote Sensing of Environment*, **51**, 74–88.

FISHER, P., and LIETH, J., 2000, Variability in flower development if Easter Lily (Lilium longiflorum Thnb.): model and decision-support system. *Computers and Electronics in Agriculture*, **26**, 53–64.

FOLEY, J., DEFRIES, R., ASNER, G., BARFORD, C., BONAN, G., CARPENTER, S., CHAPIN, F., COE, M., DAILY, G., GIBBS, H., HELKOWSKI, J., HOLLOWAY, T., HOWARD, E., KUCHARIK, C., MONFREDA, C., PATZ, J., PRENTICE, C., RAMANKUTTY, N., and SNYDER, P., 2005, Global Consequences of Land Use. *Science*, **22**, 570–574.

FOURNIER, C., and ANDRIEU, B., 1998, A 3D Architectural and Process-based Model of Maize Development. *Annals of Botany*, **81**, 233–250.

FOURNIER, C., and ANDRIEU, B., 1999, ADEL-maize:an L-system based model for the integration of growth processes from the organ to the canopy. Application to regulation of morphogenesis by light availability. *Agronomie*, **3/4**, 317–323.

FOURNIER, C., ANDRIEU, B., LJUTOVAC, S., and SAINT JEAN, S., 2000, Development of an Architectural Growth Model for Wheat: Final Report. *Report on Workpackage 30*.

FOURNIER, C., ANDRIEU, B., LJUTOVAC, S., and SAINT-JEAN, S., 2003, ADEL-wheat: A 3D Architectural Model of Wheat Development.

FOURNIER, C., DURAND, J., LJUTOVAC, S., SCHAUFELE, R., GASTAL, F., and ANDRIEU, B., 2005, A functional-structural model of elongation of the grass leaf and its relationships with the phyllochron. *New Phytologist*, **166**, 881–894.

FRANK, A., and BAUER, A., 1995, Phyllochron differences in wheat, barley and forage grasses. *Crop Science*, **35**, 19–23.

FRANK, A., and BAUER, A., 1997, Temperature effects prior to double ridge on apex development and phyllochron in spring barley. *Crop Science*, **37**, 1527–1531.

FRIEND, D., 1965, Tillering and leaf production in wheat as affected by temperature and light intensity. *Canadian Journal of Botany*, **43**, 1063–1076.

GIBSON, P., and POWER, C., 2000, Leaf Structure and Reflectance from Layered Canopies, In *Principles of Remote Sensing*, edited by P. Gibson, and C. Power (Routledge).

GITELSON, A., VINA, A., CIGANDA, V., RUNDQUIST, D., and ARKEBAUER, T., 2005, Remote estimation of canopy chlorophyll content in crops. *Geophysical Research Letters*, **32**.

GNU, 2002, The GNU Image Manipulation Programe.

GODIN, C., and SINOQUET, H., 2005, Functional-structural plant modelling. *New Phytologist*, 705–708.

GOEL, N., ROZEHNAL, I., and THOMPSON, R., 1991, A computer graphics based model for scattering from objects of arbitrary shapes in the optical region. *Remote Sensing Environment*, **36**, 73–194.

GOETZ, S., PRINCE, S., SMALL, J., and GLEASON, A., 2000, Interannual variability of global terrestrial primary production: Results of a model driven with satellite observations. *Journal of Geophysical Research D: Atmospheres*, **105**, 200077–20091.

GORDON, R., and BOOTSMA, A., 1993, Analyses of growing degree-days for agriculture in Atlantic Canada. *Climate Research*, **3**, 169–176.

GOVAERTS, Y., JACQUEMOND, S., VERTRAETE, M., and USTIN, S., 1996, Three-dimensional radiation transfer modelling in a dictoyledon leaf. *Appl. Opt.*, **35**, 6585–6598.

GRANT, R., and HESKETH, J., 1992, Gra92. *Biotronics*, **21**, 11–24.

GRAVES, A.R.AND HESS, T., MATTHEWS, R.B.AND STEPHENS, W., and MIDDLETON, T., 2002, Crop Simulation Models as Tools in Computer Laboratory and Classroom-Based Education. *Journal Natural Resource Life Science Education*, **31**, 48–54.

HAMMER, G., HILL, K., and SCHRODTER, G., 1987, Leaf area production and senscence of diverse grain sorghum hybrids. *Field Crops Research*, **17**, 305–317.

HAMMER, G., and MUCHOW, R., 1991, *Quantifying climatic risk to sorghum in Australia's semiarid tropics and subtropics: Model development and simulation p 205-232. In R.C. Muchov and J.A Bellamy (eds) Climatic Risk in crop production: Models and Management for the semiarid tropics and subtropics.* . (Wallingford, UK: C.A.B International).

HANAN, J., RENTON, M., and YORSTONE, E., 2003, *Simulating and visualising spray deposition in plant canopies.* (Australia: ACM GRAPHITE).

HANCOCK, S., LEWIS, P., FOSTER, M., DISNEY, M., and MULLER, J., 2012, Measuring tree height over topography and understory vegetation with dual wavelength lidar: a simulation study. *Agricultural Forest Meteorology*.

HARNOS, N., and KOVACS, G., 1999, Comaprison of four winter wheat simulation models using long term regional yield data. *Proceedings of the ESA International Symposium Modelling Cropping Systems, Lleida*, 197–198.

HAUN, J., 1973, Visual quantification of wheat development. *Agronomy journal*, **65**, 116–117.

HAY, R., and DELECOLLE, R., 1989, The setting of rates of development of wheat plants at crop emergence: influence of the environment on rates of leaf appearance. *Annals of Applied Biology*, **115**, 333–341.

HEIJDEN, G. V. D., VISSER, P., and HEUVELINK.E., 2007, *Functional Structural Plant Modelling in Crop Production* (Springer).

HILLIER, J., MAKOWSKI, D., and ANDRIEU, B., 2005, Maximum likelihood and bootstrap methods for plant organ growth via multi-phase kinetic models and their application to maize. *Annals of Botany*, **96**, 137–148.

HODGES, T., and RITCHIE, J., 1991, *The CERES-Wheat phenological model* (Boston: CRS Press).

HONDA, T., and OKAJIMA, H., 1970, Environmental light conditions and tiller development in the rice plant. 3. Effects of partial shading and temperature on the development of tiller buds and dry matter increments. *Bulletin of the Institute for Agricultural Research*, **22**, 1–15.

HOTSONYAME, G., and HUNT, L., 1997, Effects of sowing date, photoperiod and nitrogen on variation in main culm leaf dimensions in field-grown wheat. *Canadian Journal of Plant Science*, **78**, 35–49.

HOUBORG, R., ANDERSON, M., and DAUGHTRY, C., 2009, Utility of an image-based canopy reflectance modelling tool for remote estimation of LAI and leaf chlorophyll content at the field scale. *Remote Sensing of Environment*, **113**, 259–274.

IRONS, J., WEISMILLER, R., and PETERSON, G., 1989, Soil reflectance, In *Theory and applications of optical remote sensing*, edited by G.Asrar (New York Wiley), pp. 66–106.

IVANOV, N., BOISSARD, P., and CHAPRON, M., 1995, Computer stereo plotting for 3D reconstruction of a maize canopy. *Agricultural and Forest Meteorology*, **75**, 85–102.

JACQUEMOUD, S., BACOUR, C., POLIVE, H., and FRANGI, J., 2000, Comparison of four radiative transfer models to simulate plant canopies reflectance: direct and inverse model. *Remote Sensing Environment*, **74**, 471–481.

JACQUEMOUD, S., BARET, F., ANDRIEU, B., DANSON, M., and JAGGARD, K., 1995, Extraction of vegetation biophysical parameters by inversion of the PROSPECT+SAIL model on sugar beet canopy reflectance data. Application to TM and AVIRIS sensors. *Remote Sensing Environment*, **52**, 163–172.

JAFFUEL, S., and DAUZAT, J., 2005, Synchronism of Leaf and Tiller Emergence Relative to Position and to Main Stem Development Stage in a Rice Cultivar. *Annals of Botany*, **95**, 401–412.

JALLAS, E., SEQUEIRA, R., MARTIN, P., TURNER, S., and CRETENET, M., 2000, COTONS, a cotton simulation model for the next century.

JAME, Y., and CUTFORTH, H., 1996, Crop growth models for decision support systems. *Canadian Journal of Plant Science*, **76**, 9–19.

JAMIESON, P., BROOKING, I., PORTER, J., and WILSON, D., 1995, Prediction of leaf appearance in wheat:a question of temperature. *Field Crops Research*, **41**, 35–44.

JAMIESON, P., PORTER, J., GOUDRIANN, J., RITCHIE, J., VAN KEULEN, H., and STOL, W., 1998a, A comparison of the models AFRCWHEAT2, CERES-Wheat, SIRIUS, SUCROS2, and SWHEAT with measurements from wheat grown under drought. *Field Crops Research.*, **55**, 23–44.

JAMIESON, P., and SEMENOV, M., 2000, Modelling nitrogen uptake and redistribution in wheat. *Field Crop Research*, **68**, 21–29.

JAMIESON, P., SEMENOV, M., BROOKING, I., and FRANCIS, G., 1998b, Sirius: a mechanistic model of wheat response to environmental variation. *Europeran Journal of Agronomy*, **8**, 161–179.

JENSEN, M., 1968, Water consumption by Agricultural plants., In *Water deficits and plant growth.*, edited by T. Koslowski (New York:Academic Press), pp. 1–22.

JOCHEM, E., 2006, *Tillering in spring wheat: a 3D virtual plant modelling study*, Ph.D. thesis.

JONES, C., 1985, CERES-Maize:A stimulation model of maize growth and development. *NTIS, SPRINGFIELD, VA(USA), 1985, 195*, **195**.

JUSKIW, P., JAME, Y., and KRYZANOWSKI, L., 2001, Phenological development of spring barley in a short-season growing area. *Agronomy journal*, **93**, 370–379.

KIM, H., LUQUET, D., OOSTEROM, E., DINGKUHN, M., and HAMMER, G., 2010a, Regulation of tillering in sorghum: genotypic effects. *Annals of Botany*, 1–10.

KIM, H., OOSTEROM, E., DINGKUHN, M., LUQUET, D., and HAMMER, G., 2010b, Regulation of tillering in sorghum:environmental effects. *Annals of Botany*, 1–11.

KIMES, D., 1968, Radiative transfer in homogeneous and heterogeneous vegetation canopies, In *Photon-Vegetation Interactions. Applications in Optical Remote Sensing and Plant Ecology.*, edited by R. Myneni, and J. Ross (Springer-verlag Berlin), pp. 9–44.

KIMES, D., and KIRCHNER, J., 1982, Irradiance measurement errors due to the assumption of a Lambertian reference panel. *Remote Sensing Environment*, **12**, 141–149.

KINIRY, J., 1991, chapter Maize phasic development (ASA, CSSA, and SSSAM, Madison, WI), pp. 55–69.

KIRBY, EJM.AND FARIS, D., 1972, The effect of plant density on tiller growth and morphology in barley. *Journal of Agricultural Science*, **78**, 281–288.

KIRBY, E., APPLEYARD, M., and FELLOWES, G., 1982, Effect of sowing date on the temperature response of leaf emergence and leaf size in barley. *Plant, cell and environment*, **5**, 477–484.

KNYAZIKHIN, Y., MARSHAK, J. V., DINER, D. J., B., M. R., VERSTRAETE, M., B., P., and GOBRON, N., 1998a, Estimation of vegetation canopy leaf area index and fraction of absorbed photosynthetically active radiation from atmosphere-corrected MISR data. *Journal of Geophysical Research*, **103**, 32239–32257.

KNYAZIKHIN, Y., MARSHAK, J. V., DINER, D. J., and RUNNING, S. W., 1998b, Synergistic algorithm for estimating vegetation canopy leaf area index and fraction of absorbed photsynthetically active radiation from MODIS and MISR data. *Journal of Geophysical Research*, **103**, 32257–32277.

KURTH, W., FORSCHUNGSENTRUMS, B., and WALDOKOSYSTEME, G., 1994, Growth Grammar Interpreter GROGRA 2.4 - A software tool for the 3-dimensions interpretation of stochastic, sensitive growth grammars in the context of plant modelling.

LAFARGE, T., BROAD, I., and HAMMER, G., 2002, Tillering in Grain Sorghum over a Wide Range of Population Densities:Identification of a Common Hierarchy for Tiller Emergence, Leaf Area Development and Fertility. *Annals of Botany*, **90**, 87–98.

LAFARGE, T., and HAMMER, G., 2002, Tillering in Grain Sorghum over a Wide Range of Population Densities: Modelling Dynamics of Tiller Fertility. *Annals of Botany*, **90**, 99–110.

LANG, A., 1973, Leaf orientation of a cotton plant. *Agricultural Meteorology.*, **11**, 37–51.

LAUER, J., and SIMMONS, S., 1985, Photoassimilate partionioning of main shoot leaves in field-grown spring barley. *Crop Science*, **25**, 851–855.

LAUNEY, M., BRISSON, N., SATGER, S., HAUGGAARD-NIELSEN, H., CORRE-HELLOU, G., KASYNOVA, E., RUSKE, R., JENSEN, E., and GOODING, M., 2009, Exploring options for managing strategies for pea-barley intercropping using a modelling approach. *European Journal of Agronomy*, **2**, 85–98.

LAWLESS, C., SEMENOV, M., and JAMIESON, P., 2005, A wheat canopy model linking leaf area and phenology. *European Journal of Agronomy*, 201–234.

LEWIS, P., 2007, Canopy Modelling as a tool in remote sensing research., In *FSPM in Crop Production.*, edited by J. Vos, L. Marcelis, P. de Visser, P. Struick, and J. Evers (Springer), pp. 219–229.

LEWIS, P., 2011, Librat Source Code version 1.3.2.

LI, X., and STRAHLER, A., 1985, Optical Modelling of a Conifer Forest Canopy. *IEEE Transactions on Geoscience and Remote Sensing*, **GE-23**, 705–721.

LJUTOVAC, S., 2002, *Coordination dans l'extension des organs aériens et conséquence pour les relations entre les dimensions finales des organes chez le blé.*, Ph.D. thesis, Institute National Agronomique Paris-Grignon, Paris.

LOBELL, D., ASNER, G., ORTIZ-MONASTERIO, J., and BENNING, T., 2003, Remote Sensing of regional crop production in the Yaqui Valley, Mexico: estimates and uncertainties. *Agriculture, Ecosystems and Environment*, **94**, 205–220.

LOBELL, D., HICKE, J., ASNER, G., FIELD, C., TUCKER, C., and LOS, S., 1982-1998, Satellite estimates of productivity and light use efficiency in United States agriculture. *Global Change Biology*, **8**, 722–735.

MAAS, S., 1988, Using Satellite Data to improve model estimates of crop yield. *Agronomy Journal*, **80**, 655–662.

MAAS, S., 1991, Use of remotely sensed information in plant growth simulatio n models. *Advances in Agronomy*, **1**, 17–26.

MACELLONI, G., PALOSCIA, S., PAMPALONI, P., RUISI, R., DECAMBRE, M., VALENTIN, R., HANZY, A., PRÉVOT, L., and BRUGUIER, N., 2000, Modelling radar backscatter from crop during the growth cycle. *: submitted to Physics and Chemistry of the Earth.*

MALL, R., M., L., BHATIA, V.S.AND RATHORE, L., and SINGH, R., 2004, Mitigating climate change impact on soybean productivity in India: A simulation study. *Agriculture and Forest Meteorology*, **1**, 113–125.

MARCELIS, L., HEUVELINK, E., and GOUDRIAAN, J., 1998, Modelling biomass production and yield of horticultural crops: a review. *Scientia Horticulturae*, **74**, 83–111.

MCCALLUM, I., WAGNER, W., SCHMULLIUS, C., SHVIDENKO, A., OBERSTEINER, M., FRITZ, S., and NILSSON, S., 2009, Satellite-based terrestrial production efficiency modeling. *Carbon Balance and Management*, **4**, 8.

MCKEE, G., 1964, A coefficient for computing leaf area in hybrid corn. *Agronomy journal*, **56**, 240–241.

MCKINION, J., BAKER, D., WHISLER, F., and LAMBERT, J., 1989, Application of GOSSYM/COMAX system to cotton crop management. *Agricultural Systems*, **31**, 55–65.

MCMASTER, G., 1992, Simulating winter wheat shoot apex phenology. *Journal Agricultural Science*, **119**, 1–12.

MCMASTER, G., 2003, Spring Wheat Leaf Appearance and Temperature. Extending the paradigm? *Annals of Botany*, **91**, 697–705.

MCMASTER, G., KEPPLER, B., RICKMAN, R., WILHELM, W., and WILLIS, W., 1991, Simulation of shoot vegetative development and growth of unstressed winter wheat. *Ecological Modelling*, **53**, 189–204.

MCMASTER, G., and WILHELM, W., 1995, Accuracy of Equations Predicting the Phyllochron of Wheat. *Publication from USDA ARS/UNI, Faculty, Paper 79.*

MCMASTER, G., and WILHELM, W., 1997, Growing degree-day, one question, two interpretations. *Agriculture, Forest and Meteorology*, **83**, 291–300.

MCMASTER, G., and WILHELM, W., 1998, Is using soil temperature better than air temperature for predicting winter wheat phenology? *Agronomy journal*, **90**, 602–607.

MEINKE, H., HAMMER, G.L. VAN KEULEN, H., and RABBINGE, R., 1998, Improving wheat simulation capabilities in Australia from a cropping systems perspective III. The integrated wheat model (I-WHEAT). *European Journal of Agronomy*, **8**, 101–116.

MKHABELA, M., ASH, G., GRENIER, M., and BULLOCK, P., 2012, Evaluation of five thermal time models for modelling spring wheat phenological development on the canadian prairies. *30th Conference on Agricultutal and Forest Meteorology/First Conference on Atmospheric Biogeosciences*.

MONTEITH, J., 1977, Climate and the efficiency of crop production in Britain. *Phil. Trans. R. Soc. Lond*, **B281**, 277–297.

MONTGOMERY, E., 1911, Correlation studies in corn. *Nebraska Agric. Exp. Stn. Annu. Report*, **24**, 108–159.

MOULIA, B., and SINOQUET, H., 1993, Three dimensional digitzing systems for plant canopy geomterical structure. A review., In *Crop Structure and light microclimate:Characterization and applications*, edited by C. Varlet-Grancher, R. Bonhomme, and H. Sinoquet (Paris:INRA), pp. 183–193.

MOULIN, S., BONDEAU, A., and DELECOLLE, R., 1998, Combining agricultural crop models and satellite observations: from field to regional scales. *International Journal of Remote Sensing*, **19**, 1021–1036.

MUCHOW, R., SINCLAIR, T., and BENNETT, J., 1990, Temperature and solar radiation effects on potential maize yield across locations. *Agronomy Journal*, **82**, 338–343.

NELSON, G., ROSEGRANT, M., KOO, J., ROBERTSON, R., SULSER, T., ZHU, T., RINGLER, C., MSANGI, S., PALAZZO, A., BATKA, M., MAGALHAES, M., VALMONTE-SANTUS, R., EWING, M., and LEE, D., 2009, *Climate Change: Impact on Agricultural costs of adaptation.* (International Food Policy Research Institute.).

VAN OOSTEROM, E., HAMMER, G., KIM, H., MCLEAN, G., and DEIFEL, K., 2008, Plant design features that improve grain yield of cereals under drought, In *Global Issues, Paddock Action. Proceedings of 14th Australian Society of Agronomy Conference*, pp. 21–25.

PALOSCIA, S., MACELLONI, G., PAMALONI, P., and SIGISMONDI, S., 1999, The potential of C- and L- Band SAR in estimating vegetation biomass. *: The ERS-1 and JERS-1 experiments*, **37**, 2107–2110.

PAPROKI, A., SIRAULT, X., BERRY, S., FURBANK, R., and FRIPP, J., 2012, A novel mesh processing based technique for 3D plant analysis. *Agricultural and Forest Meteorology*, **12**, 63.

PARARAJASINGHAM, S., and HUNT, L., 1995, Effects of photoperiod on leaf appearance rate and leaf dimensions in winter and spring wheats. *Canadian Journal of Plant Science*, **76**, 43–50.

PARRY, M., O.F., C., PALUTIKOF, J., VAN DER LINDEN, P., and HANSON, C., 2001, *Contribution of Working Group II to the Fourth Assessment Report of the Intergovernmental Panel on Climate Change.* (Cambridge: Cambridge University Press).

PARRY, M., ROSENZWEIG, C., IGLESIAS, A., FISCHER, G., and LIVERMORE, M., 1999, Climate change and world food security: a new assessment. *Global Environment Change*, **9**, s51–s67.

PERTTUNEN, J., SIEVANEN, R., and NIKINMAA, E., 1998, LIGNUM:A model combining the structure and functioning of trees. *Ecological Modelling*, **108**, 189–198.

PERTTUNEN, J., SIEVANEN, R., NIKINMAA, E., SALMINEN, H., SAARENMAA, H., and VAKEVA, J., 1996, LIGNUM:A tree model based on simple structural units. *Annals of Botany*, **77**, 87–98.

PETERSON, C., KLEPPER, B., and RICKMAN, R., 1982, Tiller development at the coleoptile node in winter wheat. *Agronomy Journal*, **74**, 781–784.

PINHEIRO, J., and BATES, D., 2004, Linear and Non Linear Models. *Rgui*.

PINNSCHMIDT, H, O., BATCHELOR, W., and TENY, P., 1995, Simulation of multiple species pest damage in rice using CERES-rice. *Agricultural Systems*, **48**, 193–222.

PINTER, J., JACKSON, W., EZRA, C., and GAUSMAN, H., 1985a, Sun angle and canopy architecture effects on the spectral reflectance of six wheat cultivars. *International Journal of Remote Sensing*, **6**, 1813–1825.

PINTER, J., JACKSON, W., EZRA, C., and GAUSMAN, H., 1985b, Sun angle and canopy architecture effects on the spectral reflectance of six wheat cultivars. *International Journal of Remote Sensing*, **6**, 1813–1825.

PINTER, P., HATFIELD, J., SCHEPERS, J., BARNES, E., MORAN, M., DAUGHTRY, C., and UPCHURCH, D., 2003, Remote Sensing for Crop Management. *Photogrammetric Engineering and Remote Sensing*, **69**, 697–664.

POLUEKTOV, R., and TOPAJ, A., 2001, Crop Modeling: Nostalgia about Present or Remiscence about Future. *Agronomy Journal*, **93**, 653–659.

PORTER, J., 1993, AFRCWHEAT2, a model of the growth and development of wheat incorporating responses to water and nitrogen. *European journal of agronomy*, **2**, 69–82.

POTTER, C., RANDERSON, J., FIELD, C., MATSON, P., VITOUSEK, P., MOONEY, H., and STEVEN, A., 1993, Terrestrial ecosystem production: a process model based on global satellite and surface data. *Glob.Biogeochem.Cycles*, **7**, 811–841.

PRÉVOT, L., CHAUKI, H., TROUFLEAU, D., WEISS, M., BARET, F., and BRISSON, N., 2003, Assimilating optical and radar data into the STICS crop model for wheat. *Agronomie*, **23**, 297–303.

PRINCE, S., 1991, A model of regional primary production for use with coarse resolution satellite data. *International journal of remote sensing*, **12**, 1313–1330.

PRUSINKIEWICZ, P., 1990, Graphical Modelling using L-Systems., In *The Algorithmic Beauty of Plants*, edited by P. Prusinkiewicz (Springer-Verlag).

PRUSINKIEWICZ, P., 1998, Modeling of spatial structure and devlopment of plants: a review. *Sci Hortic*, **74**, 113–149.

R DEVELOPMENT CORE TEAM, 2005, *R: A language and environment for statistical computing*, R Foundation for Statistical Computing, Vienna, Austria, ISBN 3-900051-07-0.

RAKOCEVIC, M., SINOQUET, H., CHRISTOPHE, A., and VARLET-GRANCHER, C., 2001, Assessing the geometric structure of a white clover(Trfolium repens) canopy using 3-D digitising. *Annals of Botany*, **86**, 519–526.

DE REFFYE, P., EDELIN, C., FRANCON, J., JAEGER, M., and PUECH, C., 1988, Plant models faithful to botanical structure and development. *Computer Graphics*, **22**, 151–158.

REID, J., 202, Yield response to nutrient supply acorss a wide range of conditions 1.Model derivation. *Field Crops Research*, **77**, 161–171.

RICKMAN, R., and KLEPPER, B., 1991, Environmentally driven cereal crop growth models. *Annual Review Phytopathology*, **29**, 361–80.

RICKMAN, R., WALDMAN, S., and KLEPPER, B., 1996, MODWht3: a development driven wheat growth simulation. *Agronomy journal*, **88**, 176–185.

RITCHIE, J., and OTTER, S., 1984, Description and performance of CERES-Wheat a user-oriented wheat yield model. *Grassland Soil and Water Research Laboratory*, 159–175.

RITCHIE, J., and OTTER, S., 1991, chapter Modeling plant and soil systems (ASA, CSSA, and SSSA, Madison, WI), pp. 31–54.

ROBERTSON, G., and FOONG, S., 1977, *International Development in Oil Palm* (ISP).

ROBERTSON, M., 1994, Relationships between internode elongation, plant height and leaf appearance in maize. *Field Crops Research*, **38**, 135–145.

RODRIGUEZ, D., KELTJENS, W., and GOUDRIANN, J., 1998, Plant leaf are expansion and assimilate production in wheat(*Triticum aestivum L.*) growing under low phosphorus conditions. *Soil and Plant*, **200**, 227–240.

ROOM, P.AND HANAN, J., and PRUSINKIEWICZ, P., 1996, Virtual Plants:new prospectives for ecologists, pathologists and agricultural scientists. *Trends in Plant Science*, **1**, 33–38.

RUMULHART, D., HINTON, G., and WILLIAMS, R., 1986, *Learning internal representation by error propagation. Parallel distributed processing:Explorations in the microstructure of cognition.*

RUSHMEIER, H., and TORRENCE, K., 1990, Extending the radiosity method to include specularly reflecting and translucent materials. *ACM Trans.Graph.*, **9**, 1–27.

RUSSELLE, M., WILHELM, W., OLSON, R., and POWER, J., 1984, Growth Analysis based on degree days. *Crop Science*, **24**, 28–32.

SAIYED, I., BULLOCK, P., SAPIRSTEIN, H., FINLAY, G., and JARVIS, C., 2009, Thermal time models for estimating wheat phenological development and weather-based relationships to wheat quality. *Canadian Journal of Plant Science*, **89**, 429–439.

SAMARASINGHE, G., 2003, Growth and yields of Sri Lanka's major crops interpreted from public domain satellites. *Agric.Water Management*, **58**, 145–157.

SANDERSON, J., DAYNARD, T., and TOLLENAAR, M., 1981, A mathematical model of the shape of corn leaves. *Canadian Journal Plant Science*, **61**, 1009–1011.

SCOTFORD, I., and MILLER, P., 2004, Estimating tiller density and leaf area index of winter wheat using spectral reflectance and ultrasonic sensing techniques. *Biosystems Engineering*, **89**, 395–408.

SEHGAL, V., SASTRI, C., KALRA, N., and DADHWAL, V., 2005, Farm-Level yield mapping for precision crop management by linking remote sensing inputs and a crop simulation model. *Journal of the Indian Society of Remote Sensing*, **33**, 131–136.

SHAYKEWICH, C., 1995, An appraisal of cereal crop phenology modelling. *Canadian Journal of Plant Science*, **75**, 329–341.

SINCLAIR, T., 1986, Water and nitrogen limitations in soybean grain production. I. Model Development. *Field Crops Research*, **15**, 125–141.

SINOQUET, H., and BONHOMME, R., 1992, Modeling radiative transfer in mixed and row intercropping systems. *Agricultural and Forest Meteorology*, **62**, 219–240.

SINOQUET, H., MOULIA, B., GASTAL, F., BONHOMMED, R., and VARLET-GRANCHER, C., 1990, Modelling the radiative balance of the components of a well-mixed canopy-application to a white clover-tall fescue micture. *Acta Oecologica-International Journal of Ecology*, **11**, 469–486.

SINOQUET, H., RAKOCEVIC, M., and VARLET-GRANCHER, C., 2000, Comparison of models for daily light partioning in multispecies canopies. *Agricultural and Forest Meteorology*, **101**, 251–263.

SINOQUET, H., THANISAWANYANGKURA, S., MABROUK, H., and KASEMSAP, P., 1998, Characterisation of the light environment in canopies using 3D digitising and image processing. *Annals of Botany*, **82**, 203–212.

SKINNER, R., and NELSON, C., 1995, Elongation of grass leaf and its relationship to the phyllochron. *Crop Science*, **35**, 4–10.

SLAFER, G., and RAWSON, H., 1997, CO_2 Effects on phasic development, leaf number and rate of leaf appearance in wheat. *Annals of Botany*, **79**, 75–81.

SLAFER, G., and SAVIN, R., 1991, Developmental base temperature in different phenological phases of wheat (Triticum aestivum). *Journal of Experimental Botanyl*, **42**, 1077–1082.

SOURCES, 2013.

SPITTERS, C., KUELEN., V., and VAN KRAALINGEN, D., 1989, A Simple and Universal Crop Growth Simulator: SUCROS, In *Simulation and systems management in crop protection.*, edited by S. Ward, and H. Van Lear (Wageningen, The Netherlands), pp. 147–181.

STEWART, D., and DWYER, L., 1999, Mathematical characterization of leaf shape and area of maize hybrids. *Crop Science*, **39**, 422–427.

STEWART, J., CUENCA, R., PRUITT, W., HAGAN, R., and TOSSO, J., 1977 (Davis:University of California).

STRECK, NEREU AUGUSTO.AND WEISS, A., XUE, Q., and BAENZIGER, P., 2003, Improving predictions of developmental stages in winter wheat: a modified Wang and Engel model. *Agricultural and Forest Meteorology*, **115**, 139–150.

TAKENAKA, A., INUI, Y., and OSAWA, A., 1998, Measurement of three dimensional structure of plants with a simple device and estimation of light capture of individual leaves. *Functional Ecology*, **12**, 159–165.

TAO, F., YOKOZAWA, M., ZHANG, Z.AND XU, Y., and HAYASHI, Y., 2005, Remote Sensing of crop production in China by production efficiency models: models comparisons, estimates and incertainties. *Ecological Modelling*, **183**, 385–396.

THANISAWANYANGKURA, S., SINOQUET, H., RIVET, P., CRÉTENET, M., and JALLAS, E., 1997, Leaf orientation and sunlit leaf area distribution in cotton. *Agricultural and Forest Meteorology*, **86**, 1–15.

THOMAS, J., and GAUSMAN, H., 1977, Leaf reflectance vs leaf chlorophyll and carotenoid concentrations for eight crops. *Agronomy Journal*, **69**, 799–802.

TIVET, F., DA SILVEIRA PINHEIRO, B., DE RAISSAC, M., and DINGKUHN, D., 2001, Leaf Blade Dimensions of Rice (*Oryza sativa* L. and *Oryza glaberrima Steud*.). Relationships between Tillers and the Main Stem. *Annals of Botany*, 507–511.

TUCKER, C., 1979, Red and photographic infrared linear combinations for monitoring vegetation. *Remote Sensing of Environment*, **10**, 23–32.

VAN VUREN, D., KANUMA, M., EDMONDS, J., and RIAHIK WEYANT, J., 2011, A special issue on the RCPs. *Climate Change*, **109**, 1–4.

VERHOEF, W., 1984, Light scattering by leaf layers with application to canopy reflectance modeling: The SAIL model. *Remote Sensing of the Environment*, **16**, 125–141.

VERHOEF, W., 1985, Earth observation modelling based on layer scattering matrices. *Remote Sensing of the Environment*, **17**, 164–178.

VESCOVI, F., and GOMARASCA, M., 1998, Integration of Optical and Microwave Remote Sensing Data for Agricultural Land Use Classification. *Environmental Monitoring and Assessment*, **58**, 133–149.

WAGGONER, P., 1984, Agriculture and carbon dioxide. *American Science*, **72**, 179–184.

WANG, Y., WOODCOCK, W. E., BUERMANN, P., STENBERG, P., VOIPIO, P., SMOLANDER, H., HAME, T., TIAN, Y., HU, Y., KNYAZIKHIN, Y., and MYNENI, R. B., 2004, Evaluation of the MODIS LAI algorithm at a coniferous forest site in Finland. *Remote Sensing of Environment*, **91**, 114–127.

WATKINS, K., LU, Y., and REDDY, V., 1998, An economic evaluation of alternative pix application strategies for cotton production using GOSSYM/COMAX. *Computers and Electronics in Agriculture*, **20**, 251.

WATSON, R., ZINYOWERA, M., and MOSS, R., 1996, *Climate Change 1995: Impacts, Adaptations and Mitigation of Climate Change: Scientific-Technical Analyses. Contribution of Working Group II to the Second Assessment Report of the Intergovernmental Panel on Climate Change.* (Cambridge: Cambridge University Press).

WATSON, R., ZINYOWERA, M., and MOSS, R., 1998, *The regional impacts of climate change: an assessment of vulnerability. A special report of IPCC Working Group II* (Cambridge: Cambridge University Press).

WEIR, A., BRAGG, P., PORTER, J., and RAYNER, J., 1984, A winter wheat crop simulation model without water or nutrient limitations. *Journal Agricultural Science Cambridge*, **102**, 371–382.

WEISS, M., BARET, F., MYNENI, R., PRAGNERE, A., and KNYAZIKHIN, Y., 200, Investigation of a model inversion technique for the estimation of crop characteristics from spectral and directional reflectance data. *Agronomie*, **20**, 3–22.

WELLE, D., 2011, Global Wheat Prices Soar as Russia Cuts Crop Forecast.

WILHELM, W., and MCMASTER, G., 2003, Evaluating SHOOTGRO 4.0 as a potential winter wheat management tool in the Czech Republic. *European Journal of Agronomy*, **19**, 495–507.

WILHELM, W., MCMASTER, G., RICKMAN, R., and KLEPPER, B., 1993, Above ground vegetative development and growth of winter wheat as influenced by nitrogen and water availability. *Ecological Modelling*, **68**, 183–203.

YIN, X., and KROPFF, M., 1996, The effect of temperature on leaf appearance in rice. *Annals of Botany*, **77**, 215–221.

ZHANG, X., LOYCE, C., MEYNARD, J., and MONOD, H., 2007, Modelling the effect of cultivar resistance on yield losses of winter wheat in natural multiple disease conditions. *European journal of Agronomy*, **26**, 384–393.

ZHENG, B., SHI, L., MA, Y., DENG, Q., LI, B., and GUI, Y., 2008, Comparison of archiecture among different cultivars of hybrid rice using a spatial light model based on 3-D digitising. *Functional Plant Biology*, **35**, 900–910.